Conservation of genes and regulatory networks governing carpel development

Dissertation

for the degree Doctor of Science (Dr. rer. nat.) submitted to

Department of Biology and Chemistry Institute of Botany

AG Entwicklungsbiologie der Pflanzen

by

M. Sc. Anna Barbara Dommes

Nov 2022

Danksagung

Ich möchte Allen danken, die zur Entstehung dieser Arbeit beigetragen haben.

Insbesondere möchte ich dabei danken:

Prof. Dr. Annette Becker, für die Möglichkeit in Ihrer AG an diesem faszinierenden Thema zu arbeiten und daran zu wachsen und für ihre Unterstützung.

Allen Kollegen, für gute Zusammenarbeit, Diskussionen und eine schöne

Zeit. Dietmar Haffer, für die Anzucht von Versuchspflanzen.

Prof. Dr. Diedrich Steffens, für die Möglichkeit die Klimakammern zu nutzen.

Dr. Thomas Groß, Dr. Kai Pfannebecker, Yafei Zhao (PhD), Andrea Weisert, Dr. Katrin Ehlers und Andrea Gómez-Felipe (PhD), für die Einarbeitung, Tipps und Tricks im Labor.

Dr. Denise Herbert, Dr. Thomas Groß, Dr. Kai Pfannebecker, Andrea Gómez-Felipe (PhD), Modesto Berbel, Anja Neumann und Dr. Dieter Weber, für produktive und auch lustige Zusam- menarbeit, hilfreiche Kommentare und motivierende Worte.

Meinen Eltern, für all die Unterstützung und dafür, dass sie mich von klein auf an die Natur- wissenschaften herangeführt haben.

Den Mitgliedern der Prüfungskommission, für die investierte Zeit und Mühe.

Zusammenfassung

Pflanzen sind nicht nur Grundlage der meisten Nahrungsnetzwerke dieser Erde, sondern auch integraler Bestandteil der menschlichen Kulturen, als Lebens-, Heil-, oder Genussmittel sowie als Baustoff. Blüten sind neben dem rein ästhetischen Aspekt auch wegen der Früchte und Samen, die sich aus deren Fruchtblättern entwickeln, von besonderem Stellenwert für die Züchtung neuer Sorten. Trotzdem ist das Wissen über die Grundlagen der Fruchtblattendwicklung an vielen Stellen noch sehr lückenhaft.

Um das Verständnis der genetischen Grundlagen der Fruchtblattentwicklung zu erweitern, wurden in dieser Arbeit funktionellen Studien durch VIGS mit phylogenetischen Berechnungen, Protein-Protein-Interaktionsstudien und Analysen der potentiellen regulativen Sequenzen kombiniert. Die Versuche wurden dabei an *Eschscholzia californica* durchgeführt und deren Ergebnisse mit be-kannten Daten aus *Arabidopsis thaliana* und anderen Spezies verglichen. Ziel dieser Arbeit war die Betrachtung speziesübergreifender Mechanismen.

Die Versuchsergebnisse weisen für die bislang unbekannten Gene *EcNGA2* und *EcSPT2* auf eine Beteiligung an der Entwicklung von Griffel und Narbe hin, ebenso für ihre Paralogen *EcNGA1* und *EcSPT1*. Bislang unbekannte Interaktionen zwischen Proteinen mit Relevanz für die Fruchtblattentwicklung wurden gefunden, auf deren Grundlage auf das Vorhandensein verschiedener Kern-Proteinkomplexe mit wechselnden zusätzlichen Interaktionspartnern geschlossen werden kann. Insbesondere Dimerisierungen zwischen MADS und nicht-MADS Proteinen sind aus anderen Pflanzenspezies bislang kaum bekannt. Des Weiteren war zu beobachten, dass in jüngeren Karpellstadien eine größere Anzahl der betrachteten Gene exprimiert ist, als in älteren Stadien, woraus eine geringere Komplexität im Interaktionsnetzwerk der älteren Stadien resultiert. Auf Grundlage von Daten aus der Modellpflanze *A. thaliana* wurden in *E. californica* verwandte Gene für weiterführende Studien identifiziert und die *in silico* Analyse von Transkriptionsfaktorbindestellen als Werkzeug zur Untersuchung von Genregulation getestet. Unter den untersuchten, potenziellen regulatorischen Sequenzen fanden sich keine zwei Sequenzabschnitte mit denselben Bindemotiven und damit die Möglichkeit, dass alle untersuchten Gene unterschiedlich reguliert werden. Daher ist es notwendig die in einem bestimmten Gewebe vorliegenden Transkriptions-faktoren und ihre tatsächlichen Bindemotive zu kennen, um die von ihnen regulierten Gene zu identifizieren. Ein Transfer der Bindemotive zwischen Spezies scheint nicht so einfach möglich zu sein.

Insgesamt wurden sowohl konservierte als auch nicht-konservierte Anteile im genregulatorischen Netzwerk der Karpellentwicklung zwischen *E. californica* und *A. thaliana* gefunden. Um die Ähnlichkeit und Unterschiede weiter zu ergründen, könnten auf den hier gelegten Grundlagen eine Reihe weiterer Experimente durchgeführt werden.

Abstract

Plants are not only at the basis of most food networks on earth, but are as well a central part of human cultures, as food, feed, medicinal and recreational drugs, and as building material. Flowers are of special interest in the breeding of new varieties, not only for their ornamental value but because fruit and seeds develop from their carpels. Nonetheless, the knowledge of the basis of carpel development is incomplete in many aspects.

To broaden the understanding genetic basis of carpel development functional studies by VIGS were combined with phylogenetic calculations, protein-protein-interaction data, and analyses of potential regulating sequences. The experiments were carried out in *Eschscholzia californica* and the results compared with published data from *Arabidopsis thaliana* and further species. Aim of this work was to investigate species-spanning mechanisms.

Experimental results point to an involvement of the previously unknown genes *EcNGA2* and *EcSPT2* in style and stigma development, as well as for their paralogues *EcNGA1* and *EcSPT1*. Previously unknown interactions between proteins relevant for carpel development were observed, supporting the idea of different protein core complexes with changing additional interaction partners. Especially dimerizations be- tween MADS and non-MADS proteins are rarely reported in other plant species. Furthermore, a higher number of genes were found to be expressed in the younger carpel stages compared to older ones, resulting in a lower complexity of the protein interaction network in older stages. Based on data from the model plant *A. thaliana* related genes were identified in *E. californica* for further studies and analysis of transcription factor binding sites as a tool for examining gene regulation was tested. The examination of the potential regulatory sequences showed no two sequences containing the same binding motives and hence the possibility, that all examined genes are regulated in different ways. Thus it is necessary to know the transcription factors present in the respective tissue and their exact binding motives to identify their target genes. A transfer of binding motives between species seems not feasible.

All in all, conserved as well as not-conserved portions where found in the gene regulatory networks between *E. californica* and *A. thaliana*. To further explore the similarities and differences further experiments can be conducted based on the foundations laid out here.

Contents

1 Introduction

1.1 Flowers

Plants are at the basis of most food chains on earth, but more than that, they are a central part of human culture, shaping it and being shaped by it for generations and generations.

Due to the high nutritional value, the most interesting plant organs for human diet are fruit and seeds produced by flowers. Flowers are the most obvious structure unique to the flowering plants (angiosperms) and comprise their reproductive organs. Flowers facilitate dispersal of male gametes in form of pollen and protect the female gametes contained in the ovules. At the same time the female organs (carpels) serve to ensure efficient pollination - meeting of the male and female gametes - by promoting germination of pollen grains and growth of the pollen tubes to the ovules. Mechanisms of interspecific- and self-incompatibility are often conveyed by the carpels, as well. For these tasks a multitude of different tissue types are present, making carpels the most complex plant organs.

A typical angiosperm flower generally contains the carpels in its very centre side by side and surrounded by the male organs (stamens). Those again are surrounded by petals advertising the reproductive parts to possible pollinators, and sepals that enclosed and protected the bud during development. Usually, all floral organs are organized in concentric whorls of equal organ type, but in early diverging angiosperm species often a spiral arrangement with gradually changing organs is seen. As further deviation from the general rule tepals - perianth organs that replace petals and sepals - can be found, for example, in Anemone species or Liliaceae. After pollination and fertilization, the ovules develop into seeds, while the carpels - and sometimes other parts of the inflorescences - develop into fruits. The latter finally support dispersal of the seeds and spread of a new generation of plants (see [1] for more details).

Especially for the mechanisms of pollination and seed dispersal a huge variation can be seen among angiosperms. This diversity, along with their economic importance, sparks the question what general factors are essential for the development of flowers and especially the highly complex carpels. Carpel complexity results from a high number of different tissues, that requires a tightly controlled spacio-temporal developmental program. When looking at the evolutionary short time since the first simple carpels developed in early angiosperms (for more details see [38]), the complexity found today is even more fascinating.

In the model plant *Arabidopsis thaliana*, as well as agronomically important crops like rice (*Oryza sativa*), maize (*Zea mays*) and tomato (*Solanum lycopersicum*), a number of factors governing carpel, fruit and seed development have been identified within the last decades [2–4]. Among others, these factors comprise phytohormones and transcription factors, interacting

in a multitude of pathways to ensure correct spatio-temporal cell division and tissue differenciation in the developing organ [5, 6].

1.2 *Eschscholzia californica* as model organism

The bulk of experiments carried out for this thesis utilized the basal eudicot *Eschscholzia californica*, also known as california poppy. As the common name suggests, it is a species of the poppy family (Papaveraceae) in the order of the Ranunculales, a sister group to the core eudicots (reviewed in [8]), sharing the MRCA with the intensively studied model plant A. thaliana at an evolutionary distance of about 125 mya (compare fig. 1.1). Studies on conservation of genes and their regulatory networks between these species can provide crucial insights in early angiosperm evolution.

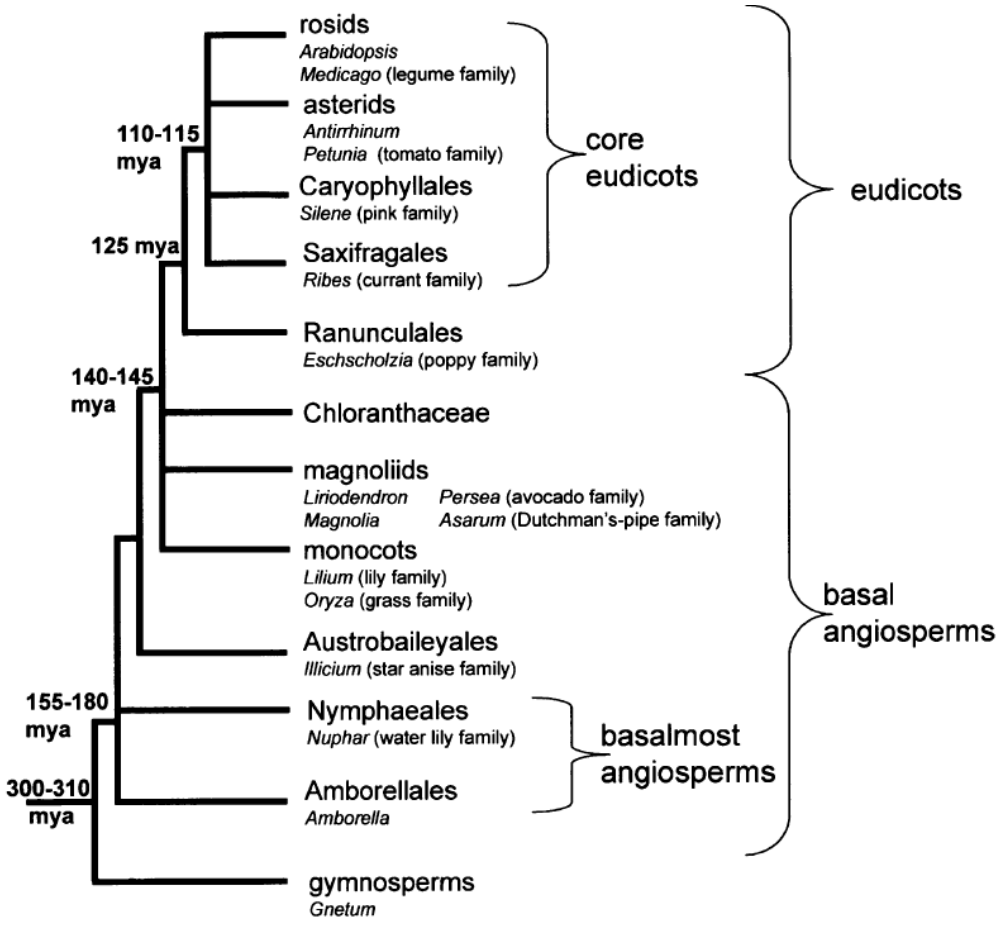

Figure 1.1: *Phylogeny of the angiosperms from [187]. The order of Ranunculales, containing E. californica is separated by 125 mya of independent evolution from the rosid clade, containing A. thaliana, from which are most literature data used in this species.*

1.2.1 Gynoecium architectures

Gynoecium architectures within the Ranunculales are highly diverse (compare fig. 1.2, [7]): The gynoecium of opium poppy (*Papaver somniferum*) is formed by a multitude of congenitally fused carpels, opening small pores at the apical end of the mature fruit. In columbines (*Aquilegia spec.*), the carpels do not fuse with one another (apocarpic gynoecium), but form a group of separate pod-like structures opening at the apical tip.

Figure 1.2: *Gynoecia of different Ranunculales species: a) Aquilegia spec., b) Papaver spec., c) E. californica (within the floral cup).*

The gynoecial architecture of *E. californica*, on the other hand, is remarkably similar to that of the *A. thaliana* (compare figs. 1.3, 1.4): Both have gynoecia composed of two congenitally fused carpels [2, 9]. Their laminar regions form valves, that will separate from the replum region after fruit maturation at determined dehiscence zones. The replum regions, dehiscence zones with separation layer, and the placenta tissues, bearing the ovules, are formed at the site of carpel fusion from the carpel margin meristem (CMM), as are style and stigma tissues [10, 11]. The *A. thaliana* gynoecium additionally develops a false septum, separating its interior into two seed chambers (locules) and enveloping the transmitting tract, a specialized matrix, guiding pollen tube growth towards the ovules [12], in the *E. californica* gynoecium these features are absent.

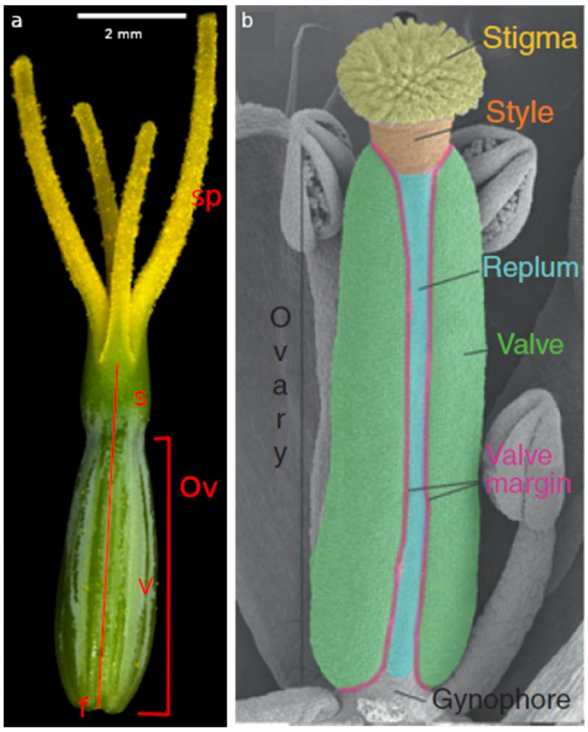

Figure 1.3: *Gynoecia of a) E. californica and b) A. thaliana [2]. sp=stigmatic protrusions, s=style, Ov=ovary, v=valve, f=fusion zone of the carpels*

Taking into account the evolutionary distance of 125 mya (compare fig. 1.4) between the order of Ranunculales (containing *E. californica*) and the rosid clade (containing *A. thaliana*) this similarity in gynoecial architectures is especially remarkable. Here the question arises, if the comparably unrelated species *A. thaliana* and *E. californica* share a common underlying regulatory network, governing the development of the quite similar gynoecia, if the similarity in gynoecium architecture evolved independently, using similar factors, or convergently.

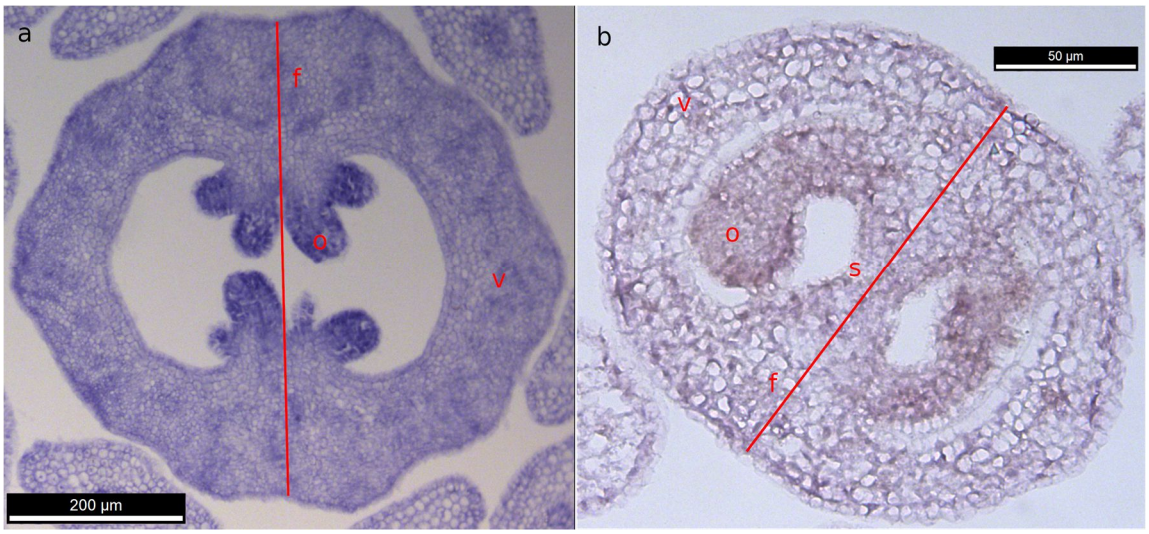

Figure 1.4: *Cross sections of gynoecia of a) E. californica and b) A. thaliana. f=fusion plane of the carpels, o=ovule, v=valve, s=septum*

1.3 Evolutionary-developmental biology

Evolutionary-developmental biology (evo-devo) seeks to gain understanding of how traits of recent species arose during evolution by changes in their developmental programs compared to that of their most recent common ancestor (MRCA). These traits are thought to be mostly brought about by changes in gene regulation and progress either as stepwise adaptations of existing traits or key innovations leading to completely new traits. To achieve this task, despite an incomplete fossil record, comparative studies are conducted to elucidate the molecular, genetic, and ecological mechanisms governing development of the examined trait in different recent species. From these results conclusions are then drawn on the characteristics of the observed trait in the MRCA of the examined species. To gain a more complete evolutionary picture, often non-model species are included alongside established model organisms in these studies. [13–19]

It is commonly assumed, that function is mostly retained after the speciation event creating the orthologues, because extensive functional changes following a mutation would most probably be detrimental if not mitigated by a redundantly working factor [294, 387, 398]. When focussing on genetic evolution, a candidate gene approach can thus be employed: Genes for comparative studies in different species are chosen based on sequence homology, assuming that some degree of related function is shared between them. The identified candidate genes then are studied and compared with respect to functional and sequence similarities.

1.3.1 Evolution of gene networks

In the course of evolution, complex traits of life where gained in part by adjustment of existing traits, to better suit the changing environmental parameters governing the organism's life or to conquer an ecological niche. This gain in trait complexity is often accompanied by a gain in complexity of gene expression regulation, placing enzymatic activities in new metabolic contexts [20, 21]. In this context, the study of changes in transcription factor activities and interactions is a possible way to understand the evolution of gene regulation, underlying new traits.

Another mode of acquiring new gene functions occurs after gene duplication events. The availability of two gene copies after a duplication event, allows independent development of both copies. While one copy maintains the ancestral function, the other copy can change without selective pressure, maybe acquiring a completely new function (neofunctionalization) or just loosing all function (pseudogenization) and getting lost over time. Another possibility for the two copies is subfunctionalization, where the ancestral function of the gene is divided between the two copies allowing independent regulational fine tuning of the resulting subfunctions [22]. In agreement with this idea, many carpel developmental genes of *A. thaliana* were found to have arisen in a stepwise manner [23].

After duplication events, both copies of transcriptional, signalling, or developmental regulators are retained at a higher than average rate [24]. Even among transcription factors, those controlling more derived processes, for example development of carpel-specific tissues, are retained as duplicates at a higher frequency than those controlling the more basal characteristics [23].

In addition to local gene duplications, whole genome duplication (WGD) events are thought to have taken place repeatedly during the evolution of plants [25], leading to growing families of related genes. WGDs result in duplication of complete pathways or networks of genes and, similar to gene duplications, allow independent evolution of both duplicates. This harbours the possibility of gaining completely new traits and is thought to be the origin for major evolutional changes [26]. The MADS-box family of transcription factors (TFs) for example, is thought to be intricately connected to the evolution of land plants and the angiosperm flower, and shows various examples of species-specific subfunctionalizations, neofunctionalizations and pseudogenizations [14, 27, 28]. After the split of the lineages leading to core eudicots and Ranunculales, two whole genome duplications and one triplication are reported in the lineage leading to *A. thaliana* [25] and one independent genome duplication was found for *E. californica* [435]. Because copy numbers of duplicated genes are subsequently reduced again, it is possible, but not likely, that there are 12 orthologous sequences in *A. thaliana* for every pair of paralogous genes in *E. californica*.

1.3.2 Evolution of the carpel

The carpel is the most obvious unifying trait of the angiosperms. Due to the enormous variation in carpel shape, co-evolving with pollinator species or changing pollination mode altogether [436], angiosperms developed to be the most species-rich group of land plants [numbers]. The origin of the carpel as variation of a leaf-like lateral organ has been established by loss-of-function and gain-of-function mutants of multiple floral homeotic genes: floral organs are reverted to leaves or leaves are converted to floral organs, respectively [29–31]. Further studies showed similar expression patterns of several genes, eg. KANADI (KAN), YABBY (YAB), HD-ZIP III, and AUXIN RESPONSE FACTORs (ARFs), in early developmental stages of carpels and leaves, before expression of carpel-specific genes induces the development of carpel-specific tissues [32–37].

For the genes regulating carpel-specific tissue development (e.g. NGATHA (NGA), HECATE (HEC), ALCATRAZ (ALC), INDEHISCENT (IND), NO TRANSMITTING TRACT (NTT), and HALF-FILLED (HAF)) higher retention rates after duplication events where found by Pfannebecker *et al.* [23] and may be a prerequisite for the enormous diversity of carpel architectures [15]. The stepwise addition of TFs to the carpel regulatory toolkit was recently reviewed in [38].

1.4 A short introduction to selected factors governing carpel tissue development in *A. thaliana*

By now, for the specification and genesis of carpel tissues a multitude of genes were shown to be required. The genes included in the experiments, conducted in the course of this study, and the tissues formed by their actions are described here in short. For every tissue first the relevant mutants will be described, then the regulatory and physical interactions of the genes and proteins will be elucidated. Genes selected for functional analysis are printed in bold.

A short overview of wild-type carpel development is given above in section 1.2.1.

1.4.1 Development of style and stigma

In *A. thaliana*, development of stylar and stigmatic tissues and gynoecium vascular patterning is promoted in a dosage-dependent manner by STYLISH 1 (STY1) and STY2, members of the SHORT INTERNODE (SHI) family of zinc-finger proteins (ZFPs) [39]. Among the single mutants only *sty1* shows subtle outer defects in style development, similar to those observed in *hec1 hec2 hec3 spatula (spt)* quadruple mutants [40], but higher-order SHI family mutants show severe defects in style and stigma development. These more pronounced defects are similar those observed in *leunig* (*lug*) mutants and *sty1 spt* or *sty1 crabs claw (crc)* double mutants [39, 41]. Other similar phenotypes are observed in higher-order mutants of NGA family members or combined NGA and SHI family mutants [42].

The **NGA family** of transcription factors in *A. thaliana* consist of four proteins, NGA1, NGA2, NGA3, and NGA4, that act dosage dependent in style and stigma development [37, 40, 42–45]. Trigueros *et al.* further described aspects of the ***NGA3* overexpression** phenotype resembling phenotypes of *HEC1*, *HEC3*, or *IND* overexpression [42].

Similar phenotypes of **NGA** and SHI family higher-order or combined mutants or overexpression lines, as well as similar expression domains of these proteins, point to cooperative action [42] or a positive feedback loop [37] between members of the two gene families. Additionally, genes of the **NGA** and SHI family are both regulated by bHLHs, HEC1 and **SPT**, respectively [40, 63]. ***SPT*** and the *HEC* genes, in turn, are repressed by ETT in the abaxial gynoecium and their ectopic expression in *ett* mutants leads to ectopic stigmatic tissue and auxin gain-of function phenotypes [46]. Ståldal *et al.* showed that *STY1* overexpression rescued the style defects of *spt-2*, *crc-1*, *seuss-1* (*seu-1*), and *seu-1 lug-1* mutants putting STY1 downstream or in parallel to these factors in style development [52]. Furthermore, Li *et al.* recently found **NGA3** as a direct regulator of the newly identified STIGMA AND STYLE STYLIST family genes *SSS1*, *SSS2*, and *SSS3*, which are angiosperm specific and involved in establishing style, stigma and transmitting tract [64].

The bHLH proteins HEC1, HEC2, HEC3, and **SPT** not only share a common expression domain, but show functional redundancy in septum, stigma and transmitting tract development

as well [46]. As a result, the *hec1 hec2 hec3* triple mutant is completely female sterile, due to complete loss of stigma and other reproductive tract tissues [47].

Heterodimerization with **SPT** was observed for HEC1, HEC2 and HEC3 in Yeast Two-Hybrid (Y2H) assays, but no HEC-HEC interactions were found [46]. Recently, additional physical interactions in Bimolecular Fluorescence Complementation (BiFC) studies were observed for **SPT**, HEC1, and HEC3 with **NGA1** and **NGA3**. Furthermore IND interacts with all aforementioned genes [46, 65]. From these and further results Ballester *et al.* propose a series of complexes forming between **NGA**, HEC, IND and **SPT** in the development of apical gynoecial tissues [65].

The ARFs ARF3, ARF6, and ARF8 play major roles in the development of carpel tissues. *ARF3*, also named *ETTIN* (*ETT*), shows a characteristic double-headed split-style mutant phenotype. It results from a lack of medial tissues from the CMM [12]. ARF6 and ARF8 are paralogues, that redundantly regulate gynoecium maturation, and carpels of the *arf6 arf8* double mutant are shorter, have shorter stigmatic papillae, and show reduced fertility [48].

The flower-specific YABBY TF ***CRC*** is expressed only in the nectaries and carpels of *A. thaliana*. ***crc* mutants** show defects in apical carpel fusion, resulting from reduced growth of medial tissues [49–51]. Ståldal *et al.* attribute the defective apical tissue differentiation of the *crc* mutant to early developmental disturbances [52]. A recent study on ***CRC*** regulation, furthermore identified ETT, **NGA2**, and ARF8, among others, as positive regulators of ***CRC*** [426].

The *PERIANTHIA* (*PAN*) gene is member of the bZIP family, expressed in developing floral organs and ovules, overlapping with *SHOOT MERISTEMLESS* (*STM*), *WUSCHEL* (*WUS*) and *AGAMOUS* (*AG*) [53–55]. It was named after the increased number of perianth organs of the *pan* mutant, which switches from a tetramerous to a pentamerous whorl organization. The defects observed in *pan* gynoecia are subtle, they develop a narrower style and occasionally show defects in carpel numbers and fusion [56, 57].

LUG encodes a glutamine-rich protein with seven C-terminal WD repeats (ending in a Tryptophan-Aspartic acid dipeptide). It is involved in the regulation of gene activity via HISTONE DEACETYLASE 19 (HDA19) or the chromatin remodelling SWITCH/SUCROSE NONFER- MENTING (SWI/SNF) complex. Without coding for a DNA-binding domain, it can exert this function only as part of larger DNA-binding protein complexes [58–61]. Reduced female fertility and horn-like protrusions from the unfused carpel tips are found in *lug* single mutants, the latter are reported as well in for *lug* double mutants with *aintegumenta* (*ant*), *apetala 1* (*ap1*), *ap2*, *ap3*, *leafy* (*lfy*), and *pistillata* (*pi*) [10, 62]. Despite its usual role as corepressor, LUG was found to positively regulate SHI family members [41].

PAN was shown to interact with the lateral organ boundary proteins BLADE ON PETIOLE1 (BOP1) and BOP2 [66]

1.4.2 Development of carpel marginal tissues

The involvement of STY1 in medial tissue formation is mostly masked in the *sty1* single mutant by redundantly acting genes like ***CRC*** and ***SPT***. *sty1* single and *sty1 sty2* double mutants have a broader replum than wild-type plants and an basalized bifurcation point of the medial veins. In the *sty1* ***crc*** and *sty1 spt* double mutants the reduction of septal tissues is much more severe than in the single mutants, implying more than an additive effect [39]. Likewise, ***crc spt*** **double mutants** show enhanced medial defects compared to the single mutants [49, 51]. The reduced growth of medial tissues observed in ***crc*** **mutants** (see section 1.4.1) is probably caused by the disrupted development of medial vasculature and stylar xylem. [51]. ***SPT*** is expressed in a broad range of developing tissues [67, 68] and its expression in the CMM in early gynoecium development was found mandatory for proper development of all derived tissues [51, 67].

The paralogous YABBY TFs FILAMENTOUS FLOWER (FIL) and YAB3 are required to form the valves and valve margins. In *fil yab3* doble mutants fruits have reduced valve margin tissues in the distal regions, while showing an increase of valve margin tissues in the proximal parts [69, 70]. Romera-Branchat *et al.* found *WUSCHEL-RELATED HOMEOBOX 13* (*WOX13*) as another factor necessary for proper valve margin and replum development. *wox13* mutants show a reduction in replum width, which is rescued in *wox13 fil* or *wox13 jagged* (*jag*) double mutants [71]. In mutants of *REPLUMLESS* (*RPL*), a three-amino-acid-loop-extension (TALE) class BEL-like (BELL) homeodomain family gene, cells in the replum region adopt valve margin identity instead of replum identity. This defect is further aggravated in *rpl wox13* double mutants, while replum formation is rescued in *rpl fil* and *rpl jag* double mutants and 35S::WOX13 *brevipedicellus* (*bp*) *rpl* plants [69, 71, 72]. Another mutation rescuing *rpl* replum defects is *knotted-like from arabidopsis thaliana 6* (*knat6*), though for *knat6* single mutants no phenotype, apart from increased root branching, was observed [73, 74].

STM is critical for the maintenance of meristematic tissues, including CMM and floral meristem (FM) [75]. Reduced *STM* expression results in floral phenotypes ranging from reduced medial tissue development to complete lack of carpels and reduced numbers of fused stamens, depending on severity. Further floral *stm* defects include fused perianth and sepals bearing ectopic ovules [75, 76].

In *lug* mutants the valves are apically converted into horn-like protrusions (section 1.4.1), while stigmatic bundles are growing from the unfused septum region [62]. Liu *et al.* found LUG necessary for the formation of all carpel marginal tissues, together with ANT [10]. This lack of medial tissue formation is accompanied by a loss of ***CRC*** expresion in the central gynoecium in *lug* mutants, while the epidermal ***CRC*** expression is unchanged [50].

In wild-type *A. thaliana* the *ARF*s 6 and 8 are expressed in carpel medial tissues. Reduced female sterility was observed in *arf8* single mutants [77], while *arf6 arf8* flowers show complete female sterility, with the transmitting tract unable to support efficient pollen tube growth [78]. This is similar to mutants of the WIP (Tryptophan-Isoleucine-Proline [79]) ZFP TF *ntt* or triple

mutants of the bHLH genes *haf*, *brassinosteroid enhanced expression 1* (*bee1*), and *bee3* [47]. Crawford *et al.* first described *ntt* mutants to lack the transmitting tract tissue in the style and septum, as well as the acidic glycoproteins, such as arabinogalactans (AGPs), that are usually produced in its extracellular matrix (ECM). As a consequence of these alterations, pollen tube growth, and thereby fertility, is reduced in *ntt* mutants [80, 81]. The tissue breakdown, usually following ECM secretion, may be caused by the AGPs and was observed to be reduced in *ntt* mutants [82]. An enhancement of the *ntt* mutant phenotype was seen in the double mutant with its interactor SEEDSTICK (STK), also known as AGAMOUS-LIKE11 (AGL11). This is probably inferred by changes in the cuticle, based on altered mannan and lipid deposition in septum cells [81]. *A. thaliana* lines, overexpressing *NTT*, show defects in the development of replum, separation layer and lignified layers, together with an enlarged replum. These may in part be caused by the reduced *FRUITFULL* (*FUL*) expression and slightly activated ***BP*** expression [83]. In *ntt* mutants, *arf6 arf8* double and *hec1 hec2 hec3* triple mutants, expression of *HAF* is severely reduced [47, 78].

Outside the replum, FIL and YAB3 act together with JAG, to promote valve and valve margin identity by activating *FUL* and *SHATTERPROOF* (*SHP*) expression, respectively, in a non-cell-autonomous way [69, 70]. In the replum *SHP* expression is inhibited by RPL via *FIL*, thus repressing valve identity. Furthermore, *RPL* expression was found to be positively regulated by BP, with which it functions then as BP-RPL heterodimer in replum development [70, 84]. Due to the direct interaction of RPL with the KNOX I TALE proteins BP and KNAT6, a competition of BP and KNAT6 for RPL as binding partner is possible [85]. WOX13 inhibits *JAG* and *FIL* expression, and thus the correct formation of a valve margin, and activates *BP* and *RPL* expression for proper replum formation [71]. Though the restoration of replum formation in 35S:WOX13 *bp rpl* plants indicates an BP/RPL-independent role in replum development for WOX13 as well [71].

As mentioned above (section 1.4.1), ETT and TFs of the HEC and **NGA** families regulate ***SPT*** and are needed for correct differentiation of CMM-derived tissues [12, 46, 64, 65].

Recently, a regulational role for AG and cytokinin on several TFs involved in development of medial tissues, namely **CRC**, **SPT**, and SHPs, was shown [427].

1.4.3 Floral meristem termination and organ identity

Floral meristem (FM) termination and the establishment of reproductive organ identity are functions of *AG* in *A. thaliana*. *ag* mutants show a typical flower-in-flower phenotype with petals replacing stamens and the carpels replaced by a new iteration of the sepal-petal-petal sequence, in some genetic backgrounds on an elongated pedicel [29, 86]. *pan* mutants grown in short-day conditions, as well show typical *ag* mutant phenotypes in addition to the altered perianth organ numbers (section 1.4.1) [87].

An involvement of LUG in FM maintenance can be assumed from the decreasing size of the FM meristem, the decreasing number of floral organs in older *lug* mutant flowers, and the enhancement of the early FM termination phenotype in *lug lfy* double mutants compared to *lfy* single mutants [62].

KNAT2 shares its expression domains in the central FM, carpels, and in the SAM with other class I KNOX genes. The expression in the axils and distal parts of the pedicels and in the dehiscence zone of the carpel is shared between *KNAT2* and *KNAT6* [74], while expression in the SAM is shared with *STM* and *BP*, which are assumed upstream regulators as well [74, 75, 90–93]. From the overlapping expression domains and the lack of a *knat2* mutant phenotype, it can be assumed, that its loss is compensated by the other KNOX I genes [94]. The *AG*-independent homeotic conversion of ovules to carpel-like structures observed after *KNAT2* induction, implies an additional role in carpel development [91]. *STM* has a specific role in carpel initiation and identity, aside from its role in meristem maintenance discussed in sections 1.4.2 and 1.4.7. Studies on *ag*, *lfy*, and *wuschel* (*wus*) mutant lines overexpressing *STM*, showed its dependency on *AG* function, but not on functional *LFY* and *WUS* [75]. Ectopic expression of KNOX I genes *KNAT2* or *STM* can promote *de novo* carpel formation and homeotic conversion of ovules to carpels [75, 91].

In addition to the split-style and gynoecial polarity defects discussed above (section 1.4.1), an increase in perianth organ numbers and a reduced number of stamen with defective anthers are described for *ett* mutants [95]. A further involvement of ARFs in FM regulation is supported by relatively recent observations: Chung *et al.* presented the idea of an YABBY/ARF complex repressing *STM* during reproductive primordium initiation via histone deacetylation by HDA19 [96]. In parallel to *ASYMMETRIC LEAVES 1* (*AS1*) and *AS2*, *ARF6* and *ARF8* were discovered to redundantly repress KNOX I genes specifically in floral organs and ectopic KNOX I gene expression phenotypes similar to the *arf6 arf8* mutant were observed by Tabata *et al.* [97]. *ARF6* and *AFR8* are miRNA-regulated, similar to *ETT* and *ARF4* [78].

The *A. thaliana WUS* and *WOX* genes are a family of homeodomain genes involved in plant developmental processes. WUS is a mobile protein expressed in the organizing centre of meristems and plays a central role in stem cell identity in a feedback loop with the CLAVATA (CLV) proteins [98–101]. In the floral meristem, in concert with LFY, WUS activates *AG* expression in the fourth whorl, AG in turn represses *WUS* directly to terminate the floral meristem. In *wus* mutants the FM terminates early, after initiating one or few stamens in the centre, while plants ectopically expressing *WUS* form flowers with additional carpels [75, 99, 102]. Another direct regulator of *AG* expression is the bZIP TF PAN [87].

AG was shown to homodimerize and heterodimerize with AP3, PI, and the **SEPALLATA** (**SEP**) proteins, in accordance with the floral quartet model [30, 103, 104]. The BELL TFs RPL, and possibly POUNDFOOLISH (PNF), positively regulate *AG* and *AP3* expression in the inner floral whorls, in parallel with LFY, UNUSUAL FLORAL ORGANS (UFO), and WUS [105–

109]. AG then regulates *WUS*, *CRC*, *KNU*, and *YUCCA 4* (*YUC4*) expression directly, to terminate the FM [107, 110–113]. It further represses of A-function genes in reproductive whorls to allow reproductive organ identity [29, 114]. Ectopic ***SEP3*** expression was found to activate *AG* expression and the **SEP3** protein binds regulatory sequences located in the second intron of the *AG* gene [115, 116]. Taken together these findings imply direct regulation of *AG* expression by **SEP3**. A recent study was conducted to identify genome-wide targets of AG-**SEP3** complexes [117].

CRC is directly activated by AG [110] and both enhance expression of the auxin biosynthetic enzyme *YUC4* to achieve FM termination [113]. *TORNADO2*, another **CRC** target gene, is involved together with YUC4 in FM termination. Yamaguchi *et al.* suggested further roles of **CRC** in FM termination via repression of *WUS* and altered cell wall composition [89, 113]. An indispensable role of ***CRC*** in FM regulation, is furthermore suggested by ***crc*** *knuckles* (*knu*), ***crc*** *rebelote* (*rbl*), ***crc spt***, ***crc*** *squint* (*sqn*), and ***crc*** *ultrapetala* (*ult*) **double mutant** phenotypes. They show a loss of FM determination and reiterating stamens and carpels, even though ***CRC*** is not expressed in the central FM, but non-cell-autonomous modes of action for ***CRC*** were identified before [49, 50, 88, 89].

1.4.4 Establishment of carpel polarity axes

The HD-ZIP III genes are expressed in the adaxial domain of the carpels and ectopic ovule formation in double mutants of their downstream targets *little zipper 3* (*zpr3*) and *zpr4* [36, 118]. These data imply a role for the HD-ZIP IIIs in carpel polarity establishment.

A. thaliana mutants of the KNOX I protein BP show defects in radial aerial organs, such as the style, in addition to the name-giving short pedicels [119–121].

In line with an auxin-dependent apical-basal polarity axis, Sohlberg *et al.* found STY1 as direct activator of YUC4-mediated auxin biosynthesis and acting synergistically with PID, ETT, and **SPT** in apical-basal gynoecium patterning [122].

ett mutants show not only a split-style phenotype, but defects in abaxial-adaxial polarity and apical-basal patterning, as well [12, 35, 46, 67]. This was attributed to an auxin gradient along the apical-basal axis of the gynoecium by Nemhauser *et al.* [123]. Simonini *et al.* detected auxin-sensitive dimer formation between ETT and IND resulting in *PID* repression [124]. Based on this, Kuhn *et al.* suggested a model, where ETT competes for IND binding with other factors, like **SPT** and HEC, depending on cellular auxin levels [125]. In this way, it negatively regulates the activity of the bHLH genes ***SPT*** and *HEC* in the abaxial gynoecium, leading to abaxial-adaxial polarity defects of the *ett* mutant. Physical interaction of ETT with the polarity factors FIL, KAN1 and KAN4 are reported, paralleling interactions of KAN, YAB, and ARF proteins in early leaf development [126–128].

Stahle *et al.* identified the ability for homo- and heterodimerization between the *A. thaliana* YABBYs FIL, YAB2, YAB3, and YAB5 and for heterodimerization with LUG/LEUNIG-

HOMOLOG (LUH) and SEU/SEUSS-LIKEs (*SLK*s) [129, 130]. The resulting complexes are involved in abaxial-adaxial cell identity regulation of all lateral organs and in SAM formation and maintenance [129]. Interestingly, *LUG* is expressed mainly adaxially in carpels and leaves [58].

In several ***crc* double mutants** adaxialization of the replum was observed, while in plants ectopically expressing ***CRC*** under control of a 35S promoter, abaxial characteristics were found on the adaxial surfaces of petals and leaves [131]. In ***crc*** single mutant carpels no obvious polarity defects were known from earlier studies, but Yamaguchi *et al.* published the observation of a slight adaxialization of *ARGONAUTE10* (*AGO10*) and *PHABULOSA* (*PHB*) expression and a laterally expanded *PIN-FORMED1* (*PIN1*) expression domain [89]. This suggests CRC is needed to later form the tissues expressing the aforementioned genes, while on the other hand, positive and negative regulation of YABBY genes by HD-ZIP III genes in polarity establishment is reported from several species [132].

Mutual negative regulation between **NGA** genes and the YABBY1 (YAB1) genes *FIL* and *YAB3* defining the style basal border was described by Alvarez *et al.*, along with common regulation of *SHP1* [37].

1.4.5 Hormonal regulation of carpel development

The involvement of hormonal regulation in carpel development has been mentioned several times above.

The YUCCA family members *YUC1* and *YUC4* are flavin-monooxygenases involved in tryptophan-dependent auxin biosynthesis [133]. They are expressed in a temporally and spatially restricted manner in the SAM, FM and floral organs, showing a high level of redundancy, which is confirmed by the subtle phenotypes of the single mutants. The *yuc1 yuc4* double mutant shows severe floral defects, which are further enhanced in higher-order mutant combinations with *yuc2* and *yuc6*, due to a severe to complete loss of vascular bundles in pedicels and flowers [134].

PINOID (*PID*) and the *WAVY ROOT GROWTH* (*WAG*) genes are members of the AGC kinase family [135]. PID is a regulator of polar auxin transport (PAT). It is upregulated in the response to auxin and facilitates the polar orientation of the auxin efflux transporters PIN1, PIN2, and PIN4 at the plasma membrane. With this action, it is part of the self-organization of auxin fluxes preceding vascular bundle formation in organ development [136–138]. *pid* mutants mimick the pin-like inflorescences of *pin* mutants [136]. *WAG1* and *WAG2* are named for their characteristic mutant root phenotype. They are thought to function in PAT similar to *PID*, in addition to presumed gravity sensing of the root [135, 139].

Maier *et al.* found a complex involvement of PAN in diverse developmental processes, such as hormone signalling and stress response, making *pan* mutants highly sensitive to environmental parameters [54].

The AUTHENTIC/ARABIDOPSIS RESPONSE REGULATORs (ARRs) of *A. thaliana* are part of a two-component response regulator system in plants relaying cytokinin (CK) signals by phosphorylation/dephosphorylation [140, 141]. Interactions of the B-type ARR ARR14 with several INDOLE-3-ACETIC ACID INDUCIBLE (IAA) proteins, GIBBERELLIC ACID INSENSITIVE (GAI), and proteins of the two-component system, imply a role of ARR14 in several hormonal pathways. Additionally, ARR14 interacts with KNAT1, the bHLH TFs **SPT** and IND, and a MEKHLA domain-less REVOLUTA (REV) construct [142–145]. The latter interactions are in agreement with known roles of other B-type ARRs in meristem regulation [146]. Findings by Herrera-Ubaldo *et al.* show an involvement of ARR14 in style and stigma development as well [147] supporting the role of phytohormones in the development of these tissues. Recently the complex interplay of CK signalling via B-type ARRs, with the TFs AG, **CRC**, **SPT** and the SHPs was examined [427].

STY1 activates auxin biosynthesis by YUC4 in the apical gynoecium, necessary for its normal development [122, 148]. This model is supported by the rescue of *sty1-1 sty2-1* double mutants stylar defects by exogenous application of auxin [52]. *STY1* in turn is regulated by LUG, giving LUG a role in the hormonal regulation of carpel development, as well [41, 52].

The **NGAs** modulate the auxin response in the apical gynoecium on several levels: (1) auxin bio-synthesis via expression of *AMIDASE 1* (*AMI1*), *TRYPTOPHAN AMINOTRANSFERASE OF ARABIDOPSIS 1* (*TAA1*), and YUCCA family flavin monooxygenases, (2) auxin signalling via ARF family proteins, and (3) auxin transport by PIN localization via the expression of the protein kinases *PID* and *WAG2* [42, 149]. In return, **NGA** gene expression is regulated by PAT [37].

SPT is activated by a combination of **NGA**, HEC, and IND activity [65], **SPT** then heterodimerizes with IND [46]. This dimer was found to regulate auxin distribution in the developing gynoecial apex by repressing *PID* and enhancing *WAG2* expression [150]. Opposite regulation of *PID* and *WAG2* by ETT, in turn restricts ***SPT*** and *HEC* expression to the apical domain of the gynoecium [46, 67]. Reyes-Olalde *et al.* found **SPT** to be involved in CK signalling in the medial domain by activating expression of the B-type ARRs *ARR1* and *ARR12*. **SPT** and ARR1 then together activate the expression of the auxin biosynthetic and signalling genes *TAA1* and *PIN3*, respectively [151]. **SPT** was found to act downstream of CK as well, because *SPT* expression is strongly reduced in the *arr1 arr10 arr12* triple mutant [427]. As CK application could not rescue all aspects of the *spt* mutant phenotype, part of the **SPT** functions are probably CK-independent. Because **SPT** and ARR1 do not interact physically, an indirect interaction via their common interaction partner HEC1 is assumed [151]. Furthermore, Carabelli *et al.* recently found an involvement of HEC and **SPT** in the HOMEOBOX-LEUCINE ZIPPER PROTEIN 3/ARABIDOPSIS THALIANA HOMEOBOX-LEUCINE ZIPPER PROTEIN 4 (HAT3/ATHB4)-mediated regulation of auxin and the resulting shift of bilateral to radial symmetry during gynoecium development [152]. For HEC1 an involvement

in gibberellic acid (GA) signalling, additionally to IND and ALC, is published, as well as in light signalling and direct transcriptional activation of **NGA1**, **NGA2**, and STY [40, 153]. Furthermore, HEC1 was shown to activate transcription of *YUC4*, *PIN1* and the A-type ARRs *ARR7* and *ARR15* [154, 155]. The apical-basal patterning defects of *ett* mutants are highly similar to *pid* or *monopteros* (*mp*, ARF5) mutants or the phenotype induced by application of the auxin transport inhibitor N-1-naphthylphthalamic acid (NPA) [95, 123, 156]. ETT was assumed to be an interpreter of auxin levels, supported by the finding, that ETT forms heterodimers with IND, BP, KNAT3, and other proteins in an auxin-sensitive manner to regulate PAT via PID [127]. Recently, an auxin-dependent binding and recruitment of chromatin remodellers to target genomic loci was observed as well [438]. An involvement of ETT in CK signalling was observed via the repression of CK biosynthesis (*ISOPENTENYLTRANS-FERASE 3* (*IPT3*), *IPT5*, *IPT7*, and *LONELY GUY 3* (*LOG3*), *LOG4 and LOG7*) and signalling (*ARABIDOPSIS HISTIDINE KINASE 4* (*AHK4*)) [157].

ARF6 and ARF8 not only regulate gynoecium maturation in a redundant fashion, but stamen maturation as well. Single *arf6* and *arf8* mutants show retarded stamen development, reduced self-pollination, and reduced female fertility; in the double mutant, apart from complete female infertility (section 1.4.1), defects in vascular patterning, cell differentiation of the petals, and bud arrest at stage 12 are observed. These double mutant phenotypes are similar to jasmonic acid (JA)- deficient or JA-insensitive mutants [48, 97]. Furthermore, the anther dehiscence phenotype can be rescued by external application of JA and response to auxin treatment is reduced in comparison to wild type [48]. Another gene involved in JA-dependent stamen maturation is AG. It activates the putative transcription factor SPOROCYTELESS (SPL) and later the JA biosynthetic gene *DEFECTIVE IN ANTHER DEHISCENCE1* (*DAD1*). *DAD1* activation possibly is dependent on ARFs 6 and 8, as well [158, 159].

Bencivenga *et al.* observed a CK-dependent repression of BELL TF *BELL 1* (*BEL1*) expression and repression of *WUS* and *PIN* in the chalaza region by BEL1 [160]. In this way BEL1, similar to and probably together with KNOX I proteins, is involved in hormonal regulation of development. A lack of non-ovule phenotypes is probably due to tissue-specific partial redundancies with other BELL proteins, like RPL [85, 161, 162]. Additionally, antagonistic roles of *BEL1* with *ARABIDOPSIS THALIANA HOMEOBOX GENE 1* (*ATH1*) and *STM* in GA biosynthesis were shown [163].

B- and C-gene (see section 1.4.6) expression was found to be repressed by the DELLA protein REPRESSOR OF GA (RGA) in the absence of GA, leading to retarded growth of petals, stamens and gynoecia [164], while SEP3 targets several non-MADS genes involved in hormonal pathways, e.g. *ARF3* and *ARF8*, *ALLENE OXIDE CYCLASE 1* (*AOC1*) and *AOC2*, *BRASSINOSTEROID INSENSITIVE 1* (*BRI1*), *PID*, and *PIN4* [116].

The HD-ZIP III genes are involved in hormonal responses to abscissic acid (ABA), auxin, and CK [143, 165–171].

A comprehensive review on the hormonal regulation of gynoecium and fruit development in *A. thaliana* has been published recently [428].

1.4.6 Floral organ identity and floral organ identity

Numerous members of the MADS-box TF family are involved in a high number of developmental processes throughout the plant life cycle [27]. Only a subset involved in flower development and flowering time will be considered here. Based on floral homeotic mutants, Coen and Meyerowitz developed the basic ABC model of floral whorl specification and most of the homeotic genes involved are from the MADS-box TF family [114]. According to the floral quartet model they act as tetrameric protein complexes, which may initiate gene expression by substituting nucleosomes in inactive chromatin and recruiting chromatin remodellers [172, 173]. A large number of intrafamily protein-protein interactions (PPI) was reviewed by Kaufmann *et al.* [20].

The A-class genes of *A. thaliana* AP1 and AP2 specify perianth identity, while outside the Brassicaceae distinct A-class genes are not well conserved [174]. The ABC model of flower development [114] specifies one function of the A-class genes in repression of the C-function in the perianth worls via recruiting of TOPLESS (TPL) and HDA19. Mutants in the A-function gene AP2 show defects in seed coat development in addition to defecs in floral organ numbers and identity [175].

The B-function of floral organ specification in *A. thaliana* is conveyed by AP3 and PI [114]. Loss of B-function results in flowers with all perianth organs transformed to sepals and stamens transformed to either filamentous structures capped with stigmatic papillae, to staminoid or solitary carpels, often the transformed stamens are fused to the gynoecium as filamentous structures or additional carpels [29]. Enhanced expression of B-function results in additional stamens and often staminoid carpels [176–178].

Besides FM termination, carpel and stamen identity, and the repression of A-function genes in reproductive whorls (sections 1.4.3 and 1.4.5), the C-class gene *AG* is involved in the development of ovules [29, 114, 159, 179–182]. Another factor involved in ovule identity is BEL1, named for the transformation of ovules into bell-like structures in *bel1* mutants [180, 182, 183]. This phenotype is reminiscent of the carpelloid ovules seen in *STM*-overexpression lines, resulting from ectopic *AG* expression in the ovules [179] but *BEL1* expression levels were not influenced by *STM* expression levels [75]. Similar to BEL1, ARABIDOPSIS BSISTER (ABS), also known as TRANSPARENT TESTA16 (TT16), is involved in ovule development by regulation of *INNER NO OUTER* (*INO*) and *WUS* via forming heterodimeric and tetrameric complexes with STK, SHP1, SHP2, **SEP3**, and AG [182, 184]. Ectopic *STK* expression is sufficient for ectopic ovule formation [185, 186]. AG, SHP1/2, **SEP**, and STK function redundantly in carpel identity, as multimeric complexes, as well [185].

The *A. thaliana* ***SEP*****s** can be divided into two clades, the *SEP3* and the *LOFSEP* genes *SEP1*,

SEP2, and *SEP4* [22, 187]. ***SEP3*** was identified as the main scaffolding protein of the B- and C-class floral homeotic proteins, conferring transcriptional activation activity to their complexes [30]. The **SEP3** protein interacts with the MADS-box TFs ABS, AG, AP1, AP3, PI, SHP1, SHP2, and STK, with the co-repressor **LUG** via SEU and chromatin remodellers [104, 188]. SEP3 was proposed as pioneer transcription factor by Theißen *et al.* recruiting chromatin remodellers to closed chromatin to enable binding of further transcription factors [173]. **SEP3** targets several MADS-box genes *AG*, *AP1*, *AP3*, ***SEP1***, and ***SEP2***, and in feedback loops ***SEP3*** again is targeted by AG, AP1, FUL, and **SEP3** [104, 116]. The **SEP1/2** proteins show redundant functions with **SEP3**, but with a weaker effect [30, 189]. They are expressed in all floral whorls, while **SEP3** is restricted to the three inner whorls, and **SEP4** is expressed in all above-ground organs [190–193]. For **SEP4**, AP1 and FUL were identified as interactors corresponding to its role in floral meristem identity [31, 104].

The *SUPERMAN* (*SUP*) gene in *A. thaliana* was shown to repress the expression of B-class genes in the fourth floral whorl. Loss-of-function results in additional stamens and stamen-carpel mosaic organs, similar to ectopic *AP3* expression [176, 177]. The *lug sup* double mutant shows additive phenotypes compared to the single mutants [62].

Even though LUG in itself is not a homeotic gene, *lug* mutants show several homeotic conversions in their flowers, especially those formed late in more apical positions. Sridhar *et al.* proposed a model, based on the finding that the co-repressor LUG via SEU can physically interact with AP1 and **SEP3**, which both are direct regulators of *AG*. This leads to repression of *AG* in the perianth whorls [188]. In addition to AP1 and **SEP3**, AGL24 and SHORT VEGETATIVE PHASE (SVP) function as adaptors for the SEU-LUG dimer in *AG* repression [194]. Other repressors of *AG* in the outer floral whorls, stem, and in the developing ovules are BEL1, RPL, and PNF [179, 195]. In *lug* mutants ectopic *AG* activation leads to ectopic activation of B-class MADS box genes and a lack of *AP1* expression [58, 62]. Interestingly, ectopic B-class gene expression is only observed in the medial sepals of *lug* mutants [62]. Furthermore, LUG is involved in miR172-regulation to control *AP2* expression [196]. AP2 function in sepal specification is assumed to be the negative regulation of **SPT** function, because ectopic ***SPT*** expression in *ap2* mutants induces ectopic *STY2* and thus carpel characteristics in sepals [63]. The homeotic changes observed in SHI family multiple mutants, on the other hand, are induced by reduced B gene expression [41]. Other proteins regulating floral homeotic genes or interacting with them are FIL, LFY, UFO, and REV [197–199].

1.4.7 Outside the *A. thaliana* carpel

The paragraphs above elucidated the functions of the considered genes in the development of *A. thaliana* carpel tissues. In the following data from other tissues and plant species are described, to gain a more complete picture of possible ancestral functions, mechanisms and interaction partners.

The role of TALE protein KNOX-BELL heterodimers for the regulation of basic developmental processes is conserved within the green plants since the green algae. Heterodimerization of the proteins masks their nuclear export signals and thus leads to accumulation in the nucleus, while at the same time the binding affinity to their target DNA is enhanced by the dimerization [85, 161, 180, 200–204].

In flowering plants TALE proteins are crucial in meristematic and quasi-meristematic [205] tissues, such as SAM, root apical meristem (RAM), inflorescence meristem (IM), CMM, and in dissected leaves. They act in partly redundant as well as in specialized ways [204–210]. The ability of moss KNOX genes to compensate loss of BP function in *A. thaliana*, but not vice versa, demonstrates that functional evolution took place in this gene family [211]. Mutual regulation among the KNOX I TFs, tissue specific expression patterns, and different binding specificities, orches- trate competing KNOX-BELL heterodimers in *A. thaliana*, as well as in monocots and pomgranate (*Punica granatum*) [85, 161, 162, 195, 200, 201, 204, 208, 210, 212–216]. This allows distinct spatio-temporal regulation of TALE functions and their target genes [85, 121, 162, 201, 213]. The different binding specificity of KNOX-BELL heterodimers could even be shown between proteins of different species [200].

The KNOX class I family of *A. thaliana* is formed by the four genes *STM*, *BP*, *KNAT2* and *KNAT6* [120, 210]. Ectopic expression of any class I KNOX gene, inhibits outgrowth and differentiation of leaves and floral organs, except for the central gynoecium, to a varying degree.

In the SAM STM is required and sufficient for cell divisions [217]. The ectopic expression of *BP* or *STM* additionally can induce *de novo* shoot meristem formation on the adaxial leaf surface [75, 84, 91]. In incipient flower primordia *STM* and *BP* are downregulated by the ARFs ETT, ARF4 and MONOPTEROS (MP/ARF5) [96]. While ETT directly targets *STM* and *BP*, MP regulates *FIL* and the resulting ETT-FIL complex mediates *STM* repression through histone deacetylation by HDA19 [96]. In *fil yab3* double mutants, *STM*, *BP*, and *KNAT2* are no longer repressed, leading to loss of lamina growth in leaves and ectopic meristem formation [218].

Because STM is essential for the maintenance of meristems in all phases of the *A. thaliana* life cycle, *stm* mutant meristems terminate prematurely in fused cotyledons, single leaves, fused flowers, central fused stamens, or separate carpels [75, 76, 91, 94, 109, 121, 205, 215, 219–222]. Stem cell maintenance by STM in the SAM was observed to function by repressing the GA biosynthesic enzyme GA20ox1, and by activating GA catabolism via GA oxidases GA2ox2 and GA2ox4. At the same time STM activates CK biosynthesis via *IPT7* [223–225] and in a positive feedback loop CK then activates *STM* and *WUS* expression [226, 227]. STM was shown to repress *AS1* and *AS2* [92, 94], thereby activating *LATERAL ORGAN BOUNDARIES* (*LOB*). LOB is a known regulator of BR catabolism via *PHYB ACTIVATION-TAGGED SUPPRESSOR 1* (*BAS1*) [228, 229]. STM acts partially redundant with, as well as upstream of *WUS*, *KNAT6*, and by de-repression of *BP*, and *KNAT2* [75, 76, 93, 96, 217, 230].

BP is primarily known for its role in inflorescence internode patterning and pedicel orientation and acts redundantly to STM in the SAM [74, 75, 84, 93, 94, 119–121, 213, 231]. In inflorescence architecture patterning, the BP-RPL dimer represses *KNAT2* and *KNAT6* via the SWI/SNF chromatin remodelling ATPase BRAHMA (BRM), and represses the lateral organ boundary genes *BOP1* and *BOP2*. These in turn activate *KNAT6* expression in the pedicel axils [74, 207, 210, 232]. Generally, the expression of *KNAT6* is mostly seen in organ boundaries of the cotyledons, pedicels, floral organs, and valves [74, 93], as well as in root phloem [73]. For proper cotyledon separation in embryonic development, Belles-Boix *et al.* proposed an involvement of KNAT6 via the STM/CUC pathway [93, 220]. Xylem formation in hybrid poplar (*Populus alba* × *Populus glandulosa*) via NAC family genes was as well shown to be regulated by the poplar KNAT2/6 ortholog PagKNAT2/6b [233]. The common involvement of KNAT2 and KNAT6 in floral organ abscission, another lignin-dependent process, was proposed to be regulated by BP, as well [234]. The observed role of BP in repressing lignin biosynthesis, is in line with its redundancy with STM in meristem maintenance, because lignin deposition is an irreversible part of cell differentiation [121, 232, 235].

Like the KNOX I proteins, their BELL interaction partners are expressed at a distinct pattern regulating not only general meristem initiation and maintenance, but depending on the formed KNOX-BELL dimers, the spatio-temporal meristem identity [201, 204, 208]. The evolutionary oldest BEL1-like protein was identified in the gymnosperm *Gnetum gnemon* making the BEL1-like genes older than the angiosperms [236]. In line with this, similar expression domains and BEL1-KNOX dimers were found in different angiosperm species [212, 237].

Antagonistic with BEL1, both, STM and ATH1 are involved in GA signalling [163], and their dimer was shown to maintain axillary meristems by activating STM expression in leaf axils [238]. Furthermore, a role for STM-ATH1 in flowering time regulation was shown, but not for a STM-RPL heterodimer [201]. In line with the partial redundancy of ATH1 and the CUC genes in the formation of basal boundaries of lateral organs [204, 206], Khan et al. suggested an KNAT6-ATH1 dimer in the formation of organ boundaries [207]. In inflorescence internodes KNAT6-ATH1 is repressed by BP-RPL, while BOP1/2 act as activators of *KNAT6* and *ATH1* [74, 207, 210]. Other factors regulating *ATH1* expression are AG, KAN1, and REV [110, 239].

Consistently with the findings from *A. thaliana*, a function in FM activity was reported for the two STM orthologues in *E. californica* and for KNOTTED 1 (KN1) in maize [209, 240]. They found a preferential expression of the two *EcSTMs* in reproductive shoot tips and early flower buds, while *EcBP* and the *EcKNAT2/6* orthologue were stronger expressed in vegetative shoot tips and developing leaves. *EcSTM1* and *EcKNAT2/6* were additionally detected in late floral buds and the latter in cotyledons as well. The functional characterization by VIGS showed premature floral meristem termination, homeotic organ transformations and defective internode

patterning for both *EcSTM*s. For *EcBP* no flower defects were observed [209]. Groot *et al.* showed *EcSTM1* expression in developing leaves and buds by RNA *in situ* hybridization, similar to *KNOX I* gene expression in *A. thaliana* [221]. In rice, maize, and Solanaceae furthermore, a role of KNOX I genes in diverse phytohormonal pathways, regulating CK, GA, auxin, and brassinosteroid (BR) metabolism and responses, was documented [223, 241–246].

The KAN TFs of the GARP family are involved in adaxial-abaxial polarity establishment and vascular development throughout a plants life cycle by regulating PIN1 localization antagonistically with HD-ZIP III proteins [166, 247]. Further genes regulated by KAN1 and REV were identified by studies conducted by Reinhardt *et al.* in 2013 and Ram *et al.* in 2020 [143, 239]. *KAN1*, *KAN2*, and *KAN4*, also called *ABERRANT TESTA SHAPE* (*ATS*), have redundant roles in embryogenesis and *kan1 kan2 kan4* triple mutants form outgrowths from the hypocotyl during embryo development, that develop into structures similar to radialized leaves [247]. Leaves formed from the SAM postembryonically are initiated as radial primordia and only later adopt polar features [247]. Eshed *et al.* describe *kan1 kan2* floral organs as 'largely adaxialized' [34], while leaf phenotypes were described as 'strikingly similar' to those of *arf3 arf4* double mutants by Pekker et al. [35]. This similarity probably stems from the physical interaction of these proteins described by Kelley *et al.* [126].

An involvement of KAN genes in leaf polarity is reported from a wide range of angiosperm species, implying a conserved function in lateral organ development [248–251].

For the ARF *ETT* an involvement in cell wall formation was identified, leading to the growth defects in *ett* mutants [252]. Redundantly with ARF4, ETT was shown to regulate adaxial-abaxial patterning in all aerial lateral organs and double mutants closely resemble *kan1 kan2* mutants [35]. Expression of both is negatively regulated by trans-acting siRNAs and enhanced by REV [143, 253, 254]. Overexpressing the ARF-regulating MIR167a of *A. thaliana* in tomato lead to comparable genetic and morphologic responses as observed in *A. thaliana*, implying a conservation of developmental regulation between both species [255]. Similarly, repression of fruit initiation without fertilization is disrupted in *A. thaliana* and tomato *arf8* mutants, inducing formation of parthenocarpic fruit [77, 256, 257].

In parallel to the stamen defects of *Atarf6* and *Atarf8* mutants, *AqARF6* and *AqARF8* of *Aquilegia coerulea* are involved in stamen, staminode and petal spur elongation, as well as *AqSTY* and *AqSTY2* expression, and thus nectary maturation [258].

Like WUS, WOX family members are involved in diverse developmental processes and promoter analysis by Wu *et al.* predicts regulation by auxin and CK signalling pathways via auxin responsive element (AuxRE), ARR-B, and ARF binding sequences [259].

In *A. thaliana* WOX1 and WOX3 are involved in sepal, petal, stamen, and leaf development.

wox1 mutants show no obvious phenotypes suggesting redundancy with other factors [260]. In *wox3* mutants lateral (with respect to the inflorescence axis) sepals and stamens are reduced or missing and in the remaining sepals the cells of the lateral margins are missing. This be rescued by expression of WUS from a WOX3 promoter [261–263]. Similarly, in double mutants of the maize WOX3 orthologues *narrow sheath 1* (*ns1*) and *ns2* the lateral domains of all lateral organs are affected [262, 263]. *wox1 wox3* double mutants of *A. thaliana* have narrow leaves, sepals, and petals, with the lateral organs often lacking. Additionally, Nakata *et al.* described the distinct WOX1/3 expression pattern, between abaxial and adaxial domains of developing leaves, governing leaf blade outgrowth and margin cell specification [261, 264]. Triple mutants of *wox1 wox3* with *wus*, *lug*, or *angustifolia 3* (*an3*) further enhance the narrow leaf phenotype [61, 265]. An involvement of WOX1 and WOX3 homologues in leaf blade outgrowth is also known from other dicot and monocot species as well [265–269]. Petunia (*Petunia × hybrida*) WOX gene *maewest* (*maw*) mutants, additionally to the sepal, petal, leaf, and stamen defects, show a split style and stigma [260]. Recently, WOX9 was found to act antagonistically to WOX1 and WOX3 in leaf blade outgrowth of *Medicago truncatula* and *Nicotiana sylvestris* [270]. Furthermore, *WOX1*, *WOX3*, and *WOX9*, together with *WOX2*,*WOX5*, and *WOX8*, were identified as partially redundant regulators of embryo development with involvement in auxin distribution and signalling [271]. Additionally, WOX5 was found to regulate the stem cells of the root apical meristem (RAM), similar to WUS in the SAM, and via related regulators [272].

For WOX4 a role in development of the procambium was described in *A. thaliana* and tomato [273], while in *M. truncatula* the WOX1 homologue STENOFOLIA (STF) was shown to achieve this, by recruiting repressors of the TPL/TPL-related (TPR) family to the *AS2* locus [269].

WOX6 is involved in ovule development, further *wox6* mutant and overexpression phenotypes are similar to *WUS* lack- or gain-of-function phenotypes, respectively [274].

Though WUS is required for functional SAM development, *WUS*-independent stem cell forma- tion has repeatedly been repoted [102, 275]. In the ovule, *WUS* is expressed in the nucellus but downregulated in the chalaza region by CK via AHK4 and BEL1, and it is required for integument development [160, 182, 276]. *WUS* is also involved in stomium and septum development of the anthers, leading finally to dehiscence and pollen release [277]. In grapevine (*Vitis vinifera*) repression of *VvWUS* and *VvAG* by *VvSUP-like* is reported and derepression was found to favor multicarpellate berries [278].

While in the *A. thaliana* gynoecium HEC1 and **SPT** together influence auxin distribution via direct regulation of its transport by PIN3 and PIN1, Schuster *et al.* demonstrated that this mechanism is irrelevant for SAM maintenance [155]. Instead, these proteins function in the SAM as complex with MP, HEC2, and the chromatin remodeler BRM to modulate auxin signalling and activate *WUS* non-cell autonomously via CK signalling. CK was identified to activate *WUS* expression in the SAM via the CK receptors ARABIDOPSIS HISTIDINE

KINASE2 (AHK2) and AHK4 and the B-type ARRs ARR1 and ARR2 [146, 227]. WUS directly represses the transcription of *HEC1*, as well as several A-type ARR genes [65, 154, 155, 279]. The A-type ARRs then negatively regulate CK signalling and thus shoot development [280, 281]. In this way HEC1 controls cell fate transitions in the SAM correspondence to environmental stimuli conveyed by phytohormones [279].

In peach (*Prunus persica*) and several Solanaceae species, ***SPT*** orthologues were shown to be involved in lignification of fruit tissues, as well as anthocyanin accumulation in the leaves of some examined Solanaceae species [282, 283]. The latter is especially interesting, as anthocyanins and lignin are derived from the same phenylpropanid pathway precursors [284].

In *A. thaliana*, YABBY TFs are primarily involved in abaxial fate determination of asymmetrical above-ground lateral organs [33, 199]. They are expressed in a polar manner in these organs, but *CRC* and *INO* are restricted to carpel tissues and nectaries or outer integuments, respectively [50, 199]. In addition to the phenotype described above, ***crc*** **mutants** do not initiate nectaries [50]. By redundantly controlling the expression of ***CRC***, the MADS-box genes *AG*, *SHP1*, and *SPH2* were found to be necessary for nectary development. In petunia an analogous regulation was discovered [285]. The shift in gynoecia dimensions observed in ***crc*** **mutants** is due to changed cell numbers and sizes [51]. The involvement of **CRC** orthologues in flower meristem termination and vascular development was shown in other species than *A. thaliana*, as well [285–289]. Interestingly, double knock-out flowers of both tomato ***CRC*** paralogues showed a loss of carpel identity in addition to FM determination and these genes were found to regulate the tomato *WUS* homologue via chromatin remodelling [289]. Non-cell-autonomous modes of action for ***CRC*** were identified in *E. californica*, pea (*Pisum sativum*), and rice [288, 290, 291].

FIL and *YAB3* expression can first be observed throughout the anlagen of lateral organs, but becomes restricted to the abaxial regions in primordia, developing leaves, and floral organs [33]. They are redundantly essential for polar development of these organs. While *yab3* mutants show no phenotype [33, 218], *fil* loss-of-function mutants develop early flowers with a multitude of defects ranging from homeotic conversions to changed organ numbers, longer pedicels, and often lacked tertiary meristems in the axils of cauline leaves [197, 198], while no vegetative phenotype is seen. In the *fil yab3* double mutant linear leaves with reduced abaxial characteristics and vasculature were observed, as well as ectopic meristem formation on adaxial leaf and cotyledon surfaces [33, 218], while ectopic *FIL* or *YAB3* expression is sufficient for induction of ectopic abaxial tissues [33]. Together these observations suggest an involvement of *FIL* and *YAB3* in abaxial tissue specification and meristem patterning in partial redundancy among each other and possibly further YABBY genes [33, 34, 197–199]. In *A. thaliana* leaves, FIL and YAB3 were found to repress KNOX I gene expression [70].

In *A. majus GRAM* and its paralogue *PROLONGATA* (*PROL*) are expressed in the abaxial

domains of lateral organs an promote abaxial cell fate, analogous to the *A. thaliana* YABBYs *FIL* and *YAB3* [292]. In monocots the situation is more complicated, because YABBY expression domains and functions are more variable [287, 291, 293–295].

The AGO family genes are involved in small RNA-mediated regulation of gene expression. The founding member *AGO1* codes for a protein binding miRNAs and some siRNAs and is involved in degradation of complementary RNAs by the RNA-induced silencing complex (RISC) [296–298]. AGO1 mutants show a number of phenotypes among them polarity defects, reminiscent of *PHB* and *PHAVOLUTA* (*PHV*) overexpression, and defective post-transcriptional gene silencing (PTGS) [299– 301].

In *A. thaliana* the five HD-ZIP III TFs PHB, PHV, REV, CNA, and ATHB8 are involved in adaxial differentiation of lateral organs, including floral organs, the establishment and maintenance of meristems and polarity in embryogenesis, as well as vasculature patterning [32, 43]. They are known to act in an antagonistic way with the KAN proteins in leaf and vasculature polarity and were found to be necessary for xylem development, differentiation, and connection, thus canalizing auxin flow in vasculature development [166, 167, 247]. Radial filamentous structures, consuming the meristems, are produced instead of shoots or flowers in seedlings or young FMs, respectively, in *phb phv rev* triple mutants or HD-ZIP III quintuple mutants [43]. Though PHB regulates CK responses in the root meristem by direct activation of the CK biosynthetic enzyme *IPT7* and via A-, and B-type ARRs, root development is not affected in *phb phv rev* triple mutants [168, 170, 302]. Furthermore, PHB, PHV, and REV, were shown to strongly interact with B-type ARRs 1, 2, 10, and 12, promoting *WUS* expression in *A. thaliana* calli [303]. Müller *et al.* found PHB to activate *MP*, as well as the MP repressors *IAA20* and *IAA30*, in an auxin-dependent manner. In this way the auxin response within the developing xylem axis is focussed and stabilized [171]. The complex transcriptional regulation of genes targeted by REV and KAN1 shows a significant overlap in establishment of polarity and meristem organization by antogonistic regulation [239, 304].

The *E. californica* PHX protein is the common orthologue to AtPHB and AtPHV. The HD-ZIP III genes of *Zinnia elegans* are involved in BR signalling during xylem development [305, 306]. Class III HD-ZIP genes from different monocot and dicot species show functional conservation [251, 305–311], which raises the question if comparable roles, via hormonal regulation, in general meristem regulation and carpel polar development are conserved in *E. californica* HD-ZIP III orthologues, such as EcPHX, as well.

In addition to apical gynoecium development, SHI family proteins act as homo- and heterodimers and synergistically with **SPT** and **CRC** in tissue proliferation [41]. SHI family multiple mutants show leaf development defects comparable to *sty2 lug* double mutants [41].

Similar to *A. thaliana*, mutations in the oat (*Hordeum vulgare*) SHI family gene *short awn2* result in style and stigma defects [312]. A study by Min *et al.* found *STY* orthologues to be involved, not only in style development, but as well in the formation of nectaries on the petal spur in *A. coerulea*, *Delphinium exaltatum*, and *Epimedium grandiflorum* [313]. In the moss *Physcomitrella patens*, the inactivation of one or both SHI genes causes reduced auxin levels and phenotypes in the reproduc- tive organs [148, 314], showing the involvement of SHI family TFs in auxin synthesis to be ancient.

Apart from apical gynoecium development, the **NGATHA** proteins function in fruit development via positive regulation of *SHP1* expression and in the development of aerial lateral organs, by regulating cell proliferation, leaf morphology, flowering time regulation, SAM maintenance [37, 40, 42–45].

Corresponding to defects in carpel, ovule, and pollen development, narrower lateral organs, and defects in vascular patterning, *LUG* expression was detected in all tissues, especially stamens and carpels [10, 58, 61, 62]. Similarily to the LUG/LUH-SEU/SLK-YAB physical interactions described above (section 1.4.4), the *Antirrhinum majus* LUG orthologue AmSTYLOSA (AmSTY) interacts with several AmYABBY proteins in yeast, among them the *FIL*/*YAB3* orthologue AmGRAMINIFOLIA (AmGRAM). *Amgram* and *Amsty* single mutant defects in organ polarity, phyllotaxis, and floral homeotic functions are strongly enhanced in the double mutants, and thought to result from repression of adaxial cell fates [315]. A direct regulation of the chromatin remodelling SWI/SNF complex by a LUG-AN3 or LUH-AN3 dimer in lateral organ blade development was reported in *A. thaliana*. Analogous interctions were also observed in *M. truncatula*, *N. sylvestris*, and maize [61, 316].

NTT has a broad native expression pattern in the leaf vasculature, petiole, shoot apex, root tip, and replum, and *KAWAK* (*KWK*), a direct target of NTT and STK, is required in fruit development [81, 83]. Furthermore, numerous interaction partners of NTT are known, among others are the MADS-box TFs AG, FUL, GORDITA (GOA), **SEP3**, SHP1, SHP2; the homeobox TFs BEL1, KNAT2, PNF, RPL, STM; **NGA1**, **NGA2**, FIL, JAG, several ARFs, HEC2, and NTT itself [81, 317]. Together with the general lack in growth of *NTT* overexpression lines, this implies a multitude of functions in plant development for NTT.

In pea and cucumber (*Cucumis sativus*) the *WAG1* orthologues, respectively *PsPK3* and *CsPK3*, were found to be light-regulated, the latter is as well regulated by exogenous IAA and GA [318, 319].

In *Vigna radiata* a *yuc* mutant is essential for the development of chasmogamous (cross-

pollinated) instead of cleistogamous (self-pollinating) flowers [320].

B_{SISTER} genes are found in gymnosperm and angiosperm female reproductive tissues, but not in ferns [321]. In Brassicaceae, two clades of *B_{SISTER}* genes coexist, the *ABS* and *GOA* clades, while one of the two is usually lost outside the Brassicaceae and the *GOA*-like genes were later shown to get lost progressively in the Brassicaceae as well [322]. In *A. thaliana*, *ABS* and *GOA* neither share phenotype, expression pattern, nor interaction partners [128, 323, 324].

b_{sister} mutants of petunia, *Brassica napus*, and rice show conserved function in ovule and embryo development, with additionally an early flowering phenotype in rice and changed fatty acid profiles in *B. napus* [325–328]. Ectopic expression of the wheat *B_{SISTER}* orthologue interferes with normal ovule development [329]. The *ABS* gene is essential for establishing endothelium identity in the ovule [330]. In *abs* mutants the endothelium cell layer shows aberrant cell morphology and a lack of seedcoat pigmentation by proanthocyanidins [331]. Studies by Ehlers *et al.* furthermore identified roles of *ABS* in coordination of cell divisions in the endothelium, endosperm proliferation, and mucilage release from the seed coat [184]. *STK* functions in seed abscission and funiculus development and, together with *ABS*, in endothelium development and cell cycle regulation of the embryo [186, 330, 332, 333]. Studies by Mizzotti *et al.* demonstrated, that STK is, possibly together with ABS, involved in seed coat pigmentation by regulating the chromatin state of the anthocyanin reductase enzyme BANYLUS (BAN) [332]. The STK function on seed abscission is mediated by direct repression of *HEC3*, causing reduced lignin deposition in the abscission zone [334]. The *abs stk* mutant shows additional defects in ovule development, fertilization and subsequent seed maturation [330].

In petunia, mutation of both D-function paralogues, *FBP7* and *FBP11*, shows similar phenotypes as the *A. thaliana stk shp1 shp2* triple mutant [186]. The induction of ovules by ectopic *STK* expression is furthermore known in alloplasmic bread wheat lines (*Triticum aestivum*) [329].

The specification of stamen identity by B- and C-class MADS-box TFs is conserved between several angiosperm species, while for petal identity an A-class gene in addition to the B-class genes is only required in some species [7, 174, 303, 335–338]. Similar to *AtAG*, the *Thalictrum thalicroides AG* orthologue conveys different functions in flower development at different developmental stages [339]. In *A. majus* on the other hand, the two C-function genes *PLENA* (*PLE*) and *FARINELLI* (*FAR*) redundantly repress B-function in the fourth whorl. Other *AtAG* functions are divided between them: *AmPLE* is orthologous to the *AtSHP* genes and functions in FM termination, while *AmFAR* is orthologous to *AtAG* and regulates stamen maturation [340]. The petunia genes *PMADS3* and *FBP6* again divide functions differently: the *AtAG* orthologue *PMADS3* mainly regulates stamen develop-ment and FM identity, while the *AmPLE* orthologue *FBP6* is involved in style and stigma develop-ment, and both genes redundantly

regulate carpel development and FM determinacy [341, 342]. FM determinacy in petunia is additionally regulated by the D-class genes *FBP7* and *FBP11*, giving an example of the functional evolution of MADS-box genes [342].

The *A. majus* genes *DEFICIENS* (*DEF*) and *GLOBOSA* (*GLO*) are orthologues of *AP3* and *PI*, respectively, and show conserved B-class function [114]. The B-function is conserved in monocots, as can be seen from mutations in *SILKY* of maize and *SUPERWOMAN* of rice [286, 343]. For the *E. californica GLO/PI* orthologue, *EcSEI*, expression pattern and mutant phenotype are typical of B-function, while *EcDEF1* is additionally expressed in carpels [344–346]. Contrary to

A. thaliana, no dimers between SEP3 and B-function protein exist in *E. californica* and *EcAG2* is positively regulated by *EcSEI* [346]. *EcDEF2* and *EcSEI* are in turn repressed by the two *EcAG* genes [345]. No data on *EcDEF3* is published. Similar to the expression of *EcDEF1* in carpels, the *GLO* orthologue *DOLL1* of *Physalis floridiana* is involved in carpel development via regulation of *Pf**CRC*** [347]. Recently, in *Phaleonopsis* orchids an involvement of different complexes of *AGL6* and B-class gene paralogues in more specialized roles in pigmentation, perianth senescence, and pedicel abscission via lignin synthesis was identified, aside of the known perianth identity specification [348]. Furthermore, a similar connection of B-function gene expression and flower senescence in *A. thaliana* and lily was detected [348]. Another function of the B-class genes outside *A. thaliana* is the regulation of fruit development in apple, as loss-of-function of the *Malus* × *domestica PI* orthologue was shown to cause parthenocarpic fruit development in several cultivars [349]. While the functional conservation of B-class MADS-box TFs appears quite high, their ability for protein-protein interactions vary between species: In *A. thaliana*, as in most core eudicot and monocot species, heterodimerization between AP3 and PI are the major form of interaction and no homodimerizations are known. Additionally, in *A. thaliana* interactions with At**SEP3**, AtAP1, and AtAG are reported [104, 350]. Oppositely, from several basal angiosperm and basal eudicot species strict homodimerization, as well as dimer formation between all B-class orthologues and intermediate dimer preferences are known [336, 346, 350, 351].

The *E. californica FUL* genes, orthologous to the *A. thaliana* A-class gene *AP1*, were characterized by Pabon-Mora *et al.* [174]. They were found to have a similar expression patterns, except for late petal development. The common knock-down phenotype affected FM and sepal identity as well as fruit development, combining functions of both *A. thaliana* A-class genes, while additionally being involved in axial meristem outgrowth.

Interactions of **SEP** homologues with AG and STK homologues, similar to *A. thaliana*, were identified in *T. thalictroides*, petunia, and rice and between proteins of both latter species. In *Alpinia hainanensis*, several combinations of **SEP3**, **SEP4**, FUL and AGL6-like proteins were found to dimerize [352]. This shows once more the high conservation of MADS-MADS interactions in angiosperms [339, 341, 352–354]. In tomato, additional roles of **SEP**

orthologous proteins in pedicel abscission and fruit ripening were observed [355, 356]. The evolutionary oldest reports of **SEP**-like proteins stem from *Pinus radiata* developing cones, showing the long history of **SEP** proteins in reproductive development [357]. In petunia, rice, maize, and orchids some aspects of the E-function were found to be redundantly conveyed by members of the *AGL6* genes [348, 358–361]. In gymnosperms and core eudicots the *AGL6* subfamily divides in two major clades, approximately dividing in vegetative and reproductive functions. *AtAGL6* was reported to function mainly in the timing of flowering and leaf movement, and only to a small extend in floral organ identity, but showing a similar pattern of interaction partners as AP1, while its close relative *AtAGL13* has **SEP2**-like roles [323, 362].

1.5 Methods for studying protein interaction and gene function in non-model species

1.5.1 VIGS

Virus-Induced Gene Silencing (VIGS) is a widely used method for generating transient gene knock downs [367, 368], where stable transformations are not feasible and no mutant collections are available. Other possibilities for this method are the study of post-embryonic mutant phenotypes of embryonically lethal mutants or the simultaneous knock down of several genes sharing a highly conserved domain.

VIGS utilizes an antiviral defence mechanism found in eukaryotes [300] to downregulate expression of the targeted gene(s). For this, a fraction of, or the complete coding sequence of the target gene(s) is intergrated into the modified VIGS vector virus genome, then the plants are infected with the resulting VIGS vector. During virus replication, a double stranded RNA intermediate is produced. Double-stranded RNA, typical for replicating viruses or small RNA precursors, is detected and cleaved by the plants DICER-like (DCL) endonucleases into fragments of 21-24 nt length with a 3’ overhang of 2 nt. The resulting short double-stranded RNAs are bound by AGO proteins. The coding ‘guiding strand’ is integrated into the RISC while the non-coding ‘passender strand’ is degraded. This complex then targets mRNAs complementary to the short fragment for degradation [296, 369], a phenomenon similar to co-suppression [370]. A comprehensive review on the molecular mechanism of VIGS was recently published by Rössner *et al.* [430].

Earlier publications using this system show its potential for high knock-down efficiency and for specifically knocking down one of two close paralogues [345, 371]. A potential draw-back of this method is the unpredictable partial silencing described by Wege *et al.* potentially masking subtle phenotypes or completely impairing knock-down phenotypes of non-cell-autonomous targets [371].

1.5.2 PPI

Protein-Protein Interactions (PPI) are a central part of life. Most cellular processes depend on protein complexes, be it metabolic pathways, signal transduction or transcription of genes. The ability of single proteins for interaction is thereby central to their functionality and versatility as part of different complexes for different cellular conditions.

Y2H

In this work the Yeast Two-Hybrid System was used to detect PPI. The genes of interest (GOIs) were expressed as fusion constructs with the GAL4 activation or binding domain (AD/BD) in yeast strains of a or α mating type, respectively. By mating of the transformed yeast strains, desired pairs of GOIs were combined and upon interaction of the fusion proteins, activation of HIS3 (growth on histidine deficient medium) and activity of lacZ (blue-white selection) were observed as reporters. The yeast system is suited for high numbers of simultaneous tests but has some minor drawbacks especially for the test of transcription factors as GOIs. As TFs often code for activation as well as binding domains of their own, these might interfere with the assay, activating transcription of the reporter genes even in the absence of an interaction partner. Additionally, HIS3 is known to show a weak background transcription, both effects giving the possibility for false positive results. False negative results can be caused by the artificial yeast system, possibly lacking plant-specific factors, like phytohormones [124], the elevated ambient temperature optimal for yeast cultivation compared to normal plant growth temperatures [354], or post-translational modifications [374], that facilitate dimerization *in planta*.

BiFC

The BiFC PPI assay is based on reconstituting a fluorescent YELLOW FLUORESCENT PROTEIN (YFP) in plant cells from two non-fluorescent halves, each fused to one protein of interest. Upon interaction between the tested proteins, both halves are brought in close proximity, allowing reconstitution of the fluorescence [377]. This allows easy assaying of interactions and the localization thereof. The time point of fluorescence determination is of interest for background determination and when comparing experiments, because usually the reconstitution is irreversible, leading to an increase of fluorescence over time and fixing unspecific or dynamic interactions [378]. False negative results may still arise when additional factors are needed for the interaction, but far less than in yeast-based assays. Furthermore, visualization of conformational changes in a maltose binding protein by Jeong *et al.* [379] highlights the influence of the orientation and positioning of the non-fluorescent fragments in the interacting dimer on resulting fluorescence. If they are too far apart or sterically hinder dimerization, no fluorescence might be detected. To diminish these latter problems, it is advisable to test several orientations of tag and gene of both fragments.

1.6 Aim of this work

In the course to unravel the evolutionary basis of carpel development, this thesis aims at exploring the grade of conservation in gene functionality and gene networks, regulating the development of carpels in different species, by integrating new experimental data from *E. californica* with published data from other species. Thus getting one step closer to finding the lowest common denominator - the basic set of factors that need to be present for carpel development across all flowering plants.

This is meant to be archieved by combining phylogenetic research, knock-down phenotypes, and protein-protein interaction data, generated in *E. californica* and comparing them with published data from *A. thaliana* and other species. The genes of interest were selected based on published functions in *A. thaliana*, followed by literature research and phylogenetic calculations, to identify the respective orthologous genes in *E. californica*. For knock-down phenotypes, VIGS experiments were conducted in *E. californica*, and interactions between *E. californica* proteins were studied in yeast- and tobacco-based systems. From the gained knowledge, a model for the evolution of a specific genetic network, in contrast of vast morphological changes, is meant to be deduced. This may be expanded to a more broad estimation for other comparable networks.

As mentioned before, fruit and seeds in their immense variability are indispensable from human diet. So the understanding of their development is not only an invigorating experience, but a sound scientific basis for further shaping of agronomic traits.

2 Materials and Methods

2.1 Materials

Chemicals and reagents were purchased from Carl Roth GmbH + Co. KG (Karlsruhe, Germany) if not stated otherwise.

2.1.1 Media, Solutions, Buffers

Agar-Agar, Kobe I (15 g/l) was added before autoclaving for preparation of solid media.

Apoplast buffer for BiFC

2 mM KCl
1 mM $CaCl_2$
1 mM $MgCl_2$ (SERVA Electrophoresis GmbH, Heidelberg, Germany) hereafter (SERVA)
50 mM Mannitol
25 mM MES pH 5.7 (Sigma)

Injection buffer for VIGS

10 mM $MgCl_2$ (SERVA)
100 µM MES (Sigma)
10 mM Acetosyringone (A. Aldrich)

LB Medium

20 g/l LB Medium - Powder according to Lennox (A6666, AppliChem GmbH, Darmstadt, Germany)
autoclave

or

10 g/l Tryptone or Peptone
5 g/l Yeast extract
5 g/l NaCl autoclave

10x LiAc

1 M LiAc
adjust pH to 7.5 with diluted Acetic Acid
autoclave

P1

100 µg/ml RNAse A (DNAse free) (Roche Diagnostics Deutschland GmbH,

Mannheim, Germany) hereafter (Roche)
50 mM Tris-HCl (pH 8.0)
10 mM EDTA

P2

0.2 M NaOH
1 % SDS

P3

60 ml 5 M KAc
11.5 ml Acetic Acid
deionized H_2O ad 100 ml

PEG/LiAc

8 ml sterile filtered 50 % PEG 3350 or 4000 in deionized water
1 ml 10x TE
1 ml 10x LiAc

Potassium Phosphate buffer 1 M pH 7.0

61.5 ml 1 M K_2HPO_4
38.5 ml 1 M KH_2PO_4

SD Medium

8.01 g Minimal SD Base (TaKaRa Bio Europe)
192 mg DO supplements -Leu(L)/-Trp(W) or –Ade(A)/–His(H)/–Leu/–Trp (Takara Bio Europe)
as necessary: 30 mg Leucine, Tryptophan, Adenine hemisulfate
deionized H_2O ad 250 ml
adjust pH to 5.8
deionized H_2O ad 300 ml
autoclave

SOC Medium

20 g/l Tryptone or Peptone 5 g/l Yeast extract
10 mM NaCl
10 mM $MgCl_2$
10 mM $MgSO_4$
2.5 mM KCl
20 mM Glucose
adjust pH to 7.0 with NaOH

Staining solution for BiFC

50 ml Apoplast buffer for BiFC
50 µl 1 g/l DAPI in H_2O
2-3 drops Silwet L-77

Staining solution for LacZ assay

8.5 g/l low-melting Agarose (Biozym Scientific GmbH, Hessisch Oldendorf, Germany) hereafter (Biozym)
0.1 M Potassium Phosphate buffer pH 7
1 g/l X-gal

10x TE buffer

0.1 M Tris
10 mM EDTA
adjust pH to 7.5 with HCl
autoclave

1x TAE buffer

40 mM Tris
0.1142 % (v/v) Acetic Acid
1 mM EDTA

YPAD Medium

20 g Tryptone or Peptone 10 g Yeast extract
100 mg Adenine hemisulfate
deionized H_2O ad 900 ml
autoclave
add 100 ml sterile filtered 20 % (w/v) Glucose in deionized H_2O

2x YT Medium

16 g/l Tryptone or Peptone 10 g/l Yeast extract
5 g/l NaCl adjust pH to 7
autoclave

2.1.2 Primers

Primers were designed using PerlPrimer v1.1.21 [363] or BioEdit v7.0.5.3 [364] and ordered at Eurofins Genomics (Ebersberg, Germany).

2.2 Methods

2.2.1 Plant material and culture

After stratification for 3 days at 4 °C in water *Eschscholzia californica* 'Aurantiaca Orange King' seeds (B & T World Seeds, Aigues Vives, France) were sown in a mixture of Einheitserde® Classic and Einheitserde® Spezial Profisubstrat (both: Einheitserde und Humuswerke, Gebr. Patzer GmbH & Co. KG, Sinntal-Altengronau, Germany) by D. Haffer and grown in 9,5 x 9 x 9 cm^3 pots (1 plant per pot). Different lighting and temperature regimes were used in long day conditions (16 h/8 h light/dark cycle): under LED growth lights (NS1-Series, Valoya Oy, Helsinki, Finland) providing 40-170 µmol/m^2s at constant 22 °C, in a growth cabinet (Percival Scientific Inc., Perry, USA) at 21 °C during day (60-220 µmol/m2s light intensity) and 16 °C during night, or in a Fitotron® CGR growth chamber (Weiss Umwelttechnik GmbH, Reiskirchen, Germany) equipped with mercury lamps (270-895 µmol/m^2s light intensity), at 60 % relative humidity and 21 °C during day and 16 °C during night. Plants were watered as needed and fertilized (WUXAL, Hauert MANNA Düngerwerke GmbH, Nürnberg, Germany) every four weeks. If necessary, the plants were sprayed with Score (Syngenta Agro GmbH, Maintal, Germany), as freshly prepared 0.1 % dilution, against powdery mildew or treated with *Steinernema feltiae* against fungus gnats and *Chrysoperla carnea* against thrips (both SAUTTER & STEPPER GmbH, Ammerbuch, Germany).

For BiFC assays *Nicotiana benthamiana* were grown from seed stocks maintained at the research group. The plants were grown on a mixture of Einheitserde® Classic and perlite (PERLIGRAN® Premium Knauf Performance Materials GmbH, Dortmund, Germany) in the greenhouse under long day conditions. Plants were treated preventively with *Steinernema feltiae* against fungus gnats every few weeks.

2.2.2 Cloning of constructs

All constructs used in this work were cloned by A. Weisert, using the primers given in the .fasta file of the respective gene in the electronic supplementals, or were already present in glycerol stocks. For a complete table of all constructs see supplemental table 13.

Further reagents and microorganisms used in cloning were: Restriction enzymes and Antarctic Phosphatase (New England Biolabs GmbH, Frankfurt am Main, Germany; hereafter (NEB)), DreamTaq and Phusion Polymerases, as well as T4 Ligase (Thermo Fisher Scientific Inc., Schw- erte, Germany) hereafter (Thermo Fisher Scientific), NucleoSpin™ Gel and PCR Clean-up Kit (Macherey-Nagel™, Düren, Germany) hereafter (Macherey-Nagel), Rifampicin (SERVA)

For downregulation of a target gene by VIGS, specific sequences of up to 450 bp of the gene's coding sequence were cloned into the multiple cloning site (MCS) of pTRV2 [365]. The resulting VIGS constructs were transformed into *A. tumefaciens* strain GV3101 [366] for transient plant transformation.

To test protein-protein interaction between *E. californica* proteins in yeast two hybrid assays their coding sequence was cloned in the MCS of the pGADT7 and pGBKT7 plasmids (Clontech Laboratories Inc., TaKaRa Bio) hereafter (Clonetech).

To test for interactions between chosen proteins *in planta* their coding sequences where amplified from cDNA with specific primers (included in the .fasta file of each gene in the electronic supplementals) and inserted in the MCS behind the C- or N-terminal half of YFP (tag) in pNBV. The complete fusion cassette of tag-cds was then cloned into pMLBART. The resulting BiFC constructs were transformed into *A. tumefaciens* GV3101 [366] for transient plant transformation.

2.2.3 Transformation of chemocompetent bacteria

After thawing 100 µl aliquots of chemocompetent cells on ice, 10 ng of purified plasmid DNA were added and mixed with the bacteria by tipping the tube. The mixture was incubated on ice for 15-30 min before a heat shock of 45 secs at 42 °C was given. Subsequently, the cells were directly cooled on ice for 2 min before 1 ml of pre-warmed SOC media was added. After incubation for 1 h at 28 °C (*A. tumefaciens*) or 37 °C (*E. coli*) and 180 rpm the cells were spun down and the pellet resuspended in 100 µl LB. 10 µl of the suspension diluted with 90 µl or the remaining 90 µl cell suspension were plated on LB plates containing antibiotics as necessary and incubated at 28 °C for two days (*A. tumefaciens*) or 37 °C for one day (*E. coli*).

2.2.4 Transformation of electrocompetent bacteria

While thawing 50 µl aliquots of electrocompetent cells on ice, clean electroporation cuvettes (Eppendorf AG, Hamburg, Germany) hereafter (Eppendorf) were pre-chilled. To each aliquot 10 ng of purified plasmid DNA were added and mixed with the bacteria by tipping the tube. The mixture was transferred bubble-free to a cuvette and subjected to a pulse (up to 6 ms) of 2.5 kV in an Eporator® (Eppendorf). The cells were directly transferred to 1 ml pre-warmed SOC media and incubated for 1 h at 28 °C (*A. tumefaciens*) or 37 °C (*E. coli*) and 180 rpm. Subsequently, the cells were spun down and the pellet resuspended in 100 µl LB. 10 µl of the suspension diluted with 90 µl or the remaining 90 µl cell suspension were plated on LB plates containing antibiotics as necessary and incubated at 28 °C for two days (*A. tumefaciens*) or 37 °C for one day (*E. coli*).

2.2.5 Virus-Induced Gene Silencing

In this work TRV-derived VIGS constructs, based on Liu *et al.* [365] where used.

For the inoculation of *E. californica* seedlings (approximately 3 leaf stage) 4 ml cultures of *A. tumefaciens* GV3101 [366], containing the chosen VIGS-constructs, were prepared in liquid LB, containing kanamycin and gentamicin at a concentration of 50 ng/ml each. The cultures were incubated overnight at 28 °C with shaking (180 rpm). In addition to the cultures containing pTRV2 constructs with a gene of interest, one culture each of pTRV2 without insert and pTRV2 containing a part of the phytoene desaturase (PDS) cds [371] were prepared and per pTRV2 culture one culture of pTRV1 [365]. The next morning, fresh 40 ml liquid LB (50 ng/ml

kanamycin, 50 ng/ml gentamicin) cultures were inoculated with each one of the overnight cultures and incubated at 28 °C and shaking (180 rpm) until an OD_{600} of 0.6-0.8 was reached. The cultures were spun down (4000 rpm, 15 min, RT) and each resulting pellet resuspended in 20 ml inoculation buffer containing 10 µM acetosyringone. To allow a sufficient production of virulence factors for efficient transformation the bacteria were incubated in the acetosyringone-containing buffer at RT for 2 h.

After induction one culture of pTRV1 was mixed with every one culture of pTRV2 and injected with a syringe and 0.45 mm needle directly beneath the SAM of an *E. californica* seedling. The plants were then kept at 5 °C over night before being transferred to normal growing conditions on the next morning.

Figure 2.1: *Overview of the steps of a VIGS experiments. Adapted from [368].*

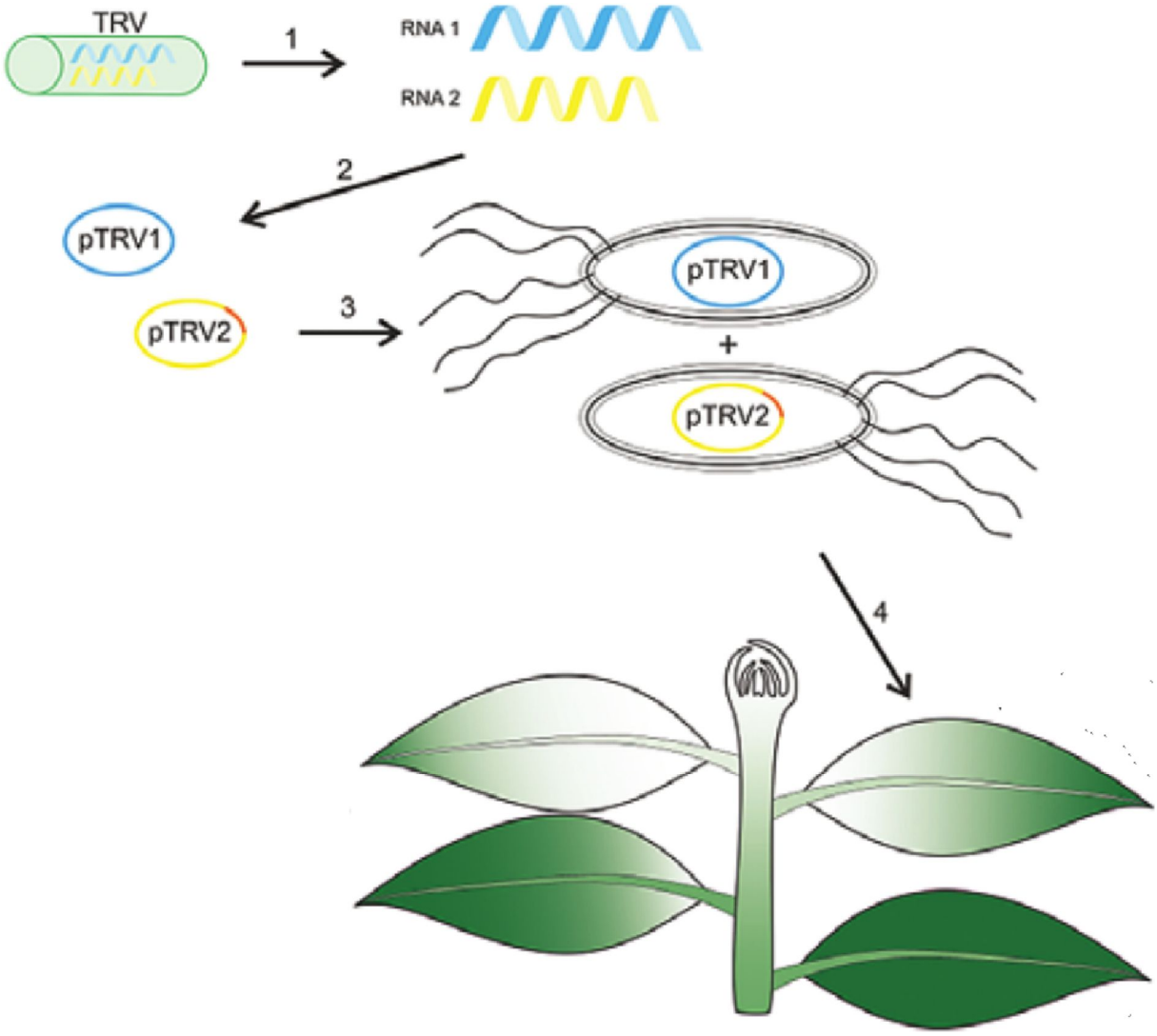

2.2.6 Phenotyping of E. californica VIGS flowers

For expression analysis by qRT-PCR the first bud of each plant was harvested into liquid nitrogen (Linde) at sizes of 2-6 mm diametre and stored at -80 °C. The following three flowers on each plant reaching anthesis, were phenotyped as described below, as frequency of phenotype declines in later flowers [371].

Petals were removed and photographed with a Canon PowerShot S5 IS (Canon Inc.) or COOLPIX B500 (Nikon Corporation) at a constant distance from the lens next to a ruler. The reproductive floral structures were documented separately at a Leica stereoscope (M165C, Leica Microsystems GmbH, Wetzlar, Germany) hereafter (Leica), equipped with a Leica DFC450 camera. When no phenotypes could be visuably identified, thirteen parameters, indicated in figure 3.17, were measured in the VIGS experiments V2 to V8, using ImageJ 1.52p (Wayne Rasband, `http://imagej.nih.gov/ij`) and compared between treatment and the control groups of the respective experiment by statistical means using GraphPad Prism5 (Graph- Pad Software, San Diego, California, USA). These data were supplemented by position of the flower on the plant, numbers of petals and stamens, and in one experiment floral shoot lengths. Because the positional data could not be correlated to phenotype incidence, they are not shown or discussed further.

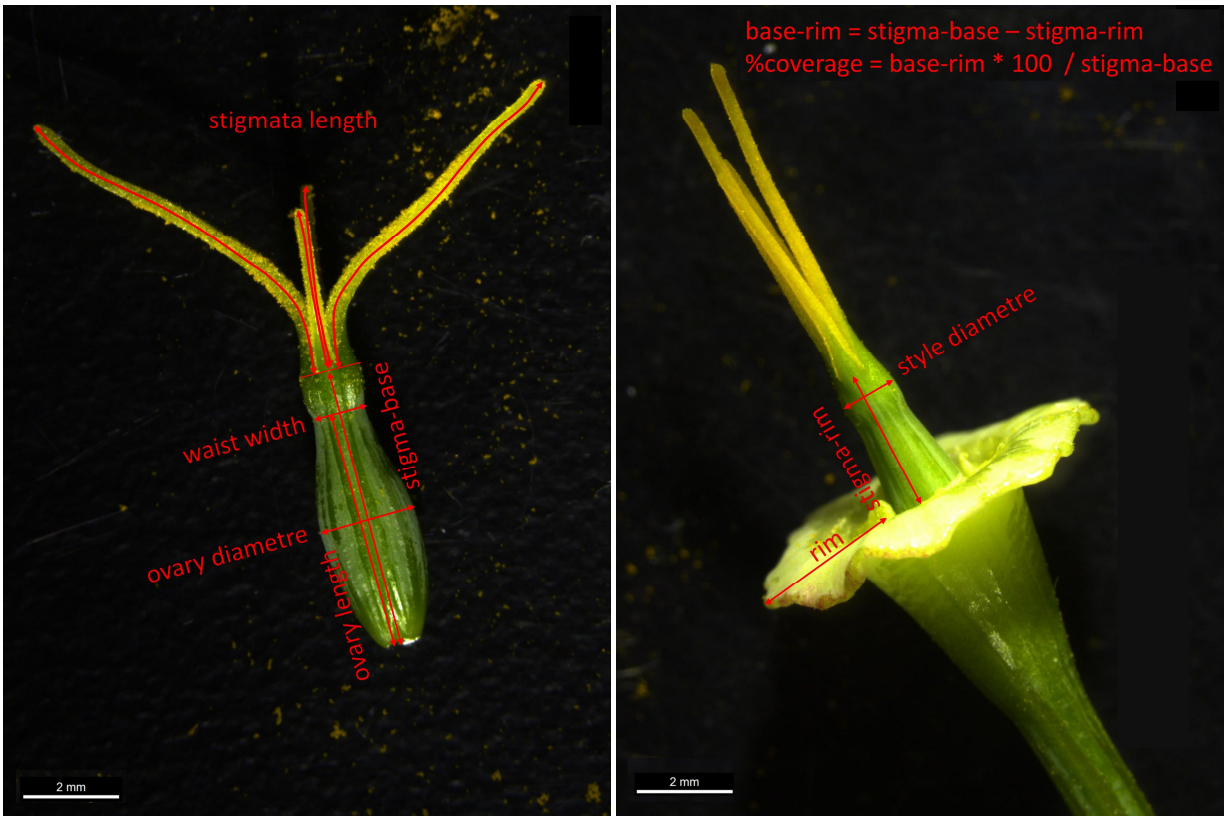

Figure 3.17: *Parameters measured in each flower for statistical phenotyping in the experiments V2 to V8. Additionally, the position on the plant, number of petals, and number of stamens were recorded.*

To confirm the observed VIGS phenotypes were caused by a down regulation of the targeted GOI, the respective expression levels were quantified by qPCRs performed with total RNA extracted from the first bud of selected plants. The respective plants were selected based on severity of the presumed VIGS phenotype or chosen at random where no phenotype was identified, usually 3 to 10 per treatment. In V8 only two plants showing a presumed phenotype were found in the *EcNGA1* VIGS plants, so only these two were used. The relative expression of the target genes compared to the expression of *EcGAPDH* as housekeeping gene was determined by the $2^{\Delta\Delta Ct}$ method [386].

2.2.7 RNA extraction

E. californica buds were ground to a fine powder with mortar and pestle in liquid nitrogen. RNA extraction was then performed using a NucleoSpin™ RNA Plant (Macherey-Nagel) kit according to the manufacturer's instructions. DEPC treated water was used for the elution step.

Concentration and quality of the resulting RNA was measured spectrophotometrically using a NanoDrop™ 2000c (Thermo Fisher Scientific)

2.2.8 Agarose gel electrophoresis

The quality of nucleic acids was checked by applying 0.5-1 µg of RNA or 5 µl of PCR product mixed with 1 µl 6x loading dye (NEB) on an 1 % agarose gel (LE Agarose, Biozym) supplemented with 0.002 % DNA stain G (SERVA). Alternatively, gels were stained after electrophoresis for 10 min with 1 drop EtBr per 100ml deionized H_2O and a washing step in deionized H_2O. As size standard a MassRuler DNA Ladder Mix (Thermo Fisher Scientific) as used and the electrophoresis was run at 7 V/cm in 1x TAE.

2.2.9 cDNA synthesis

First strand cDNA was prepared using RevertAid H Minus Reverse Transcriptase (Thermo Fisher Scientific) with random hexamer primers (for qRT-PCR) or oligo(dT) primers (for amplification of the complete cds) according to the manufacturer's instructions. As template 1 µg of DNase A treated RNA was used.

2.2.10 qPCR

Primers were designed using PerlPrimer v1.1.21 [363]. Care was taken to choose pimer pairs with similar melting temperatures not predicted to form dimers. Furthermore, repetetive or conserved regions in the target sequence were avoided, as well as regions chosen for the design of VIGS constructs. To reduce the chance of more than one amplificate potential primers were subjected to a BLASTN query versus the *E. californica* RNASeq databases of the Becker lab and a melting curve analysis after each use. The amplification efficiency of new primer pairs for qPCR was tested in a cDNA dilution series (1:10 to 1:10,000). Primer pairs with an amplification efficiency of approximately 2 were used for expression analyses.

The qRT-PCR was performed by A. Weisert using the Luna® Universal qPCR Master Mix (NEB) according to the manufacturer's instructions and detection by a LightCycler®480 II (Roche). One run comprised 60 s 95 °C followed by 45 cycles of 10 s 95 °C, 10 s 60 °C and 10 s 72 °C. One to four technical replicates were prepared per sample. For melting curve analysis, as well as primer efficiency test the LightCycler®480 (Roche) Software was used.

2.2.11 Plasmid isolation from bacteria

For high-throughput plasmid isolation the following protocol was used (for composition of the buffers see section 2.1.1):

Approximately 1.5 ml *E. coli* culture were spun down for 30 s at 13,000 x g at RT. The

supernatant was removed completely and the pellet resuspended in 200 µl buffer P1. The cells were lysed by adding 200 µl buffer P2 and gently inverting repeatedly. The proteins and remaining SDS were precipitated by 200 µl buffer P3 and 25 µl $CHCl_3$ were added for improved phase separation, before centrifugation for 10 min at 4 °C and at least 14,000 x g. The clear supernatant was transferred to a fresh tube and 400 µl isopropanol were added to precipitate the plasmid DNA. The precipitated DNA was pelleted by centrifugation (10 min, 4 °C, ≥14,000 x g). The supernatant was removed and the pellet washed with 500 µl 70 % (v/v) Ethanol. After centrifugation (5 min, 4 °C, ≥ 14,000 x g) the supernatant was completely removed and the pellet dried at 37 °C until getting clear. The dry pellet was then dissolved in 50 µl sterile, deionized H_2O.

For transformation of yeast or cloning, plasmids were isolated using a NucleoSpin™ Plasmid EasyPure (Macherey-Nagel) kit according to the manufacturer's instructions.

2.2.12 Protein-Protein Interaction Assays

Two PPI assays were utilized in this work to determine the dimerization abilities of target proteins.

Y2H

In this work the CLONETECH MATCHMAKER GAL4 Two-Hybrid System was used. The genes of interest (GOIs) were expressed as fusion constructs with the GAL4 activation or binding domain (AD/BD), respectively. pGADT7 constructs coding for the AD-GOI fusion were transformed into the yeast strain AH109 (a mating type, Clontech) and the pGBKT7 constructs coding for the BD-GOI fusion were transformed into the Y187 strain (α mating type, Clontech), as described in section 2.2.12 and tested for autoactivation as described below. By mating of the transformed yeast strains, desired pGADT7 and pGBKT7 pairs were combined. Upon interaction of the fusion proteins, the GAL4 activation and binding activities are recombined in the protein dimer and can activate the transcription of reporter genes present in the mated yeast. Here, growth on histidine deficient medium (SD-H) and activity of lacZ (blue-white selection) were observed as reporters.

Yeast transformation

For yeast transformation the respective strains were streaked out on YPAD plates four days before the transformation. After three days on plate, three cultures for each strain were started in 25 ml YPAD. Each culture was inoculated with one yeast colony and grown for 20 h at 28-30 °C and 200-215 rpm.

On the next day the most densely grown culture (OD_{600} at 1-1.5) of each strain was chosen to inoculate a fresh 300 ml YPAD culture with an OD_{600} of 0.2-0.3. The fresh culture was grown at 28-30 °C and 200-215 rpm until an OD_{600} of 0.4-0.6. Then the cells were spun down (1000 x g, 5 min, RT) in 6 50 ml falcon tubes and the resulting pellets resuspended in 6-7 ml sterile 1x TE. The resuspended cells were pooled in one tube and subsequently spun down again (1000 x g, 5 min, RT), before being resuspended in 0.5-1.5 ml 1x TE/1x LiAc (depending on the amount needed) and kept at RT. Carrier DNA 2 mg/ml was denatured by boiling for 5 min and immediately cooled on ice. For each transformation 1 µg of the respective plasmid DNA, 100

µg denatured carrier DNA, 600 µl PEG/LiAc, and 100 µl competent yeast cells were transferred to a fresh 1.5 ml tube, pre-chilled on ice. The transformation mix was mixed gently and incubated at 28-30 °C and 200-215 rpm for 0.5 h. Then 70 µl DMSO (SIGMA) were added and the tubes mixed by inverting, before the cells were subjected to a heat shock at 42 °C for 15 min with mixing every five minutes. Subsequently, the tubes were immediately chilled on ice for 1-2 min before being spun down for 5 sec and resuspended in 120 µl sterile 1x TE each. The transformants were plated on SD selection plates and grown at 28-30 °C for three days.

Test for autoactivation of BD-constructs

pGBKT7 plasmids (Clontech), containing the open reading frames of the genes of interest, were tested for autoactivation by spotting 5 µl of an overnight cultures of yeast strain Y187 (Clontech) containing the respective plasmids on different SD media: SD -W, SD -W/-A, SD -W/-H, SD -W/- H/+1 mM 3-AT, SD -W/-H/+5 mM 3-AT, SD -W/-H/+10 mM 3-AT and incubating for 3-5 days at 30 °C. Cultures growing on media containing 3-AT were not used for the Y2H experiments.

Yeast mating

Overnight cultures, containing the respective open reading frames in the pGADT7 or pGBKT7 plasmids, where prepared for yeast mating and 5 µl of those cultures where then spotted on full SD plates in the same spot, always combining one pGADT7 containing with one pGBKT7 containing culture. Mating on full SD was carried out over night at 30 °C (and a weekend at 4 °C), on the next day some of the resulting diploid yeast was transferred to double selection plates (SD -L/-W) and incubated at 30 °C for two days. On the second day a bit of each spot was transferred to 100 µl of sterile water with a sterile toothpick and 5 µl of the suspension was spotted on a fresh SD -L/-W plate. After another two days diploid yeast of each mating was resuspended in 100 µl of MQ and spotted on selection plates (SD -L/-W/-H/+1 mM 3-AT) and new SD -L/-W plates. After 7 more days at 20 °C yeast from each spot was transferred to two copies of fresh SD -L/-W/-H/+1 mM 3-AT plates into four adjacent spots. After three days at 20 °C one copy was used for LacZ assay and the second for a final check of plasmids.

LacZ assay

For the LacZ assay, yeast growing on SD -L/-W/-H/+1 mM 3-AT plates was made permeable by incubation for 10 min in chloroform vapour. For this the bottom of a glass Petri dish was covered with a few ml of $CHCl_3$ and the open SD selection plate was put upside down on top of the glass dish. To further increase permeability of the yeast cells the colonies on the plate were covered with droplets of $CHCl_3$, which were let evaporate two times, in a next step. During the $CHCl_3$ incubation, 10 ml staining solution was prepared (X-gal is not stable at 40 °C) and was spotted on the yeast colonies after the $CHCl_3$ was evaporated for the second time. After solidification of the staining solution the plates incubated were at 20 °C in the dark for 24 h. The intensity of the staining was documented before, after 1 h and 24 h after start of the incubation.

DNA isolation from yeast

To verify the interacting proteins, total DNA was extracted from each yeast spot positive for

both reporter gene activities as described by Hoffmann *et al.* [375] and transformed into *E. coli*. The electrocompetent *E. coli* strains DB3.1 and JM109 where tested, as well as chemocompetent strain DH5α [376]. Best results where achieved for transformations in electrocompetent DB3.1 with 1 µl of aqueous supernatant in 50 µl of competent cells. In some cases further purification of the DNA as described by Hoffmann *et al.* [375] and an increase to 10 µl of DNA extract per transformation was needed. The transformants were selected for presence of pGADT7 or pGBKT7 on LB plates containing ampicillin (SERVA) or kanamycin ( ), respectively, at a final concentration of 50 ng/ml. Overnight cultures of the transformants where prepared in liquid LB, plasmids were extracted as described in section 2.2.11 and sequenced from the T7 primer at Microsynth Seqlab GmbH (Göttingen, Germany).

BiFC

The BiFC PPI assay is based on reconstituting a fluorescent YELLOW FLUORESCENT PROTEIN (YFP) in plant cells from two non-fluorescent halves, each fused to one protein of interest.

For each BiFC test three 10 ml overnight cultures of *A. tumefaciens* GV3101 [366] were prepared in liquid LB or 2x YT at 28 °C and shaking at 180 rpm: one containing the p19 plasmid, and two containing the open reading frames of two genes of interest in pMLBART (one of the GOIs fused to the N-terminal (YN), the other to the C-terminal (YC) half of YFP). p19 cultures were supplemented with 50 ng/ml kanamycin, the GOI cultures with 50 ng/ml gentamicin and spectinomycin each. On the next day the cells of the overnight cultures were harvested and resuspended in 10 mM $MgCl_2$ containing 0.15 mg/ml acetosyringone to yield a final volume of 0.5 ml per test with an OD of 1.2 for the GOIs and 0.25 ml per test with an OD of 2.4 for p19.

For sufficient production of virulence factors by *A. tumefaciens*, enhancing the transformation efficiency, the bacteria suspensions described above were incubated 2 h at RT before a mixture of the 3 suspensions was injected with a needleless syringe into the abaxial surface of 3 leaves on 3 *N. benthamiana* plants.

On the third day after inoculation a strip was cut from each inoculated leaf close to the injection site and harvested into staining solution on ice. The sections were degassed by applying vacuum for 20 min on ice and then incubated for 30 min at RT in the dark. To check for fluorescence, the pieces were put with the abaxial side upwards into a drop of deionized water directly before examination and covered with a cover slip. The leaf cuttings were examined with a Leica microscope (DM5500 B, Leica), equipped with a camera (Leica DFC 450, Leica), and cuttings showing YFP fluorescence were documented each with a bright-field image showing the status of the cells, an image showing the DAPI fluorescence of the nuclei (A4 filter) and another image showing YFP fluorescence (L5 filter), where the proteins of interest interact physically. When no YFP fluorescence was seen, only one site per leaf piece was documented (complete results are shown in figures 3.29, 3.30, and suppl. fig. 9).

2.2.13 Orthologues search in *Eschscholzia californica*

To find *E. californica* homologues of relevant carpel developmental regulators known in *A. thaliana*, the protein sequences from *A. thaliana* were as a first step used in a BLASTP [380] search at the JGI Phytozome v12.1 plant genomics resource (https://phytozome.jgi.doe.gov/pz/portal.html). The five most similar (by E-value) sequences of each, *Aquilegia coerulea*, *Amborella trichopoda*, and *A. thaliana* were collected for further steps. Additionally, one isoform each of the five most similar proteins of *Papaver somniferum* based on a BLASTP search using the NCBI BLAST® tool (https://blast.ncbi.nlm.nih.gov/Blast.cgi) were added. The corresponding coding nucleotide sequences of all genes were collected as well.

The resulting collection of protein sequences was aligned using the MAFFT tool (https://www.ebi.ac.uk/Tools/msa/mafft/) using a tree building number and maxiterate of 100 and all other parameters on standard values. The resulting alignment was subjected to a Neighbour Joining phylogeny calculation using MEGA v7.0.26 [381] with standard settings and 500 bootstrap replications.

Based on this first phylogeny further BLASTN searches were performed using BioEdit v7.0.5.3 [364]: The coding sequences of the two most related protein sequences per species were used as query and the *E. californica* RNAseq data of the Becker lab as local databases. The resulting five most similar *E. californica* transcript sequences for each query from each database were collected. Sequences that were only found in one transcript dataset were marked, then duplicates were removed. The remaining sequences were used as queries for BLASTN searches against the Eschscholzia Genome Database (Kazusa DNA Research Institute, Chiba, Japan) [382]. Sequences that were present in at least two of these three independently assembled databases were seen as reliable and used for phylogenetic reconstruction (see supplemental table 7 for the complete list of identified orthologues).

Alignments containing transcript and genomic sequences and primer sequences, where applicable, for orthologues identified here or published before are attached as .fasta files in the electronic supplement.

2.2.14 Phylogeny reconstruction including *E. californica* coding sequences

For each *E. californica* gene of interest (GOI) a new phylogeny (maximum likelihood, 500 bootstraps, for complete analysis settings refer to the .txt files provided in the electronic supplemental) was calculated, including the translated cds of the reliable *E. californica* transcript and at least one outgroup sequence specified in the literature (see figure descriptions in sections 3.1 and 3.2), in addition to the collected protein sequences used in the first phylogeny (see section 2.2.13). As before MAFFT and MEGA were used. The resulting phylogenetic tree was improved by removing any sequences that were outside the "core phylogeny" consisting of the GOI and its close relatives and the chosen outgroup sequence and recalculating. The final figure was created using TreeGraph2 [383]. A complete list of all sequences used in the final

phylogenies is found in supplemental table 8.

2.2.15 Promoter analysis of *Eschscholzia californica* genes

For the promoter analysis of *E. californica* genes the online Plant Promoter Analysis Navigator v3.0 (PlantPAN; http://PlantPAN.itps.ncku.edu.tw [384]) was used. 5 kb of genomic sequence directly upstream of the identified transcription start site of the gene of interest was copied into the TFBS tool and the PlantPAN 3.0 database with all species was selected for the motif search, as optional promoter elements default values were used.

The resulting list of TF binding motifs was searched for entries of selected transcription factors by locus ID. A summary of all binding sites is given in supplemental table 12.

3 Results

3.1 VIGS experiments in *Eschscholzia californica*

VIGS experiments were conducted to test the functional conservation of *E. californica* genes, which are orthologous to known *A. thaliana* carpel developmental regulators.

To monitor the VIGS efficiency of each inoculation, one group of plants in each experiment was inoculated with a pTRV2-*EcPDS* construct as positive control [371]. Regardless of culture conditions, PDS knock down in each of the 7 to 15 *EcPDS* VIGS plants of each experiment was seen at 9-13 DPI. Phenotypic changes were in accordance to the literature [371].

In several experiments, regardless of the targeted genes, partial loss of floral organ identity, leading to sepal-leaf, sepal-petal, or petal-stamen mosaic organs, was observed. Even though some treatments showed a higher tendency for mosaic organs, the overall frequency was too low for evaluation as phenotype. These mosaic organs were observed only at a low frequency, shown in supplemental table 1. Where sepals assume partial leaf character, additional buds may form in axillar position inside the first whorl. Another fraction of buds throughout the experiments showed partly unfused sepals, but without obvious shift of identity (suppl. tab. 2). The buds with unfused sepals were often aborted, probably because a disturbed sepal cap leaves the developing bud vulnerable to humidity loss and pathogens.

3.1.1 VIGS effects in *E. californica* depend on growth conditions

For growing healthy plants, their required environmental conditions need to be taken into consideration. This is even more crucial when the plants are kept indoors, allowing no natural rhythm of changes in light, temperature or seasons. Working with flowers therefore requires consideration of the basic requirements of the respective species, for healthy growth and flower induction, like light and watering regime, temperature and humidity, and possibly vernalization.

In early VIGS experiments, *E. californica* was grown in the group's culture room on a bench equipped with Valoya NS1-LED growth lights (Valoya, Helsinki, Finland). The light regime provided 16 h of light (40-170 µmol/m^{2}s) and 8 h of darkness at a continuous temperature of 22 °C. In these conditions, the plants grew to a height of more than 40 cm on supports and were easily infected by fungi and thrips. The leaves had a fresh green colour and little wax covering.

The first buds in these conditions were collected 13 to 36 days after inoculation (DAI) and the experiments were stopped 50 to 116 days thereafter. On average, 40 % of the expected buds and flowers were harvested during these experiments. The low number of harvested buds and flowers was due to a high abortion rate of buds. After knock-down of different target genes in three independent experiments including the previously published *EcCRC* [288], no significantly different phenotype compared to the control plants treated with pTRV2 empty

could be detected. The untreated plants formed smaller and more diverse flowers compared to TRV-treated plants. Due the low number of fully developed flowers, the phenotyping results of these experiments V1 to V3 are not considered further. To establish an adequate plant quality with lower bud abortion rates and more uniform flowers, different growth conditions were tested.

Figure 3.1: *Comparison of a bench-grown plant (left) and a chamber-grown plant (right) of E. californica. The plants in the chamber grew more compact with darker leaves covered with wax, and were more resistant to fungal and insect pathogens. They produced bigger, more uniform flowers at a faster rate.*

A test of a growth cabinet (Percival Scientific Inc. Perry, USA) for VIGS experiments in *E. californica* was conducted with 16 h of light (60-220 µmol/m^{2}s) and 8 h of darkness, with a day temperature of 21 °C and a temperature drop to 16 °C during night. The plants started flowering 18 DAI and the experiment ended 85 DAI with 93 % of the expected buds and flowers harvested. Although these plants aborted less buds, they as well were easily infected and grew in a comparable habitus as in the earlier experiments. Ultimately, this lead to space problems during the harvest and watering inside the growth cabinet.

For the following experiments a Fitotron® CGR growth chamber (Weiss Umwelttechnik GmbH, Reiskirchen, Germany) equipped with mercury lamps was used at 16 h of light (270-895 µmol/m^{2}s) at 21 °C and 8 h of darkness at 16 °C and a constant humidity of 60 %. Here the plants showed little to no infections, dark green, waxy leaves and only needed support after the third flower opened, if any at all. Nonetheless, plants were fixed to supports to reduce entangling of the branches. The first flowers appeared approximately 19 DAI and after an average of 59 DAI the experiments ended with around 94 % of the expected buds and flowers harvested.

In conclusion, meeting the plants' requirements in growth conditions is crucial for comparable wild type phenotypes and for an effective knock-down of the target gene by VIGS. The plants in the growth chamber grew healthier, flowered earlier and aborted less buds than in the growth cabinet or on the bench of the culture room. While the conditions in the growth cabinet induced flowering earlier, the plant health and habitus were similar to the bench-grown plants. Together with the enclosed space hindering plant handling, this growing condition was found unsuitable. For growing healthy and productive *E. californica* a temperature drop during the night and a lighting of 300-800 µmol/m^{2}s is advisable. Below 300 µmol/m^{2}s the plants had lighter green colour and at 895 µmol/m^{2}s a high amount of anthocyanins was produced, probably due to light stress. An overview of the growing conditions of all experiments, containing information on flower formation, is given in table 3.1.

Table 3.1: *Overview of evaluated VIGS experiments. In each VIGS experiment, the first bud of each plant was harvested as a bud and the next 3 flowers opening were harvested at anthesis for documentation and phenotyping. % values consider dead and PDS VIGS plants are not required for harvest.* [2] *61 plants were removed before floral transition at 80 dpi.* [3] *preliminary experiment, flowers were only collected from control plants because no evident phenotype was oberserved in the knock-downs.*

experiment	growth conditions	# plants treated	first bud dpi	last flower dpi	% buds collected	% flowers analysed	# buds collected	# flowers analysed	# buds aborted
V1-V3	bench	383	∅ 25	∅ 101	∅ 40	∅ 40	143	437	538
V5[2]	growth cabinet	180	18	85	96	89	133	365	154
V4	growth chamber	123	17	63	99	99	109	326	5
V6a	growth chamber	85	22	55	97	94	52	148	8
V8a	growth chamber	90	17	72	100	100	79	237	8
V8b	growth chamber	90	17	65	99	97	69	204	2
total	growth chamber	613	∅19	∅ 59	∅ 95	∅ 98	388	938	24
total		1176					664	1740	717

3.1.2 Phenotypic changes induced by VIGS in *E. californica*

Table 3.2: *Overview of targeted genes in the evaluated VIGS experiments. The experiments V6 and V8 were split in two inoculation batches, for technical reasons, indicated by letters. Individual treatment groups are separated by a comma; co-inoculations are indicated by a '+'.*

experiment	target gene(s)
V4	*EcCRC, EcSPT1, EcCRC+EcSPT1*
V5	*EcSEP1, EcSEP3, EcSEP1+EcSEP3*
V6a	*EcSPT1, EcCRC+EcSPT1*
V8a	*EcNGA1, EcNGA2, EcNGA1+EcNGA2,*
V8b	*EcNGA, EcNGA+EcNGA1+EcNGA2, EcSPT1+EcSPT2*

In the experiments V3, V4, and V5, the construct published by Orashakova *et al.* knocking down the only *EcCRC* orthologue [130, 288], was used to monitor VIGS efficiency in flowers. *E. californica* with *EcCRC* knocked down shows several changes in the gynoecium, the most striking being a lack of determination of the floral meristem, leading to additional gynoecia formed within the fourth whorl. Other aspects of the *EcCRC* knock-down phenotype are a disturbed lignification of the ovary wall, omitting the ridge-like reinforcements and dehiscence

zone seen in wild type. A disturbed development of the carpel marginal tissues leads to a reduced or lacking initiation of placenta and ovules on the inside of the affected gynoecia, usually combined with a reduced ovary diameter.

In addition to these phenotypic changes described in [288], a green stripe along the outside of the fusion domain of the gynoecium and a change in the number of stigmatic protrusions was observed in this work. The green stripe is thought to be a disturbance of the wax depositions, which usually cover the gynoecium surface and are easily removed by touching the surface. Of the stigmatic protrusions, only the marginal stigmatic protrusions were affected by the change in numbers, with one or both being reduced to stumps or completely missing,or in other flowers two orderly spaced protrusions replacing one compared to the wild type as seen in figures 3.2 and 3.3.

V4+V6: SPT1+CRC VIGS

On the one hand, the knock down of *EcCRC* was used as a positive control to establish the right growing conditions for *E. californica* during VIGS experiments (section 3.1.1). On the other hand, the additional marginal stigmatic protrusions observed here might be a split style/stigma phenotype similar to what is observed in *A. thaliana* [49-51]. The *A. thaliana* phenotype is enhanced in *spt crc* mutants [49, 51].

To see, if the putative split style/stigma *EcCRC* phenotype can be enhancend in a comparable manner to *A. thaliana,* a co-inoculation of *EcCRC* and *EcSPT1* VIGS constructs was first tested in experiment V4 and further plants added by V6a.

By knock down of *EcSPT1* by VIGS treatment, the proportions of the gynoecium were changed statistically significant to a higher floral cup. Together with only a slight increase in ovary length (fig. 3.4), this resulted in a slightly higher coverage of the *EcSPT1* VIGS gynocia by the floral cup (supplemental fig. 1). In rare cases, the lower part of the stigmatic protrusions was buried in the floral cup as well. The ovary length, and thus total gynoecium length, was significantly increased in *EcCRC* VIGS-treated plants compared to pTRV2-empty treated plants, while the height of the floral cup only slightly increased (fig. 3.4). Compared to the *EcCRC+EcSPT1* double knock down, the height of the floral cup was unchanged in *EcSPT1* and *EcCRC* single VIGS plants, while ovary length and gynoecium length was significantly increased in *EcCRC* single VIGS. Together these changes lead to a significantly bigger part of the gynoecium above the rim in *EcCRC* compared to *EcSPT1+EcCRC* knock downs (fig. 3.4).

Due to the immensely reduced ovary diametre observed in *EcCRC* VIGS plants, the ovary-length-to-diameter and rim-diametre-to-ovary-diametre ratios are significantly higher in these plants than in pTRV2-empty treated plants (fig 3.5). Because of the significant increase in ovary length compared to pTRV2-empty and *EcSPT1+EcCRC* treated plants, the ovary-length-to-diameter ratio is as well significantly increased in these comparisons (fig 3.5).

Additionally, the stigmatic protrusions in marginal positions were significantly shorter in the VIGS treated than in pTRV2-empty control plants, leading to a significant increase in length

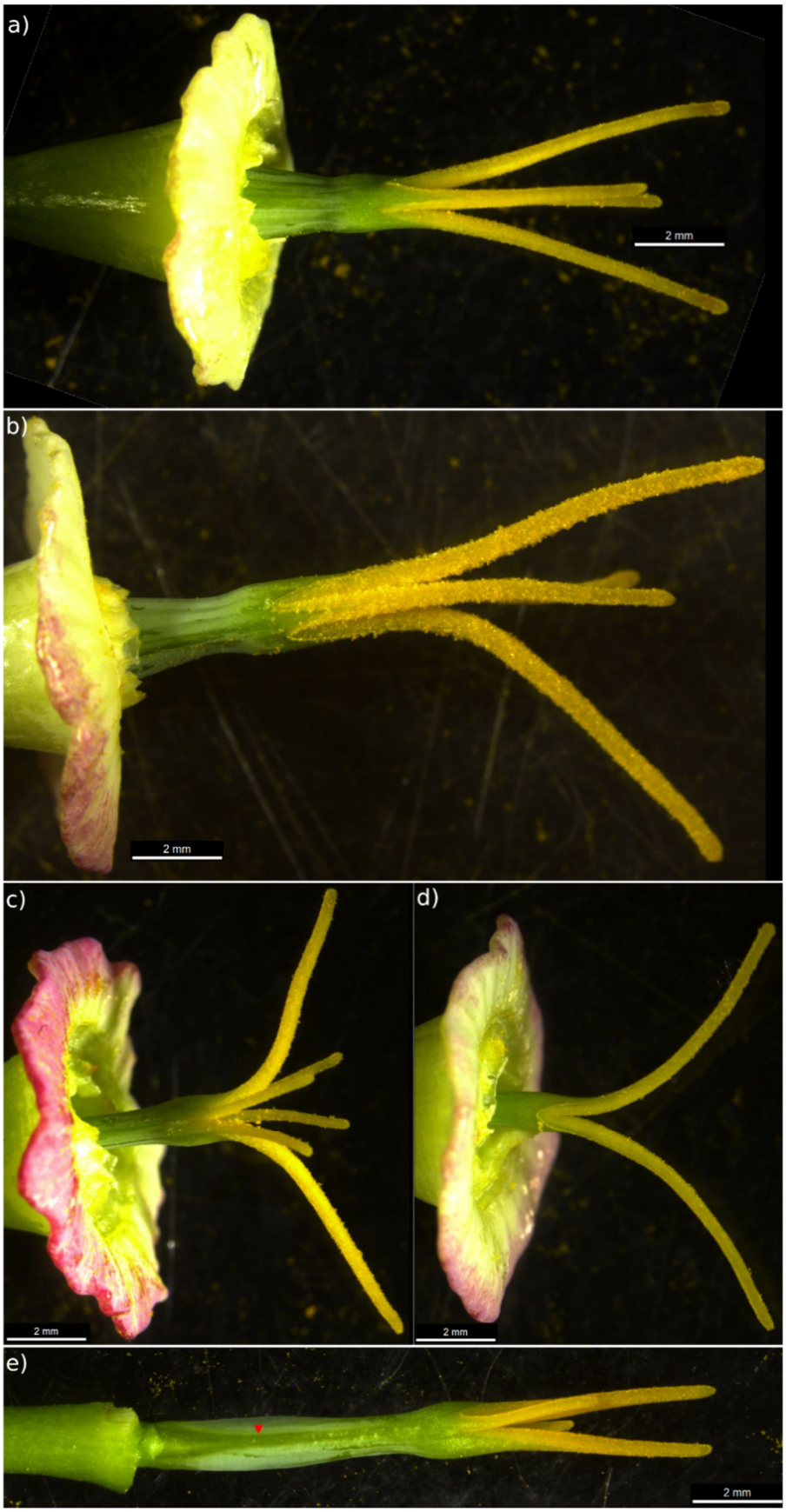

Figure 3.2: *Knock-down of EcCRC in E. californica produces a distinguishable phenotype described in [288]. Additionally, compared to the wild type (a) and pTRV2-empty treated control plants (b), changes in number of stigmatic protrusions (c) and (d) and wax deposition in the carpel fusion zone (e, red arrowhead) were found in this work.*

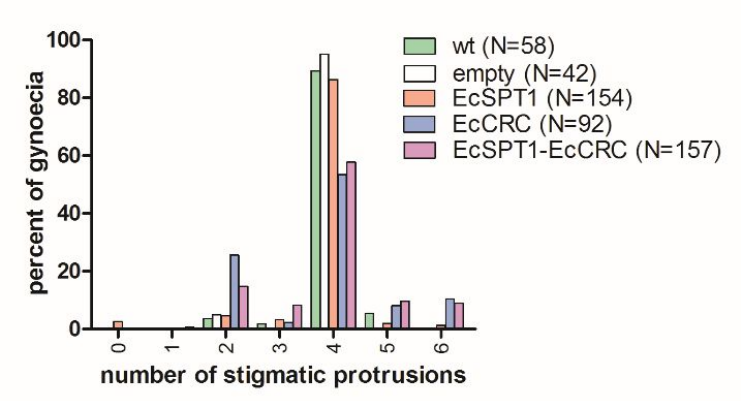

Figure 3.3: *Number of stigmatic protrusions on 523 gynoecia phenotyped for V4 and V6. In EcSPT1 knock-down, pTRV2-empty treated plants, and wild type over 80 % of the flowers had four stigmatic protrusions, while of the plants VIGS-treated for EcCRC knock-down only 53 to 63 % of the flowers had four stigmatic protrusions.*

ratios of the average laminar versus average marginal stigmatic protrusion lengths within a flower. The strength of the effects on the marginal stigmatic protrusions were significantly less pronounced in *EcSPT1* knock-down gynoecia compared to the *EcCRC* single and *EcCRC+EcSPT1* double knock down (fig. 3.6). The frequency of double or lacking marginal stigmatic protrusions was comparable in EcCRC and EcSPT1+EcCRC VIGS gynoecia (42 % and 36 % of flowers affected, respectively; 59 % and 62 % of plants affected, respectively), and nearly not found in EcSPT1 single VIGS (2 % of flowers and 4 % of plants affected). As well *EcCRC* and *EcSPT1+EcCRC* VIGS plants flowered significantly earlier (figs. 3.7a, 3.17a), pointing to an involvement of these genes in flowering time regulation.

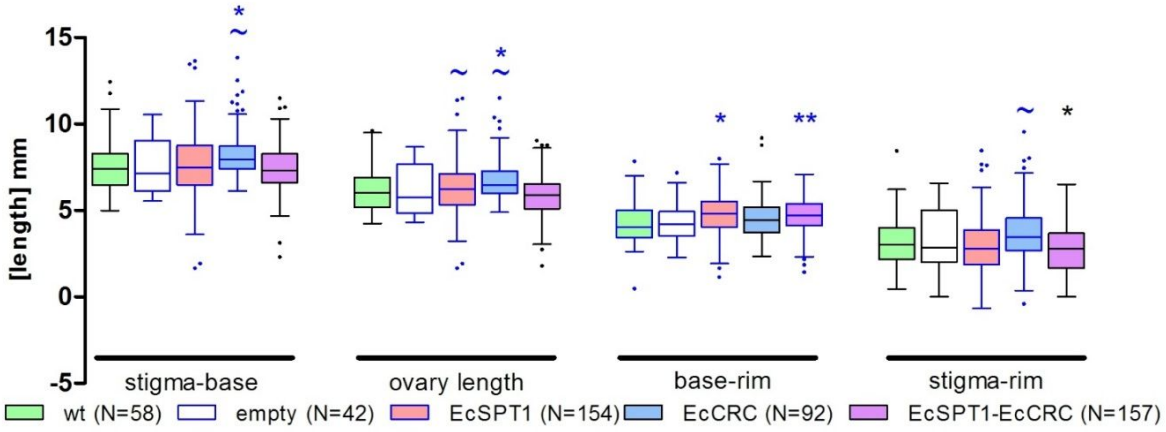

Figure 3.4: *Absolute dimensions of 523 gynoecia phenotyped for V4 and V6. Knock-down of EcSPT1, EcCRC, and both in E. californica lead to a number of small changes in gynoecia geometry: In EcCRC treated plants the length of the ovary is significantly increased leading to an increased stigma-base length. At the same time the height of the floral cup significantly increased in EcSPT1 and EcSPT1+EcCRC treated plants, while in EcCRC treated plants this change was not significant. In combination this leads to a significantly increased stigma-rim and stigma-base length in EcCRC, and statistically increased ovary lengths for both knock downs, compared to the double knock downs. Data sets marked in blue vary significantly from normal distribution in Kolmogorov-Smirnov (KS) test (with Dallal-Wilkinson-Lilie (DWL) for P value). Asterisks show statistically significant differences from pTRV2-empty treated plants: (*) 0.01 < p < 0.05, (**) 0.001 < p < 0.01, (***) p < 0.001. ~ show statistically significant differences from EcCRC+EcSPT1 treated plants Significance was tested by Student's t-test for normally distributed samples or Mann-Whitman U test for not-normally distributed samples.*

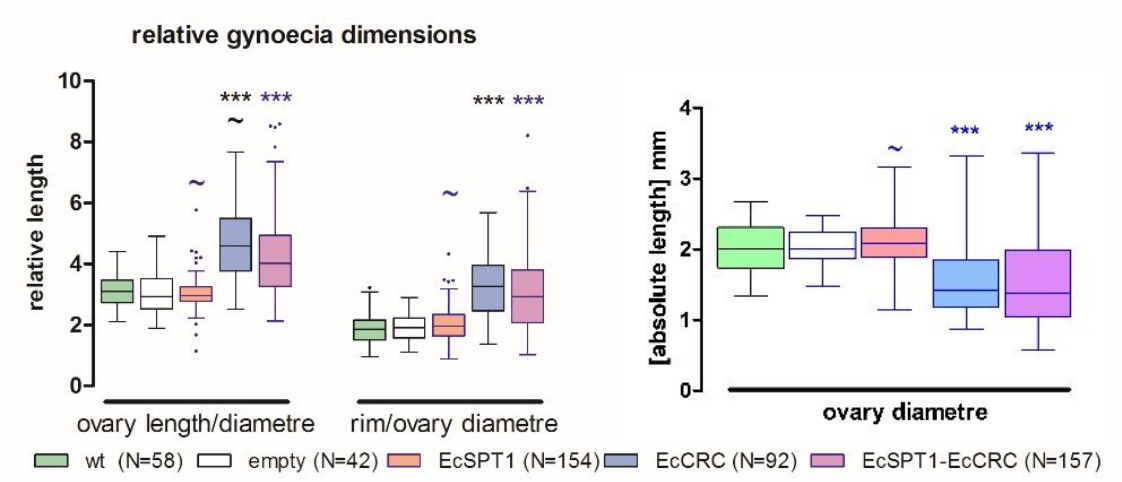

Figure 3.5: *Ovary dimensions of 523 gynoecia phenotyped for V4 and V6. Knock down of EcSPT1, EcCRC or both in E. californica led to a number of small changes in gynoecia geometry: EcCRC and EcSPT1+EcCRC knock downs showed a significantly reduced ovary diameter compared to the other treatments, causing the significant increase in ovary length/diameter and rim width/ovary diameter ratios in EcCRC and EcCRC+EcSPT1 VIGS flowers compared to the controls. Border colours and significances are defined as in fig. 3.4.*

After careful re-examination of the data it was found, that the differences in frequency of a rarely observed defect in ovule development can be understood as another possible change in phenotype by knock-down of *EcSPT1* and *EcCRC*. With a possible preference for *EcCRC* and *EcSPT1+EcCRC* VIGS plants (empty: 4 flowers (4 %) on 2 plants (6 %), *EcSPT1*: 2 flowers (2 %) on 1 plant (2 %), *EcCRC*: 5 flowers (5 %) on 4 plants (13 %), *EcSPT1+EcCRC*: 13 flowers (8 %) on 10 plants (19 %)), at anthesis the ovules show a candle-like appearance (compare figure 3.8). Instead of being anatropous and green, some or all ovules inside a given gynoecium appear orthotropous and white, sitting on a fat green structure. From different severities of this appearance it is assumed here, that integument development is halted before

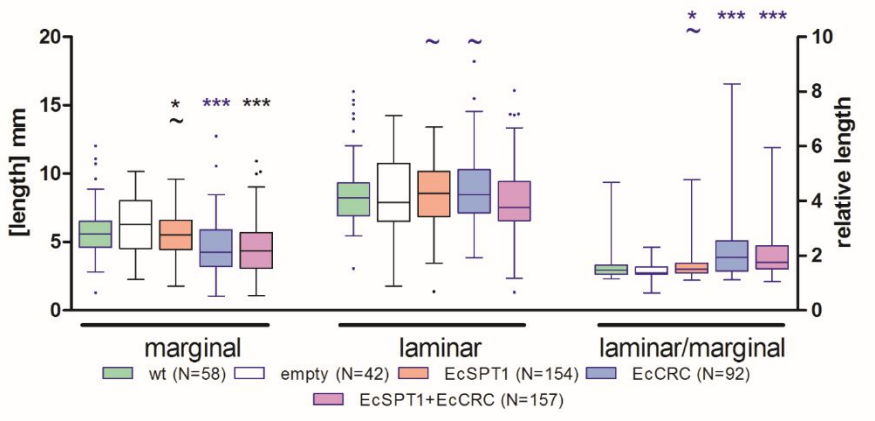

Figure 3.6: *Stigmatic protrusion length of 523 gynoecia phenotyped for V4 and V6. The absolute length of the marginal stigmatic protrusions is significantly reduced in all VIGS treated plants compared to the pTRV-empty control. Thus, the relative length of the laminar compared to marginal stigmatic protrusions is significantly increased in EcSPT1, EcCRC and EcSPT+CRC knock-downs. Length smaller than 1 mm were not included in the statistics to avoid bias by strongly reduced marginal stigmatic protrusions. Border colours and significances as defined in fig. 3.4.*

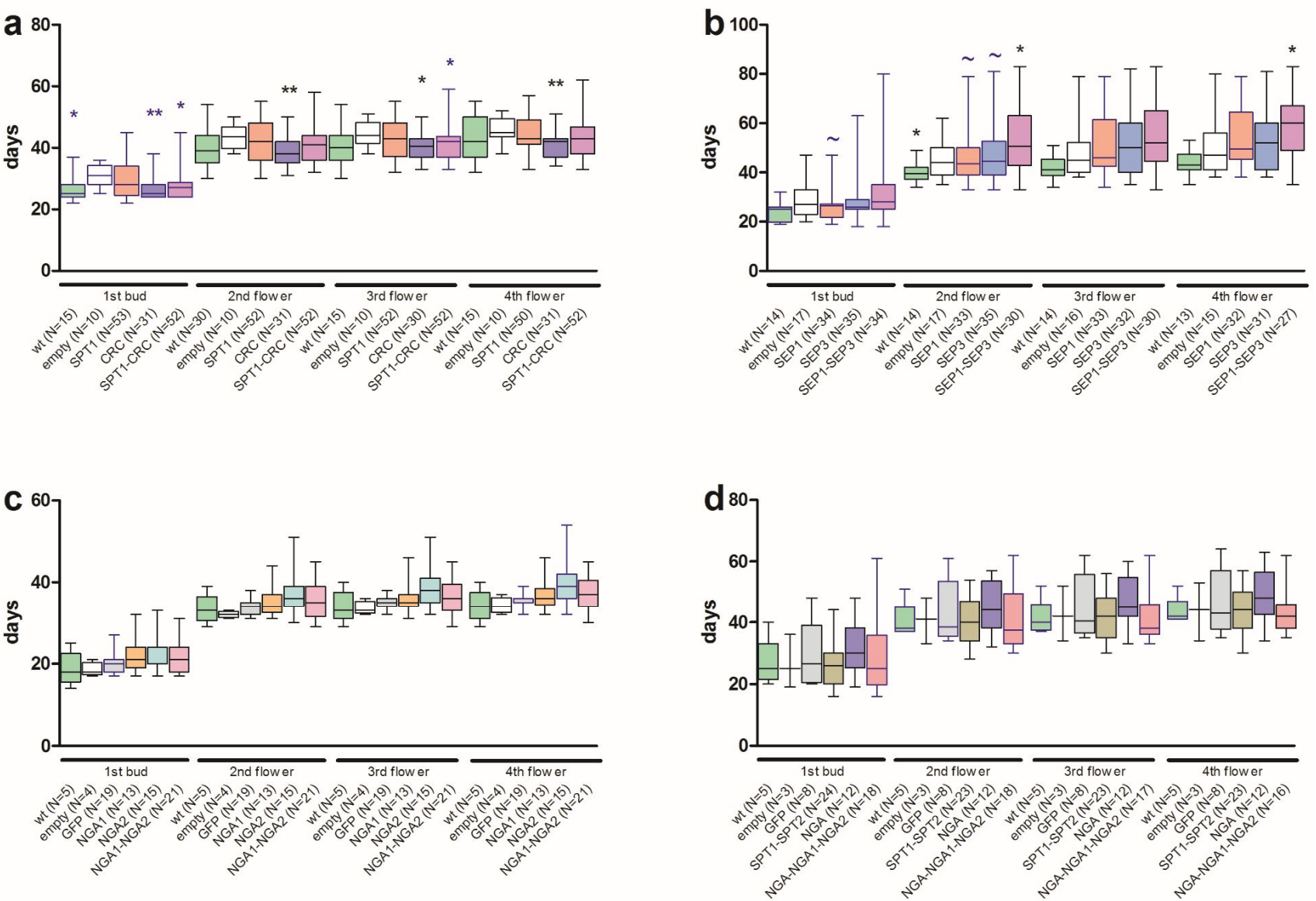

Figure 3.7: *The number of days after inoculation on which a flower was harvested in experiments V4, V5, V6, and V8. Colours and significances are defined as in fig. 3.18. Floral transition and formation of subsequent flowers was delayed signifycant-ly in knock-down of EcSEPs and slightly in EcNGA and EcNGA2, while it was significantly earlier in EcCRC and EcSPT1+EcCRC double knock-downs. pTRV2-empty treated plants in some experiments flower significantly later than wt.*

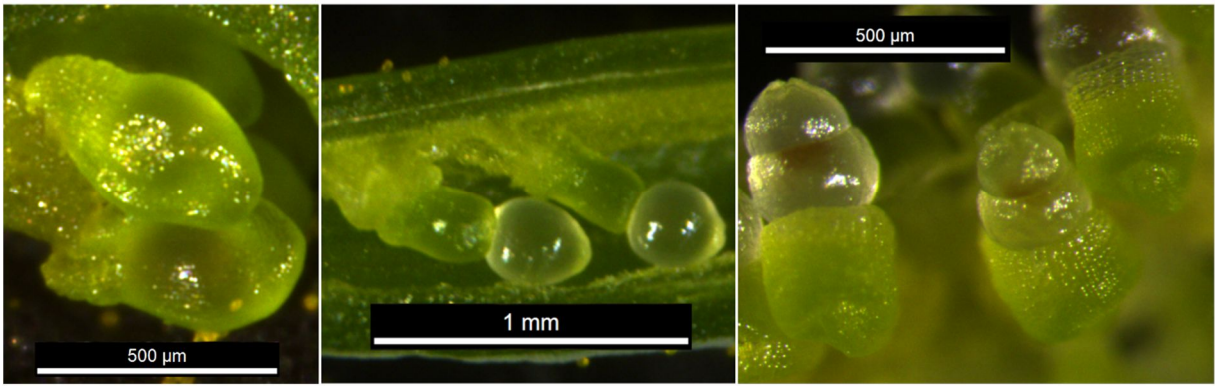

Figure 3.8: *Candle-like ovules. left: wild type ovules at anthesis, middle and right: integument development appears halted in different stages in gynoecia at anthesis. The white structure is interpreted here as nucellus not covered by integuments (middle), or covered only by the inner integument at the proximal half and the funiculus becomeing visible at the base of the outgrowing outer integument (right).*

the integuments grow out to cover the nucellus while at the same time bending the ovule in the anatropous position. Instead the outer integument appears to be folded around the funiculus, resulting in the fat green structure mentioned before.

Of each treatment group, plants showing a phenotype in VIGS were chosen for qPCR analysis. For EcCRC the phenotype is published, for *EcSPT1* single and double VIGS plants with a higher floral cup were selected (fig. 3.9). The remaining *EcSPT1* expresion levels in *EcSPT1* VIGS plants were 24 %-59 % and in *EcSPT1+EcCRC* double knock downs 65 %-80 %. Of *EcCRC* expression in *EcCRC* VIGS plants 3 %-8 % remained and in *EcSPT1+EcCRC* 3 %-70 %.

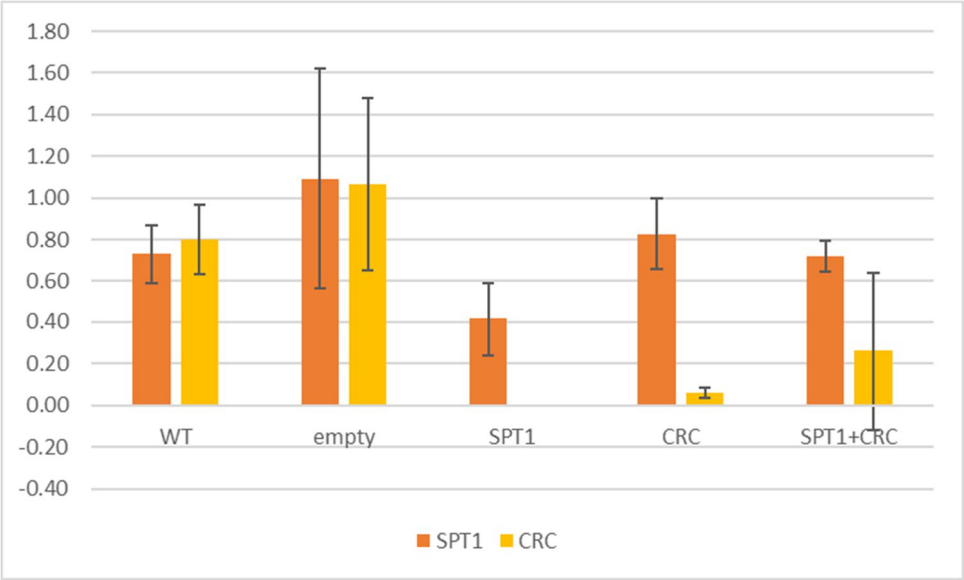

Figure 3.9: *Expression analysis in VIGS plants and controls based on 3 biological replicates. Expression is normalized to GAPDH and relative to the average expression in pTRV2-empty treated plants: Remaining EcSPT1 expresion levels in EcSPT1 were 24 %-59 % and in EcSPT1+EcCRC 65 %-80 %. Remaining EcCRC expression was in EcCRC 3 %-8 % and in EcSPT1+EcCRC 3 %-70 %.*

Taken together, no increase of the putative split style/stigma *EcCRC* VIGS phenotype was observed in a combined *EcSPT1+EcCRC* knock down, wether in severity nor in frequency. The length reduction of the marginal stigmatic protrusions was comparable between

EcCRC and *EcSPT1+EcCRC* VIGS plants, while the length reduction was less pronounced in *EcSPT1* knock down. That this change is not significant in comparison with the pTRV2-empty treated control plants, is probably due to the high variation in the control group. On the other hand, the laminar stigmatic protrusions were significantly shorter in the *EcSPT1+EcCRC* double VIGS plants than in either single VIGS, which hints at an additive effect of both genes in the longitudinal growth of the laminar stigmatic protrusions. Furthermore, an increase of gynoecia containing one to only candle-like ovules, increased in the *EcSPT1+EcCRC* VIGS compared to the *EcCRC* single VIGS. This may hint at a combined effect of both genes in *E. californica* ovule development and an effect on flowering time was observed (fig. 3.7, 3.17). The generally only subtle changes in *EcSPT1* VIGS might be explained by (1) the role of *SPT* in flower development is not conserved in *E. californica*, (2) the floral phenotyp of the *EcSPT1* knock down is masked by other factors, or (3) the used VIGS construct is not causing an efficient knock down. A list of gene copy numbers is found in the supplemental table 8.

In *A. thaliana* direct regulation of *STY2* and *YUC4* by SPT and CRC, respectively, is published [63, 113]. Based on this, expression levels of *EcSTY-L* [391] and *EcYUC1/4* were monitored as well. For this a single *EcYUC1/4* ortholog was identified here (compare fig 3.10). To identify possible positive or negative correlation, the ratio of between expression of the possible regulating and the possibly regulated gene was determined for each pair. No correlation could be found (see suppl. table 3).

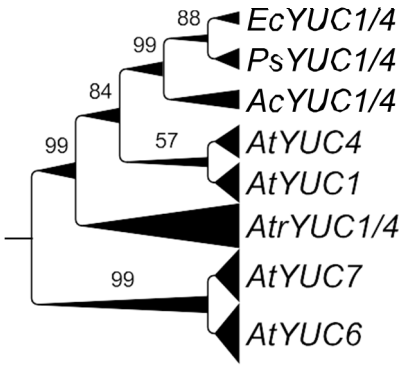

Figure 3.10: *ML tree YUC1/4 genes rooted with AtYUC6/7. Calculated, using protein sequences from another Papaveraceae species (P. somniferum (Ps)), another ranunculales species (Aquilegia caerulea (Ac)), the basal angiosperm Amborella trichopoda (Atr) in addition to the sequences from A. thaliana (At) and E. californica (Ec); 500 bootstraps. Outgroups chosen according to [320]. Bootstrap values higher than 50 were accepted as reliable. Branch lengths are depicted as width of the triangle at the respective branch. Unnamed paralogous sequences are numbered for better overview.*

V8: SPT1+SPT2 VIGS

In *E. californica* a second *SPT*-like gene was discovered here, which forms a well supported group together with the other Ranunculales *SPT*-like genes (fig. 3.11).

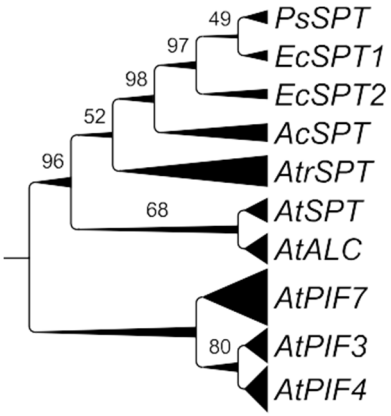

Figure 3.11: *ML tree of EcSPT genes rooted with AtPHYTOCHROME INTERACTING FACTORS3/4/7. Calculated, using protein sequences from another Papaveraceae species (P. somniferum (Ps)), another ranunculales species (Aquilegia caerulea (Ac)), the basal angiosperm Amborella trichopoda (Atr) in addition to the sequences from A. thaliana (At) and E. californica (Ec); 500 bootstraps. Outgroup chosen according to [23]. Bootstrap values higher than 50 were accepted as reliable. Branch lengths are depicted as width of the triangle at the respective branch. Unnamed paralogous sequences are numbered for better overview.*

Cross-silencing of *EcSPT2* by the used *EcSPT1* VIGS construct or compensation of *EcSPT1* knock-down by upregulaton of its paralogue *EcSPT2*, was not detected, based on unchanged expression levels of *EcSPT2* in *EcSPT1* VIGS plants (fig. 3.12).

After *EcSPT2* was discovered (fig. 3.11), the functional redundancies were explored by a *EcSPT1+EcSPT2* double knock-down in V8b and comparison to the *EcSPT1* VIGS data.

Figure 3.12: *Expressionn analysis of EcSPT1 and EcSPT2 in EcSPT1 VIGS plants generated in V4. All expression*

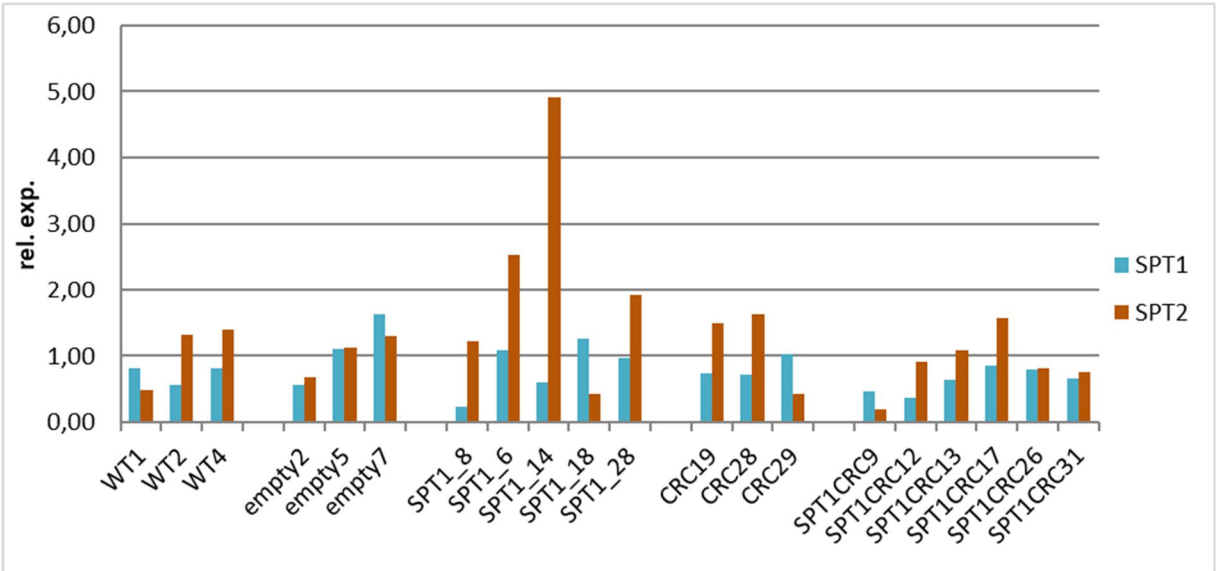

levelsnormalized to GAPDH and relative to the average expression level of pTRV2-empty treated plants. No cross-silencing or compensatorial upregulation of EcSPT2 were observed.

By a simultaneous knock down of *EcSPT1* and *EcSPT2*, the ovary length was reduced significantly compared to pTRV2-empty treated control plants, leading to a significant decrease in stigma-to-base length and significantly smaller part of the gynoecia above the cup's rim. At the same time, the increase in height of the floral cup, observed in *EcSPT1* knock downs, was no longer significant in the *EcSPT1+EcSPT2* double VIGS plants (fig. 3.13).

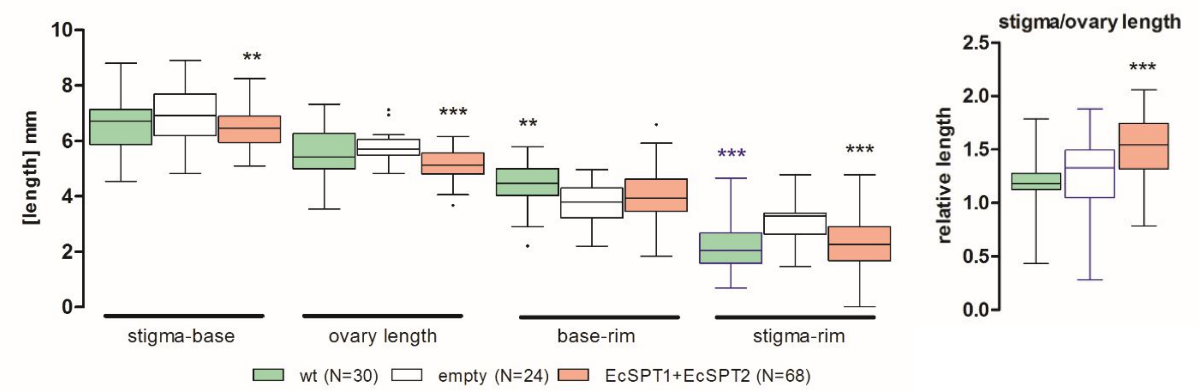

Figure 3.13: *Dimensions of 122 gynoecia phenotyped in V8b. The waist diametre is reduced significantly as is the ratio of ovary length versus diametre, the latter results from the reduced ovary length. The reduced ovary length results as well in higher stigma-to-ovary length ratio. The significant reduction of the absolute rim width, as well as in relation to the ovary diametre, is less pronounced in the double VIGS plants than in the wild type. Border colours and significances are defined as in fig. 3.4.*

Similarily to the *EcSPT1* single knock down, a significant decrease in length of the marginal stigmatic protrusions was observed in the *EcSPT1+EcSPT2* double VIGS plants, while the laminar stig-matic protrusions were slightly increased in length, compared to both control groups. This in combination, lead to a highly significant increase in the length ratio of the averages lengths of laminar and marginal stigmatic protrusions within a flower, similar to what was observed in *EcCRC* and *EcSPT1+EcCRC* VIGS plants (figs. 3.6, 3.14).

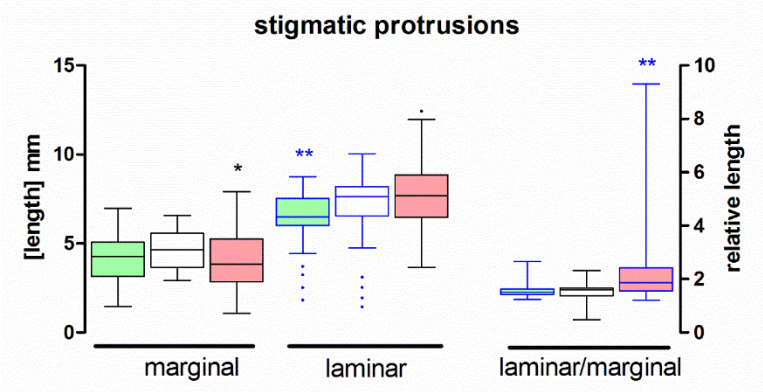

Figure 3.14: *Dimensions of 122 gynoecia phenotyped in V8b. Simultaneous knock down of EcSPT1 and EcSPT2 (red, 68 flowers) in E. californica lead to a number of small changes in gynoecia geometry compared to pTRV2-empty controls (white, 24 flowers). In VIGS treated plants the length of the marginal stigmatic protrusions and of the ovary decreased significantly. At the same time the ratio of the average marginal vs. laminar stigmatic protrusion lengths within a flower increased significantly, as did the ratio of the average marginal stigmatic protrusion vs. ovary length. Colours and significances are defined as in figs. 3.4 and 3.13.*

Both, the significantly reduced ovary length and the slightly increased average length of the laminar stigmatic protrusions of the *EcSPT1+EcSPT2* double VIGS plants lead to a highly significant increased ratio of these parameters (compare figures 3.14). The ratio of ovary length versus diameter is reduced significantly, as the latter results from the reduced ovary length (fig. 3.13). For several parameters measured in this experiment, significant differences between the wild-type plants and the pTRV2-empty treated control plants impede interpretation of the results. The subtle phenotype changes observed in EcSPT1+EcSPT2 VIGS plants were only discovered by statistical evaluation after the wetlab phase had been finished, so no qPCR data are available for this treatment group.

Taken together, the results of the combined knock-down of *EcSPT1+EcSPT2* point to a redundant function for *EcSPT1* and *EcSPT2* in regulation of the ovary length, which opposes the role of *EcCRC*. In the regulation of stigmatic protrusion length *EcSPT1* and *EcCRC* seem to have additional effects on laminar stigmatic protrusions, while on the stigmatic protrusions length ration the effect of *EcCRC* is not increased by the weaker *EcSPT1* effect but similar to the combined effect of *EcSPT1* and *EcSPT2*. A full overview of phenotype-frequencies is given in supplemental table 4.

V5: EcSEPALLATA VIGS

A striking phenotype is known for the *A. thaliana sep1 sep2 sep3 sep4* quadruple mutants, where all floral organs are converted to leaves. In *E. californica*, only two *SEPALLATA* genes are known: *EcSEP1* which is orthologous to the *LOFSEP* clade genes *AtSEP1*, *AtSEP2*, and *AtSEP4*, and *EcSEP3*, an orthologue of *AtSEP3* [30, 31, 187]. For assessment of the different functions of the homologues, individual as well as combined knock-downs were generated.

In these VIGS experiments, no homeotic phenotype reminiscent of the *A. thaliana* quadruple *sep* mutant phenotype was observed. Instead, unsually long stamens, stamens with green connectives but producing mature pollen grains, or with unusually broad connectives were observed only in *EcSEP1* (1/35 plants), *EcSEP3* (14/33 plants*)*, and *EcSEP1+EcSEP3* (22/30 plants) knock downs (figs. 3.15 and 3.16). On average, only two of the three phenotyped flowers per plant and usually only 3 to 8 stamens per flower showed clear phenotypic differences to the controls. Stamens with only slightly green or broader connectives could be found mostly in the *EcSEP*s knock-down plants, but in one pTRV2-empty treated control plant as well and thus were interpreted as part of the normal phenotypic variation (supplemental table 5). A frequency distribution of stamen widths is seen in supplemental fig. 5).

Additionally, plants treated with both *EcSEP*s VIGS constructs flowered significantly later, while the single *EcSEP* VIGS treated plants showed no significant change in flowering time (see figure 3.7b). This pattern suggests an additive effect of *EcSEP1* and *EcSEP3* on the timing of flowering. At the same time the number of days passing between harvest of the first bud and the fourth fower is significantly increased in *EcSEP1* and *EcSEP1+ EcSEP3* VIGS plants compared to pTRV2-treated plants (fig. 3.17b). Interestingly, the number of days passing between harvest of the first bud and fourth flower in the single *EcSEP1* VIGS-treated plants

were not normally distributed. The detailed analysis of the distribution of days when a flower is formed shows a shoulder or second peak instead of a gaussian distribution, indicative of two overlappig populations in these treatments (figures 3 and 4 in the supplementals).

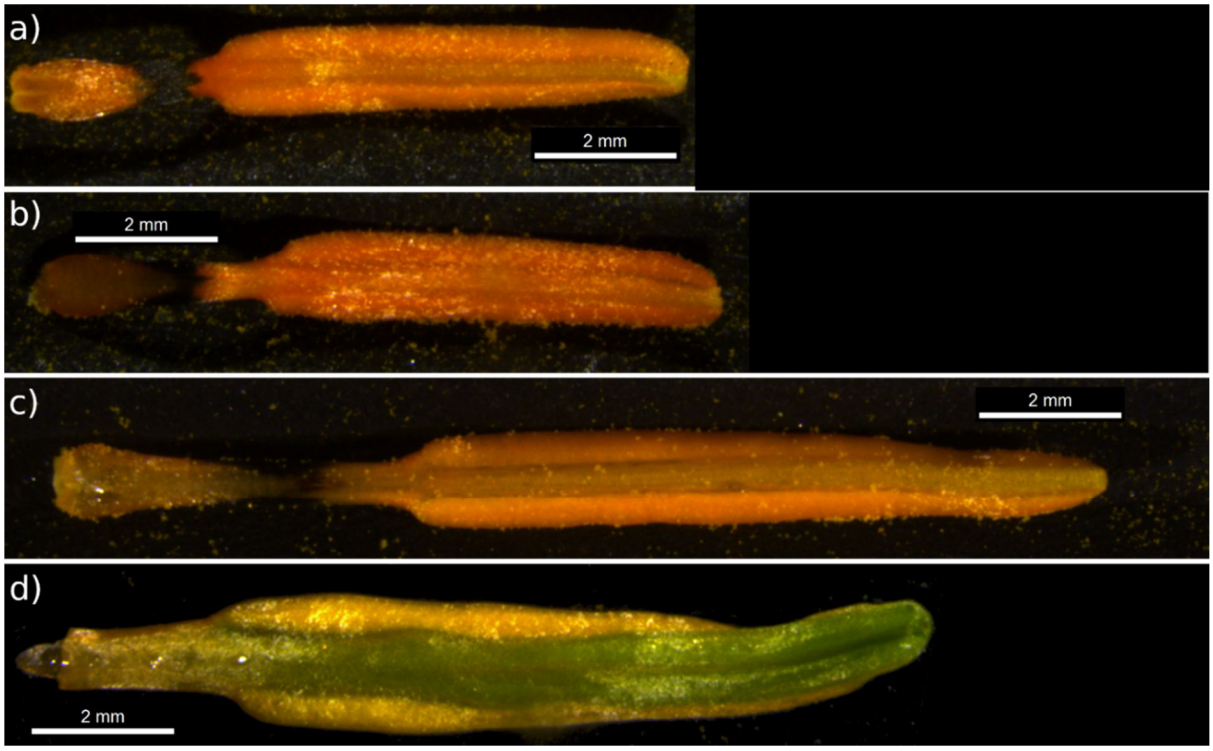

Figure 3.15: *Presumed stamen phenotype of the EcSEPs knock-down at anthesis. a) wild type stamen b) pTRV2 empty c) long stamen as seen in some EcSEP3 VIGS flowers. d) extremely broad and green stamen as seen in one EcSEP1+EcSEP3 VIGS plant. Stamens with green or broad connectives were seen in several flowers of knock-down plants of this experiment.*

Figure 3.18 and table 3.3 show the expression levels of *EcSEP*s in *EcSEP1* and *EcSEP3* single VIGS, as well as *EcSEP1+EcSEP3* double VIGS plants, compared to the average Δct in pTRV2-empty VIGS control plants. A causal correlation between broad, green connectives and *EcSEP*s expression was not found. Plants with an increased as well as a reduced expression level of *EcSEP*s were among the plants showing this phenotype. The same is true for the late flowering phenotype.

Table 3.3: *Expression values of EcSEPs normalized on the average Δct the of pTRV2-empty treated control plants and flowering times in days post inoculation for the EcSEPs VIGS plants chosen for qPCR analysis.*

	relative expression		dpi			
plant	***SEP1***	***SEP3***	**1st bud**	**2nd flower**	**3rd flower**	**4th flower**
WT_5	1.66	1.86	25	39	42	43
WT_6	1.55	1.20	25	41	42	44
WT_11	1.14	1.56	19	35	35	38
WT_12	0.80	2.48	32	49	51	53
WT_14	1.93	2.80	26	45	46	47
empty_6	1.02	1.33	25	44	44	63
empty_9	2.51	2.01	33	39	40	80
empty_14	1.83	0.58	33	52	53	54
empty_15	0.11	0.94	27	48	48	50
empty_18	1.87	0.69	21	40	40	42
***SEP1*_3**	1.22		19	40	59	79
***SEP1*_11**	0.18		21	39	46	48
***SEP1*_17**	1.19		27	45	45	46
***SEP1*_27**	0.34		21	33	34	38
***SEP1*_30**	0.59		29	47	76	
***SEP1*_43**	0.26		27	46	56	75
***SEP3*_4**		1.31	25	39	40	40
***SEP3*_5**		0.54	25	39	43	52
***SEP3*_7**		0.51	25	59	59	67
***SEP3*_19**		0.68	28	48	50	52
***SEP3*_27**		1.06	22	42	43	45
***SEP3*_29**		1.04	20	35	38	54
***SEP3*_34**		0.36	22	42	60	75
***SEP1+3*_8**	0.14	0.24	28	48	49	60
***SEP1+3*_10**	0.04	0.20	25	43	45	49
***SEP1+3*_17**	0.54	0.70	32	56	59	60
***SEP1+3*_18**	0.48	0.70	25	42	44	46
***SEP1+3*_19**	0.91	1.19	63	62	72	72
***SEP1+3*_20**	3.63	3.60	54	72	74	74
***SEP1+3*_23**	0.52	1.16	18	33	33	35
***SEP1+3*_25**	0.40	0.77	32	73	75	
***SEP1+3*_28**	0.12	0.25	25	41	42	47
***SEP1+3*_38**	1.60	0.94	32	55	59	60

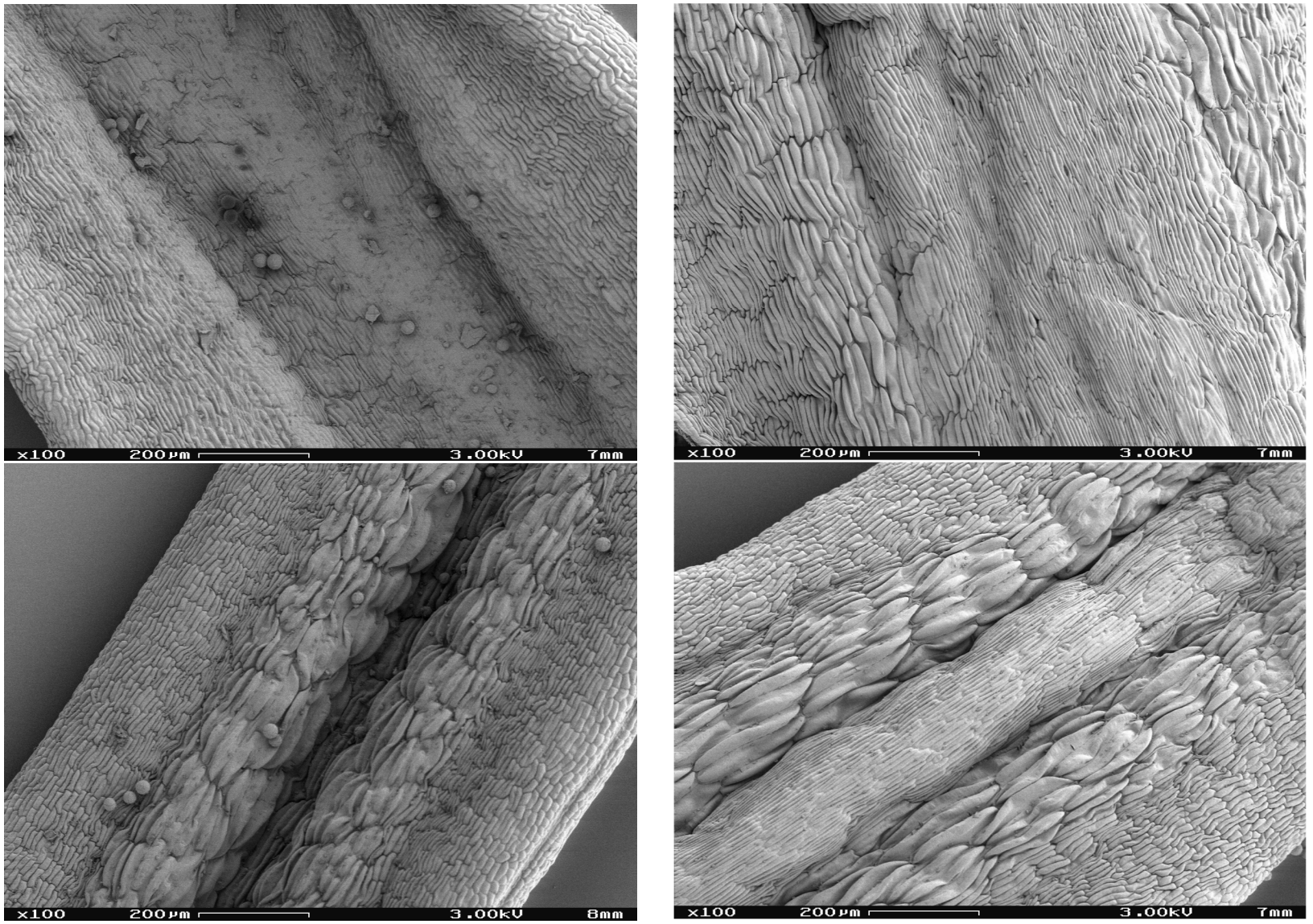

Figure 3.16: *Presumed stamen phenotype of the EcSEPs knock-down. SEM pictures of an extremely broad EcSEP1+EcSEP3 stamen (upper) and a wild-type stamen (lower). Compared to wt no obvious change in connective cell identity or size can be seen, but cell number is increased. The round structures are pollen grains. (a) abaxial side: The large-lumen cells lining the wt connective-theka border are missing in the VIGS stamen. (b) adaxial side: The large-lumen cells lining the wt connective-theka border are far less pronounced in the VIGS stamen.*

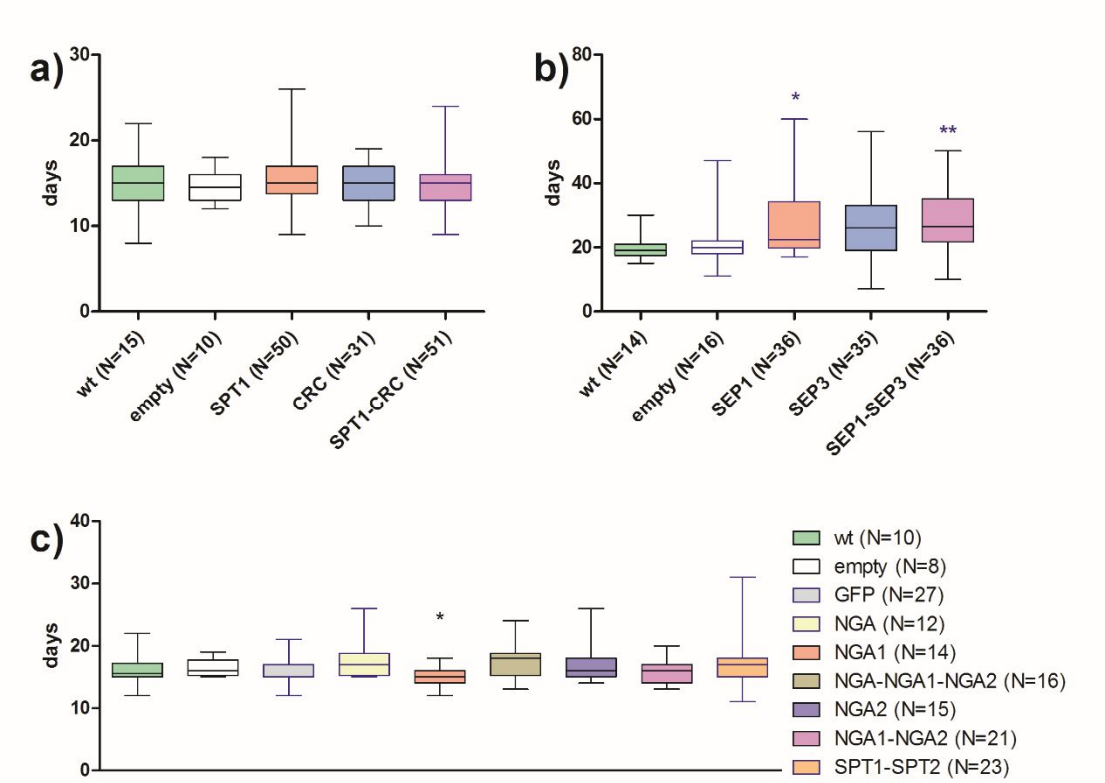

Figure 3.17: *The number of days passing between the harvest of the first bud and the fourth flower of each plant for V4, V5, V6, and V8 are shown. Colours and significances are defined as in fig. 3.18. Floral transition took place later in the experiment conducted in the climate cabinet (b) compared to those conducted in the climate chamber (a+c). Flower formation rate was reduced in E. californica after VIGS treatment for knock-down of EcSEP1 and both EcSEPs (b) and EcNGA (c), but not affected in the other treatments.*

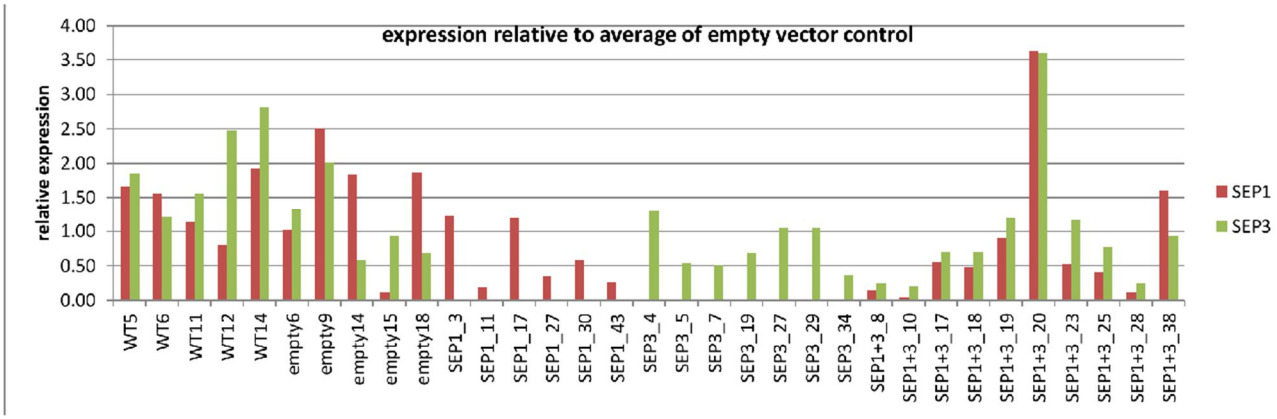

Figure 3.18 *qPCR analysis of VIGS treated E. californica monitoring expression levels of EcSEP1 and EcSEP3. Plants were selected by presumed stamen phenotype or randomly for control plants.*

Not only the EcSEPALLATAs were found to have an effect on flowerering time, the same is true for knock-downs *EcNGA*. In the detailed analysis of flowering times, two populations can be found as well in *EcSPT1* knock-down and a combination of all three *EcNGA*s. Another interesting observation in this work was a single flower in the *EcSEP1+EcSEP3* double VIGS: This showed a phenotype reminiscent of a mild *EcNGA*-VIGS (see fig. 3.19).

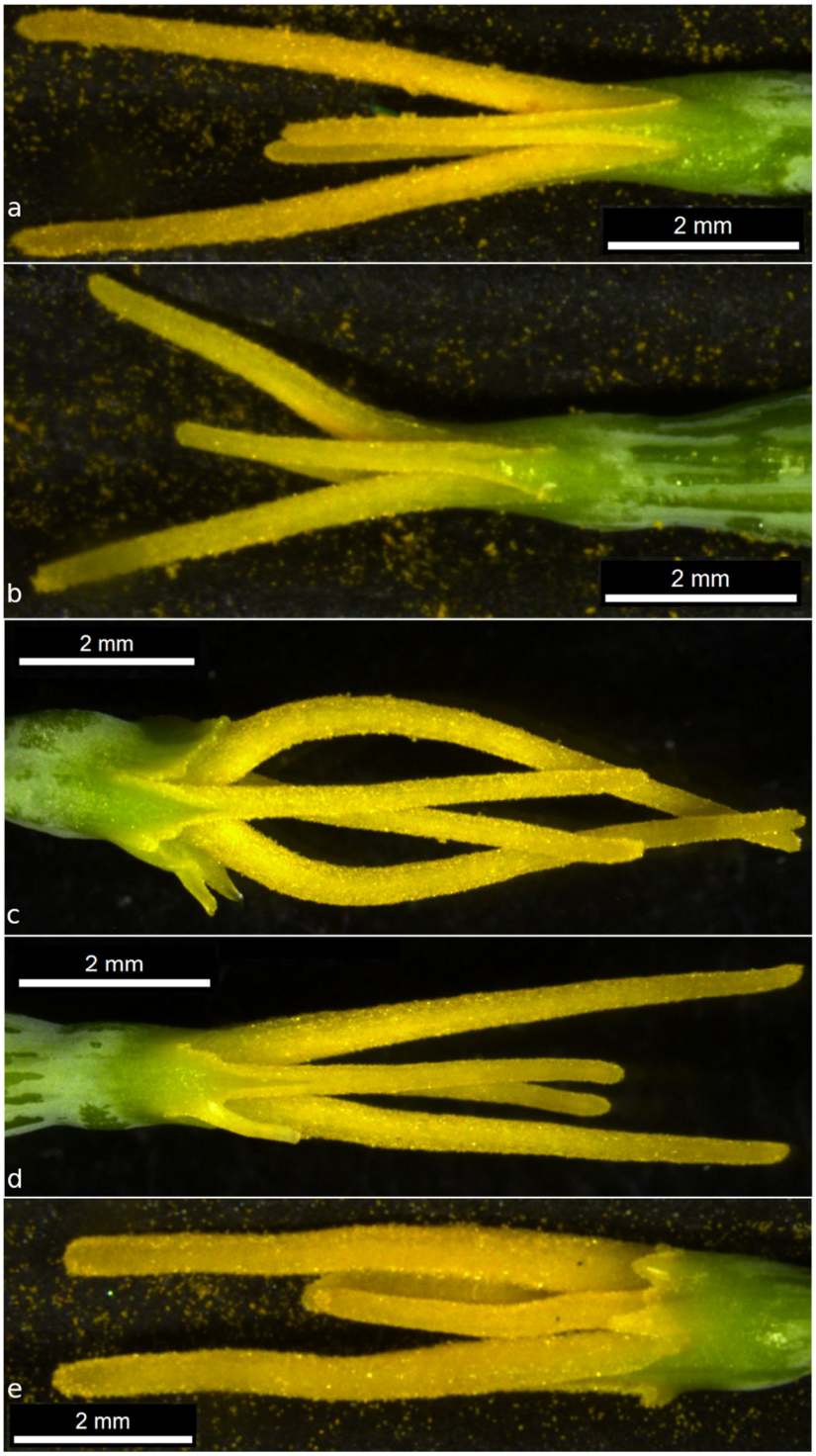

Figure 3.19: *Comparison of defects in style and stigma development in E. californica VIGS treated plants. Mild EcNGA phenotypes c) EcNGA2 VIGS, d) EcNGA1+EcNGA2 VIGS compared to a) wt from V5 b) pTRV2 empty controlfrom V5, and e) a unique flower from EcSEP1+SEP3 double VIGS. All knock down plants schow additional, tiny stigmatic protrusions. Wt and pTRV2 empty controls from V8 see fig. 3.29.*

V8: EcNGATHA VIGS

For the four *NGATHA* genes from *A. thaliana* redundant roles in style/stigma development are published [37, 40, 42-45]. Mutant phenotypes further show redundant action with SHI and bHLH family proteins [42]. Four *P. somniferum NGA* sequences and one *A. caerulea*

NGA were retrieved from NCBI. Opposed to this, only two homologues in *E. californica* were published before [23]. Here EcNGA2, a third EcNGA paralog was discovered, which forms with the other Ranunculales NGAs a sister group to the AtNGA proteins (compare fig. 3.20).

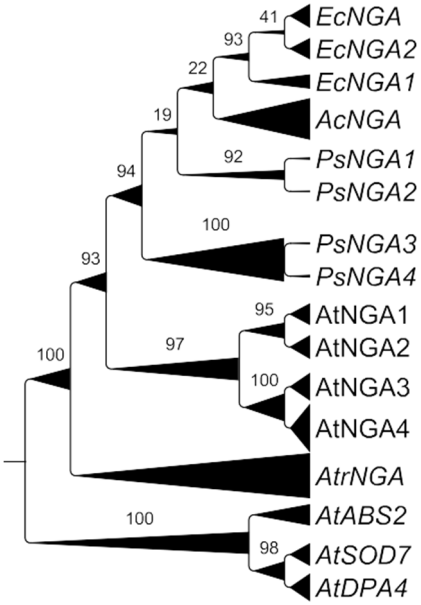

Figure 3.20: *ML tree of NGA genes rooted with AtNGA-LIKEs. Calculated, using protein sequences from another Papaveraceae species (P. somniferum (Ps)), another ranunculales species (Aquilegia caerulea (Ac)), the basal angiosperm Amborella trichopoda (Atr) in addition to the sequences from A. thaliana (At) and E. californica (Ec); 500 bootstraps. Outgroup chosen according to [23]. Bootstrap values higher than 50 were accepted as reliable. Branch lengths are depicted as width of the triangle at the respective branch. Unnamed paralogous sequences are numbered for better overview.*

To dissect the functional conservation of the previously known *EcNGA* [385], *EcNGA1* [23] and the newly discovered *EcNGA2* (fig. 3.14), pTRV2-based VIGS constructs for all three genes were assembled and tested alone or in combinations. For *EcNGA*, the construct published before [385] was used. Because of a high conservation between the coding sequences it was not posssible to completely avoid the conserved sequences described by Fourquin and Ferrándiz [385]: the pTRV2-EcNGA and pTRV2-EcNGA1 constructs contain the NGA-I motif, while the pTRV2-NGA2 construct contains part of the B3 DNA binding domain.

Though often only one flower of a given plant was affected (9 of 14 affected plants), single, double, and triple VIGS experiments involving *EcNGA2* showed phenotypes similar to those published for *EcNGA* before ([385], fig. 3.22): overproliferation of stylar tissues forming flaps, lacking stigmatic tissues or with a multitude of stigma-like extensions protruding from the edge. The stylar flaps replaced the normal stigmatic protrusions to a lesser or greater extend, with the laminar pair more often affected than the marginal. In severe cases, style and stigma tissues were strongly reduced or even completely absent, revealing ovules in the open apical end of the ovary, or in mild cases a skirt of additional, tiny, stigma-like extensions surrounded the normally developed stigmatic protrusions (fig. 3.22, suppl. table 6). The latter phenotype was the only one ever seen in any of the other conducted experiments: in a single flower of a *EcSEP*s double VIGS plant.

All single inoculations showed different phenotypes of style and stigma developmental defects: Residual expression levels of *EcNGA* of 66-124 %, produced phenotypes similar to published mild *EcNGA* VIGS phenotypes, a skirt of additional tiny stigmatic protrusions, or a lack of stigmatic papillae similar to *EcNGA* VIGS plants. In *EcNGA1* VIGS expression levels were reduced to 70-90 %, resulting in a lack of stigmatic papillae on the tips of otherwise normal stigmatic protrusions or reduced development of stigma and/or style tissues, while ovules were fully developed. This is different from the reduced style/stigma development sometimes observed in plants from all treatments of all experiments, where ovules fail to develop after initiation and style and stigma development is halted. Plants treated with pTRV2-*EcNGA2* in single or multiple knock-downs showed the defects published for mild to strong *EcNGA* VIGS phenotypes: flaps of stylar tissue lined with short sigma-like protrusions replacing the laminar stigmatic prostrusions (4 (9 %) flowers on 3 (20 %) plants of *EcNGA2* VIGS, 15 (23.8 %) flowers on 9 (36 %) plants in *EcNGA1+EcNGA2* VIGS, 3 (5.9 %) flower on 3 (15 %) plants in the triple VIGS), or a skirt of additional tiny stigmatic protrusions similar to *EcNGA* knock-down. A complete overview of observed carpel penotypes is found in table 6 in the supplemental data section. A slight delay in flowering time was observed in *EcNGA* single VIGS and *EcNGA+EcNGA1+EcNGA2* triple knock-down, while at the same time for *EcNGA1* a significant earlier flowering time was observed (fig. 3.7d, 3.17c). In general it can be noted, that EcNGA and EcNGA2 are more similar in sequence relationship and in VIGS phenotype compared to EcNGA1.

Based on a discernible phenotype, 2 to 6 buds of each treatment group were used for the expression analysis of *EcNGA*s VIGS plants (fig. 3.21). Similar to *EcSPT1* and the *EcSEPs*, the targetet genes were not necesserily expressed at strongly reduced levels in the first bud of a plant which later formed flowers with phenotype compared to the pTRV2-empty control group.

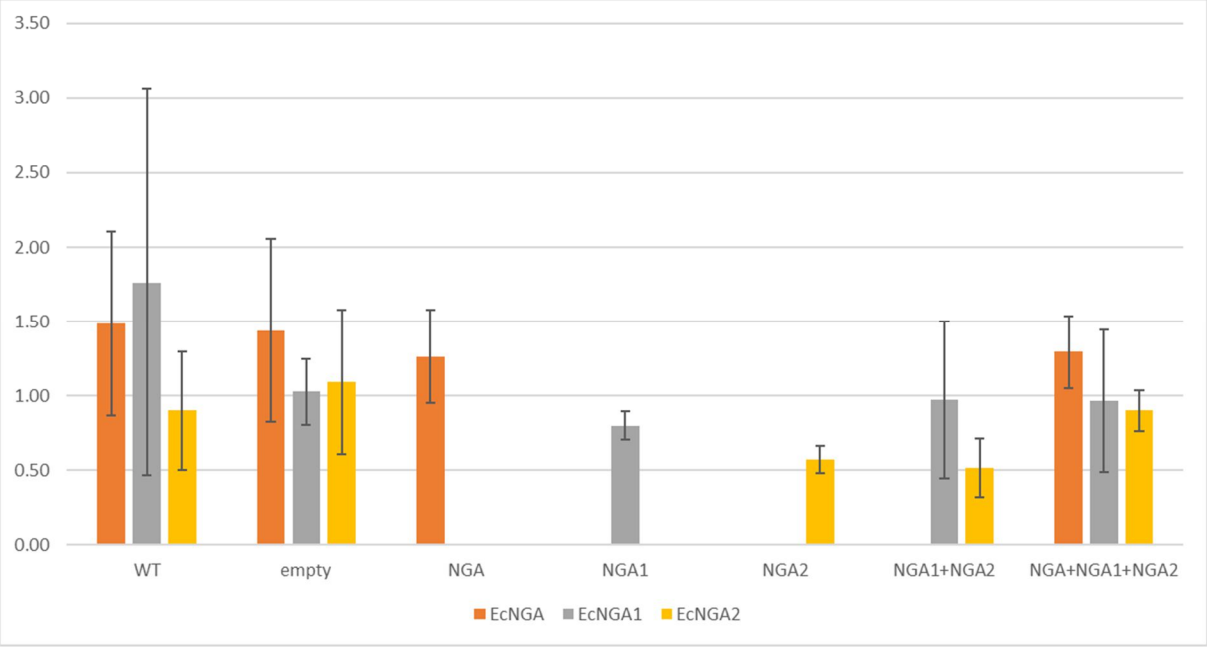

Figure 3.21: *Expression analysis of EcNGA knock-downs. Expression is normalzied to EcGAPDH and given relative to the expression in the empty vector control.*

Figure 3.22: *Defects in style and stigma development in E. californica plants VIGS treated for knock-down of EcNGAs. All flowers defects were observed in flowers at anthesis. a) wild-type style and stigma, b) pTRV empty control, c) - e) show different amounts of stylar overproliferation with stigma-like extensions, c) EcNGA1+EcNGA2 VIGS, d) EcNGA1+EcNGA2 VIGS, e) EcNGA2 VIGS, f) lack of stigmatic papillae at the tip of otherwise normal stigmatic protrusions in EcNGA1 VIGS, g) complete lack of stigmatic tissues in EcNGA2 VIGS*

Like for *EcSPT1* and *EcCRC*, putative regulatory downstream target genes of the *EcNGAs* were idenified based on data from *A. thaliana*. To reveal possible conserved regulatory pathways, the putative auxin signalling factors *EcYUC1/4*, *EcPIDs* and *EcWAG* were chosen for an expression analysis. In *E. californica* and the other considered Ranunculales species, one gene was identified as orthologue to the *AtWAGs*. For both *AtPIDs* one orthologue each was identified in *P. somniferum*, in the other considered species varying numbers of orthologues were identifed: For *AtPID2* one orthologue was identified each in all considered species, while for *AtPID* two orthologues were identified in *E. californica* but none in *A. trichipoda* and *A. caerulea* (fig. 3.23).

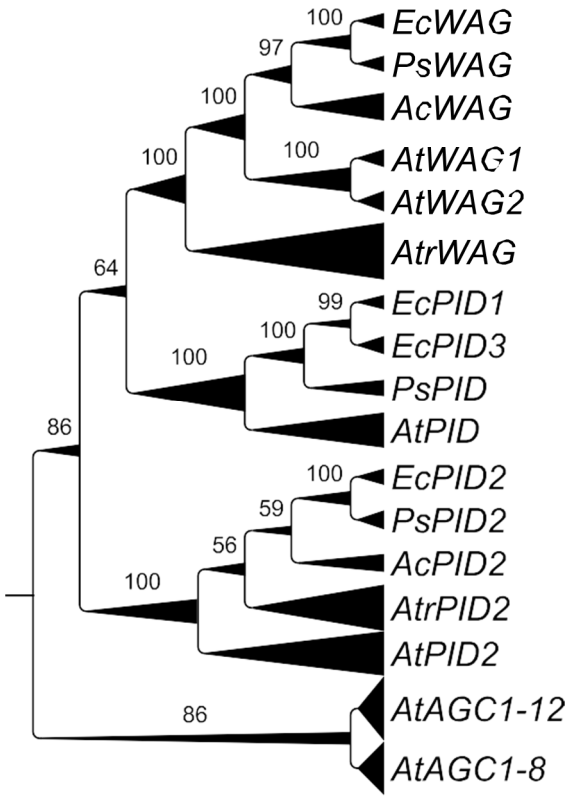

Figure 3.23: *ML tree of AGCVIII protein kinase family members PIDs and WAGs rooted with AtAGC1-12 and AtAGC1-8. Calculated, using protein sequences from another Papaveraceae species (P. somniferum (Ps)), another ranunculales species (Aquilegia caerulea (Ac)), the basal angiosperm Amborella trichopoda (Atr) in addition to the sequences from A. thaliana (At) and E. californica (Ec); 500 bootstraps. Outgroups chosen according to [135]. Bootstrap values higher than 50 were accepted as reliable. Branch lengths are depicted as width of the triangle at the respective branch. Unnamed paralogous sequences are numbered for better overview.*

Like for the *EcSPT1-EcSTY-L* and *EcCRC-EcYUC1/4* putative regulation pairs, no correlation of the expression of one or more putatively regulating EcNGAs with the putative downstream target gene expression could be detected (fig. 3.24).

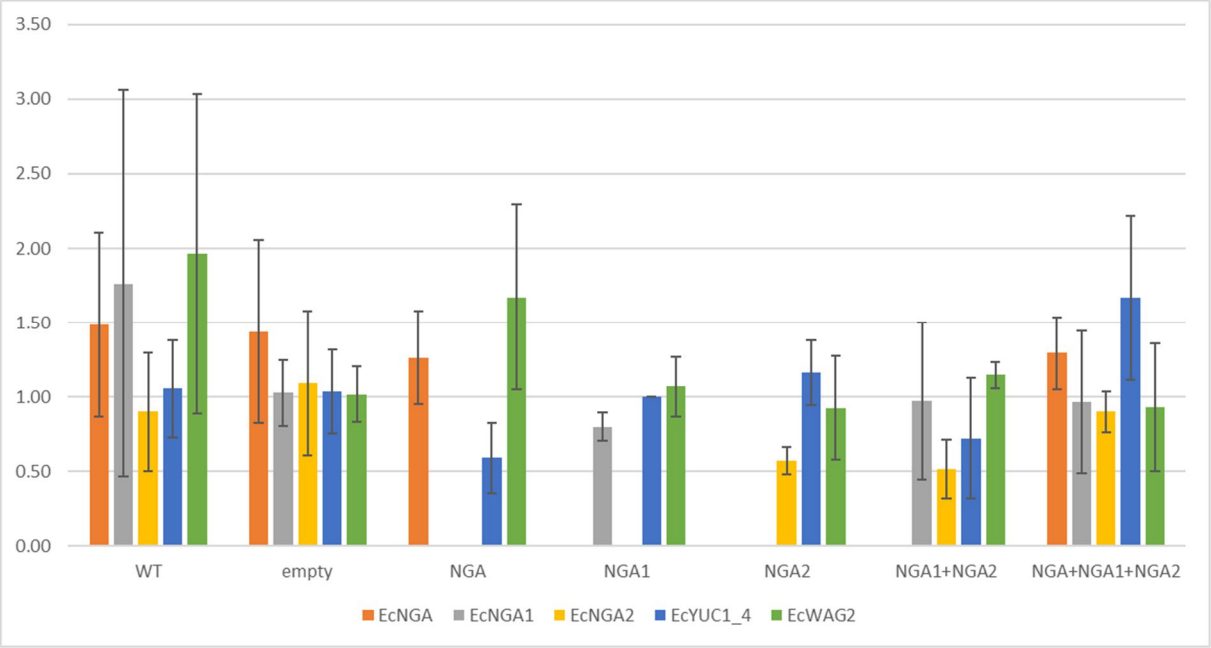

Figure 3.24: *Expression analysis of YUC1/4 and WAG2 in EcNGA VIGS plants. Expression data are based on 2 to 6 biological replicates per treatment group, depending on the number of plants showing phenotypic differences to the controls. Expression is normalized to EcGAPDH expression and plotted relative to the average expression of that gene in pTRV2-empty treated plants.*

In VIGS experiments conducted here, generally a low penetration of the effect within a plant batch, and even within single plants was observed, with affected flowers found side by side with unaffected ones throughout the experiments. Only the pTRV2-*EcCRC* construct, published by Orashakova *et al.* 2009 had a good efficiency and consistency. The high variation in expression strength within the wild-type control plants and the unpredictable changes in phenotype induced by pTRV2-empty treatment posed further obstacles in evaluation of VIGS experiments in *E. californica*.

As a general rule, the empty vector control treated plants often differed significantly from untreated plants in the monitored parameters. To avoid this, a construct containing a GFP fragment was tested as control in the last experiment. As expected, no obvious flower phenotype was observed after inoculation with the GFP VIGS construct (data not shown). Expression of the *EcNGAs* and *EcYUC1/4* was analyzed as an example in *pTRV-GFP* treated plants (suppl. fig. 6). The *EcNGAs* seem expressed in a comparable manner in all treatment groups, *EcYUC1/4* expression seems to be lower in the *GFP* VIGS plants. Because no further VIGS experiments were carried out, statistical analysis was omitted, but would be advisable before further use.

3.2 Y2H and BiFC show high numbers of interfamily Protein-Protein-Interactions in *E. californica*

Because this thesis is not limited to the evaluation of functional conservation of single genes, protein-protein interaction (PPI) networks of *E californica* proteins were generated here for comparison with published data of other species. In the Y2H and BiFC PPI assays a total of 54 different interactions could be detected, of which twelve were reproduced in two or three independent testings.

3.2.1 Identification of further candidate genes in *E. californica*

New candidate genes for PPI studies in *E. californica* were identified as part of this work. Based on PPI studies in *A. thaliana* conducted by H. Herrera-Ubaldo (personal communication), carpel developmental regulators were chosen, of which orthologues were identified in the Eschscholzia Genome Database (EGD) by the Kazusa DNA Research Institute (Chiba, Japan) [382], and new *E. californica* carpel transcriptome data [395], as well as their transcript and genomic sequences. As proposed before, no *ALC*-, *HAF* -, *IND*-, or *SHP*-like transcript or genomic sequences were found in the *E. californica* sequence databases [23, 388].

In the process of assigning genomic loci to the known *E. californica* transcript sequences (e.g. [209, 346, 385]; see supplemental table 7 for complete list), further related transcript and genomic sequences were identified. All alignments, containing transcript and genomic sequences as well as any used primer sequences, are attached as .fasta files in the electronic supplement.

During re-evaluation of the previously identified transcript sequences in comparison with the new RNAseq data, no genomic data or transcript data for the *EcLUG2* transcript published in [391] could be found. Instead the previously identified *EcLUG2* transcript resembles a mixture composed of sequences identical to parts of the other three *EcLUG* transcripts and might be an assembly artefact or caused by a number of homologous recombination events. Figure 3.25 shows an exemplary fragment of the alignment. The complete alignment can be found in supplemental figure 8.

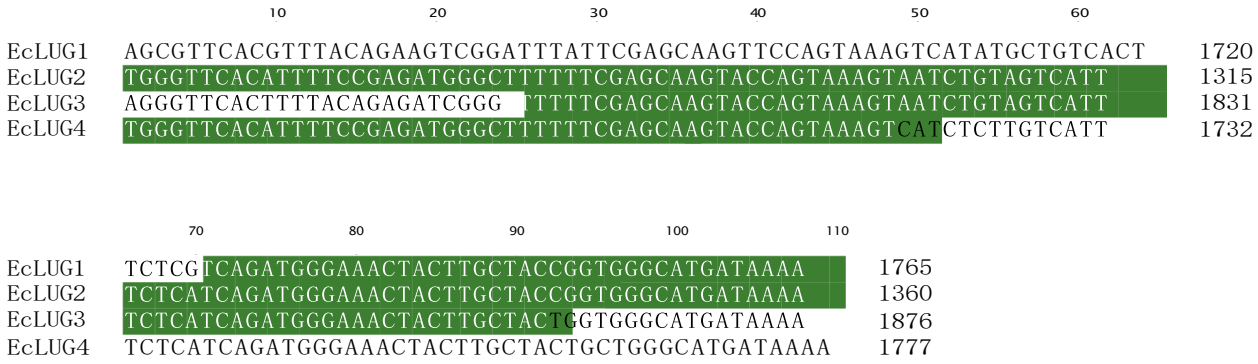

Figure 3.25: *Nucleotide positions 1800 to 1909 of an alignment of EcLUG genes. The sequences identical to the EcLUG2 sequence are marked in green.*

Another *EcLUG* transcript was identified here instead and is referred to as *EcLUG4* in this work. Together with the two previously identified *EcLUG* genes, *EcLUG1* and *EcLUG3*, it forms a well-supported group with the other Ranunculales *LEUNIG* genes (1 in *P. somniferum* and 2 in *A. carulea*), which together with the single *AtLUG* and 2 *A. trichopoda LUG* genes is clearly divided from the *LEUNIG HOMOLOGs* as well as the outgroup (compare fig. 3.26).

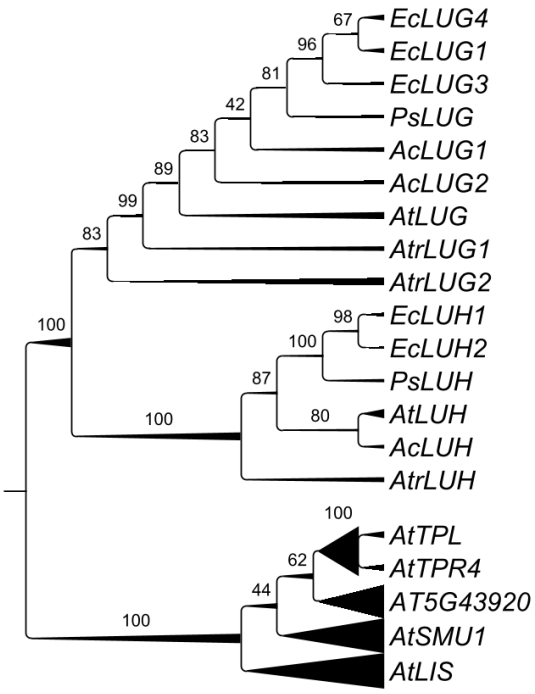

Figure 3.26: *ML tree of LUG and LUH proteins rooted with AtLACHESIS (AtLIS), AtSUPPRESSOR OF MEC-8 AND UNC-52 1 (AtSMU1), AT5G43920.1, AtTPL, and AtTPR4. Calculated, using protein sequences from another Papaveraceae species (P. somniferum (Ps)), another ranunculales species (A caerulea (Ac)), the basal angiosperm Amborella trichopoda (Atr) in addition to the sequences from A. thaliana (At) and E. californica (Ec); 500 bootstraps. Outgroup as defined in [391]. Bootstrap values higher than 50 were accepted as reliable. Branch lengths are depicted as width of the triangle at the respective branch. Unnamed paralogous sequences are numbered for better overview. The previously unknown EcLUG sequence is named EcLUG4 here, while the potentially artificial EcLUG2 sequence is not included.*

Of EcATH1.2, EcARR14, and EcBEL1 only one homologue each was identified in *E. californica* forming well-supported groups with the respective Ranunculales homologues and clear separation from the respective outgroups (fig.3.27). Constructs containing EcLUG1, EcATH1.2, EcARR14, and EcBEL1 were cloned for the PPI experiments conducted here.

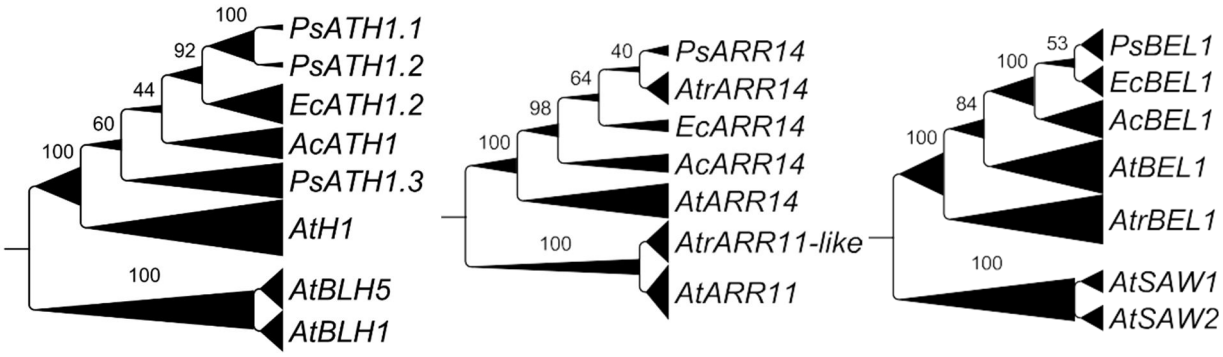

(a) **(b)** **(c)**

Figure 3.27: *ML tree of (a) EcATH1 rooted with A. thaliana BEL1-LIKE HOMEOBOX (BLH) proteins 1 and 5, (b) B-type AUTHENTIC RESPONSE REGULATORs (ARR) proteins rooted with ARR11 of A. thaliana and A. trichopoda and (c) BLH transcription factors rooted with AtSAWTOOTH1 (AtSAW1) and 2. Calculated, using protein sequences from another Papaveraceae species (P. somniferum (Ps)), another ranunculales species (A caerulea (Ac)), the basal angiosperm Amborella trichopoda (Atr) in addition to the sequences from A. thaliana (At) and E. californica (Ec); 500 bootstraps. Outgroups chosen according to(a) [216], (b) [281], and (c) [393]. Bootstrap values higher than 50 were accepted as reliable. Branch lengths are depicted as width of the triangle at the respective branch. Unnamed paralogous sequences are numbered for better overview.*

In the PPI experiments a EcAGL6 construct published before [394] was used. Here a close paralogue was identified for EcAGL6-like1, referred to as EcAGL6-like2. Both form a well-supported group with the other Ranunculales and *A. trichopoda* AGL6-like genes and show clear separation from AtAGL6 and AtAGL13, as well as from the outgroup (fig.3.28).

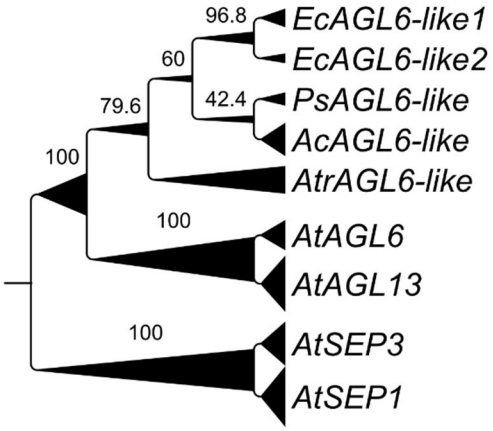

Figure 3.28: *ML tree of AGL6-like proteins rooted with two SEP proteins of A. thaliana. Calculated, using protein sequences from another Papaveraceae species (P. somniferum (Ps)), another ranunculales species (A caerulea (Ac)), the basal angiosperm Amborella trichopoda (Atr) in addition to the sequences from A. thaliana (At) and E. californica (Ec); 500 bootstraps. Outgroup chosen according to [187]. Bootstrap values higher than 50 were accepted as reliable. Branch lengths are depicted as width of the triangle at the respective branch. Unnamed paralogous sequences are numbered for better overview. For EcAGL6-like a closely related homologue was identified here. The previously known gene is indicated as EcAGL6-like1, the newly identified as EcAGL6-like2.*

In Y2H assays, tests were considered as positive for interaction, if the mated yeast grew on triple drop-out media (SD-L/-W/-H) and showed staining in the blue-white assay. Mated yeast that neither grew nor showed staining was interpreted as no interaction of the tested proteins. If the mated yeast only showed growth or staining, the result was interpreted as inconclusive and was not considered for the results presented here.

Neither were results of tests considered, if one construct showed interactions in negative control tests with the empty AD- or BD-plasmids, containing no test protein, or if one tested protein showed no interactions with any protein partner included in the test. The latter refers to 13 Y2H constructs, as well as three BiFC constructs, showing no interactions in any of the matchings. Signals in the negative control combinations with empty Y2H plasmids excluded both Y2H constructs for EcTCP2, the BD-EcSPT1, BD-EcWIP, BD-EcYAB1, and BD-EcYAB2 Y2H constructs, as well as the YC-EcARR14 BiFC construct giving a fluorescence signal with an empty YN construct in the BiFC assays. The two different EcSEP1 constructs used here contain variants that differ by two amino acids and showed comparable results in all tests except the one against AD-EcNGA.

The results of all conducted Y2H experiments of this thesis are summarized in table 3.4. Interactions are marked with ‘+’ or ‘++’, no observed interactions with ‘-‘ and inconclusive results with ‘+-‘. Green cells refer to a comparable result than is published for the respective *A. thaliana* orthologues, orange cells, indicate different behaviour from the respective *A. thaliana* orthologues, constructs marked in red showed interactions when combined with the empty ‘opposite’ construct and the data were excluded from the further interpretation.

Positive results for some BD constructs in the test with an empty AD plasmid were unexpected, because all yeasts transformed with the BD plasmid were tested for autoactivation before, showing no growth on the selective media. Based on the negative autoactivation test for all BD constructs, the positive results seen for some of them in the Y2H screen may stem from direct interactions of the tested proteins with the activation domain coded by the empty AD plasmid.

For the BiFC test, YFP signals in the cell nuclei, visible after 1 s of exposure were interpreted as interaction, no YFP signal after 6 s of exposure was interpreted as no interaction. YFP signals visible after 6 s of exposure but not after 1 s were considered uncertain and in need of further testing (compare figs. 3.29 and 3.30). Combinations of proteins giving these weak signals might not interact in physiological concentrations, or only in absence of the preferred interaction partners, or the interactions occurring between the native proteins might be sterically hindered by the fluorescence tag fused to the proteins in BiFC. Further tests with the tags fused in other positions to the proteins, might give clearer results.

Table 3.4: *Table of all tested interactions in the Y2H assays. '-': no interaction, '+': weak interaction, '++': strong interaction, '+-': inconclusive result, green cells: same interaction type published for Arabidopsis thaliana, orange cells: opposite interaction type published for Arabidopsis thaliana, white cells: no data from Arabidopsis thaliana, red cells: data not considered further due to interaction in negative control*

AD \ BD	empty	EcAG1ikc	EcAG2ΔMADS	EcAGL11orf	EcBP	EcCRC	EcDEF1ΔMADS	EcDEF2ΔMADS	EcEBS	EcLUG1	EcNGA	EcPHX	EcSEP1cds	EcSEP1cds +6nt	EcSEP3	EcSEP3 (ORF)	EcSPT1	EcSTM1	EcSTM2	EcTCP2	EcWIP	EcYAB1	EcYAB2
empty	-	+-	-	-	-	-	-	-	-	-	-	-	-	-	-	-	+	-	-	+-	+	+	+
EcAG1ikc	-	-	-	-	-	-	-	-	-	-	-		-	-		-	+	-	-	+-	+	-	+
EcAG2ΔMADS	-	-	++	-	+	-	++	++	-		-	+	+	+	-	-	+	+-	+	+-	+	+	+
EcAGL11orf	-	-	-	-	-	-	-	-	-	-	-	-	-	-	-	-	+			+-	+	-	+
EcAGL6	-	-	-	-	-	-	-	-	-		-		-	-	-	-	+	-		+-	+	-	+
EcATH1.2	-	-	-	-	++	-		-	-	-	-	+-	-	-	-	-	+		++	+-		++	++
EcCRC	-	-	-	-	-	-	-	-	-	-	+-		-	-	-	-	++	-	-	+	+	+	+
EcDEF1ΔMAD	-	-	+	-	-	-	++	+	-	-	-		++	++	-	-	+	-	+	+-	+	+	+
EcDEF2ΔMAD	-	-	+	-	-	-	-	-	-	-			++	+	-		+	-	-	+-	+	+	+
EcDEF3ΔMAD	-	-	+	-	-	-	-	+	-	-	-		++	+	-		+	-	-	+-	+	+	+
EcEBS	-	-	+	-	-	-	+		-	-	-	-	++	++	-	-	+	-	-	-	+-	+	+
EcLUG1	-	-	-	-	-	-	-	-	-	-	-	-	-	-	-	-	+	-	-	+-	+-	-	+
EcNGA	-	+-	+	-	+-	++	++	++	-	-	++		+	-	-	-	++	+	+	+	+	++	++
EcPHX	-	-	-	-	+-	-	-	+-	-	-	-	+	-	-	-	-	++	+-	+	+-	+	+	+
EcSEIΔMADS	-	-	-	-	-		++	++	-	-	-		-	-	-	-	++	+	-	+-	+	+-	+
EcSEP1cds	-	-	++	-	++	-	++	++	-	-	-		+	+	-	-	++	-	+	+-	+	+	+
EcSEP3	-	-	-	-	-	-	-	-	-	-	-	+	-	-	-	-	++		-	+-	+	+-	+
EcSEP3 (ORF)	-	-	-	-	-	-	-	-	-	-	-	-	-	-	-		++	-	-	+-		-	+
EcSTM1	-	-	-	-	+-	-	-	-	-	-	-		-	-	-		++	+-	+-	-	+-	+	+
EcSTM2	-	-	++	-	+	-	-	++	-	-	-		+-	-	-		++	+	+	-	-	+	+
EcTCP2	+	++	+-	+-	++	-	++	++	-	-	++		+	+-	+	++	++	++	++	+	+	++	++
EcWIP	-	-	-	-	-	-	-	-	-		-	-	-	-	-		++	-	-	+-	+-	-	+
EcYAB1	-	-	-	-		-	-	-	-	-	-	-	-	-	-	-	++	-	-	+-	+	+	+
EcYAB2	-	-	-	-	-	-	-	-	-	-		-		-	-		++	-	-	+-	+-	-	+

The fluorescent granulae, seen in some tested combinations, are thought to be protein aggregations caused by high expression of the BiFC constructs or high stress levels in the cells. If possible, cells containing granulae were excluded from the evaluation. They could be seen in all leaves transformed with the YC-BP constructs, but as well in other combinations.

For 70 combinations of EcMADS-box proteins tested here, Y2H or BiFC data were published before [346, 394]. Of these, 26 could be reproduced in this study, 32 were not retested. While eleven were identified as not-interacting here but as interacting before and one interaction was identified here, but was non-interacting before. In addition to the old AD-EcSEP3(ORF) and BD-EcSEP3(ORF) constructs, new AD- and BD-EcSEP3 constructs (AD-EcSEP3, BD-EcSEP3) were used here. For both sets, no interactions were found except for the AD-SEP3/BD-PHX interaction of the new construct.

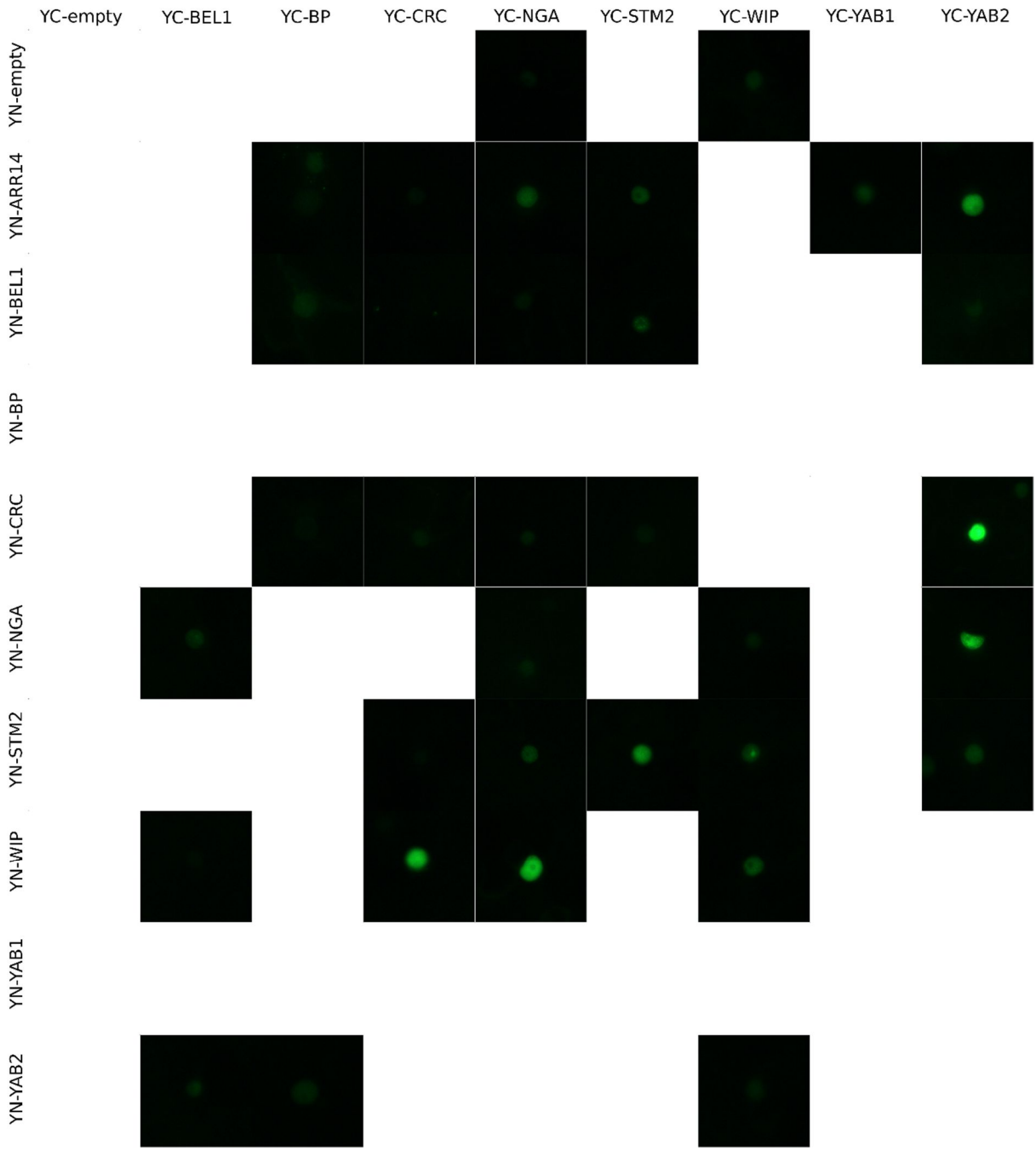

Figure 3.29: *Summary of all BiFC experiments. YFP fluorescence at 1 s exposition time in tobacco leaves. The fluorescence signal is concentrated in the nuclei of the transformed cells. A clearly visible signal after 1 s was interpreted as interaction.*

All conducted Y2H tests are summarized in table 3.4 and figures 3.29 and 3.30 show the results of the conducted BiFC tests. All positive interactions discovered in this work are combined in a protein interaction network shown in figure 3.31, for a tabular overview see table 10 in the supplemental material. From these interactions, three protein pairs were found, sharing most interaction partners identified in this work: EcSTM2 and EcNGA, EcDEF1 and EcDEF2, and EcAG2 and EcSEP1.

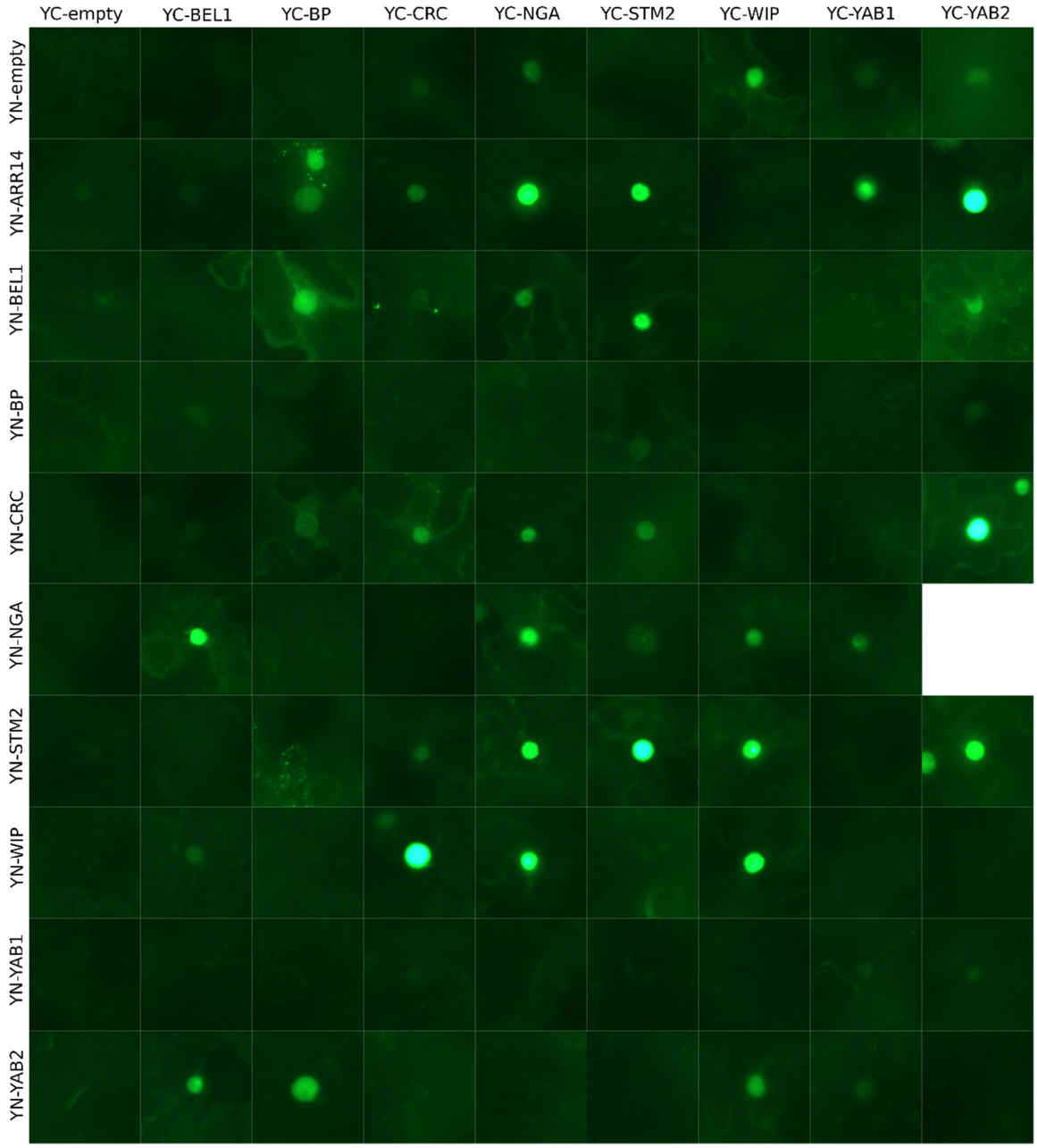

Figure 3.30: *Summary of all BiFC experiments. YFP fluorescence at 6 s exposition time in tobacco leaves. The fluorescence signal is mostly concentrated in the nuclei of the transformed cells, but in some combinations fluorescent granulae are observed in the periphery. No signal after 6 s was interpreted as no interaction.*

EcSTM2 and EcNGA interact with a majority of the tested proteins from a variety of families: ARR, BEL, KNOX I, MADS-box and WIP TFs. Only the interaction of EcNGA with YABBY family TFs is not shared by EcSTM2, while the interactions with ECBP, EcATH1, and EcPHX are restricted to EcSTM2. EcAG2 and EcSEP1 both interact with the majority of MADS-box transcription factors as well as EcBP, EcSTM2, and EcNGA. Similarily proteins interacting with both, EcDEF1 and EcDEF2, are mostly from the MADS-box TF family, except for EcSTM2 and EcNGA. Interestingly, both tested YABBY proteins interact directly with EcNGA, as well as with other EcNGA interactors. The MADS-box proteins on the other hand form a tight-knit network within the transcription factor family with only a limited number of non-MADS proteins being connected to it.

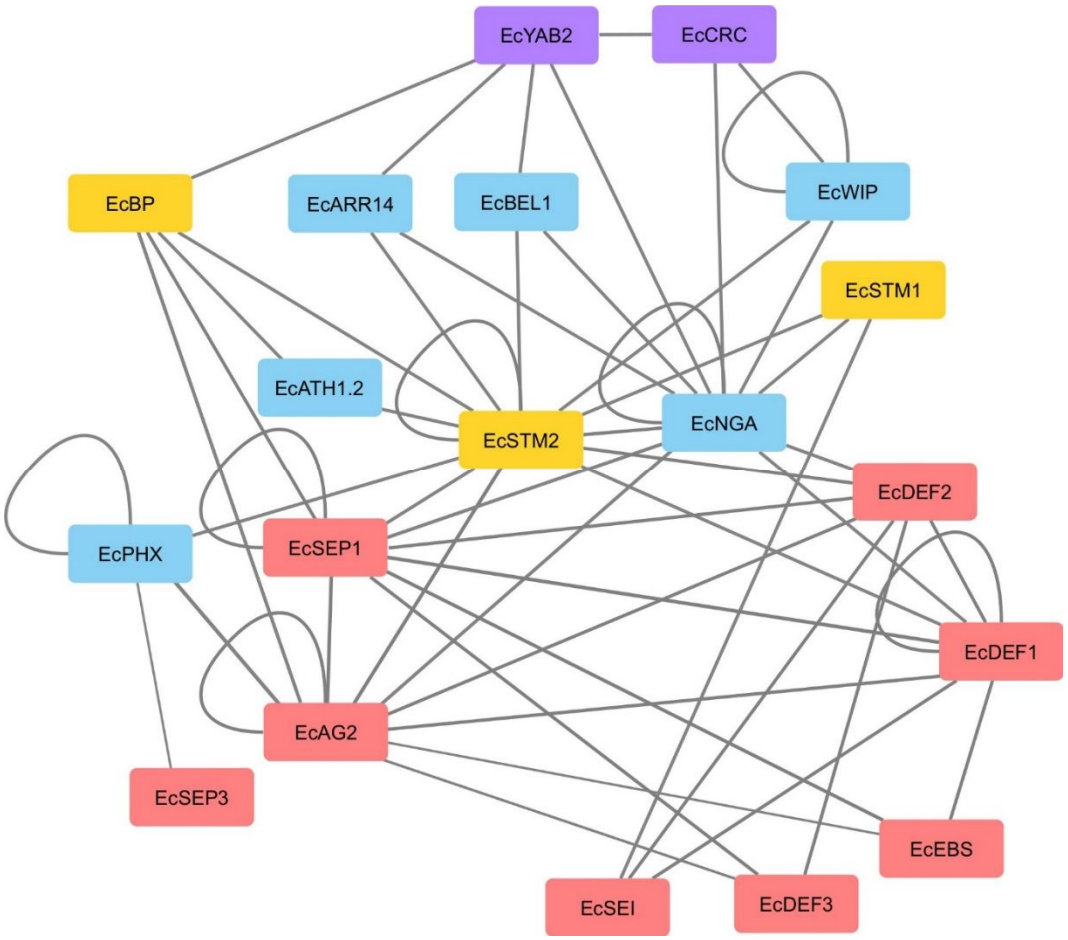

Figure 3.31: *Summary of physical interactions between E. californica proteins observed in Y2H and BiFC assays. Boxes: proteins, lines: interactions; orange: class I KNOX protein, violet: YABBY protein, red: MADS-box protein, blue: other protein family.*

3.3 Protein-Protein-Interaction networks in *E. californica* vary in their complexity between tissues and developmental stages

To determine if the protein-protein interactions detected in the conducted Y2H and BiFC assays are of biological relevance, possible co-expression of the target genes was assessed. Expression strength as transcripts per million (TPM) was calculated by O. Rupp based on carpel transcript data by K. Kivivirta [395] and SRA files available at the NCBI server (ERR364334, ERR364335, ERR364336, ERR364337, ERR364338, SRR341948). If expression (TPM>0) was detected in at least one of the replicates, the respective gene was assumed to be expressed in the respective organ and developmental stage and therefore a potential interactor. The figures 3.32 to 3.34 show the resulting stage- and tissue-specific PPI subnetworks. No TPM data are available for *EcDEF2* and *EcWIP*, because the only transcripts of these genes in the dataset contained more than one ORF. Supplemental table 11 summarizes all TPM values of the relevant transcripts.

In young bud stages (S1 and S2 according to [395]) and the stem sample (SRA file ERR364335) all proteins shown in fig. 3.31 are found, except that the TPM values of *EcDEF2* and *EcWIP* are unknown. In medium buds (S3 according to [395]) no expression of EcBP, EcSTM2, EcEBS, and EcDEF3 was found (fig. 3.32, upper), while in old buds (S4 according to [395]) EcEBS and EcDEF3 ae expressed but no EcSEI (fig. 3.32, lower). From the flower bud sample (SRA file ERR364337), the considered YABBY TFs, EcATH1.2, EcNGA, and the MADS-box TFs EcAG2, EcDEF3, EcEBS, and EcSEI are absent (fig. 3.33, upper), while in the developing fruit sample (SRA file ERR364338) only EcSTM2 and EcDEF3 are missing (fig.3.33, lower). In the root samples (SRA files ERR364336 + SRR341948) the network ist reduced by absense of the considered YABBY TFs, EcATH1.2, EcAG2, EcDEF3, EcEBS, and EcSEI (fig 3.34, upper) und further reduced to EcPHX, EcARR14, EcBEL1, EcSTM1, EcNGA, EcDEF1, and maybe EcWIP and EcDEF2 in the leaf sample (SRA file ERR364334 ,fig. 3.34, lower).

Interestingly, the complexity of the observed protein interaction networks decreases from early to late stages of bud development. Expression of the KNOX I genes *EcBP* and *EcSTM2* is absent in older bud stages and that of the B-class genes *EcDEF3* and *EcSEI* declines (compare suppl. table 11). On the other hand, the expression of the B_{SISTER} gene *EcEBS* is absent in the bud stage S3 but rises again in the bud stage S4 and continues in the fruit.

In the examined stem sample all tested factors are expressed, like in the early bud stages S1 and S2. In the bud, root and leaf SRA files no, expression of *EcATH1.2*, the tested YABBY genes (*EcYAB2* and *EcCRC*), and most of the tested MADS-box TFs (*EcAG2*, *EcSEI*, *EcDEF3*, and *EcEBS*) was found. Further genes not expressed in some stages are *EcNGA* in the bud sample, and the *EcSEP*s and KNOX I genes *EcBP* and *EcSTM2* in the leaf sample.

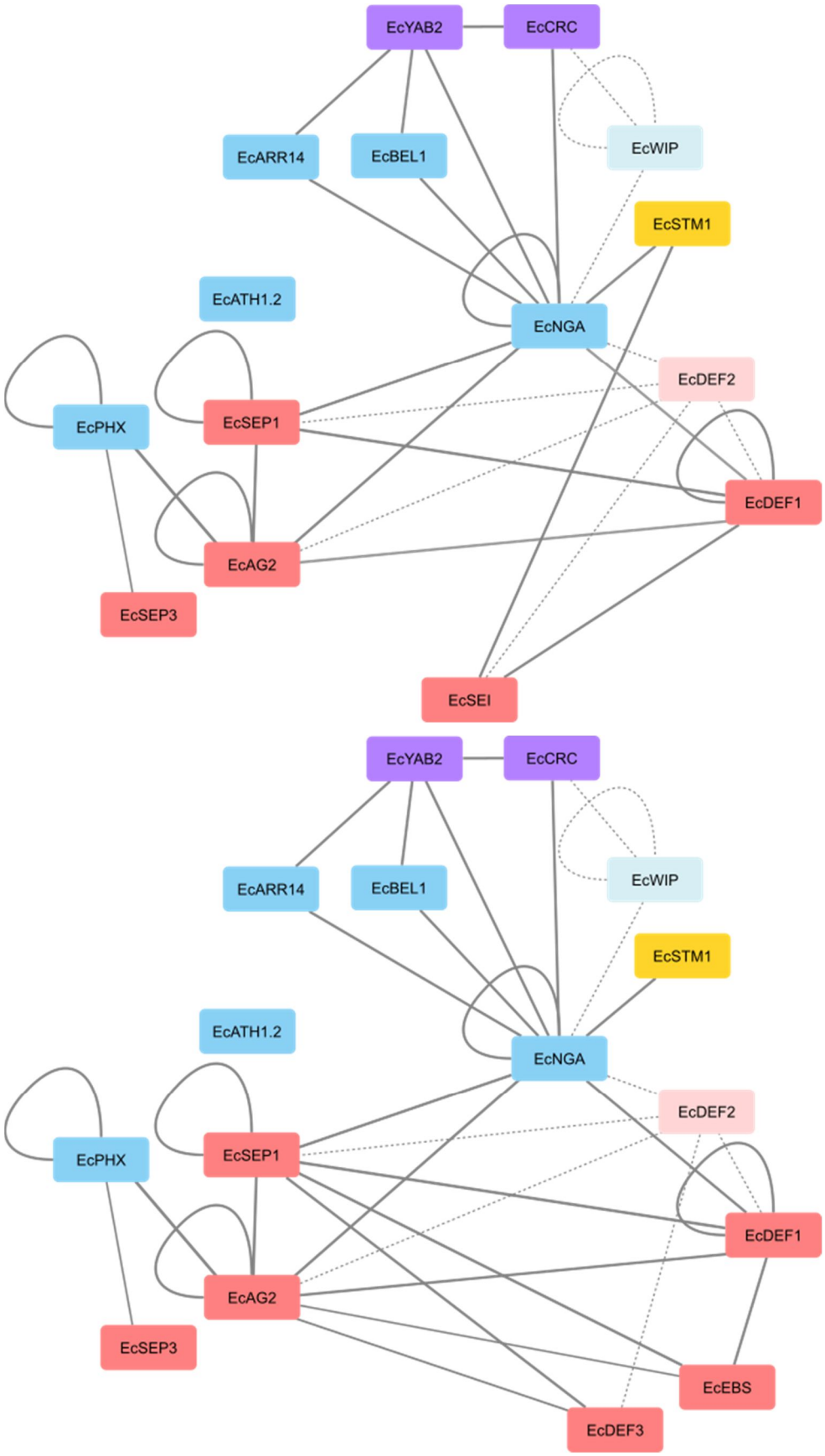

Figure 3.32: *Interaction networks of E. californica carpels in medium (upper: S3), and old (lower: S4) buds (stages defined in [395]). Interactions in the network are based on PPIs detected here (section 3.3) and expression data for the respective stages calculated as TPM values, rounded to one digit (section 4). Colours as described for fig. 3.31. Lighter coloured boxes indicate unknown TPM values, interactions of these proteins are shown as dashed lines.*

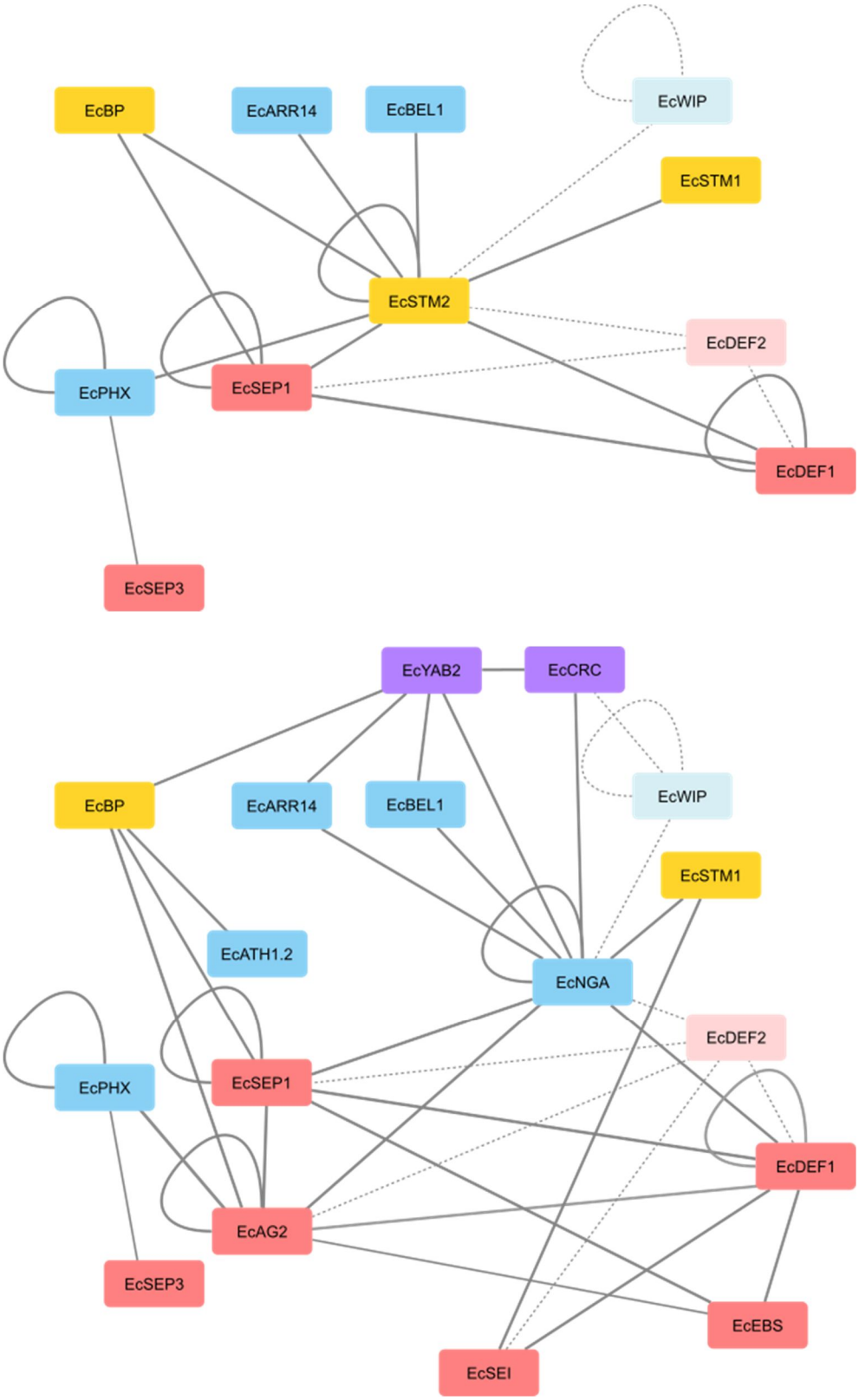

Figure 3.33: *Interaction networks of E. californica tissues (SRA files) based on PPI (section 3.3) and expression data for the respective stages calculated as TPM values (suppl. sec. 4, TPM>0). The SRA files were based on following tissues samples: flower bud ERR364337 (upper), developing fruit ERR364338 (lower). Colous as defined in fig. 3.32.*

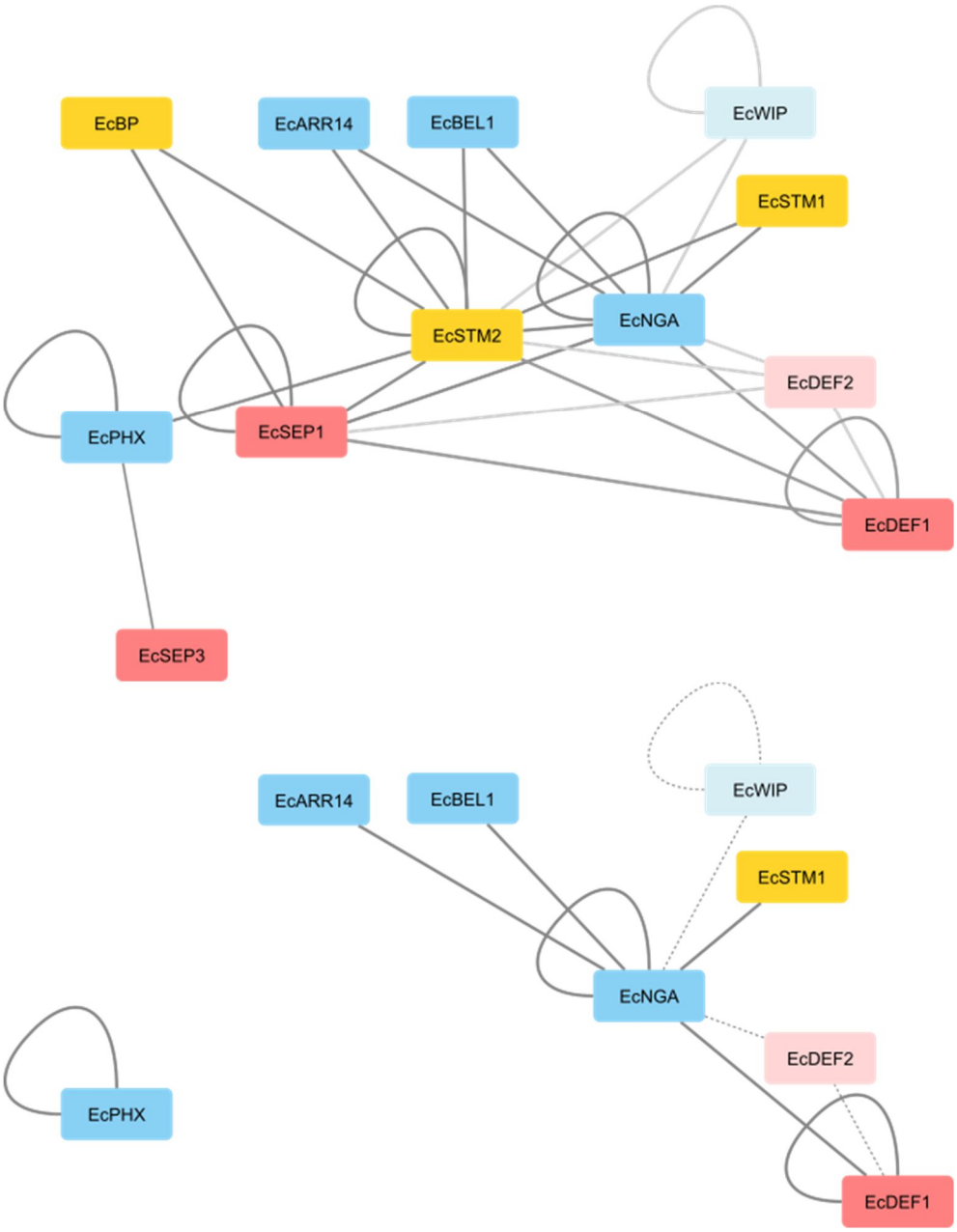

Figure 3.34: *Interaction networks of E. californica tissues (SRA files) based on PPI (section 3.3) and expression data for the respective stages calculated as TPM values (suppl. sec. 4, TPM>0) The SRA files were based on following tissues samples: stem ERR364335 (upper), root ERR364336 + SRR341948 (middle), and leaf ERR364334 (lower). Colours as described for fig. 3.32.*

4 Discussion

4.1 Effectiveness of VIGS is dependent on many factors

VIGS experiments conducted in this work demonstrated points, that need to be considered in the planning of further experiments: (1) Growth conditions were identified to have a major impact on plant development and bud abortion rate, as well as reproducibility of phenotypes in control plants and VIGS efficiency (section 3.1). (2) A low penetration of the knock-down phenotype within a plant was observed here and in other labs and species, as well [258, 371], leading to highly varying phenotype severity between the flowers of a plant. This can explain the lack of correlation of target gene expression in the first bud with the phenotype of later flowers, as discussed above. The low percentage of affected flowers thus complicates or even prevents the detection of subtle phenotypes by statistical means. Double knock-down of the GOI in combination with a flower-specific pigment is used in *A. caerulea* and might be adapted for *E. californica*, since some carotinoids were found to be flower-specific [432]. In [414], use of a GFP-tagged TRV vector system is presented, which is visible *in planta* using hand-held UV lamps. (3) A high remaining expression rate of the target genes was detected in many buds (compare table 3.3 and figs. 3.9, 3.18, and 3.21). The described problems probably are dependent on the constructs used, because for the *EcCRC* VIGS remaining expression rates below 10 % were determined for plants showing the CRC knock-down phenotype and usually all flowers of a plant were equally affected. It thus seems advisable to test several constructs for each target gene. Recently, the influence of secondary structure of the siRNAs on VIGS efficientcy was highlighted [430] (4) In many cases the values measured for parameters in wt control plants where not distributed normally and empty vector controls differed significantly from untreated wt plants. This may be caused by a too low number of individuals (≤14) included per experiment. Similarly, the low number of affected flowers could be balanced out by more inoculated plants. An influence of the empty vector on control plants was reported before [437], so a GFP-containing VIGS construct was tested as a possible control construct and showed no obvious differences from the untreated plants.

All in all, VIGS experiments were enhanced by optimizing growth conditions and could be further improved by selection of controls.

4.2 The complexity of Protein-Protein-Interaction networks varies between tissues and developmental stages

PPI data in this work were generated by yeast-based as well as *in planta* methods. In some

cases, interactions were observed in BiFC but not in Y2H or *vice versa*. This can have several reasons, that need to be considered: (1) The Y2H assay was incubated at 30 °C for optimal yeast growth conditions, but plant protein dimers may not be stable at these elevated temperatures compared to normal plant growth conditions. Temperature-sensitive interactions are reported for some *A. thaliana* proteins [354]. (2) Native protein conformations may be disturbed by the tags used in the assays or high ambient temperatures. (3) Additional factors may be needed for interactions between the plant proteins, that are not present in yeast cells. This may be scaffolding proteins or non-protein factors like phytohormones [127, 438]. (4) Spontaneous false-negative or false-positive results may occur, that can be reduced by testing of more technical replicates.

Taking into account not only the PPI data generated in this work (supplemental table 9), but as well previously published interaction data on *E. californica* proteins [346, 394], interaction networks of the considered proteins were created for different developmental stages and tissues (compare figs. 4.1 to 4.5). Similar to the networks shown in figures 3.31 to 3.34, the overall complexity decreases in the extended networks over the course of bud development (fig. 4.1 and fig. 4.2) and further in root and leaf tissues (fig. 4.3 to 4.5). The additional data from the literature add EcAG1 into the networks of buds and stem and increase the general density by adding further MADS-MADS-interactions. This suggests a higher amount of transcription factors may be needed for initiating the different carpel tissues (in young bud stages) than for their outgrowth (in older bud stages), as is suggested for *A. thaliana* [397]. Alternatively, the observation may be biased by the chosen set of transcription factors considered in this work, because in the underlying datasets the total number of sequences counted as expressed (TPM >0) is more or less constant over all stages.

Protein pairs, sharing most interaction partners, were identified above (sec.3.2). They may form core complexes, recruiting different interaction partners in a specific spatio-temporal pattern. Stage-specific changes in regulatory PPI were identified before [397], for the MADS-box proteins AtAP1 and AtSEP3, possibly acting as pioneer TFs in tetrameric MADS-box TF complexes [173, 396]. For several MADS and non-MADS TFs, stage-specific expression during gynoecium development in *A. thaliana* was shown, resulting in a stage-specific subset of interactors for each protein [397]. This further supports the idea of protein complexes of changing composition in the progress of differentiation and development of *E. californica* carpel tissues. The possible EcSTM2-EcNGA hub may be recruited to the promoter regions by tetrameric MADS-box TF complexes as a first step, followed by secondary binding of more stage- and tissue-specific non-MADS TFs. For the homologous *A. thaliana* proteins, no direct PPI with MADS proteins is reported, instead BEL and NTT both interact with SEP3, AG, and STM, and NTT as well with NGA2. Thus, in both species a protein complex containing the respective homologoues of STM, NGA, AG, SEP, BEL, and WIP/NTT could form connected by species-specific interactions (compare fig. 4.7). This may be interpreted as a kind of conserved module of the network. Rewiring conserved modules may be a much simpler way to restructure existing networks for new functions, than rewiring all proteins of the network

independently.

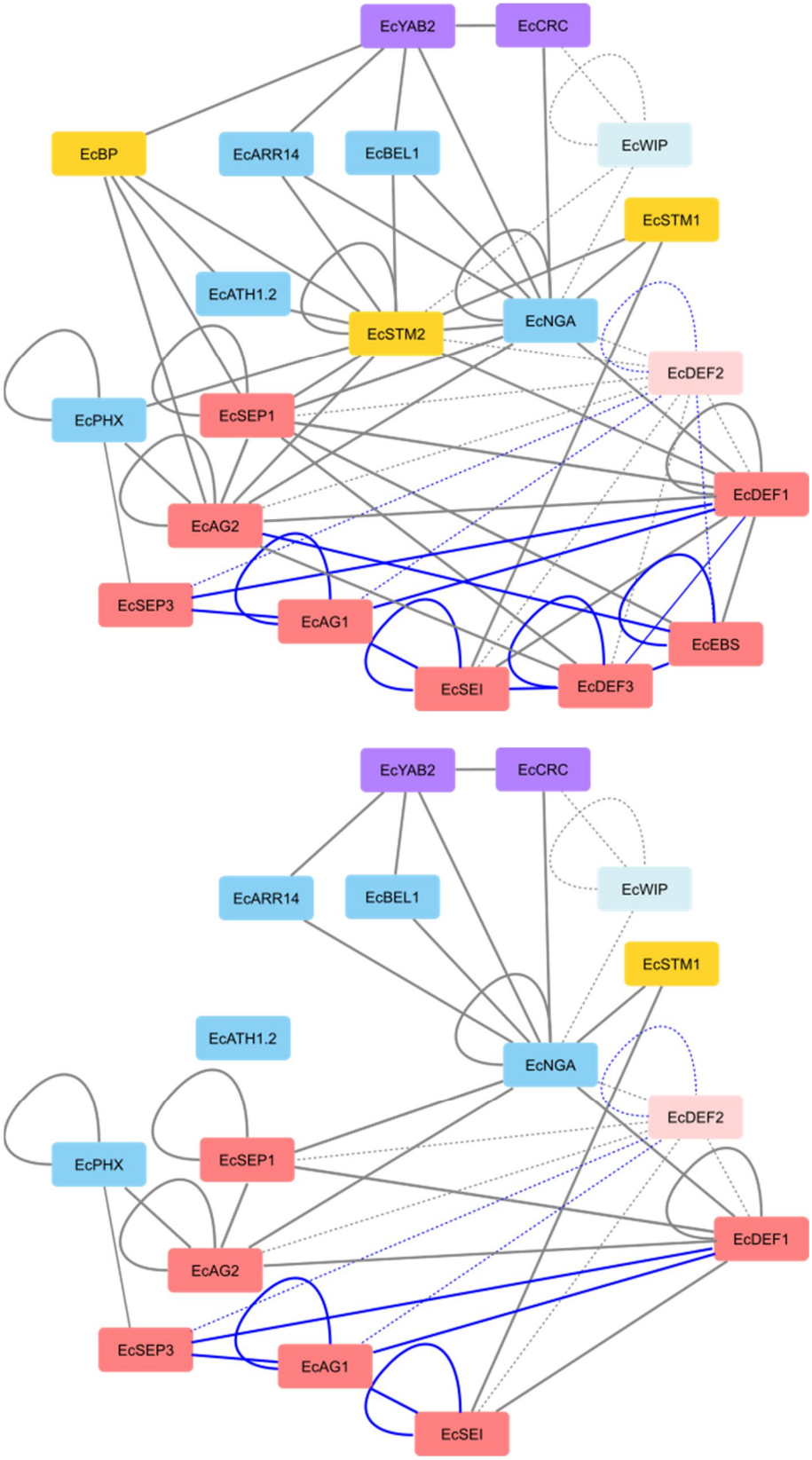

Figure 4.1: *Interaction networks of E. californica (upper) carpels in young buds (S1, S2) and stem (SRA file NCBI-ID ERR364335), and (lower) medium buds (S3, stages defined in [395]). Interactions in the network are based on PPIs detected here (section 3.2), interactions published previously, and expression data for the respective stages calculated as TPM values (section 4). Boxes: proteins, lines: interactions; orange: class I KNOX protein, violet: YABBY protein, red: MADS-box protein, blue: other protein family. Lighter coloured boxes indicate unknown TPM*

values, interactions of these proteins are shown as dashed lines. Previously published interactions are shown as blue lines.

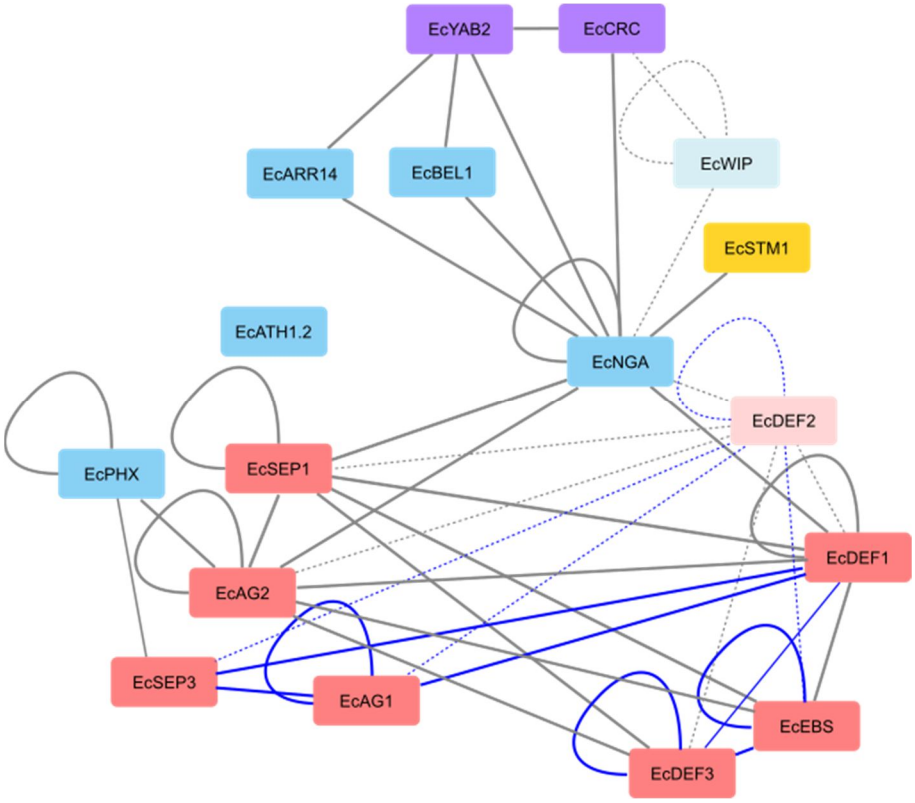

Figure 4.2: *Interaction networks of E. californica carpels in old (S4) buds (stages defined in [395]). Interactions in the network are based on PPIs detected here (section 3.2), interactions published previously, and expression data for the respective stages calculated as TPM values (section 4). Colour as defined for fig. 4.1.*

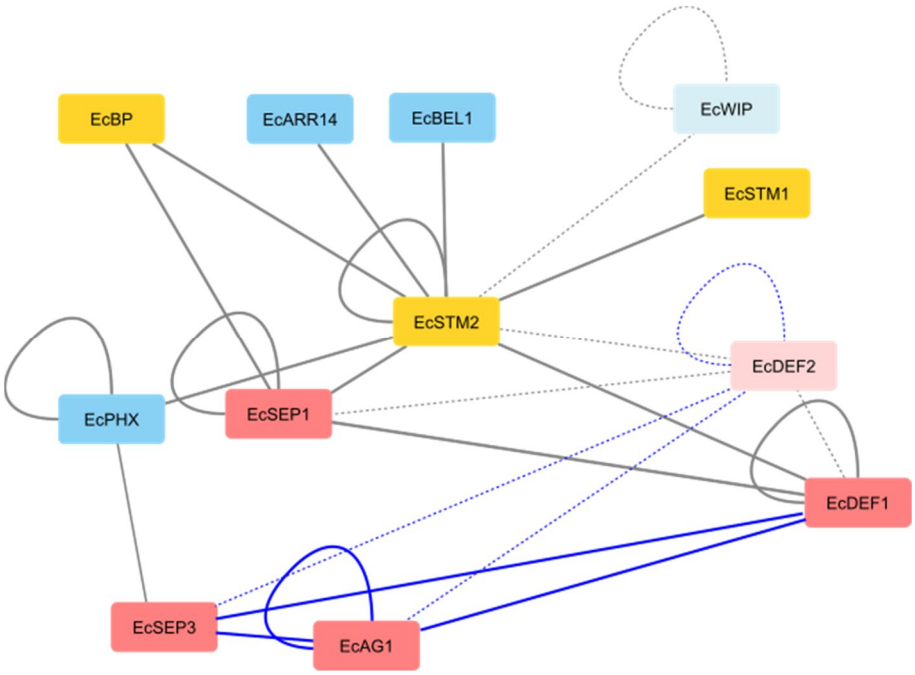

Figure 4.3: *Tissue specific interaction network of E. californica flower bud (NCBI-ID ERR364337) based on PPIs detected here, as well as previously published data (section 3.2, [346, 394]) and expression data for the respective tissues calculated as TPM values from SRA files (section 4, TPM>0). Colour as defined for fig. 4.1.*

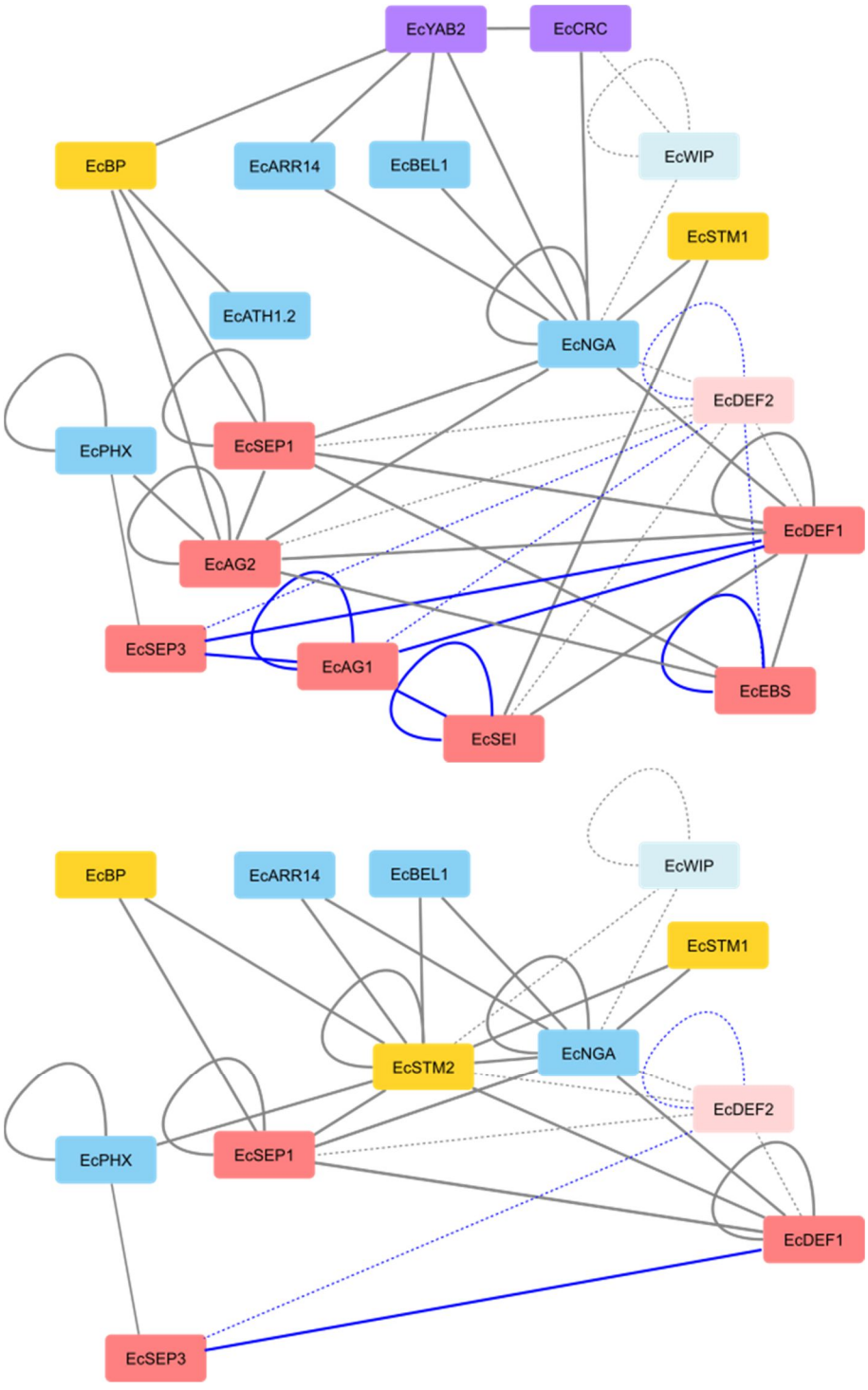

Figure 4.4: *Tissue specific interaction networks of E. californica based on PPIs detected here, as well as previously published data (section 3.2, [346, 394]) and expression data for the respective tissues calculated as TPM values from SRA files (section 4, TPM>0). The SRA files are based on following tissue samples: developing fruit (lower, NCBI-ID ERR364338) and root (lower, NCBI-IDs ERR364336 + SRR341948). Colour as defined for fig. 4.1.*

In roots, calculated TPM values showed no expression of most of the considered MADS-box factors, the two examined YABBY genes and EcATH1.2, while TPM values for all the other genes were greater than zero (table 5). This might hint at a more general role for the expressed factors in growing tissues, and a more specific reproductive function of the not-expressed genes.

The expression of all examined genes, not only in early carpel stage samples but also in the stem sample observed here (table 5), implies an unexpected high similarity between stem and

young buds, this may result from a high similarity of the SAM and the FM. The calculated lack of expression of most of these genes in developing leaves speaks against a more general expression of these genes in aerial tissues.

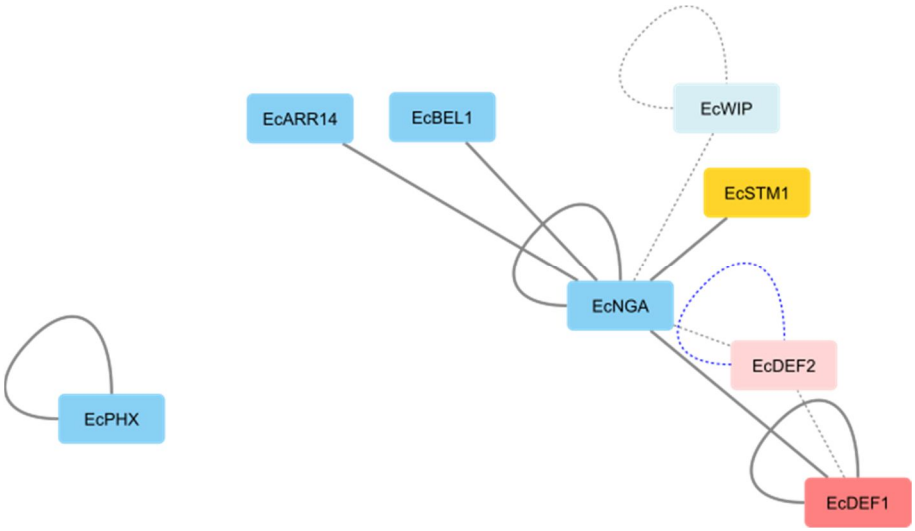

Figure 4.5: *Tissue specific interaction networks of E. californica based on PPIs detected here, as well as previously published data (section 3.2, [346, 394]) and expression data for the respective tissues calculated as TPM values from SRA files (section 4, TPM>0). The SRA file is based on following leaf tissue sample NCBI-ID ERR364334. Colour as defined for fig. 4.1.*

The expression of *EcSTM1* in leaves seen in the TPM data used here (table 5) are in accordance with RNA *in situ* hybridization data published by Groot *et al.* [221]. Interestingly the expression of *EcYAB2* in leaves and buds, as observed by Bartholmes *et al.* [130], was not reflected by the TPM values calculated here based on leaf or bud SRA files.

Taken together, the complexity of the Protein-Protein-Interaction networks generated in this thesis decreased during carpel development and further in fully differenciated tissues like leaves and roots. Several potential core complexes were identified here, the interaction partners of which change between different developmental stages as well as tissues. As well, the thought of conserved modules was put forward.

4.3 Gene networks regulating carpel development are partially conserved between *E. californica* and *A. thaliana*

To compare the stage [395] specific PPIs in *E. californica* and *A. thaliana*, interaction networks for both species were generated (fig. 4.6 to 4.9) based on the PPI observed in this study, complemented by interaction data from the literature and expression data calculated by O. Rupp, based on published transcript data as described in the results section [346, 394, 395, 397]. For *E. californica*, proteins with TPM >0 in at least one of the replicates were assumed to be expressed (as above), for *A. thaliana*, proteins with TPM values >10 were counted as expressed (compare [397]). Paralogous proteins are depicted as combined boxes for better comparison. Coloured shadings refer to functional information on the *A. thaliana* homologues:

Functions in carpel medial tissue development are published for AtAG, AtBP, AtCRC, AtFIL and AtYAB2, and AtNTT. The AtSEPs, AtAG, AtAP3, AtPI, and AtSTM are involved in floral organ identity. AtSTM is also involved in flowering time regulation, together with AtATH1. Proteins involved in meristematic tissues are AtAG, AtARR14, AtBP, AtCRC, AtFIL and AtYAB2, AtSTM, and AtPHB and AtPHV. AtAG and AtSTM are also involved in ovule development, together with AtABS and AtBEL1. AtFIL, AtYAB2, AtPHB, and AtPHV define organ polarity. AtNGAs are known for their involvement in style and stigma development.

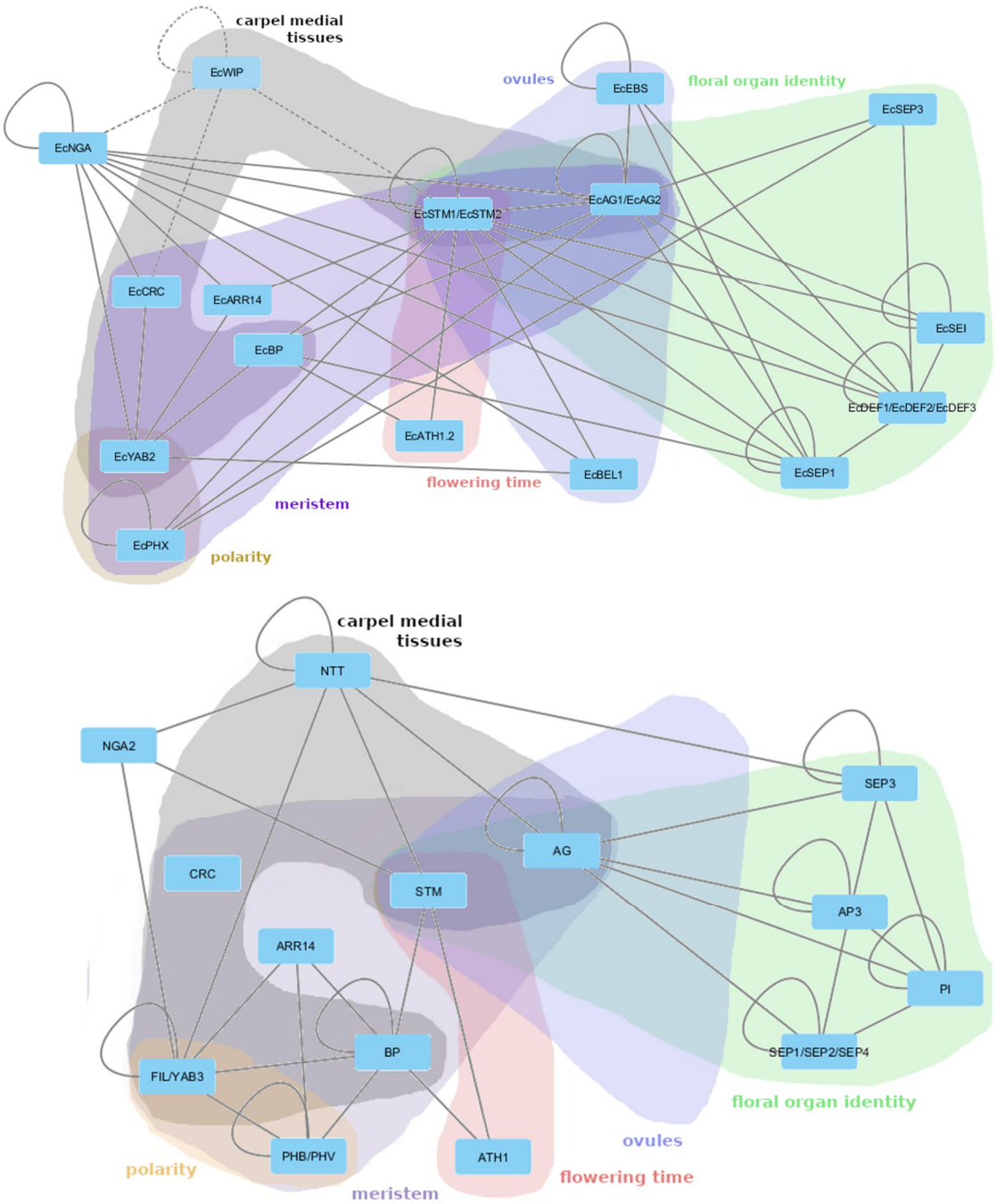

Figure 4.6: *Interaction networks of orthologous proteins in E. californica (upper, TPM>0) and A. thaliana (lower, TPM>10) proteins in carpels at initiation stages (S1 [395]) based on this study and published data [346, 394, 395, 397]. Shaded areas in both networks indicate published function of the A. thaliana proteins. Dashed lines and lighter coloured box indicates unknown expression strength.*

As described in the results section, the most obvious difference between the interaction networks is the higher connectedness between the *E. californica* proteins, compared to the higher specifity in binding partners in *A. thaliana*.

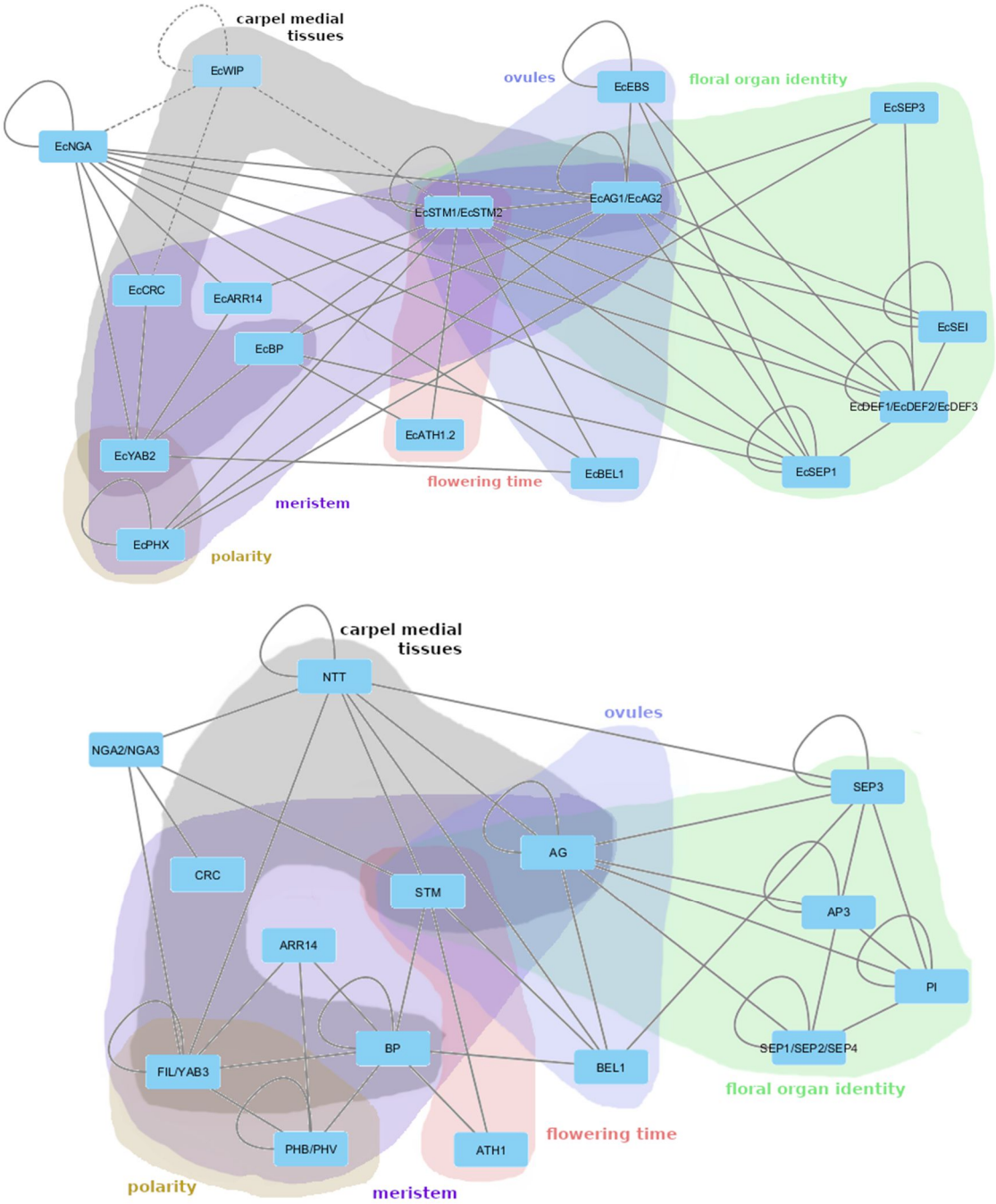

Figure 4.7: *Interaction networks of orthologous proteins in E. californica (upper, TPM>0) and A. thaliana (lower, TPM>10) proteins in carpels at carpel wall elongantion stages (S2 [395]) based on this study and published data [346, 394, 395, 397]. Shaded areas in both networks indicate published function of the A. thaliana proteins. Dashed lines and lighter coloured box indicates unknown expression strength.*

While EcSTM and EcNGA are hubs for nearly the complete network in *E. californica*, the gap between interconnected MADS and interconnected non-MADS in *A. thaliana* is bridged only by interactions of AG, SEP3, NTT, and BEL1, among the considered genes. The different binding specifity between proteins of the two species might suggest a difference in functional

specifity, as well. An increase in specifity can allow for higher complexity [434], which manifests itself in *A. thaliana* in additional gynoecial tissues (e.g. septum and transmitting tract) and additional carpel developmental factors (HAF/BEEs, SHPs, etc.).

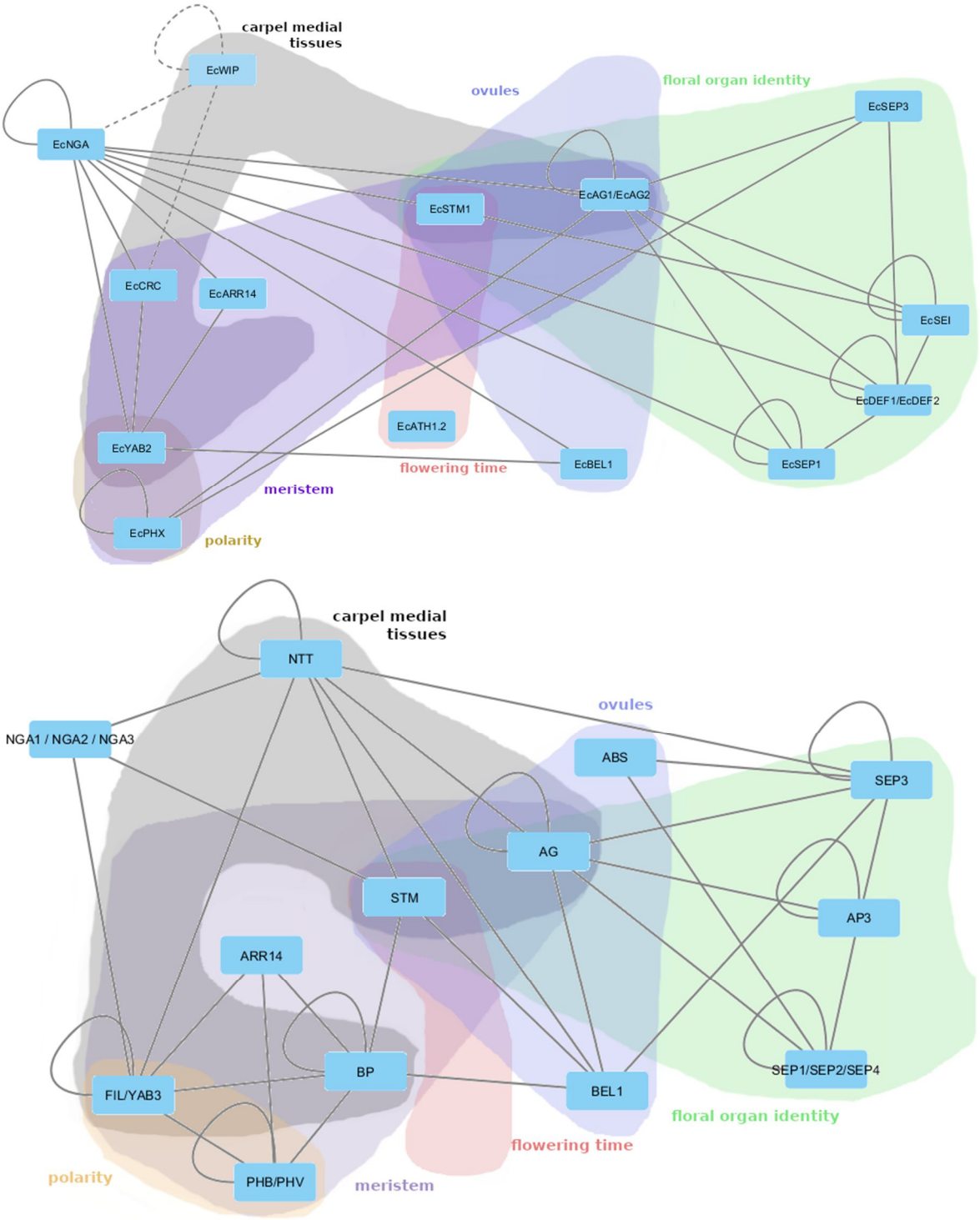

Figure 4.8: *Interaction networks of orthologous proteins in E. californica (upper, TPM>0) and A. thaliana (lower, TPM>10) proteins in carpels at meiosis stages (S3 [395]) based on this study and published data [346, 394, 395, 397]. Shaded areas in both networks indicate published function of the A. thaliana proteins. Dashed lines and lighter coloured box indicates unknown expression strength.*

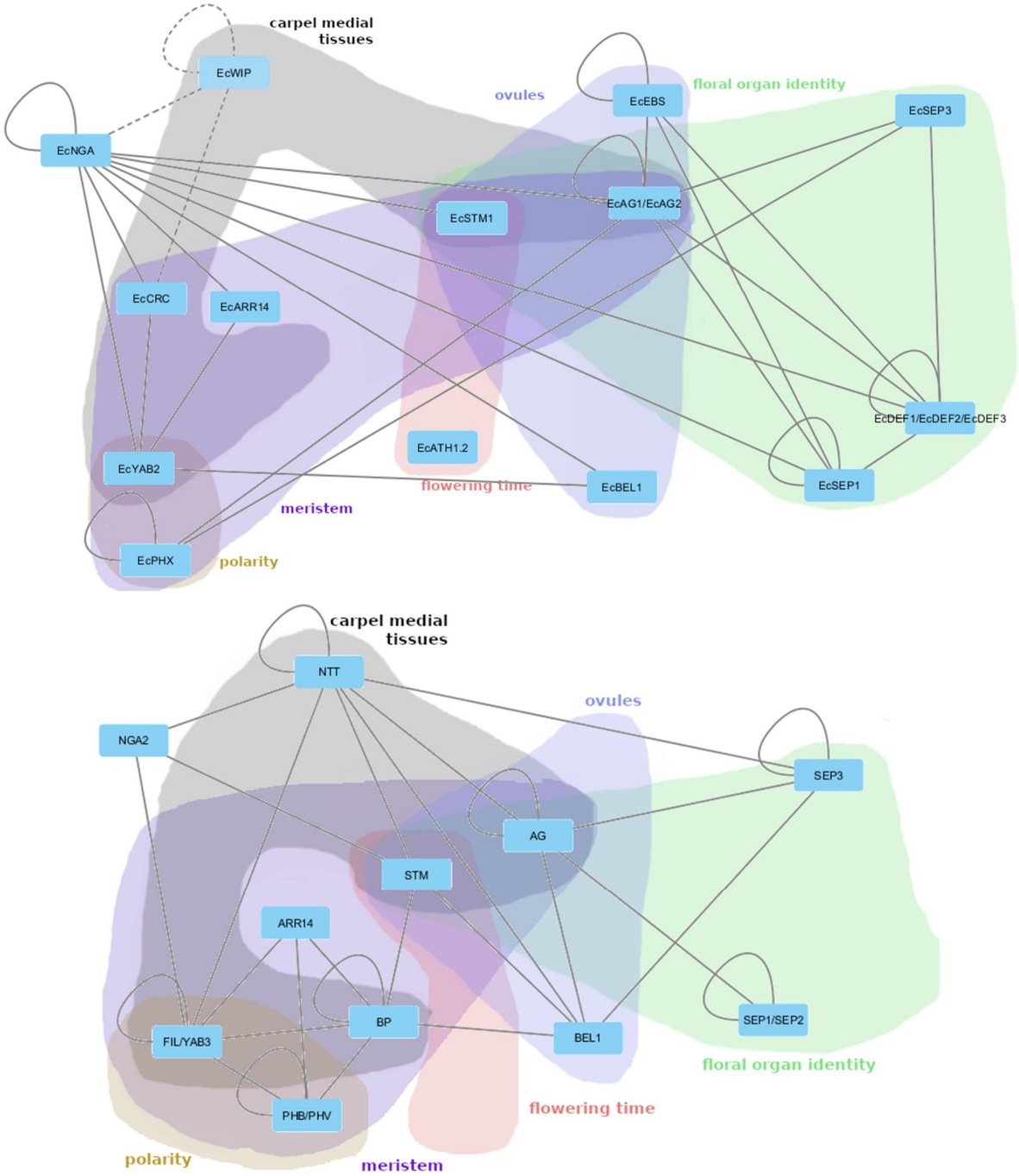

Figure 4.9: *Interaction networks of orthologous proteins in E. californica (upper, TPM>0) and A. thaliana (lower, TPM>10) proteins in carpels at post-meiosis stages (S4 [395]) based on this study and published data [346, 394, 395, 397]. Shaded areas in both networks indicate published function of the A. thaliana proteins. Dashed lines and lighter coloured box indicates unknown expression strength.*

4.3.1 Development of style and stigma

The knock down phenotypes of *EcNGA*, *EcNGA1*, and *EcNGA2* (fig. 3.22) in this work fit well with the reported role of NGA proteins in style and stigma development of *E. californica*, *N benthamiana*, and *A. thaliana* [37, 42, 385]. This coincides with the expression domain of *EcNGA* in the tips of the stigmatic protrusions [385]. No data specifically on *EcNGA1* and *EcNGA2* expression is published so far. The observed

differences in knock-down phenotypes for the different EcNGATHA proteins indicate more specific roles in carpel development compared with NGATHA proteins from *A. thaliana*, for which redundant roles are reported. The higher similarity of VIGS phenotypes of EcNGA and EcNGA2 compared to EcNGA1 (supplemental table 6) is consistent with the relationships between the three genes found in the phylogenetic analysis (fig. 3.20).

In the Y2H and BiFC PPI assays conducted, a multitude of interactions was shown for EcNGA, several of which are analogous to known PPI in *A. thaliana* (figs. 4.6 to 4.9): The interactions between *E. californica* NGA, WIP, STM1 and STM2 proteins, are similar to heterodimerizations of AtNGA1 and AtNGA2 with AtNTT and of AtNGA3 with AtSTM observed by Herrera-Ubaldo *et al.* [81, 147]. As well, interactions of EcNGA with the YABBY proteins EcCRC and EcYAB2 were observed. These bear resemblance to the reported heterodimerizations between AtNGA2 or AtNGA4 with AtFIL [128], and AtNGA3 and AtNGA4 with AtCRC [128, 147], respectively.

Among the plant-specific YABBY TFs, that are often involved in polarity establishment of lateral organs, besides more specific roles [33, 34, 197-199, 218, 286, 291-295], CRC is involved in carpel polarity, style/stigma and nectary formation in *A. thaliana*, as well as cell wall composition [113]. In this study, a change of the number of marginal stigmatic protrusions was observed in *EcCRC* knock down plants. The stigmatic protrusions were either missing or doubled, this could be interpreted as different severities of a split style/stigma phenotype, reported for *A. thaliana crc* mutants.

The expression domains of *EcCRC* and *EcNGA* do not overlap in buds after stage 4 (stages defined in [9]), as shown in RNA *in situ* hybridization data [288, 385], so an interaction *in vivo* might be limited to earlier stages of flower development and to stems. On the other hand, non-cell autonomous modes of action are assumed for *CRC* in several species, including *E. californica*, [50, 288, 290, 291] facilitating interactions of EcCRC with EcNGA, as well as the phenotype in the stigmatic protrusions of *EcCRC* VIGS plants observed here (fig. 3.3), where no *EcCRC* expression is documented in wild type [288].

Taken together, the EcNGA-EcCRC dimerization shown here, fits well with the observation of roles in style and stigma development for both proteins in the VIGS experiments conducted here and published before [288, 385].

The other YABBY protein found to interact with EcNGA in this study is EcYAB2. EcYAB2 is paralogous to EcYAB1 and both are orthologues to the *AtYAB1/FIL* and *AtYAB3* genes, that are involved in abaxial-adaxial polarity and carpel margin development. EcYAB2 was found to interact, aside from EcNGA, with the common EcSTM2-EcNGA interactors EcARR14, EcBEL1, and EcBP (fig. 4.1). This might reflect EcNGA scaffold activity in later carpel stages, where the KNOX I genes EcSTM2 and EcBP are no longer expressed, for example in style and stigma development. EcCRC was found to interact with EcYAB2, EcNGA, and the common EcSTM2-EcNGA interactor EcWIP, the latter interaction is not known from *A. thaliana* [81].

Along with a physical interaction between EcNGA and EcSEP1 in the Y2H studies conducted for this work, the single flower in the *EcSEP1+EcSEP3* double VIGS showing an *EcNGA*-VIGS-like phenotype (see fig. 3.19) harbours the possibility of a shared involvement of EcSEPs and EcNGAs in the regulation of *E. californica* style and stigma development. This is in line with the regulation of *CRC* by NGA2 and SEP3 in A. thaliana [426].

In the *EcCRC* VIGS, expression levels and phenotype (figs. 3.2, 3.3, bookmark47 and 3.9, [288]) correlated and showed preference for defects of the marginal gynoecium region: The marginal stigmatic protrusions where usually the ones affected by the observed change in numbers – absent or doubled. This may be an analogous observation to the split style in *A. thaliana crc* mutants. The presumed change in wax deposition was restricted to the marginal fusion domains of the carpels, as well. Additionally, the effects observed by Orashakova *et al.* include lack of placenta and ovules, which implies part of the EcCRC function in defining the carpel margin domain.

In *A. thaliana*, the split style/stigma phenotype of the *crc* mutant is enhanced in *spt crc* double mutants [49, 51]. SPT in *A. thaliana* is, among other, involved in septum, stigma, and transmitting tract development [46]. For this reason, the *EcCRC* VIGS was combined here with *EcSPT1*.

In the *EcSPT1* VIGS (fig. 3.6) statistically significant reductions in the absolute length of the laminar stigmatic protrusions was found, as well as in the ratio of the average length of laminar versus marginal stigmatic protrusions per flower. This was more pronounced in the *EcCRC* single knock down, and *EcSPT1+EcCRC* and *EcSPT1+EcSPT2* double VIGS plants (figs. 3.6). Unspecific knock down effects of *EcSPT1* VIGS on the expression of the close paralogue *EcSPT2* could be excluded (compare fig. 3.12). Though no phenotype comparable to the *spt* mutant in *A. thaliana* [49, 67] was observed here, the data confirm a role of the *EcSPT* genes in style and stigma development. The discovery that the style/stigma phenotypes of *EcSPT1*, *EcSPT2*, and *EcSPT1+EcSPT2* VIGS knock downs are not obvious, but only very subtle, implies that there may be further redundant factors to be found in *E. californica*. Based on the reported functional redundancy of SPT with the three HEC proteins in *A. thaliana* [46, 155], the EcHECs would be a worthwhile starting point. Especially, as the three *EcHEC* genes, identified in transcript data before, might be supplemented by two further *EcHEC*s, for which genomic loci were located here (compare suppl. sec. 2.1).

EcWIP is the putative *E. californica* orthologue of *AtNTT*, also called *AtWIP2* [23]. *AtNTT* can establish physical interactions in Y2H with a high number of proteins belonging to different families [81, 317]. Some of these interactions were also observed in the BiFC assay here between the orthologous *E. californica* proteins (see supplemental table 10): Comparable to AtNTT, EcWIP is able to form homodimers and heterodimers with EcSTM2 and EcNGA *in planta*. The interaction observed between EcWIP and EcCRC in BiFC was not detected for the *A. thaliana* homologous proteins in Y2H by Herrera-Ubaldo *et al.* [81].

The heterodimerizations observed in the BiFC assays for EcYAB2 with EcARR14, EcBP, EcCRC, and EcNGA (suppl. table 10) fit well with interactions between the orthologous *A. thaliana* proteins [81, 128, 147], while for the EcYAB2-EcBEL1 interaction no data from *A. thaliana* are available. No analogous interaction to the EcCRC-EcYAB2 dimerization was observed in *A. thaliana* [147].

Taken together the observed roles of EcNGAs, EcCRC, and EcSPTs in style and stigma development are similar to reported functions of the orthologous *A. thaliana* proteins. EcNGA furthermore seems to fuctions as a central hub in the style and stigma developmental protein interaction network. Further phenotypes of knock downs of *EcCRC* and the *EcSPTs* affecting the marginal stimatic protrusions were observed.

4.3.2 Establishment of carpel polarity axes

Orashakova *et al.* reported a reduced ovary diameter in *EcCRC* VIGS plants [288]. In addition to this, a significant increase in ovary length was observed here. In line with these observations, changed gynoecia dimensions were reported for *A. thaliana crc* mutants before [51]. In the *EcSPT1+EcCRC* VIGS plants, ovary length was no longer affected and in *EcSPT1+EcSPT2* double VIGS plants it was significantly shorter. This suggests a combined effect of both *EcSPT* genes opposit to the *EcCRC* effect on ovary length. The homodimerization of EcPHX in Y2H (table 3.4) is analogous to the homodimer formations of the HD-ZIP III proteins AtPHB and AtPHV [118, 412].

4.3.3 Hormonal regulation of carpel development

Several interactions between proteins were observed in *E. californica*, of which *A. thaliana* orthologues are involved in hormonal regulation. The detected EcSTM2-EcWIP interaction (fig. 4.1) might play a similar role in cytokinin signalling as reported by Marsch-Martínez *et al.* for the AtSTM-AtNTT heterodimer [317]. As well, the heterodimerization of EcPHX with EcSTM2 suggests a role in meristem regulation and phytohormone signalling for EcPHX, similar to the published roles of the HD-ZIP III proteins of *A. thaliana* [170, 171].

The observed EcARR14-EcSTM2 heterodimerization may replace the published AtARR14-AtBP interaction [403] in *E. californica*. For the EcARR14-EcNGA dimer, no similar interactions are known from *A. thaliana*. Contrasting the findings from *A. thaliana* [147], dimerizations between the EcNGA and EcAG2 or EcARR14 were identified here, and this interaction of EcNGA and EcAG2 is further supported by overlapping expression domains in the incipient petal, stamen, and gynoecium primordia, in stage 3 buds, and in the tips of developing third and fourth whorl organs [346, 385].

The EcARR14-EcbHLH interactions, analogous to interactions of AtARR14 with AtSPT and AtIND in Y2H [145], are another interesting addition to the data presented here. Both AtbHLH

proteins are known to be involved in fruit dehiscence and auxin distribution, harbouring the possibility of an involvement of their common interactor ARR14 in these processes, as well.

Taken together, the above interactions of EcARR14 with EcWIP and EcPHX via EcSTM2, as well as with EcNGA and EcbHLHs, gives the possibility of ARR14 proteins as a central hub for phytohormone signalling in the carpel, connecting CK, GA and auxin signalling pathways.

4.3.4 Floral meristem termination and floral organ identity

MADS and KNOX genes are promenent factors of floral organ identity and meristem regulation. The EcAGs were described before by Yellina *et al.* to have similar, but not completely identical roles in FM termination and reproductive organ identity, as the AtAG [345]. Similarily, the *E. californica* homologues to *A. thaliana* AP3 and PI B-function genes, were shown have similarities as well as differences in numbers and functions [346, 394]. The differences and similarities of B- and C-function genes described before, were further verified in this work by additional PPI data:

In the Y2H tests performed for this work (table 3.4), interactions were found between EcAG2 and most other MADS-box factors included in this study. Exceptions are EcAG1, EcSEI and EcSEP3, fitting with Y2H results by Lange *et al.* and similar to data from *A. thaliana* [104, 185, 346]. In addition to these intrafamily interactions, EcNGA and EcPHX2, as well as the KNOX I proteins EcBP and EcSTM, were found here to heterodimerize with EcAG2. No similar interactions are published so far for AtAG.

The quite different sets of MADS interaction partners of the two EcAG proteins (compare fig. 4.1) support the suggested subfunctionalization between the *E. californica* paralogues [345]. Additionally, in different stages of bud development different EcAG2 interaction partners are expressed (compare figs. 4.1 to 4.9). This may point to changing roles for EcAG2, depending on tissues and developmental stages and is consistent with data from *A. thaliana* and *T. thalictroides* [159, 339, 397].

The role of the two EcSTMs in floral development was demonstrated before by Stammler *et al.* [209]. The observed subfunctionalization is supported by the differences in numbers of interaction partners and expression in carpel development observed here (figs. 4.1 to 4.9): While a low number of interaction partners and expression during all carpel stages was found for *EcSTM1*, EcSTM2 has a high number of interaction partners but is expressed only in the pre-meiotic stages of carpel development. For this, the expression of *EcSTM2* observed in older bud stages by Stammler *et al.* has to be extra-carpellar. Combining this with the fact, that *EcSTM2* VIGS plants show more severely reduced stamen numbers compared to *EcSTM1* VIGS plants, an involvement of EcSTM2 in the stamen-generating ring meristem of *E. californica* [433] is possible.

Among the *E. californica* B-function genes, the three AP3/DEF orthologues form homodimers and heterodimers with the PI/GLO orthologue EcSEI, with EcAG2, and with EcSEP1, analogous to the situation in *A. thaliana* (fig. 4.7). EcDEF3 shows a reduced number of interaction partners compared to the other EcDEFs and EcSEI interacts with none of the two EcSEPs, only EcAG1, and EcSTM1 intead of EcSTM2. Apart from the intrafamily dimers, the *E. californica* B-function proteins EcDEF1 and EcDEF2, but not EcDEF3, can form heterodimers with non-MADS-box TFs (compare table 3.4), similar interactions were not observed for the *A. thaliana* proteins, so far. As for the EcAGs, this points to non-redundant functions for the homologous proteins. Because the interaction partners of EcDEF1 and EcDEF2 were idenitcal among the tested proteins, possible functional differences will more be based on differential expression between the two genes as was observed before [346].

Two SEPALLATA homologues were previously identified in *E. californica* [187]. In Y2H, a higly different set of interactors for both proteins was observed here: While SEP1 interated with NGA, the two KNOXs STM2 and BP, as well as the MADS-box proteins AG2, EBS and all three DEFs (see table 3.4), for SEP3 a striking absence of interactions was found, when compared to the literature, for example from *A. thaliana* [104, 182, 323] or *Amborella trichopoda* [351]. In Y2H, SEP3 only dimerized with EcPHX. Interactions between HD-ZIP IIIs and MADS-box transcription factors, as seen for EcAG2-EcPHX and EcSEP3-EcPHX heterodimers, are not known from the literature for any species, but may just have never been assessed so far, as HD-ZIP IIIs are mainly known to play roles in the regulation of SAM, vascular development, auxin transport, and lateral organ polarity [411]. Lange *et al.* further published EcSEP3 interactions with EcAG1, EcDEF1 and EcDEF2 in BiFC [346]. Heterodimerization of EcSEI with EcSEP3 and EcSEP3 homodimerization are widely conserved among species [104, 350–352, 404] and available data on SEPALLATAs from *T. thalictroides* show interactions of ThtSEP3 with ThtAG1, ThtPI, and ThtSEP3 [339, 350], implying further interactions of the EcSEPALLATAs undiscovered so far. No interaction data from *Arabidopsis thaliana* is published for the orthologues of most of these proteins so far, only Brambilla *et al.* published an interaction between AtSEP3 and AtBEL1 [182].

In the VIGS studies conducted here to gather functional data on the EcSEPs, no typical E-function could be observed for these proteins: Instead of the the striking homeotic conversion of all floral organs to leaves in complete loss of function mutants of *A. thaliana*, stamen development and flowering time were affected (figures 3.15 to 3.17). Because a single functional SEP allele in *A. thaliana* is sufficient to alleviate the conversion of floral organs to leaves [31], the remaining *EcSEP* expression may be sufficient for normal floral organ development. Additionally, the observed stamen effects hint at a possible similarity between *E. californica* and *T. thalictroides* SEP protein functions, because Soza *et al.* found partially redundant roles for *T. thalictroides SEPALLATA*s in organ boundary maintenance and in sepal and stamen identity, leading, among other, to broader filaments in VIGS experiments [338]. Considering this, the mosaic organs observed in *EcSEP* knock downs might point to a similar

function in *E. californica*. Although mosaic organs were as well observed in other VIGS treatments and in control plants (see suppl. table 1). The delayed flowering found in *EcSEP1* and *EcSEP3* VIGS plants (compare figs. 3.7 and 3.17), is reminiscent to a late-flowering phenotype in rice caused by reduced expression of two rice SEPALLATA orthologues, *OsMADS7* and *OsMADS8* [399]. The enhanced phenotype in the double knock down of both *EcSEP*s suggests an additive effect of *EcSEP1* and *EcSEP3* on the timing of flowering. This may be caused either by a later floral transition and delayed development of further flowers or an overall slower floral development. Another possibility for the lack of homeotic conversions are redundancies with additional proteins, that take over in the absence of the EcSEP proteins. It may even be the case, that related proteins, like one or both EcAGL6s (fig. 3.28), completely take over this function in *E. californica* instead of the SEPALLATAs. SEPALLATA-like functions were, after all, reported for the AGL6 proteins from petunia and several monocot species, as well as an involvement of AtAGL6 in flowering time [348, 358–361, 410]. Furthermore, PPI between EcSEP1 and EcSTM2 was detected here, which is not reported for the orthologous *A. thaliana* proteins, while an involvement of the STM-ATH1 dimer in flowering time regulation is published [201]. Thus, the EcSEP1-EcSTM2 interaction might connect the EcSEPs to flowering time regulation, though no data on involvement of the EcSTMs in flowering time regulation is published. Interestingly, compared to their *A. thaliana* orthologues, neither EcAG2 nor EcSEP1 interacts with EcAG1, EcSEI or EcSEP3, which in turn interact only with a limited set of other proteins. The only interaction of EcAG2, that is not shared with EcSEP1, is the one with the HD-ZIP III TF EcPHX, which moreover binds EcSEP3 (fig. 4.1). In this way, EcPHX could act as a scaffold in the formation of a complex including both EcAG2 and EcSEP3, comparable to the AG-SEP3 complex known from *Arabidopsis thaliana* [182, 185, 323], without necessity of a direct EcAG2-EcSEP3 interaction.

In this study, for EcEBS only heterodimerizations with EcAG2 and EcDEF1 were found, while all tests with non-MADS TFs were negative, as where all tests including the BD-EcEBS construct. The latter interacted with AD-constructs of EcAG2, all EcDEF proteins, as well as EcEBS in experiments conducted earlier [394], for this reason, retesting these combinations would be useful. Interestingly, while ABS expression is only detected in bud stage S3 [395] corresponding to meiosis, EBS is not detected during meiosis, but at earlier and later stages of bud development (compare figs 4.5 to 4.9). This implies different roles for the BSISTER orthologues of both species or a switch from negative regulation of ovule development in *E. californica* to positive regulation in *A. thaliana*. Another interesting fact observed here, is the higher frequency of ovules halting development during integument outgrowth in *EcCRC* and *EcSPT1+EcCRC* VIGS plants (fig. 3.8), compared to control and *EcSPT1* single VIGS plants. Taken together with the absence of *E. californica* orthologues of *A. thaliana* ovule development factors (SHPs, INO) from transcript databases and the draft genome, the above findings consitently point to major differences between *E. californica* and *A thaliana* ovule development.

Except for EcSEP3, the ability to homodimerize was shown in this study for all examined MADS-box TFs. The ability of the *E. californica* B-class proteins for homo- and heterodimerization is similar to published reports on the *T. thalictroides* AP3 and PI homologues [350], but no comparable interaction of EcSEI with any of the two EcSEP homologues was detected. The absence of EcSEP3 homodimerizations and heterodimerizations with EcSEI form the PPI data generated in this study (table 3.4) are partly in line with data published by Lange *et al.* [346].

The Y2H and BiFC studies of this work (see supplemental table 9) showed BELL-KNOX I interactions between the *E. californica* proteins EcATH1.2, EcBEL1, EcBP, EcSTM1, EcSTM2 in different combinations. The weak interaction of EcBEL1 with EcSTM2 is consistent with data from *A. thaliana* [214], while no EcBP-EcBEL1 interaction was observed in the BiFC assays, despite of an analogous interaction in *A. thaliana* [162]. In addition to the KNOX I TF EcSTM2, EcBEL1 interacted with EcNGA and EcYAB2, coincidentally the same interaction partners as found for EcARR14. For EcATH1.2 only interactions with the KNOX I proteins EcBP and EcSTM2 were found, while EcATH1.2-EcSTM1 heterodimerization still needs to be tested. Similar heterodimers with AtBP and AtSTM are published for AtATH1 and AtBEL1 in *A. thaliana* [145, 214]. In contrast to the limited number of interaction partners identified for the BELL proteins in *E. californica*, the KNOX I proteins dimerized with a high variety of TF families (fig. 4.1). Among these are heterodimerizations with MADS-box family TFs, the HD-ZIP III protein EcPHX, and KNOX I hetero- and homodimerizations. For many of those interactions no data from *A. thaliana* are available. Interactions of all three tested KNOX I with MADS-box family members might represent the ability of *E. californica* KNOX I-BEL dimers to form larger complexes with MADS-box TFs, similar to the published AtBEL1-(AtAG-AtSEP) interaction [182].

Taken together, several published instances of subfunctionalizations in *E. californica* are backed up by the observation of differences in expression and interaction partners between the paralogues. For the *EcSEPALLATA* genes, a change in function compared to *A. thaliana* was be observed. Furthermore, the colleted data hint at differences in ovule developmental regulation between *A. thaliana* and *E. californica*.

4.3.5 Outside the *A. thaliana* carpel

The floral cup surrounding the *E. californica* ovary is a structure not present in *A. thaliana* flowers, thus no data on it's development can be transferred from the model species. In *EcSPT1* and *EcSPT1+EcCRC* VIGS plants, but not *EcCRC* single knock downs (fig. 3.4) a statistically significant increase of the height of the floral cup compared to the empty vector treated plants was found. In the *EcSPT1+EcSPT2* (fig. 3.13) double VIGS plants, the in the height of the floral cup was no longer statistically significant, but a statistically significant reduction in ovary

length was observed. The knock-down phenotype in the double VIGS compared to the *EcSPT1* single VIGS, points at an effect of EcSPT2 alone on the length of the ovary, while the milder effects on the height of the floral cup of the knock down hint at opposite roles of the *EcSPT* genes in floral cup development. Until now, there are no publications concerning the biological function of the floral cup in *E. californica*. A protective function for the carpels and ovules could be conceived: A higher floral cup would result in better protected ovaries, but at the same time pollination efficiency could decrease, when the stigmatic protrusions are buried deeper between the stamens or even partially covered by the floral cup.

Wu *et al.* [409] reported an influence of AtSPT on flowering time and a slight delay of flowering was also observed in *EcSPT1* single as well as *EcSPT1+EcSPT2* double VIGS experiments (see figures 3.7 and 3.17), but these effects were not statistically significant.

5 Conclusion

Based on the observations of this thesis and published data it can be concluded, that gene networks regulating *E. californica* carpel development are only partially conserved compared to *A. thaliana*.

Most protein interactions tested in this study, were not reported for *A. thaliana* or other species before, except for MADS-MADS interactions. Some physical interactions are conserved between species, while others are observed instead between related proteins or not at all. Notably, an abundance of physical interactions between non-MADS and MADS-box transcription factors was found here, that is not yet described in this extend for any other species. Especially interesting in this context may be the fact, that in *E. californica*, as well as in *A. thaliana* interactions between NGA, STM, BEL1 and WIP are observed. Both groups of proteins probably form heteromultimers, which can interact with the MADS-box TFs AG and SEP homologues. Contrasting *A. thaliana*, where the interaction with the MADS-box proteins is conferred by BEL1 and WIP2/NTT, in *E. californica* the interaction is established via STM2 and NGA. This implies, that interactions between smaller modules forming the overall PPI network might be better conserved than the individual interactions between two sets of orthologues.

Exemplary for conserved protein functions and interactions, physical interaction between EcCRC and EcNGA proteins and their common involvement together with *EcSPTs* in apical carpel development are named.

Subfunctionalizations between *E. californica* paralogues of AG and STM are exampels of diverged functions. The differences in VIGS phenotypes published before [209, 345] are well-supported by data generated here: Not only are the respective paralogues expressed in different stages of bud development, but as well distinct sets of protein interaction partners were observed. Similar differences can be assumed for the newly discovered paralogues of EcNGA and EcSPT, for which phenotypical differences of VIGS knock-downs were observed here.

Strong indications were found as well, that regulation of ovule development in *E. californica* is different from described *A. thaliana* processes: Firstly, in *E. californica* no orthologues for INO, and SHPs were detected, secondly the *E. californica* ABS orthologue was found to be not expressed in the meiosis stage carpel transcriptome, but in all others and last but not least integument outgrowth was found to be halted more often in *EcCRC* and *EcSPT1+EcCRC* VIGS flowers than in the controls, implying an involvement of these genes.

This broadens the findings of Li *et al.* concerning MADS-box transcription factors "comparing the network in different species showed that conservativeness and variability co–exist in composition, organization, and structure of the complex interactions among proteins encoded by these genes" [352] to other protein families.

6 Future experiments

In the following, further experiments and questions resulting from this work will be discussed.

To complement the generated Y2H data, BiFC tests could be conducted for the proteins showing no interactions in Y2H and the proteins interacting specifically with the protein product of the empty AD vector. Furthermore, integration of the newly discovered EcNGA and EcSPT paralogues in PPI testing will enhance our understanding of their subfunctionalization.

Because cell-to-cell movement of KN1, LeT6, DEF, GLO, LFY, and AP1 proteins was shown before [415–418], observing the localization of the orthologous *E. californica* proteins might be interesting, in addition to RNA *in situ* hybridization experiments to determine the expression domains of the proteins tested in PPI assays. This could give valuable information on the *in vivo* possibility of the observed PPI.

As a second point, further functional studies might give interesting insights: Due to the intertwinement of EcNGA and EcCRC, simultaneous knock down of the *EcNGA* genes and *EcCRC* could be of interest. The presumed hub positions of EcSTM2-EcNGA, EcAG2-EcSEP1, and EcDEF1-EcDEF2 dimers identified here would be another interesting target of functional studies.

For this, further improvements of VIGS experiments can be helpful: For example, implementing the propositions of Rössner *et al.* [430] in the construction of VIGS vectors. As well, further improvement of cultivation, e.g. by adjusting the administration of fertilizer to the faster development under stronger light, could enhance the reproducibility of experiments. Furthermore, a visible marker of knock-down efficiency could facilitate the evaluation of the phenotypes. A combined knock down as used for other species with a flower-specific pigment [336, 413] or the use of a GFP-tagged TRV vector system, might be feasible.

7 Bibliography

[1] Coombe, B. G., 1976. The development of fleshy fruits. *Annual Review of Plant Physiology*, **27**, 207.

[2] Ferrándiz, C., C. Fourquin, N. Prunet, et al., 2010. Carpel development. vol. 55 of *Advances in Botanical Research*, 1–73.

[3] Shikata, M., K. Hoshikawa, T. Ariizumi, et al., 2016. TOMATOMA Update: Phenotypic and metabolite information in the Micro-Tom mutant resource. *Plant & Cell Physiology*, **57**, e11.

[4] Shen, C., G. Li, L. Dreni, et al., 2021. Molecular control of carpel development in the grass family. *Frontiers in Plant Science*, **12**, 635500.

[5] Marsch-Martínez, N. and S. de Folter, 2016. Hormonal control of the development of the gynoecium. *Current Opinion in Plant Biology*, **29**, 104.

[6] Di Marzo, M., I. Roig-Villanova, E. Zanchetti, et al., 2020. MADS-Box and bHLH Transcription Factors Coordinate Transmitting Tract Development in Arabidopsis thaliana. *Frontiers in Plant Science*, **11**, 526.

[7] Damerval, C. and A. Becker, 2017. Genetics of flower development in Ranunculales - a new, basal eudicot model order for studying flower evolution. *New Phytologist*, **216**, 361.

[8] Judd, W. S. and R. G. Olmstead, 2004. A survey of tricolpate (eudicot) phylogenetic relationships. *American Journal of Botany*, **91**, 1627.

[9] Becker, A., S. Gleissberg, and D. R. Smyth, 2005. Floral and vegetative morphogenesis in California poppy (Eschscholzia californica Cham.). *International Journal of Plant Sciences*, **166**, 537.

[10] Liu, Z., R. G. Franks, and V. P. Klink, 2000. Regulation of gynoecium marginal tissue formation by LEUNIG and AINTEGUMENTA. *Plant Cell*, **12**, 1879.

[11] Liljegren, S. J., A. H. K. Roeder, S. A. Kempin, et al., 2004. Control of fruit patterning in Arabidopsis by INDEHISCENT. *Cell*, **116**, 843.

[12] Sessions, R. A. and P. C. Zambryski, 1995. Arabidopsis gynoecium structure in the wild type and in ettin mutants. *Development*, **121**, 1519.

[13] Gilbert, S. F., 2003. The morphogenesis of evolutionary developmental biology. *International Journal of Developmental Biology*, **47**, 467.

[14] Kramer, E. M., M. A. Jaramillo, and V. S. Di Stilio, 2004. Patterns of gene duplication and functional evolution during the diversification of the AGAMOUS subfamily of MADS box genes in angiosperms. *Genetics*, **166**, 1011.

[15] Scutt, C. P., M. Vinauger-Douard, C. Fourquin, et al., 2006. An evolutionary perspective on the regulation of carpel development. *Journal of Experimental Botany*, **57**, 2143.

[16] Carroll, S. B., 2008. Evo-devo and an expanding evolutionary synthesis: a genetic theory of morphological evolution. *Cell*, **134**, 25.

[17] Becker, A., K. Alix, and C. Damerval, 2011. The evolution of flower development: current understanding and future challenges. *Annals of Botany*, **107**, 1427.

[18] Hall, B. K., 2012. Evolutionary Developmental Biology (Evo-Devo): Past, Present, and Future. *Evolution: Education and Outreach*, **5**, 184.

[19] Moyroud, E. and B. J. Glover, 2017. The evolution of diverse floral morphologies. *Current Biology*, **27**, R941.

[20] Kaufmann, K., R. Melzer, and G. Theißen, 2005. MIKC-type MADS-domain proteins: structural modularity, protein interactions and network evolution in land plants. *Gene*, **347**, 183.

[21] Wagner, A., 2011. The molecular origins of evolutionary innovations. *Trends in Genetics*, **27**, 397.

[22] Malcomber, S. T. and E. A. Kellogg, 2005. SEPALLATA gene diversification: brave new whorls. *Trends in Plant Science*, **10**, 427.

[23] Pfannebecker, K. C., M. Lange, O. Rupp, et al., 2017. Seed plant-specific gene lineages involved in carpel development. *Molecular Biology and Evolution*, **34**, 925.

[24] Maere, S., S. de Bodt, J. Raes, et al., 2005. Modeling gene and genome duplications in eukaryotes. *Proceedings of the National Academy of Sciences of the United States of America*, **102**, 5454.

[25] Jiao, Y., N. J. Wickett, S. Ayyampalayam, et al., 2011. Ancestral polyploidy in seed plants and angiosperms. *Nature*, **473**, 97.

[26] Jin, X., J. Ren, E. Nevo, et al., 2017. Divergent Evolutionary Patterns of NAC Transcription Factors Are Associated with Diversification and Gene Duplications in Angiosperm. *Frontiers in Plant Science*, **8**, 1156.

[27] Becker, A. and G. Theißen, 2003. The major clades of MADS-box genes and their role in the development and evolution of flowering plants. *Molecular Phylogenetics and Evolution*, **29**, 464.

[28] Zhao, Q., A. L. Weber, M. D. McMullen, et al., 2011. MADS-box genes of maize: frequent targets of selection during domestication. *Genetics Research*, **93**, 65.

[29] Bowman, J. L., D. R. Smyth, and E. M. Meyerowitz, 1991. Genetic interactions among floral homeotic genes of Arabidopsis. *Development*, **112**, 1.

[30] Honma, T. and K. Goto, 2001. Complexes of MADS-box proteins are sufficient to convert leaves into floral organs. *Nature*, **409**, 525.

[31] Ditta, G., A. Pinyopich, P. Robles, et al., 2004. The SEP4 gene of Arabidopsis thaliana functions in floral organ and meristem identity. *Current Biology*, **14**, 1935.

[32] McConnell, J. R. and M. K. Barton, 1998. Leaf polarity and meristem formation in Arabidopsis. *Development*, **125**, 2935.

[33] Siegfried, K. R., Y. Eshed, S. F. Baum, et al., 1999. Members of the YABBY gene family specify abaxial cell fate in Arabidopsis. *Development*, **126**, 4117.

[34] Eshed, Y., A. Izhaki, S. F. Baum, et al., 2004. Asymmetric leaf development and blade expansion in Arabidopsis are mediated by KANADI and YABBY activities. *Development*, **131**, 2997.

[35] Pekker, I., J. P. Alvarez, and Y. Eshed, 2005. Auxin response factors mediate Arabidopsis organ asymmetry via modulation of KANADI activity. *Plant Cell*, **17**, 2899.

[36] Dinneny, J. R., D. Weigel, and M. F. Yanofsky, 2006. NUBBIN and JAGGED define stamen and carpel shape in Arabidopsis. *Development*, **133**, 2285.

[37] Alvarez, J. P., A. Goldshmidt, I. Efroni, et al., 2009. The NGATHA distal organ development genes are essential for style specification in Arabidopsis. *Plant Cell*, **21**, 1373.

[38] Becker, A., 2020. A molecular update on the origin of the carpel. *Current Opinion in Plant Biology*, **53**, 15.

[39] Kuusk, S., J. J. Sohlberg, J. A. Long, et al., 2002. STY1 and STY2 promote the formation of apical tissues during Arabidopsis gynoecium development. *Development*, **129**, 4707.

[40] Gaillochet, C., S. Jamge, F. van der Wal, et al., 2018. A molecular network for functional versatility of HECATE transcription factors. *The Plant Journal*, **95**, 57.

[41] Kuusk, S., J. J. Sohlberg, D. Magnus Eklund, et al., 2006. Functionally redundant SHI family genes regulate Arabidopsis gynoecium development in a dose-dependent manner. *The Plant Journal*, **47**, 99.

[42] Trigueros, M., M. Navarrete-Gómez, S. Sato, et al., 2009. The NGATHA genes direct style development in the Arabidopsis gynoecium. *Plant Cell*, **21**, 1394.

[43] Alvarez, J. P., I. Pekker, A. Goldshmidt, et al., 2006. Endogenous and synthetic microRNAs stimulate simultaneous, efficient, and localized regulation of multiple targets in diverse species. *Plant Cell*, **18**, 1134.

[44] Kwon, S. H., B. H. Lee, E. Y. Kim, et al., 2009. Overexpression of a Brassica rapa NGATHA gene in Arabidopsis thaliana negatively affects cell proliferation during lateral organ and root growth. *Plant & Cell Physiology*, **50**, 2162.

[45] Lee, B. H., S. H. Kwon, S.-J. Lee, et al., 2015. The Arabidopsis thaliana NGATHA transcription factors negatively regulate cell proliferation of lateral organs. *Plant Molecular Biology*, **89**, 529.

[46] Gremski, K., G. Ditta, and M. F. Yanofsky, 2007. The HECATE genes regulate female reproductive tract development in Arabidopsis thaliana. *Development*, **134**, 3593.

[47] Crawford, B. C. W. and M. F. Yanofsky, 2011. HALF FILLED promotes reproductive tract development and fertilization efficiency in Arabidopsis thaliana. *Development*, **138**, 2999.

[48] Nagpal, P., C. M. Ellis, H. Weber, et al., 2005. Auxin response factors ARF6 and ARF8 promote jasmonic acid production and flower maturation. *Development*, **132**, 4107.

[49] Alvarez, J. P. and D. R. Smyth, 1999. CRABS CLAW and SPATULA, two Arabidopsis genes that control carpel development in parallel with AGAMOUS. *Development*, **126**, 2377.

[50] Bowman, J. L. and D. R. Smyth, 1999. CRABS CLAW, a gene that regulates carpel and nectary development in Arabidopsis, encodes a novel protein with zinc finger and helix-loop-helix domains. *Development*, **126**, 2387.

[51] Alvarez, J. P. and D. R. Smyth, 2002. CRABS CLAW and SPATULA genes regulate growth and pattern formation during gynoecium development in Arabidopsis thaliana. *International Journal of Plant Sciences*, **163**, 17.

[52] Ståldal, V., J. J. Sohlberg, D. M. Eklund, et al., 2008. Auxin can act independently of CRC, LUG, SEU, SPT and STY1 in style development but not apical-basal patterning of the Arabidopsis gynoecium. *New Phytologist*, **180**, 798.

[53] Chuang, C. F., M. P. Running, R. W. Williams, et al., 1999. The PERIANTHIA gene encodes a bZIP protein involved in the determination of floral organ number in Arabidopsis thaliana. *Genes & Development*, **13**, 334.

[54] Maier, A. T., S. Stehling-Sun, S.-L. Offenburger, et al., 2011. The bZIP Transcription Factor PERIANTHIA: A Multifunctional Hub for Meristem Control. *Frontiers in Plant Science*, **2**, 79.

[55] Dröge-Laser, W., B. L. Snoek, B. Snel, et al., 2018. The Arabidopsis bZIP transcription factor family-an update. *Current Opinion in Plant Biology*, **45**, 36.

[56] Running, M. P. and E. M. Meyerowitz, 1996. Mutations in the PERIANTHIA gene of Arabidopsis specifically alter floral organ number and initiation pattern. *Development*, **122**, 1261.

[57] Bowman, J. L., S. F. Baum, Y. Eshed, et al., 1999. Molecular Genetics of Gynoecium Devel- opment in Arabidopsis. vol. 45 of *Current Topics in Developmental Biology*, 155–205.

[58] Conner, J. and Z. Liu, 2000. LEUNIG, a putative transcriptional corepressor that regulates AGAMOUS expression during flower development. *Proceedings of the National Academy of Sciences of the United States of America*, **97**, 12902.

[59] Sridhar, V. V., A. Surendrarao, D. Gonzalez, et al., 2004. Transcriptional repression of target genes by LEUNIG and SEUSS, two interacting regulatory proteins for Arabidopsis flower development. *Proceedings of the National Academy of Sciences of the United States of America*, **101**, 11494.

[60] Liu, Z. and V. Karmarkar, 2008. Groucho/Tup1 family co-repressors in plant development. *Trends in Plant Science*, **13**, 137.

[61] Zhang, F., H. Wang, S. Kalve, et al., 2019. Control of leaf blade outgrowth and floral organ development by LEUNIG, ANGUSTIFOLIA3 and WOX transcriptional regulators. *New Phytologist*, **223**, 2024.

[62] Liu, Z. and E. M. Meyerowitz, 1995. LEUNIG regulates AGAMOUS expression in Arabidopsis flowers. *Development*, **121**, 975.

[63] Groszmann, M., T. Paicu, and D. R. Smyth, 2008. Functional domains of SPATULA, a bHLH transcription factor involved in carpel and fruit development in Arabidopsis. *The Plant Journal*, **55**, 40.

[64] Li, W., X. Huang, J. Zou, et al., 2020. Three STIGMA AND STYLE STYLISTs pattern the fine architectures of apical gynoecium and are critical for male gametophyte-pistil inter- action. *Current Biology*, **30**, 4780.

[65] Ballester, P., M. A. Martínez-Godoy, M. Ezquerro, et al., 2021. A transcriptional complex of NGATHA and bHLH transcription factors directs stigma development in Arabidopsis. *Plant Cell*.

[66] Hepworth, S. R., Y. Zhang, S. McKim, et al., 2005. BLADE-ON-PETIOLE-dependent signaling controls leaf and floral patterning in Arabidopsis. *Plant Cell*, **17**, 1434.

[67] Heisler, M. G., A. Atkinson, Y. H. Bylstra, et al., 2001. SPATULA, a gene that controls development of carpel margin tissues in Arabidopsis, encodes a bHLH protein. *Development*, **128**, 1089.

[68] Groszmann, M., Y. Bylstra, E. R. Lampugnani, et al., 2010. Regulation of tissue-specific expression of SPATULA, a bHLH gene involved in carpel development, seedling germination, and lateral organ growth in Arabidopsis. *Journal of Experimental Botany*, **61**, 1495.

[69] Dinneny, J. R., D. Weigel, and M. F. Yanofsky, 2005. A genetic framework for fruit patterning in Arabidopsis thaliana. *Development*, **132**, 4687.

[70] Alonso-Cantabrana, H., J. J. Ripoll, I. Ochando, et al., 2007. Common regulatory networks in leaf and fruit patterning revealed by mutations in the Arabidopsis ASYMMETRIC LEAVES1 gene. *Development*, **134**, 2663.

[71] Romera-Branchat, M., J. J. Ripoll, M. F. Yanofsky, et al., 2013. The WOX13 homeobox gene promotes replum formation in the Arabidopsis thaliana fruit. *The Plant Journal*, **73**, 37.

[72] Roeder, A. H. K., C. Ferrándiz, and M. F. Yanofsky, 2003. The role of the REPLUMLESS homeodomain protein in patterning the Arabidopsis fruit. *Current Biology*, **13**, 1630.

[73] Dean, G., S. Casson, and K. Lindsey, 2004. KNAT6 gene of Arabidopsis is expressed in roots and is required for correct lateral root formation. *Plant Molecular Biology*, **54**, 71.

[74] Ragni, L., E. Belles-Boix, M. Günl, et al., 2008. Interaction of KNAT6 and KNAT2 with BREVIPEDICELLUS and PENNYWISE in Arabidopsis inflorescences. *Plant Cell*, **20**, 888.

[75] Scofield, S., W. Dewitte, and J. A. H. Murray, 2007. The KNOX gene SHOOT MERISTEMLESS is required for the development of reproductive meristematic tissues in Arabidopsis. *The Plant Journal*, **50**, 767.

[76] Endrizzi, K., B. Moussian, A. Haecker, et al., 1996. The SHOOT MERISTEMLESS gene is required for maintenance of undifferentiated cells in Arabidopsis shoot and floral meristems and acts at a different regulatory level than the meristem genes WUSCHEL and ZWILLE. *The Plant Journal*, **10**, 967.

[77] Vivian-Smith, A., M. Luo, A. Chaudhury, et al., 2001. Fruit development is actively restricted in the absence of fertilization in Arabidopsis. *Development*, **128**, 2321.

[78] Wu, M.-F., Q. Tian, and J. W. Reed, 2006. Arabidopsis microRNA167 controls patterns of ARF6 and ARF8 expression, and regulates both female and male reproduction. *Development*, **133**, 4211.

[79] Appelhagen, I., G. Huep, G.-H. Lu, et al., 2010. Weird fingers: functional analysis of WIP domain proteins. *FEBS Letters*, **584**, 3116.

[80] Crawford, B. C. W., G. Ditta, and M. F. Yanofsky, 2007. The NTT gene is required for transmitting-tract development in carpels of Arabidopsis thaliana. *Current Biology*, **17**, 1101.

[81] Herrera-Ubaldo, H., P. Lozano-Sotomayor, I. Ezquer, et al., 2019. New roles of NO TRANSMITTING TRACT and SEEDSTICK during medial domain development in Arabidopsis fruits. *Development*, **146**.

[82] Gao, M. and A. M. Showalter, 1999. Yariv reagent treatment induces programmed cell death in Arabidopsis cell cultures and implicates arabinogalactan protein involvement. *The Plant Journal*, **19**, 321.

[83] Chung, K. S., J. H. Lee, J. S. Lee, et al., 2013. Fruit indehiscence caused by enhanced expression of NO TRANSMITTING TRACT in Arabidopsis thaliana. *Molecules and Cells*, **35**, 519.

[84] Lincoln, C., J. Long, J. Yamaguchi, et al., 1994. A knotted1-like homeobox gene in Arabidopsis is expressed in the vegetative meristem and dramatically alters leaf morphology when overexpressed in transgenic plants. *Plant Cell*, **6**, 1859.

[85] Bhatt, A. M., J. P. Etchells, C. Canales, et al., 2004. VAAMANA–a BEL1-like homeodomain protein, interacts with KNOX proteins BP and STM and regulates inflorescence stem growth in Arabidopsis. *Gene*, **328**, 103.

[86] Yanofsky, M. F., H. Ma, J. L. Bowman, et al., 1990. The protein encoded by the Arabidopsis homeotic gene agamous resembles transcription factors. *Nature*, **346**, 35.

[87] Maier, A. T., S. Stehling-Sun, H. Wollmann, et al., 2009. Dual roles of the bZIP transcription factor PERIANTHIA in the control of floral architecture and homeotic gene expression. *Development*, **136**, 1613.

[88] Prunet, N., P. Morel, A.-M. Thierry, et al., 2008. REBELOTE, SQUINT, and ULTRAPETALA1 function redundantly in the temporal regulation of floral meristem termination in Arabidopsis thaliana. *Plant Cell*, **20**, 901.

[89] Yamaguchi, N., J. Huang, Y. Xu, et al., 2017. Fine-tuning of auxin homeostasis governs the transition from floral stem cell maintenance to gynoecium formation. *Nature Communications*, **8**, 1125.

[90] Dockx, J., N. Quaedvlieg, G. Keultjes, et al., 1995. The homeobox gene ATK1 of Arabidop- sis thaliana is expressed in the shoot apex of the seedling and in flowers and inflorescence stems of mature plants. *Plant Molecular Biology*, **28**, 723.

[91] Pautot, V., J. Dockx, O. Hamant, et al., 2001. KNAT2: Evidence for a link between knotted- like genes and carpel development. *Plant Cell*, **13**, 1719.

[92] Byrne, M. E., R. Barley, M. Curtis, et al., 2000. Asymmetric leaves1 mediates leaf patterning and stem cell function in Arabidopsis. *Nature*, **408**, 967.

[93] Belles-Boix, E., O. Hamant, S. M. Witiak, et al., 2006. KNAT6: an Arabidopsis homeobox gene involved in meristem activity and organ separation. *Plant Cell*, **18**, 1900.

[94] Byrne, M. E., J. Simorowski, and R. A. Martienssen, 2002. ASYMMETRIC LEAVES1 reveals knox gene redundancy in Arabidopsis. *Development*, **129**, 1957.

[95] Sessions, A., J. L. Nemhauser, A. McColl, et al., 1997. ETTIN patterns the Arabidopsis floral meristem and reproductive organs. *Development*, **124**, 4481.

[96] Chung, Y., Y. Zhu, M.-F. Wu, et al., 2019. Auxin Response Factors promote organogenesis by chromatin-mediated repression of the pluripotency gene SHOOT MERISTEMLESS. *Nature Communications*, **10**, 886.

[97] Tabata, R., M. Ikezaki, T. Fujibe, et al., 2010. Arabidopsis AUXIN RESPONSE FACTOR6 and 8 regulate jasmonic acid biosynthesis and floral organ development via repression of class 1 KNOX genes. *Plant & Cell Physiology*, **51**, 164.

[98] Mayer, K. F., H. Schoof, A. Haecker, et al., 1998. Role of WUSCHEL in regulating stem cell fate in the Arabidopsis shoot meristem. *Cell*, **95**, 805.

[99] Schoof, H., M. Lenhard, A. Haecker, et al., 2000. The stem cell population of Arabidopsis shoot meristems is maintained by a regulatory loop between the CLAVATA and WUSCHEL genes. *Cell*, **100**, 635.

[100] Brand, U., J. C. Fletcher, M. Hobe, et al., 2000. Dependence of stem cell fate in Arabidopsis on a feedback loop regulated by CLV3 activity. *Science*, **289**, 617.

[101] Yadav, R. K., M. Perales, J. Gruel, et al., 2011. WUSCHEL protein movement mediates stem cell homeostasis in the Arabidopsis shoot apex. *Genes & Development*, **25**, 2025.

[102] Laux, T., K. F. Mayer, J. Berger, et al., 1996. The WUSCHEL gene is required for shoot and floral meristem integrity in Arabidopsis. *Development*, **122**, 87.

[103] Fan, H. Y., Y. Hu, M. Tudor, et al., 1997. Specific interactions between the K domains of AG and AGLs, members of the MADS domain family of DNA binding proteins. *The Plant Journal*, **12**, 999.

[104] Smaczniak, C., R. G. H. Immink, J. M. Muiño, et al., 2012. Characterization of MADS-domain transcription factor complexes in Arabidopsis flower development. *Proceedings of the National Academy of Sciences of the United States of America*, **109**, 1560.

[105] Levin, J. Z. and E. M. Meyerowitz, 1995. UFO: an Arabidopsis gene involved in both floral meristem and floral organ development. *Plant Cell*, **7**, 529.

[106] Busch, M. A., K. Bomblies, and D. Weigel, 1999. Activation of a floral homeotic gene in Arabidopsis. *Science*, **285**, 585.

[107] Lenhard, M., A. Bohnert, G. Jürgens, et al., 2001. Termination of stem cell maintenance in Arabidopsis floral meristems by interactions between WUSCHEL and AGAMOUS. *Cell*, **105**, 805.

[108] Lohmann, J. U., R. L. Hong, M. Hobe, et al., 2001. A molecular link between stem cell regulation and floral patterning in Arabidopsis. *Cell*, **105**, 793.

[109] Yu, L., V. Patibanda, and H. M. S. Smith, 2009. A novel role of BELL1-like homeobox genes, PENNYWISE and POUND-FOOLISH, in floral patterning. *Planta*, **229**, 693.

[110] Gómez-Mena, C., S. de Folter, M. M. R. Costa, et al., 2005. Transcriptional program controlled by the floral homeotic gene AGAMOUS during early organogenesis. *Development*, **132**, 429.

[111] Sun, B., Y. Xu, K.-H. Ng, et al., 2009. A timing mechanism for stem cell maintenance and differentiation in the Arabidopsis floral meristem. *Genes & Development*, **23**, 1791.

[112] Liu, X., Y. J. Kim, R. Müller, et al., 2011. AGAMOUS terminates floral stem cell maintenance in Arabidopsis by directly repressing WUSCHEL through recruitment of Polycomb Group proteins. *Plant Cell*, **23**, 3654.

[113] Yamaguchi, N., J. Huang, Y. Tatsumi, et al., 2018. Chromatin-mediated feed-forward auxin biosynthesis in floral meristem determinacy. *Nature Communications*, **9**, 5290.

[114] Coen, E. S. and E. M. Meyerowitz, 1991. The war of the whorls: genetic interactions controlling flower development. *Nature*, **353**, 31.

[115] Castillejo, C., M. Romera-Branchat, and S. Pelaz, 2005. A new role of the Arabidopsis SEPALLATA3 gene revealed by its constitutive expression. *The Plant Journal*, **43**, 586.

[116] Kaufmann, K., J. M. Muiño, R. Jauregui, et al., 2009. Target genes of the MADS transcription factor SEPALLATA3: integration of developmental and hormonal pathways in the Arabidopsis flower. *PLoS Biology*, **7**, e1000090.

[117] Lai, X., A. Stigliani, J. Lucas, et al., 2020. Genome-wide binding of SEPALLATA3 and AGAMOUS complexes determined by sequential DNA-affinity purification sequencing. *Nucleic Acids Research*, **48**, 9637.

[118] Kim, Y.-S., S.-G. Kim, M. Lee, et al., 2008. HD-ZIP III activity is modulated by competitive inhibitors via a feedback loop in Arabidopsis shoot apical meristem development. *Plant Cell*, **20**, 920.

[119] Douglas, S. J., G. Chuck, R. E. Dengler, et al., 2002. KNAT1 and ERECTA regulate inflorescence architecture in Arabidopsis. *Plant Cell*, **14**, 547.

[120] Venglat, S. P., T. Dumonceaux, K. Rozwadowski, et al., 2002. The homeobox gene BREVIPEDICELLUS is a key regulator of inflorescence architecture in Arabidopsis. *Proceedings of the National Academy of Sciences of the United States of America*, **99**, 4730.

[121] Mele, G., N. Ori, Y. Sato, et al., 2003. The knotted1-like homeobox gene BREVIPEDICELLUS regulates cell differentiation by modulating metabolic pathways. *Genes & Development*, **17**, 2088.

[122] Sohlberg, J. J., M. Myrenås, S. Kuusk, et al., 2006. STY1 regulates auxin homeostasis and affects apical-basal patterning of the Arabidopsis gynoecium. *The Plant Journal*, **47**, 112.

[123] Nemhauser, J. L., L. J. Feldman, and P. C. Zambryski, 2000. Auxin and ETTIN in Arabidopsis gynoecium morphogenesis. *Development*, **127**, 3877.

[124] Simonini, S., S. Bencivenga, M. Trick, et al., 2017. Auxin-induced modulation of ETTIN activity orchestrates gene expression in Arabidopsis. *Plant Cell*, **29**, 1864.

[125] Kuhn, A., B. Runciman, W. Tasker-Brown, et al., 2019. Two auxin response elements fine-tune PINOID expression during gynoecium development in Arabidopsis thaliana. *Biomolecules*, **9**.

[126] Kelley, D. R., A. Arreola, T. L. Gallagher, et al., 2012. ETTIN (ARF3) physically interacts with KANADI proteins to form a functional complex essential for integument development and polarity determination in Arabidopsis. *Development*, **139**, 1105.

[127] Simonini, S., J. Deb, L. Moubayidin, et al., 2016. A noncanonical auxin-sensing mechanism is required for organ morphogenesis in Arabidopsis. *Genes & Development*, **30**, 2286.

[128] Trigg, S. A., R. M. Garza, A. MacWilliams, et al., 2017. CrY2H-seq: a massively multiplexed assay for deep-coverage interactome mapping. *Nature Methods*, **14**, 819.

[129] Stahle, M. I., J. Kuehlich, L. Staron, et al., 2009. YABBYs and the transcriptional corepressors LEUNIG and LEUNIG_HOMOLOG maintain leaf polarity and meristem activity in Arabidopsis. *Plant Cell*, **21**, 3105.

[130] Bartholmes, C., O. Hidalgo, and S. Gleissberg, 2012. Evolution of the YABBY gene family with emphasis on the basal eudicot Eschscholzia californica (Papaveraceae). *Plant Biology*, **14**, 11.

[131] Eshed, Y., S. F. Baum, and J. L. Bowman, 1999. Distinct mechanisms promote polarity establishment in carpels of Arabidopsis. *Cell*, **99**, 199.

[132] Yamada, T., S. Yokota, Y. Hirayama, et al., 2011. Ancestral expression patterns and evolutionary diversification of YABBY genes in angiosperms. *The Plant Journal*, **67**, 26.

[133] Zhao, Y., S. K. Christensen, C. Fankhauser, et al., 2001. A role for flavin monooxygenase-like enzymes in auxin biosynthesis. *Science*, **291**, 306.

[134] Cheng, Y., X. Dai, and Y. Zhao, 2006. Auxin biosynthesis by the YUCCA flavin monooxy- genases controls the formation of floral organs and vascular tissues in Arabidopsis. *Genes & Development*, **20**, 1790.

[135] Galván-Ampudia, C. S. and R. Offringa, 2007. Plant evolution: AGC kinases tell the auxin tale. *Trends in Plant Science*, **12**, 541.

[136] Benjamins, R., A. Quint, D. Weijers, et al., 2001. The PINOID protein kinase regulates organ development in Arabidopsis by enhancing polar auxin transport. *Development*, **128**, 4057.

[137] Friml, J., X. Yang, M. Michniewicz, et al., 2004. A PINOID-dependent binary switch in apical-basal PIN polar targeting directs auxin efflux. *Science*, **306**, 862.

[138] Sauer, M., J. Balla, C. Luschnig, et al., 2006. Canalization of auxin flow by Aux/IAA-ARF-dependent feedback regulation of PIN polarity. *Genes & Development*, **20**, 2902.

[139] Santner, A. A. and J. C. Watson, 2006. The WAG1 and WAG2 protein kinases negatively regulate root waving in Arabidopsis. *The Plant Journal*, **45**, 752.

[140] Ishida, K., T. Yamashino, A. Yokoyama, et al., 2008. Three type-B response regulators, ARR1, ARR10 and ARR12, play essential but redundant roles in cytokinin signal transduction throughout the life cycle of Arabidopsis thaliana. *Plant & Cell Physiology*, **49**, 47.

[141] Zeng, J., X. Zhu, M. S. Haider, et al., 2017. Genome-wide identification and analysis of the type-B authentic response regulator gene family in peach (Prunus persica). *Cytogenetic and Genome Research*, **151**, 41.

[142] D'Agostino, I. B., J. Deruère, and J. J. Kieber, 2000. Characterization of the response of the Arabidopsis response regulator gene family to cytokinin. *Plant Physiology*, **124**, 1706.

[143] Reinhart, B. J., T. Liu, N. R. Newell, et al., 2013. Establishing a framework for the ad/abaxial regulatory network of Arabidopsis: ascertaining targets of class III HOMEODOMAIN LEUCINE ZIPPER and KANADI regulation. *Plant Cell*, **25**, 3228.

[144] Marín-de la Rosa, N., A. Pfeiffer, K. Hill, et al., 2015. Genome wide binding site analysis reveals transcriptional coactivation of cytokinin-responsive genes by DELLA proteins. *PLoS Genetics*, **11**, e1005337.

[145] Altmann, M., S. Altmann, P. A. Rodriguez, et al., 2020. Extensive signal integration by the phytohormone protein network. *Nature*, **583**, 271.

[146] Zhang, T.-Q., H. Lian, C.-M. Zhou, et al., 2017. A two-step model for de novo activation of WUSCHEL during plant shoot regeneration. *Plant Cell*, **29**, 1073.

[147] Herrera-Ubaldo, H., S. E. Campos, P. López-Gómez, et al., 2022. The protein-protein interaction landscape of transcription factors during gynoecium development in Arabidopsis. *Molecular Plant*.

[148] Eklund, D. M., M. Thelander, K. Landberg, et al., 2010. Homologues of the Arabidopsis thaliana SHI/STY/LRP1 genes control auxin biosynthesis and affect growth and development in the moss Physcomitrella patens. *Development*, **137**, 1275.

[149] Martínez-Fernández, I., S. Sanchís, N. Marini, et al., 2014. The effect of NGATHA altered activity on auxin signaling pathways within the Arabidopsis gynoecium. *Frontiers in Plant Science*, **5**, 210.

[150] Girin, T., T. Paicu, P. Stephenson, et al., 2011. INDEHISCENT and SPATULA interact to specify carpel and valve margin tissue and thus promote seed dispersal in Arabidopsis. *Plant Cell*, **23**, 3641.

[151] Reyes-Olalde, J. I., V. M. Zúñiga-Mayo, J. Serwatowska, et al., 2017. The bHLH transcription factor SPATULA enables cytokinin signaling, and both activate auxin biosynthesis and transport genes at the medial domain of the gynoecium. *PLoS Genetics*, **13**, e1006726.

[152] Carabelli, M., L. Turchi, G. Morelli, et al., 2021. Coordination of biradial-to-radial symmetry and tissue polarity by HD-ZIP II proteins. *Nature Communications*, **12**, 4321.

[153] Arnaud, N., T. Girin, K. Sorefan, et al., 2010. Gibberellins control fruit patterning in Arabidopsis thaliana. *Genes & Development*, **24**, 2127.

[154] Schuster, C., C. Gaillochet, A. Medzihradszky, et al., 2014. A regulatory framework for shoot stem cell control integrating metabolic, transcriptional, and phytohormone signals. *Developmental Cell*, **28**, 438.

[155] Schuster, C., C. Gaillochet, and J. U. Lohmann, 2015. Arabidopsis HECATE genes function in phytohormone control during gynoecium development. *Development*, **142**, 3343.

[156] Bennett, S. R., J. P. Alvarez, G. Bossinger, et al., 1995. Morphogenesis in pinoid mutants of Arabidopsis thaliana. *The Plant Journal*, **8**, 505.

[157] Zúñiga-Mayo, V. M., A. Gómez-Felipe, H. Herrera-Ubaldo, et al., 2019. Gynoecium development: networks in Arabidopsis and beyond. *Journal of Experimental Botany*, **70**, 1447.

[158] Ito, T., F. Wellmer, H. Yu, et al., 2004. The homeotic protein AGAMOUS controls microsporogenesis by regulation of SPOROCYTELESS. *Nature*, **430**, 356.

[159] Ito, T., K.-H. Ng, T.-S. Lim, et al., 2007. The homeotic protein AGAMOUS controls late stamen development by regulating a jasmonate biosynthetic gene in Arabidopsis. *Plant Cell*, **19**, 3516.

[160] Bencivenga, S., S. Simonini, E. Benková, et al., 2012. The transcription factors BEL1 and SPL are required for cytokinin and auxin signaling during ovule development in Arabidopsis. *Plant Cell*, **24**, 2886.

[161] Bellaoui, M., M. S. Pidkowich, A. Samach, et al., 2001. The Arabidopsis BELL1 and KNOX TALE homeodomain proteins interact through a domain conserved between plants and an- imals. *Plant Cell*, **13**, 2455.

[162] Byrne, M. E., A. T. Groover, J. R. Fontana, et al., 2003. Phyllotactic pattern and stem cell fate are determined by the Arabidopsis homeobox gene BELLRINGER. *Development*, **130**, 3941.

[163] García-Martinez, J. L. and J. Gil, 2001. Light Regulation of Gibberellin Biosynthesis and Mode of Action. *Journal of Plant Growth Regulation*, **20**, 354.

[164] Yu, H., T. Ito, Y. Zhao, et al., 2004. Floral homeotic genes are targets of gibberellin signaling in flower development. *Proceedings of the National Academy of Sciences of the United States of America*, **101**, 7827.

[165] Donner, T. J., I. Sherr, and E. Scarpella, 2009. Regulation of preprocambial cell state acquisition by auxin signaling in Arabidopsis leaves. *Development*, **136**, 3235.

[166] Ilegems, M., V. Douet, M. Meylan-Bettex, et al., 2010. Interplay of auxin, KANADI and Class III HD-ZIP transcription factors in vascular tissue formation. *Development*, **137**, 975.

[167] Brandt, R., M. Salla-Martret, J. Bou-Torrent, et al., 2012. Genome-wide binding-site analysis of REVOLUTA reveals a link between leaf patterning and light-mediated growth responses. *The Plant Journal*, **72**, 31.

[168] Dello Ioio, R., C. Galinha, A. G. Fletcher, et al., 2012. A PHABULOSA/cytokinin feedback loop controls root growth in Arabidopsis. *Current Biology*, **22**, 1699.

[169] Ursache, R., S. Miyashima, Q. Chen, et al., 2014. Tryptophan-dependent auxin biosynthesis is required for HD-ZIP III-mediated xylem patterning. *Development*, **141**, 1250.

[170] Sebastian, J., K. H. Ryu, J. Zhou, et al., 2015. PHABULOSA controls the quiescent center-independent root meristem activities in Arabidopsis thaliana. *PLoS Genetics*, **11**, e1004973.

[171] Müller, C. J., A. E. Valdés, G. Wang, et al., 2016. PHABULOSA mediates an auxin signaling loop to regulate vascular patterning in Arabidopsis. *Plant Physiology*, **170**, 956.

[172] Theißen, G. and H. Saedler, 2001. Floral quartets. *Nature*, **409**, 469.

[173] Theißen, G., R. Melzer, and F. Rümpler, 2016. MADS-domain transcription factors and the floral quartet model of flower development: linking plant development and evolution. *Development*, **143**, 3259.

[174] Pabón-Mora, N., B. A. Ambrose, and A. Litt, 2012. Poppy APETALA1/FRUITFULL orthologs control flowering time, branching, perianth identity, and fruit development. *Plant Physiology*, **158**, 1685.

[175] Jofuku, K. D., B. G. den Boer, M. van Montagu, et al., 1994. Control of Arabidopsis flower and seed development by the homeotic gene APETALA2. *Plant Cell*, **6**, 1211.

[176] Bowman, J. L., H. Sakai, T. Jack, et al., 1992. SUPERMAN, a regulator of floral homeotic genes in Arabidopsis. *Development*, **114**, 599.

[177] Jack, T., G. L. Fox, and E. M. Meyerowitz, 1994. Arabidopsis homeotic gene APETALA3 ec- topic expression: Transcriptional and posttranscriptional regulation determine floral organ identity. *Cell*, **76**, 703.

[178] Lee, I., D. S. Wolfe, O. Nilsson, et al., 1997. A LEAFY co-regulator encoded by UNUSUAL FLORAL ORGANS. *Current Biology*, **7**, 95.

[179] Ray, A., K. Robinson-Beers, S. Ray, et al., 1994. Arabidopsis floral homeotic gene BELL (BEL1) controls ovule development through negative regulation of AGAMOUS gene (AG). *Proceedings of the National Academy of Sciences of the United States of America*, **91**, 5761.

[180] Reiser, L., Z. Modrusan, L. Margossian, et al., 1995. The BELL1 gene encodes a homeodomain protein involved in pattern formation in the Arabidopsis ovule primordium. *Cell*, **83**, 735.

[181] Sieburth, L. E. and E. M. Meyerowitz, 1997. Molecular dissection of the AGAMOUS con-trol region shows that cis elements for spatial regulation are located intragenically. *Plant Cell*, **9**, 355.

[182] Brambilla, V., R. Battaglia, M. Colombo, et al., 2007. Genetic and molecular interactions between BELL1 and MADS box factors support ovule development in Arabidopsis. *Plant Cell*, **19**, 2544.

[183] Robinson-Beers, K., R. E. Pruitt, and C. S. Gasser, 1992. Ovule development in wild-type Arabidopsis and two Female-sterile mutants. *Plant Cell*, **4**, 1237.

[184] Ehlers, K., A. S. Bhide, D. G. Tekleyohans, et al., 2016. The MADS box genes ABS, SHP1, and SHP2 are essential for the coordination of cell divisions in ovule and seed coat development and for endosperm formation in Arabidopsis thaliana. *PloS One*, **11**, e0165075.

[185] Favaro, R., A. Pinyopich, R. Battaglia, et al., 2003. MADS-box protein complexes control carpel and ovule development in Arabidopsis. *Plant Cell*, **15**, 2603.

[186] Pinyopich, A., G. S. Ditta, B. Savidge, et al., 2003. Assessing the redundancy of MADS-box genes during carpel and ovule development. *Nature*, **424**, 85.

[187] Zahn, L. M., H. Kong, J. H. Leebens-Mack, et al., 2005. The evolution of the SEPALLATA subfamily of MADS-box genes: a preangiosperm origin with multiple duplications throughout angiosperm history. *Genetics*, **169**, 2209.

[188] Sridhar, V. V., A. Surendrarao, and Z. Liu, 2006. APETALA1 and SEPALLATA3 interact with SEUSS to mediate transcription repression during flower development. *Development*, **133**, 3159.

[189] Pelaz, S., G. S. Ditta, E. Baumann, et al., 2000. B and C floral organ identity functions require SEPALLATA MADS-box genes. *Nature*, **405**, 200.

[190] Flanagan, C. A. and H. Ma, 1994. Spatially and temporally regulated expression of the MADS-box gene AGL2 in wild-type and mutant arabidopsis flowers. *Plant Molecular Biology*, **26**, 581.

[191] Huang, H., M. Tudor, C. A. Weiss, et al., 1995. The Arabidopsis MADS-box gene AGL3 is widely expressed and encodes a sequence-specific DNA-binding protein. *Plant Molecular Biology*, **28**, 549.

[192] Savidge, B., S. D. Rounsley, and M. F. Yanofsky, 1995. Temporal relationship between the transcription of two Arabidopsis MADS box genes and the floral organ identity genes. *Plant Cell*, **7**, 721.

[193] Mandel, M. A. and M. F. Yanofsky, 1998. The Arabidopsis AGL 9 MADS box gene is expressed in young flower primordia. *Sexual Plant Reproduction*, **11**, 22.

[194] Gregis, V., A. Sessa, L. Colombo, et al., 2006. AGL24, SHORT VEGETATIVE PHASE, and APETALA1 redundantly control AGAMOUS during early stages of flower development in Arabidopsis. *Plant Cell*, **18**, 1373.

[195] Bao, X., R. G. Franks, J. Z. Levin, et al., 2004. Repression of AGAMOUS by BELLRINGER in floral and inflorescence meristems. *Plant Cell*, **16**, 1478.

[196] Grigorova, B., C. Mara, C. Hollender, et al., 2011. LEUNIG and SEUSS co-repressors regulate miR172 expression in Arabidopsis flowers. *Development*, **138**, 2451.

[197] Sawa, S., T. Ito, Y. Shimura, et al., 1999. FILAMENTOUS FLOWER controls the formation and development of Arabidopsis inflorescences and floral meristems. *Plant Cell*, **11**, 69.

[198] Chen, Q., A. Atkinson, D. Otsuga, et al., 1999. The Arabidopsis FILAMENTOUS FLOWER gene is required for flower formation. *Development*, **126**, 2715.

[199] Bowman, J. L., Y. Eshed, and S. F. Baum, 2002. Establishment of polarity in angiosperm lateral organs. *Trends in Genetics*, **18**, 134.

[200] Smith, H. M. S., I. Boschke, and S. Hake, 2002. Selective interaction of plant homeodomain proteins mediates high DNA-binding affinity. *Proceedings of the National Academy of Sciences of the United States of America*, **99**, 9579.

[201] Cole, M., C. Nolte, and W. Werr, 2006. Nuclear import of the transcription factor SHOOT MERISTEMLESS depends on heterodimerization with BLH proteins expressed in discrete sub-domains of the shoot apical meristem of Arabidopsis thaliana. *Nucleic Acids Research*, **34**, 1281.

[202] Lee, J.-H., H. Lin, S. Joo, et al., 2008. Early sexual origins of homeoprotein heterodimerization and evolution of the plant KNOX/BELL family. *Cell*, **133**, 829.

[203] Mukherjee, K., L. Brocchieri, and T. R. Bürglin, 2009. A comprehensive classification and evolutionary analysis of plant homeobox genes. *Molecular Biology and Evolution*, **26**, 2775.

[204] Rutjens, B., D. Bao, E. van Eck-Stouten, et al., 2009. Shoot apical meristem function in Arabidopsis requires the combined activities of three BEL1-like homeodomain proteins. *The Plant Journal*, **58**, 641.

[205] Girin, T., K. Sorefan, and L. Ostergaard, 2009. Meristematic sculpting in fruit development. *Journal of Experimental Botany*, **60**, 1493.

[206] Gómez-Mena, C. and R. Sablowski, 2008. ARABIDOPSIS THALIANA HOMEOBOX GENE1 establishes the basal boundaries of shoot organs and controls stem growth. *Plant Cell*, **20**, 2059.

[207] Khan, M., P. Tabb, and S. R. Hepworth, 2012. BLADE-ON-PETIOLE1 and 2 regulate Arabidopsis inflorescence architecture in conjunction with homeobox genes KNAT6 and ATH1. *Plant Signaling & Behavior*, **7**, 788.

[208] Li, Y., L. Pi, H. Huang, et al., 2012. ATH1 and KNAT2 proteins act together in regulation of plant inflorescence architecture. *Journal of Experimental Botany*, **63**, 1423.

[209] Stammler, A., S. S. Meyer, A. R. Plant, et al., 2013. Duplicated STM-like KNOX I genes act in floral meristem activity in Eschscholzia californica (Papaveraceae). *Development Genes and Evolution*, **223**, 289.

[210] Zhao, M., S. Yang, C.-Y. Chen, et al., 2015. Arabidopsis BREVIPEDICELLUS interacts with the SWI2/SNF2 chromatin remodeling ATPase BRAHMA to regulate KNAT2 and KNAT6 expression in control of inflorescence architecture. *PLoS Genetics*, **11**, e1005125.

[211] Frangedakis, E., D. Saint-Marcoux, L. A. Moody, et al., 2017. Nonreciprocal complementa- tion of KNOX gene function in land plants. *New Phytologist*, **216**, 591.

[212] Müller, J., Y. Wang, R. Franzen, et al., 2001. In vitro interactions between barley TALE homeodomain proteins suggest a role for protein-protein associations in the regulation of Knox gene function. *The Plant Journal*, **27**, 13.

[213] Smith, H. M. S. and S. Hake, 2003. The interaction of two homeobox genes, BREVIPEDICELLUS and PENNYWISE, regulates internode patterning in the Arabidopsis inflorescence. *Plant Cell*, **15**, 1717.

[214] Hackbusch, J., K. Richter, J. Müller, et al., 2005. A central role of Arabidopsis thaliana ovate family proteins in networking and subcellular localization of 3-aa loop extension homeodomain proteins. *Proceedings of the National Academy of Sciences of the United States of America*, **102**, 4908.

[215] Kanrar, S., O. Onguka, and H. M. S. Smith, 2006. Arabidopsis inflorescence architecture requires the activities of KNOX-BELL homeodomain heterodimers. *Planta*, **224**, 1163.

[216] Wang, Y., Y. Zhao, M. Yan, et al., 2020. Genome-wide identification and expression analysis of TALE gene family in pomegranate (Punica granatum L.). *Agronomy*, **10**, 829.

[217] Lenhard, M., G. Jürgens, and T. Laux, 2002. The WUSCHEL and SHOOTMERISTEM- LESS genes fulfil complementary roles in Arabidopsis shoot meristem regulation. *Development*, **129**, 3195.

[218] Kumaran, M. K., J. L. Bowman, and V. Sundaresan, 2002. YABBY polarity genes mediate the repression of KNOX homeobox genes in Arabidopsis. *Plant Cell*, **14**, 2761.

[219] Long, J. A., E. I. Moan, J. I. Medford, et al., 1996. A member of the KNOTTED class of homeodomain proteins encoded by the STM gene of Arabidopsis. *Nature*, **379**, 66.

[220] Aida, M., T. Ishida, and M. Tasaka, 1999. Shoot apical meristem and cotyledon formation during Arabidopsis embryogenesis: interaction among the CUP-SHAPED COTYLEDON and SHOOT MERISTEMLESS genes. *Development*, **126**, 1563.

[221] Groot, E. P., N. Sinha, and S. Gleissberg, 2005. Expression patterns of STM-like KNOX and Histone H4 genes in shoot development of the dissected-leaved basal eudicot plants Chelidonium majus and Eschscholzia californica (Papaveraceae). *Plant Molecular Biology*, **58**, 317.

[222] Kimura, S., D. Koenig, J. Kang, et al., 2008. Natural variation in leaf morphology results from mutation of a novel KNOX gene. *Current Biology*, **18**, 672.

[223] Hay, A., H. Kaur, A. Phillips, et al., 2002. The gibberellin pathway mediates KNOTTED1- Type homeobox function in plants with Different body plans. *Current Biology*, **12**, 1557.

[224] Jasinski, S., P. Piazza, J. Craft, et al., 2005. KNOX action in Arabidopsis is mediated by coordinate regulation of cytokinin and gibberellin activities. *Current Biology*, **15**, 1560.

[225] Yanai, O., E. Shani, K. Dolezal, et al., 2005. Arabidopsis KNOXI proteins activate cytokinin biosynthesis. *Current Biology*, **15**, 1566.

[226] Jung, J.-H., J. Yun, Y.-H. Seo, et al., 2005. Characterization of an Arabidopsis gene that mediates cytokinin signaling in shoot apical meristem development. *Molecules and Cells*, **19**, 342.

[227] Gordon, S. P., V. S. Chickarmane, C. Ohno, et al., 2009. Multiple feedback loops through cytokinin signaling control stem cell number within the Arabidopsis shoot meristem. *Proceedings of the National Academy of Sciences of the United States of America*, **106**, 16529.

[228] Neff, M. M., S. M. Nguyen, E. J. Malancharuvil, et al., 1999. BAS1: A gene regulating brassinosteroid levels and light responsiveness in Arabidopsis. *Proceedings of the National Academy of Sciences of the United States of America*, **96**, 15316.

[229] Bell, E. M., W.-c. Lin, A. Y. Husbands, et al., 2012. Arabidopsis LATERAL ORGAN BOUNDARIES negatively regulates brassinosteroid accumulation to limit growth in organ boundaries. *Proceedings of the National Academy of Sciences of the United States of America*, **109**, 21146.

[230] Roth, O., J. P. Alvarez, M. Levy, et al., 2018. The KNOXI transcription factor SHOOT MERISTEMLESS regulates floral fate in Arabidopsis. *Plant Cell*, **30**, 1309.

[231] Chuck, G., C. Lincoln, and S. Hake, 1996. KNAT1 induces lobed leaves with ectopic meristems when overexpressed in Arabidopsis. *Plant Cell*, **8**, 1277.

[232] Khan, M., M. Xu, J. Murmu, et al., 2012. Antagonistic interaction of BLADE-ON-PETIOLE1 and 2 with BREVIPEDICELLUS and PENNYWISE regulates Arabidopsis inflorescence architecture. *Plant Physiology*, **158**, 946.

[233] Zhao, Y., X. Song, H. Zhou, et al., 2020. KNAT2/6b, a class I KNOX gene, impedes xylem differentiation by regulating NAC domain transcription factors in poplar. *New Phytologist*, **225**, 1531.

[234] Shi, C.-L., G.-E. Stenvik, A. K. Vie, et al., 2011. Arabidopsis class I KNOTTED-like homeobox proteins act downstream in the IDA-HAE/HSL2 floral abscission signaling pathway. *Plant Cell*, **23**, 2553.

[235] Groover, A. and A. M. Jones, 1999. Tracheary element differentiation uses a novel mechanism coordinating programmed cell death and secondary cell wall synthesis. *Plant Physiol- ogy*, **119**, 375.

[236] Becker, A., M. Bey, T. R. Bürglin, et al., 2002. Ancestry and diversity of BEL1-like homeobox genes revealed by gymnosperm (Gnetum gnemon) homologs. *Development Genes and Evolution*, **212**, 452.

[237] Dong, Y. H., J. L. Yao, R. G. Atkinson, et al., 2000. MDH1: an apple homeobox gene belonging to the BEL1 family. *Plant Molecular Biology*, **42**, 623.

[238] Cao, X., J. Wang, Y. Xiong, et al., 2020. A self-activation loop maintains meristematic cell fate for branching. *Current Biology*, **30**, 1893.

[239] Ram, H., S. Sahadevan, N. Gale, et al., 2020. An integrated analysis of cell-type specific gene expression reveals genes regulated by REVOLUTA and KANADI1 in the Arabidopsis shoot apical meristem. *PLoS Genetics*, **16**, e1008661.

[240] Kerstetter, R. A., D. Laudencia-Chingcuanco, L. G. Smith, et al., 1997. Loss-of-function mutations in the maize homeobox gene, knotted1, are defective in shoot meristem maintenance. *Development*, **124**, 3045.

[241] Sakamoto, T., N. Kamiya, M. Ueguchi-Tanaka, et al., 2001. KNOX homeodomain protein directly suppresses the expression of a gibberellin biosynthetic gene in the tobacco shoot apical meristem. *Genes & Development*, **15**, 581.

[242] Chen, H., A. K. Banerjee, and D. J. Hannapel, 2004. The tandem complex of BEL and KNOX partners is required for transcriptional repression of ga20ox1. *The Plant Journal*, **38**, 276.

[243] Bolduc, N. and S. Hake, 2009. The maize transcription factor KNOTTED1 directly regulates the gibberellin catabolism gene ga2ox1. *Plant Cell*, **21**, 1647.

[244] Shani, E., H. Ben-Gera, S. Shleizer-Burko, et al., 2010. Cytokinin regulates compound leaf development in tomato. *Plant Cell*, **22**, 3206.

[245] Bolduc, N., A. Yilmaz, M. K. Mejia-Guerra, et al., 2012. Unraveling the KNOTTED1 regulatory network in maize meristems. *Genes & Development*, **26**, 1685.

[246] Tsuda, K., N. Kurata, H. Ohyanagi, et al., 2014. Genome-wide study of KNOX regulatory network reveals brassinosteroid catabolic genes important for shoot meristem function in rice. *Plant Cell*, **26**, 3488.

[247] Izhaki, A. and J. L. Bowman, 2007. KANADI and class III HD-Zip gene families regulate embryo patterning and modulate auxin flow during embryogenesis in Arabidopsis. *Plant Cell*, **19**, 495.

[248] Kerstetter, R. A., K. Bollman, R. A. Taylor, et al., 2001. KANADI regulates organ polarity in Arabidopsis. *Nature*, **411**, 706.

[249] Candela, H., R. Johnston, A. Gerhold, et al., 2008. The milkweed pod1 gene encodes a KANADI protein that is required for abaxial/adaxial patterning in maize leaves. *Plant Cell*, **20**, 2073.

[250] Zhang, G.-H., Q. Xu, X.-D. Zhu, et al., 2009. SHALLOT-LIKE1 is a KANADI transcription factor that modulates rice leaf rolling by regulating leaf abaxial cell development. *Plant Cell*, **21**, 719.

[251] Whitewoods, C. D., B. Gonçalves, J. Cheng, et al., 2020. Evolution of carnivorous traps from planar leaves through simple shifts in gene expression. *Science*, **367**, 91.

[252] Andres-Robin, A., M. C. Reymond, A. Dupire, et al., 2018. Evidence for the regulation of gynoecium morphogenesis by ETTIN via cell wall dynamics. *Plant Physiology*, **178**, 1222.

[253] Fahlgren, N., T. A. Montgomery, M. D. Howell, et al., 2006. Regulation of AUXIN RESPONSE FACTOR3 by TAS3 ta-siRNA affects developmental timing and patterning in Arabidopsis. *Current Biology*, **16**, 939.

[254] Hunter, C., M. R. Willmann, G. Wu, et al., 2006. Trans-acting siRNA-mediated repression of ETTIN and ARF4 regulates heteroblasty in Arabidopsis. *Development*, **133**, 2973.

[255] Liu, N., S. Wu, J. van Houten, et al., 2014. Down-regulation of AUXIN RESPONSE FACTORS 6 and 8 by microRNA 167 leads to floral development defects and female sterility in tomato. *Journal of Experimental Botany*, **65**, 2507.

[256] Goetz, M., A. Vivian-Smith, S. D. Johnson, et al., 2006. AUXIN RESPONSE FACTOR8 is a negative regulator of fruit initiation in Arabidopsis. *Plant Cell*, **18**, 1873.

[257] Goetz, M., L. C. Hooper, S. D. Johnson, et al., 2007. Expression of aberrant forms of AUXIN RESPONSE FACTOR8 stimulates parthenocarpy in Arabidopsis and tomato. *Plant Physiology*, **145**, 351.

[258] Zhang, R., Y. Min, L. D. Holappa, et al., 2020. A role for the Auxin Response Factors ARF6 and ARF8 homologs in petal spur elongation and nectary maturation in Aquilegia. *New Phytologist*, **227**, 1392.

[259] Wu, C.-C., F.-W. Li, and E. M. Kramer, 2019. Large-scale phylogenomic analysis suggests three ancient superclades of the WUSCHEL-RELATED HOMEOBOX transcription factor family in plants. *PloS One*, **14**, e0223521.

[260] Vandenbussche, M., A. Horstman, J. Zethof, et al., 2009. Differential recruitment of WOX transcription factors for lateral development and organ fusion in Petunia and Arabidopsis. *Plant Cell*, **21**, 2269.

[261] Matsumoto, N. and K. Okada, 2001. A homeobox gene, PRESSED FLOWER, regulates lateral axis-dependent development of Arabidopsis flowers. *Genes & Development*, **15**, 3355.

[262] Nardmann, J., J. Ji, W. Werr, et al., 2004. The maize duplicate genes narrow sheath1 and narrow sheath2 encode a conserved homeobox gene function in a lateral domain of shoot apical meristems. *Development*, **131**, 2827.

[263] Shimizu, R., J. Ji, E. Kelsey, et al., 2009. Tissue specificity and evolution of meristematic WOX3 function. *Plant Physiology*, **149**, 841.

[264] Nakata, M., N. Matsumoto, R. Tsugeki, et al., 2012. Roles of the middle domain-specific WUSCHEL-RELATED HOMEOBOX genes in early development of leaves in Arabidopsis. *Plant Cell*, **24**, 519.

[265] Zhang, F. and M. Tadege, 2015. Repression of AS2 by WOX family transcription factors is required for leaf development in Medicago and Arabidopsis. *Plant Signaling & Behavior*, **10**, e993291.

[266] Scanlon, M. J., R. G. Schneeberger, and M. Freeling, 1996. The maize mutant narrow sheath fails to establish leaf margin identity in a meristematic domain. *Development*, **122**, 1683.

[267] Cho, S.-H., S.-C. Yoo, H. Zhang, et al., 2013. The rice narrow leaf2 and narrow leaf3 loci encode WUSCHEL-related homeobox 3A (OsWOX3A) and function in leaf, spikelet, tiller and lateral root development. *New Phytologist*, **198**, 1071.

[268] Ishiwata, A., M. Ozawa, H. Nagasaki, et al., 2013. Two WUSCHEL-related homeobox genes, narrow leaf2 and narrow leaf3, control leaf width in rice. *Plant & Cell Physiology*, **54**, 779.

[269] Zhang, F., Y. Wang, G. Li, et al., 2014. STENOFOLIA recruits TOPLESS to repress ASYM- METRIC LEAVES2 at the leaf margin and promote leaf blade outgrowth in Medicago trun- catula. *Plant Cell*, **26**, 650.

[270] Wolabu, T. W., H. Wang, D. Tadesse, et al., 2021. WOX9 functions antagonistic to STF and LAM1 to regulate leaf blade expansion in Medicago truncatula and Nicotiana sylvestris. *New Phytologist*, **229**, 1582.

[271] Breuninger, H., E. Rikirsch, M. Hermann, et al., 2008. Differential expression of WOX genes mediates apical-basal axis formation in the Arabidopsis embryo. *Developmental Cell*, **14**, 867.

[272] Sarkar, A. K., M. Luijten, S. Miyashima, et al., 2007. Conserved factors regulate signalling in Arabidopsis thaliana shoot and root stem cell organizers. *Nature*, **446**, 811.

[273] Ji, J., J. Strable, R. Shimizu, et al., 2010. WOX4 promotes procambial development. *Plant Physiology*, **152**, 1346.

[274] Park, S. O., Z. Zheng, D. G. Oppenheimer, et al., 2005. The PRETTY FEW SEEDS2 gene encodes an Arabidopsis homeodomain protein that regulates ovule development. *Development*, **132**, 841.

[275] Green, K. A., M. J. Prigge, R. B. Katzman, et al., 2005. CORONA, a member of the class III homeodomain leucine zipper gene family in Arabidopsis, regulates stem cell specification and organogenesis. *Plant Cell*, **17**, 691.

[276] Gross-Hardt, R., M. Lenhard, and T. Laux, 2002. WUSCHEL signaling functions in inter- regional communication during Arabidopsis ovule development. *Genes & Development*, **16**, 1129.

[277] Deyhle, F., A. K. Sarkar, E. J. Tucker, et al., 2007. WUSCHEL regulates cell differentiation during anther development. *Developmental Biology*, **302**, 154.

[278] Liang, J., P. Guan, Z. Liu, et al., 2020. The VvSUPERMAN-like gene is differentially expressed between bicarpellate and tricarpellate florets of Vitis vinifera L. Cv. 'Xiangfei' and its heterologous expression reduces carpel number in tomato. *Plant & Cell Physiology*, **61**, 1760.

[279] Gaillochet, C., T. Stiehl, C. Wenzl, et al., 2017. Control of plant cell fate transitions by transcriptional and hormonal signals. *eLife*, **6**.

[280] Werner, T., V. Motyka, M. Strnad, et al., 2001. Regulation of plant growth by cytokinin. *Proceedings of the National Academy of Sciences of the United States of America*, **98**, 10487.

[281] To, J. P. C., G. Haberer, F. J. Ferreira, et al., 2004. Type-A Arabidopsis response regulators are partially redundant negative regulators of cytokinin signaling. *Plant Cell*, **16**, 658.

[282] Tani, E., A. Tsaballa, C. Stedel, et al., 2011. The study of a SPATULA-like bHLH transcrip- tion factor expressed during peach (Prunus persica) fruit development. *Plant Physiology and Biochemistry*, **49**, 654.

[283] Ortiz-Ramírez, C. I., M. A. Giraldo, C. Ferrándiz, et al., 2019. Expression and function of the bHLH genes ALCATRAZ and SPATULA in selected Solanaceae species. *The Plant Journal*, **99**, 686.

[284] Dardick, C. and A. M. Callahan, 2014. Evolution of the fruit endocarp: molecular mechanisms underlying adaptations in seed protection and dispersal strategies. *Frontiers in Plant Science*, **5**, 284.

[285] Morel, P., K. Heijmans, K. Ament, et al., 2018. The floral C-lineage genes trigger nectary development in Petunia and Arabidopsis. *Plant Cell*, **30**, 2020.

[286] Nagasawa, N., M. Miyoshi, Y. Sano, et al., 2003. SUPERWOMAN1 and DROOPING LEAF genes control floral organ identity in rice. *Development*, **130**, 705.

[287] Yamaguchi, T., N. Nagasawa, S. Kawasaki, et al., 2004. The YABBY gene DROOPING LEAF regulates carpel specification and midrib development in Oryza sativa. *Plant Cell*, **16**, 500.

[288] Orashakova, S., M. Lange, S. Lange, et al., 2009. The CRABS CLAW ortholog from California poppy (Eschscholzia californica, Papaveraceae), EcCRC, is involved in floral meristem termination, gynoecium differentiation and ovule initiation. *The Plant Journal*, **58**, 682.

[289] Castañeda, L., E. Giménez, B. Pineda, et al., 2022. Tomato CRABS CLAW paralogues interact with chromatin remodelling factors to mediate carpel development and floral determinacy. *New Phytologist*.

[290] Fourquin, C., A. Primo, I. Martínez-Fernández, et al., 2014. The CRC orthologue from Pisum sativum shows conserved functions in carpel morphogenesis and vascular development. *Annals of Botany*, **114**, 1535.

[291] Toriba, T. and H.-Y. Hirano, 2014. The DROOPING LEAF and OsETTIN2 genes promote awn development in rice. *The Plant Journal*, **77**, 616.

[292] Golz, J. F., M. Roccaro, R. Kuzoff, et al., 2004. GRAMINIFOLIA promotes growth and polarity of Antirrhinum leaves. *Development*, **131**, 3661.

[293] Juarez, M. T., R. W. Twigg, and M. C. P. Timmermans, 2004. Specification of adaxial cell fate during maize leaf development. *Development*, **131**, 4533.

[294] Liu, H.-l., Y.-Y. Xu, Z.-H. Xu, et al., 2007. A rice YABBY gene, OsYABBY4, preferentially expresses in developing vascular tissue. *Development Genes and Evolution*, **217**, 629.

[295] Nakayama, H., T. Yamaguchi, and H. Tsukaya, 2010. Expression patterns of AaDL, a CRABS CLAW ortholog in Asparagus asparagoides (Asparagaceae), demonstrate a stepwise evolution of CRC/DL subfamily of YABBY genes. *American Journal of Botany*, **97**, 591.

[296] Vaucheret, H., F. Vazquez, P. Crété, et al., 2004. The action of ARGONAUTE1 in the miRNA pathway and its regulation by the miRNA pathway are crucial for plant development. *Genes & Development*, **18**, 1187.

[297] Qi, Y., A. M. Denli, and G. J. Hannon, 2005. Biochemical specialization within Arabidopsis RNA silencing pathways. *Molecular Cell*, **19**, 421.

[298] Vaucheret, H., 2008. Plant ARGONAUTES. *Trends in Plant Science*, **13**, 350.

[299] Bohmert, K., I. Camus, C. Bellini, et al., 1998. AGO1 defines a novel locus of Arabidopsis controlling leaf development. *The EMBO Journal*, **17**, 170.

[300] Fagard, M., S. Boutet, J. B. Morel, et al., 2000. AGO1, QDE-2, and RDE-1 are related proteins required for post-transcriptional gene silencing in plants, quelling in fungi, and RNA interference in animals. *Proceedings of the National Academy of Sciences of the United States of America*, **97**, 11650.

[301] Kidner, C. A. and R. A. Martienssen, 2004. Spatially restricted microRNA directs leaf polarity through ARGONAUTE1. *Nature*, **428**, 81.

[302] Carlsbecker, A., J.-Y. Lee, C. J. Roberts, et al., 2010. Cell signalling by microRNA165/6 directs gene dose-dependent root cell fate. *Nature*, **465**, 316.

[303] Zhang, T., Y. Zhao, I. Juntheikki, et al., 2017. Dissecting functions of SEPALLATA-like MADS box genes in patterning of the pseudanthial inflorescence of Gerbera hybrida. *New Phytologist*, **216**, 939.

[304] Brandt, R., M. Cabedo, Y. Xie, et al., 2014. Homeodomain leucine-zipper proteins and their role in synchronizing growth and development with the environment. *Journal of Integrative Plant Biology*, **56**, 518.

[305] Ohashi-Ito, K. and H. Fukuda, 2003. HD-zip III homeobox genes that include a novel member, ZeHB-13 (Zinnia)/ATHB-15 (Arabidopsis), are involved in procambium and xylem cell differentiation. *Plant & Cell Physiology*, **44**, 1350.

[306] Ohashi-Ito, K., M. Kubo, T. Demura, et al., 2005. Class III homeodomain leucine-zipper proteins regulate xylem cell differentiation. *Plant & Cell Physiology*, **46**, 1646.

[307] Juarez, M. T., J. S. Kui, J. Thomas, et al., 2004. microRNA-mediated repression of rolled leaf1 specifies maize leaf polarity. *Nature*, **428**, 84.

[308] McHale, N. A. and R. E. Koning, 2004. MicroRNA-directed cleavage of Nicotiana sylvestris PHAVOLUTA mRNA regulates the vascular cambium and structure of apical meristems. *Plant Cell*, **16**, 1730.

[309] Itoh, J.-I., K.-I. Hibara, Y. Sato, et al., 2008. Developmental role and auxin responsiveness of Class III homeodomain leucine zipper gene family members in rice. *Plant Physiology*, **147**, 1960.

[310] Zhu, Y., D. Song, J. Sun, et al., 2013. PtrHB7, a class III HD-Zip gene, plays a critical role in regulation of vascular cambium differentiation in Populus. *Molecular Plant*, **6**, 1331.

[311] Fukushima, K. and M. Hasebe, 2014. Adaxial-abaxial polarity: the developmental basis of leaf shape diversity. *Genesis*, **52**, 1.

[312] Yuo, T., Y. Yamashita, H. Kanamori, et al., 2012. A SHORT INTERNODES (SHI) family transcription factor gene regulates awn elongation and pistil morphology in barley. *Journal of Experimental Botany*, **63**, 5223.

[313] Min, Y., J. I. Bunn, and E. M. Kramer, 2019. Homologs of the STYLISH gene family control nectary development in Aquilegia. *New Phytologist*, **221**, 1090.

[314] Landberg, K., E. R. A. Pederson, T. Viaene, et al., 2013. The moss Physcomitrella patens reproductive organ development is highly organized, affected by the two SHI/STY genes and by the level of active auxin in the SHI/STY expression domain. *Plant Physiology*, **162**, 1406.

[315] Navarro, C., N. Efremova, J. F. Golz, et al., 2004. Molecular and genetic interactions between STYLOSA and GRAMINIFOLIA in the control of Antirrhinum vegetative and re- productive development. *Development*, **131**, 3649.

[316] Nelissen, H., D. Eeckhout, K. Demuynck, et al., 2015. Dynamic changes in ANGUSTIFO- LIA3 complex composition reveal a growth regulatory mechanism in the maize leaf. *Plant Cell*, **27**, 1605.

[317] Marsch-Martínez, N., V. M. Zúñiga-Mayo, H. Herrera-Ubaldo, et al., 2014. The NTT transcription factor promotes replum development in Arabidopsis fruits. *The Plant Journal*, **80**, 69.

[318] Chono, M., K. Nemoto, H. Yamane, et al., 1998. Characterization of a protein kinase gene responsive to auxin and gibberellin in cucumber hypocotyls. *Plant & Cell Physiology*, **39**, 958.

[319] Khanna, R., X. Lin, and J. C. Watson, 1999. Photoregulated expression of the PsPK3 and PsPK5 genes in pea seedlings. *Plant Molecular Biology*, **39**, 231.

[320] Chen, J., P. Somta, X. Chen, et al., 2016. Gene mapping of a mutant mungbean (Vigna radiata L.) using new molecular markers suggests a gene encoding a YUC4-like protein regulates the chasmogamous flower trait. *Frontiers in Plant Science*, **7**, 830.

[321] Becker, A., K. Kaufmann, A. Freialdenhoven, et al., 2002. A novel MADS-box gene subfam- ily with a sister-group relationship to class B floral homeotic genes. *Molecular Genetics and Genomics*, **266**, 942.

[322] Hoffmeier, A., L. Gramzow, A. S. Bhide, et al., 2018. A dead gene walking: Convergent degeneration of a clade of MADS-box genes in crucifers. *Molecular Biology and Evolution*, **35**, 2618.

[323] de Folter, S., R. G. H. Immink, M. Kieffer, et al., 2005. Comprehensive interaction map of the Arabidopsis MADS Box transcription factors. *Plant Cell*, **17**, 1424.

[324] Erdmann, R., L. Gramzow, R. Melzer, et al., 2010. GORDITA (AGL63) is a young paralog of the Arabidopsis thaliana B(sister) MADS box gene ABS (TT16) that has undergone neofunctionalization. *The Plant Journal*, **63**, 914.

[325] de Folter, S., A. V. Shchennikova, J. Franken, et al., 2006. A Bsister MADS-box gene involved in ovule and seed development in petunia and Arabidopsis. *The Plant Journal*, **47**, 934.

[326] Deng, W., G. Chen, F. Peng, et al., 2012. Transparent testa16 plays multiple roles in plant development and is involved in lipid synthesis and embryo development in canola. *Plant Physiology*, **160**, 978.

[327] Chen, G., W. Deng, F. Peng, et al., 2013. Brassica napus TT16 homologs with different genomic origins and expression levels encode proteins that regulate a broad range of endothelium-associated genes at the transcriptional level. *The Plant Journal*, **74**, 663.

[328] Lee, D. S., L. J. Chen, C. Y. Li, et al., 2013. The Bsister MADS gene FST determines ovule patterning and development of the zygotic embryo and endosperm. *PloS One*, **8**, e58748.

[329] Yamada, K., T. Saraike, N. Shitsukawa, et al., 2009. Class D and B(sister) MADS-box genes are associated with ectopic ovule formation in the pistil-like stamens of alloplasmic wheat (Triticum aestivum L.). *Plant Molecular Biology*, **71**, 1.

[330] Mizzotti, C., M. A. Mendes, E. Caporali, et al., 2012. The MADS box genes SEEDSTICK and ARABIDOPSIS BSISTER play a maternal role in fertilization and seed development. *The Plant Journal*, **70**, 409.

[331] Nesi, N., I. Debeaujon, C. Jond, et al., 2002. The TRANSPARENT TESTA16 locus encodes the ARABIDOPSIS BSISTER MADS domain protein and is required for proper develop- ment and pigmentation of the seed coat. *Plant Cell*, **14**, 2463.

[332] Mizzotti, C., I. Ezquer, D. Paolo, et al., 2014. SEEDSTICK is a master regulator of develop- ment and metabolism in the Arabidopsis seed coat. *PLoS Genetics*, **10**, e1004856.

[333] Ezquer, I., C. Mizzotti, E. Nguema-Ona, et al., 2016. The developmental regulator SEEDSTICK controls structural and mechanical properties of the Arabidopsis seed coat. *Plant Cell*, **28**, 2478.

[334] Balanzà, V., I. Roig-Villanova, M. Di Marzo, et al., 2016. Seed abscission and fruit dehiscence required for seed dispersal rely on similar genetic networks. *Development*, **143**, 3372.

[335] Liu, Y., N. Nakayama, M. Schiff, et al., 2004. Virus induced gene silencing of a DEFICIENS ortholog in Nicotiana benthamiana. *Plant Molecular Biology*, **54**, 701.

[336] Kramer, E. M., L. Holappa, B. Gould, et al., 2007. Elaboration of B gene function to include the identity of novel floral organs in the lower eudicot Aquilegia. *Plant Cell*, **19**, 750.

[337] Pabón-Mora, N., H. Suárez-Baron, B. A. Ambrose, et al., 2015. Flower Development and Perianth Identity Candidate Genes in the Basal Angiosperm Aristolochia fimbriata (Piperales: Aristolochiaceae). *Frontiers in Plant Science*, **6**, 1095.

[338] Soza, V. L., C. D. Snelson, K. D. Hewett Hazelton, et al., 2016. Partial redundancy and functional specialization of E-class SEPALLATA genes in an early-diverging eudicot. *Devel- opmental Biology*, **419**, 143.

[339] Galimba, K. D., T. R. Tolkin, A. M. Sullivan, et al., 2012. Loss of deeply conserved C-class floral homeotic gene function and C- and E-class protein interaction in a double-flowered ranunculid mutant. *Proceedings of the National Academy of Sciences of the United States of America*, **109**, E2267.

[340] Davies, B., P. Motte, E. Keck, et al., 1999. PLENA and FARINELLI: redundancy and regulatory interactions between two Antirrhinum MADS-box factors controlling flower development. *The EMBO Journal*, **18**, 4023.

[341] Kapoor, M., S. Tsuda, Y. Tanaka, et al., 2002. Role of Petunia pMADS3 in determination of floral organ and meristem identity, as revealed by its loss of function. *The Plant Journal*, **32**, 115.

[342] Heijmans, K., K. Ament, A. S. Rijpkema, et al., 2012. Redefining C and D in the Petunia ABC. *Plant Cell*, **24**, 2305.

[343] Ambrose, B. A., D. R. Lerner, P. Ciceri, et al., 2000. Molecular and genetic analyses of the Silky1 gene reveal conservation in floral organ specification between eudicots and monocots. *Molecular Cell*, **5**, 569.

[344] Zahn, L. M., J. Leebens-Mack, C. W. de Pamphilis, et al., 2005. To B or Not to B a flower: the role of DEFICIENS and GLOBOSA orthologs in the evolution of the angiosperms. *Journal of Heredity*, **96**, 225.

[345] Yellina, A. L., S. Orashakova, S. Lange, et al., 2010. Floral homeotic C function genes repress specific B function genes in the carpel whorl of the basal eudicot California poppy (Eschscholzia californica). *EvoDevo*, **1**, 13.

[346] Lange, M., S. Orashakova, S. Lange, et al., 2013. The seirena B class floral homeotic mutant of California Poppy (Eschscholzia californica) reveals a function of the enigmatic PI motif in the formation of specific multimeric MADS domain protein complexes. *Plant Cell*, **25**, 438.

[347] Gong, P., C. Song, H. Liu, et al., 2021. Physalis floridana CRABS CLAW mediates neofunctionalization of GLOBOSA genes in carpel development. *Journal of Experimental Botany*, **72**, 6882.

[348] Hsu, H.-F., W.-H. Chen, Y.-H. Shen, et al., 2021. Multifunctional evolution of B and AGL6 MADS box genes in orchids. *Nature Communications*, **12**, 902.

[349] Yao, J.-L., Y.-H. Dong, and B. A. M. Morris, 2001. Parthenocarpic apple fruit production conferred by transposon insertion mutations in a MADS-box transcription factor. *Proceedings of the National Academy of Sciences of the United States of America*, **98**, 1306.

[350] Galimba, K. D., J. Martínez-Gómez, and V. S. Di Stilio, 2018. Gene Duplication and Transference of Function in the paleoAP3 Lineage of Floral Organ Identity Genes. *Frontiers in Plant Science*, **9**, 334.

[351] Melzer, R., A. Härter, F. Rümpler, et al., 2014. DEF- and GLO-like proteins may have lost most of their interaction partners during angiosperm evolution. *Annals of Botany*, **114**, 1431.

[352] Li, X., T. Fan, J. Song, et al., 2014. Functional conservation and divergence of four ginger AP1/AGL9 MADS-box genes revealed by analysis of their expression and protein-protein interaction, and ectopic expression of AhFUL gene in Arabidopsis. *PloS One*, **9**, e114134.

[353] Favaro, R., R. G. H. Immink, V. Ferioli, et al., 2002. Ovule-specific MADS-box proteins have conserved protein-protein interactions in monocot and dicot plants. *Molecular Genetics and Genomics*, **268**, 152.

[354] Immink, R. G. H., T. W. J. Gadella, S. Ferrario, et al., 2002. Analysis of MADS box protein- protein interactions in living plant cells. *Proceedings of the National Academy of Sciences of the United States of America*, **99**, 2416.

[355] Vrebalov, J., D. Ruezinsky, V. Padmanabhan, et al., 2002. A MADS-box gene necessary for fruit ripening at the tomato ripening-inhibitor (rin) locus. *Science*, **296**, 343.

[356] Liu, D., Di Wang, Z. Qin, et al., 2014. The SEPALLATA MADS-box protein SLMBP21 forms protein complexes with JOINTLESS and MACROCALYX as a transcription activa- tor for development of the tomato flower abscission zone. *The Plant Journal*, **77**, 284.

[357] Mouradov, Glassick, Hamdorf, et al., 1998. Family of MADS-Box genes expressed early in male and female reproductive structures of Monterey pine. *Plant Physiology*, **117**, 55.

[358] Ohmori, S., M. Kimizu, M. Sugita, et al., 2009. MOSAIC FLORAL ORGANS1, an AGL6-like MADS box gene, regulates floral organ identity and meristem fate in rice. *Plant Cell*, **21**, 3008.

[359] Rijpkema, A. S., J. Zethof, T. Gerats, et al., 2009. The Petunia AGL6 gene has a SEPALLATA-like function in floral patterning. *The Plant Journal*, **60**, 1.

[360] Thompson, B. E., L. Bartling, C. Whipple, et al., 2009. bearded-ear encodes a MADS box transcription factor critical for maize floral development. *Plant Cell*, **21**, 2578.

[361] Li, H., W. Liang, R. Jia, et al., 2010. The AGL6-like gene OsMADS6 regulates floral organ and meristem identities in rice. *Cell Research*, **20**, 299.

[362] Dreni, L. and D. Zhang, 2016. Flower development: the evolutionary history and functions of the AGL6 subfamily MADS-box genes. *Journal of Experimental Botany*, **67**, 1625.

[363] Marshall, O. J., 2004. PerlPrimer: cross-platform, graphical primer design for standard, bisulphite and real-time PCR. *Bioinformatics*, **20**, 2471.

[364] Hall, T. A., 1999. BioEdit: a user-friendly biological sequence alignment editor and analysis program for Windows 95/98/NT. *Nucleic Acids Symposium Series*, **41**, 95.

[365] Liu, Y., M. Schiff, R. Marathe, et al., 2002. Tobacco Rar1, EDS1 and NPR1/NIM1 like genes are required for N-mediated resistance to tobacco mosaic virus. *The Plant Journal*, **30**, 415.

[366] Rotino, G. L. and S. Gleddie, 1990. Transformation of eggplant (Solanum melongena L.) using a binary Agrobacterium tumefaciens vector. *Plant Cell Reports*, **9**, 26.

[367] Becker, A. and M. Lange, 2010. VIGS - genomics goes functional. *Trends in Plant Science*, **15**, 1.

[368] Dommes, A. B., T. Gross, D. B. Herbert, et al., 2019. Virus-induced gene silencing: empowering genetics in non-model organisms. *Journal of Experimental Botany*, **70**, 757.

[369] Song, J.-J., S. K. Smith, G. J. Hannon, et al., 2004. Crystal structure of Argonaute and its implications for RISC slicer activity. *Science*, **305**, 1434.

[370] Napoli, C., C. Lemieux, and R. Jorgensen, 1990. Introduction of a chimeric chalcone synthase gene into Petunia results in reversible co-suppression of homologous genes in trans. *Plant Cell*, **2**, 279.

[371] Wege, S., A. Scholz, S. Gleissberg, et al., 2007. Highly efficient virus-induced gene silencing (VIGS) in California poppy (Eschscholzia californica): an evaluation of VIGS as a strategy to obtain functional data from non-model plants. *Annals of Botany*, **100**, 641.

[372] Abramoff, M. D., P. J. Magalhaes, and S. J. Ram, 2004. Image processing with ImageJ. *Biophotonics International*, **11**, 36.

[373] Schneider, C. A., W. S. Rasband, and K. W. Eliceiri, 2012. NIH Image to ImageJ: 25 years of image analysis. *Nature Methods*, **9**, 671.

[374] Friso, G. and K. J. van Wijk, 2015. Posttranslational protein modifications in plant metabolism. *Plant Physiology*, **169**, 1469.

[375] Hoffman, C. S. and F. Winston, 1987. A ten-minute DNA preparation from yeast efficiently releases autonomous plasmids for transformaion of Escherichia coli. *Gene*, **57**, 267.

[376] Taylor, R. G., D. C. Walker, and R. R. McInnes, 1993. E. coli host strains significantly affect the quality of small scale plasmid DNA preparations used for sequencing. *Nucleic Acids Research*, **21**, 1677.

[377] Hu, C.-D., Y. Chinenov, and T. K. Kerppola, 2002. Visualization of interactions among bZIP and Rel family proteins in living cells using Bimolecular Fluorescence Complementation. *Molecular Cell*, **9**, 789.

[378] Shyu, Y. J. and C.-D. Hu, 2008. Fluorescence complementation: an emerging tool for biological research. *Trends in Biotechnology*, **26**, 622.

[379] Jeong, J., S. K. Kim, J. Ahn, et al., 2006. Monitoring of conformational change in maltose binding protein using split green fluorescent protein. *Biochemical and Biophysical Research Communications*, **339**, 647.

[380] Altschul, S. F., W. Gish, W. Miller, et al., 1990. Basic local alignment search tool. *Journal of Molecular Biology*, **215**, 403.

[381] Kumar, S., G. Stecher, and K. Tamura, 2016. MEGA7: Molecular Evolutionary Genetics Analysis version 7.0 for bigger datasets. *Molecular Biology and Evolution*, **33**, 1870.

[382] Hori, K., Y. Yamada, R. Purwanto, et al., 2018. Mining of the uncharacterized cytochrome P450 genes involved in alkaloid biosynthesis in California poppy using a draft genome sequence. *Plant & Cell Physiology*, **59**, 222.

[383] Stöver, B. C. and K. F. Müller, 2010. TreeGraph 2: combining and visualizing evidence from different phylogenetic analyses. *BMC Bioinformatics*, **11**, 7.

[384] Chow, C.-N., T.-Y. Lee, Y.-C. Hung, et al., 2019. PlantPAN3.0: a new and updated resource for reconstructing transcriptional regulatory networks from ChIP-seq experiments in plants. *Nucleic Acids Research*, **47**, D1155.

[385] Fourquin, C. and C. Ferrándiz, 2014. The essential role of NGATHA genes in style and stigma specification is widely conserved across eudicots. *New Phytologist*, **202**, 1001.

[386] Livak, K. J. and T. D. Schmittgen, 2001. Analysis of relative gene expression data using real-time quantitative PCR and the 2(-Delta Delta C(T)) Method. *Methods*, **25**, 402.

[387] Conte, M. G., S. Gaillard, G. Droc, et al., 2008. Phylogenomics of plant genomes: a methodology for genome-wide searches for orthologs in plants. *BMC Genomics*, **9**, 183.

[388] Zahn, L. M., J. H. Leebens-Mack, J. M. Arrington, et al., 2006. Conservation and diver- gence in the AGAMOUS subfamily of MADS-box genes: evidence of independent sub- and neofunctionalization events. *Evolution & Development*, **8**, 30.

[389] Xing, H., R. N. Pudake, G. Guo, et al., 2011. Genome-wide identification and expression profiling of auxin response factor (ARF) gene family in maize. *BMC Genomics*, **12**, 178.

[390] Zumajo-Cardona, C., A. Vasco, and B. A. Ambrose, 2019. The evolution of the KANADI gene family and leaf development in lycophytes and ferns. *Plants*, **8**.

[391] Pfannebecker, K. C., M. Lange, O. Rupp, et al., 2017. An evolutionary framework for carpel developmental control genes. *Molecular Biology and Evolution*, **34**, 330.

[392] Zhao, J., M. Liu, L. Jiang, et al., 2014. Cucumber SUPERMAN has conserved function in stamen and fruit development and a distinct role in floral patterning. *PloS One*, **9**, e86192.

[393] Sharma, P., T. Lin, C. Grandellis, et al., 2014. The BEL1-like family of transcription factors in potato. *Journal of Experimental Botany*, **65**, 709.

[394] Tekleyohans, D. G., 2014. *Functional and molecular characterization of Bsister genes in the two model species: Arabidopsis thaliana and Eschscholzia californica*. Ph.D. thesis, Justus-Liebig- Universität, Otto-Behaghel-Str. 8, 35394 Gießen.

[395] Kivivirta, K., D. Herbert, M. Lange, et al., 2019. A protocol for laser microdissection (LMD) followed by transcriptome analysis of plant reproductive tissue in phylogenetically distant angiosperms. *Plant Methods*, **15**, 151.

[396] Pajoro, A., P. Madrigal, J. M. Muiño, et al., 2014. Dynamics of chromatin accessibility and gene regulation by MADS-domain transcription factors in flower development. *Genome Biology*, **15**, R41.

[397] Kivivirta, K. I., D. Herbert, C. Roessner, et al., 2021. Transcriptome analysis of gynoecium morphogenesis uncovers the chronology of gene regulatory network activity. *Plant Physiology*, **185**, 1076.

[398] Majic, P. and J. L. Payne, 2020. Enhancers facilitate the birth of de novo genes and gene integration into regulatory networks. *Molecular Biology and Evolution*, **37**, 1165.

[399] Li, H., W. Liang, Y. Hu, et al., 2011. Rice MADS6 interacts with the floral homeotic genes SUPERWOMAN1, MADS3, MADS58, MADS13, and DROOPING LEAF in specifying floral organ identities and meristem fate. *Plant Cell*, **23**, 2536.

[400] Osnato, M., E. Lacchini, A. Pilatone, et al., 2020. Transcriptome analysis reveals rice OsMADS13 as an important repressor of the carpel development pathway in ovules. *Journal of Experimental Botany*.

[401] Arora, R., P. Agarwal, S. Ray, et al., 2007. MADS-box gene family in rice: genome-wide identification, organization and expression profiling during reproductive development and stress. *BMC Genomics*, **8**, 242.

[402] Lee, J.-Y., S. F. Baum, S.-H. Oh, et al., 2005. Recruitment of CRABS CLAW to promote nectary development within the eudicot clade. *Development*, **132**, 5021.

[403] Arabidopsis Interactome Mapping Consortium, 2011. Evidence for network evolution in an Arabidopsis interactome map. *Science*, **333**, 601.

[404] Ferrario, S., R. G. H. Immink, A. Shchennikova, et al., 2003. The MADS box gene FBP2 is required for SEPALLATA function in Petunia. *Plant Cell*, **15**, 914.

[405] Ishikawa, M., Y. Ohmori, W. Tanaka, et al., 2009. The spatial expression patterns of DROOPING LEAF orthologs suggest a conserved function in grasses. *Genes & Genetic Systems*, **84**, 137.

[406] Wang, A., J. Tang, D. Li, et al., 2009. Isolation and functional analysis of LiYAB1, a YABBY family gene, from lily (Lilium longiflorum). *Journal of Plant Physiology*, **166**, 988.

[407] Reinhardt, D., 2003. Vascular patterning: More than just auxin? *Current Biology*, **13**, R485.

[408] Ortiz-Ramírez, C. I., S. Plata-Arboleda, and N. Pabón-Mora, 2018. Evolution of genes associated with gynoecium patterning and fruit development in Solanaceae. *Annals of Botany*, **121**, 1211.

[409] Wu, M., S. Upreti, Yan, et al., 2018. SPATULA regulates floral transition and photomorphogenesis in a PHYTOCHROME B-dependent manner in Arabidopsis. *Biochemical and Biophysical Research Communications*, **503**, 2380.

[410] Koo, S. C., O. Bracko, M. S. Park, et al., 2010. Control of lateral organ development and flowering time by the Arabidopsis thaliana MADS-box Gene AGAMOUS-LIKE6. *The Plant Journal*, **62**, 807.

[411] Ariel, F. D., P. A. Manavella, C. A. Dezar, et al., 2007. The true story of the HD-Zip family. *Trends in Plant Science*, **12**, 419.

[412] Sessa, G., C. Steindler, G. Morelli, et al., 1998. The Arabidopsis Athb-8, -9 and -14 genes are members of a small gene family coding for highly related HD-ZIP proteins. *Plant Molecular Biology*, **38**, 609.

[413] Quadrana, L., M. C. Rodriguez, M. López, et al., 2011. Coupling virus-induced gene silencing to exogenous green fluorescence protein expression provides a highly efficient system for functional genomics in Arabidopsis and across all stages of tomato fruit development. *Plant Physiology*, **156**, 1278.

[414] Tian, J., H. Pei, S. Zhang, et al., 2014. TRV-GFP: a modified Tobacco rattle virus vector for efficient and visualizable analysis of gene function. *Journal of Experimental Botany*, **65**, 311.

[415] Lucas, W. J., S. Bouché-Pillon, D. P. Jackson, et al., 1995. Selective trafficking of KNOTTED1 homeodomain protein and its mRNA through plasmodesmata. *Science*, **270**, 1980.

[416] Perbal, M. C., G. Haughn, H. Saedler, et al., 1996. Non-cell-autonomous function of the Antirrhinum floral homeotic proteins DEFICIENS and GLOBOSA is exerted by their polar cell-to-cell trafficking. *Development*, **122**, 3433.

[417] Sessions, A., M. F. Yanofsky, and D. Weigel, 2000. Cell-cell signaling and movement by the floral transcription factors LEAFY and APETALA1. *Science*, **289**, 779.

[418] Kim, M., W. Canio, S. Kessler, et al., 2001. Developmental changes due to long-distance movement of a homeobox fusion transcript in tomato. *Science*, **293**, 287.

[419] Kim, S., P. S. Soltis, and D. E. Soltis, 2013. AGL6-like MADS-box genes are sister to AGL2- like MADS-box genes. *Journal of Plant Biology*, **56**, 315.

[420] Pabón-Mora, N., O. Hidalgo, S. Gleissberg, et al., 2013. Assessing duplication and loss of APETALA1/FRUITFULL homologs in Ranunculales. *Frontiers in Plant Science*, **4**, 358.

[421] Pabón-Mora, N., G. K.-S. Wong, and B. A. Ambrose, 2014. Evolution of fruit development genes in flowering plants. *Frontiers in Plant Science*, **5**, 300.

[422] Gomariz-Fernández, A., V. Sánchez-Gerschon, C. Fourquin, et al., 2017. The Role of SHI/STY/SRS Genes in Organ Growth and Carpel Development Is Conserved in the Distant Eudicot Species Arabidopsis thaliana and Nicotiana benthamiana. *Frontiers in Plant Science*, **8**, 814.

[423] Zhao, Y., K. C. Pfannebecker, A. B. Dommes, et al., 2018. Evolutionary diversification of CYC/TB1-like TCP homologs and their recruitment for the control of branching and floral morphology in Papaveraceae (basal eudicots). *New Phytologist*, **220**, 317.

[424] Kölsch, A. and S. Gleissberg, 2006. Diversification of CYCLOIDEA-like TCP genes in the basal eudicot families Fumariaceae and Papaveraceae s.str. *Plant Biology*, **8**, 680.

[425] Tanious, F. A., J. M. Veal, H. Buczak, et al., 1992. DAPI (4',6-diamidino-2-phenylindole) binds differently to DNA and RNA: minor-groove binding at AT sites and intercalation at AU sites. *Biochemistry*, **31**, 3103.

[426] Gross, T. and A. Becker, 2021. Transcription Factor Action Orchestrates the Complex Expression Pattern of CRABS CLAW in Arabidopsis. *Genes*, **12**, 1663.

[427] Gómez-Felipe, A., D. Kierzkowski and S. de Folter, 2021. The Relationship between AGAMOUS and Cytokinin Signaling in the Establishment of Carpeloid Features, *Plants*, **10**, 827.

[428] Herrera-Ubaldo, H. and S. de Folter, 2022. Gynoecium and fruit development in Arabidopsis. *Development*, **149**.

[429] Shannon P., A. Markiel, O. Ozier, et al., 2003. Cytoscape: a software environment for integrated models of biomolecular interaction networks. *Genome Research* **13**: 2498–2504.

[430] Rössner, C., D. Lotz and A. Becker, 2022. VIGS Goes Viral: How VIGS Transforms Our Understanding of Plant Science. *Annual Review of Plant Biology*, **73**, 703-728.

[431] Martínez-Gómez, J., K. D. Galimba, et al., 2020. Spontaneous homeotic mutants and genetic control of floral organ identity in a ranunculid. *Evolution & Development*

[432] Maoka, T., Y. Fujiwara, K. Hashimoto, et al., 2000. A new *retro*-Carotinoid from the Petals of the Californian Yellow Poppy Eschscholtzia californica. *Journal of Natural Products*, **63**, 1288-1289.

[433] Kong, D. and A. Becker, 2021. Then There were Plenty – Ring Meristems Giving Rise to Many Stamen Whorls. *Plants*, **10**, 1140.

[434] Alhindi, T., Z. Zhang, P. Ruelens et al., 2017. Protein interaction evolution from promiscuity to specifity with reduced flexibility in an increasingly complex network. *Scientific Reports*, **7**, 44948.

[435] Cui, L., P. K. Wall, J. H. Leebens-Mack, et al., 2006. Widespread denome duplications throughout the history of flowering plants. *Genome research*, **16**, 738-749.

[436] Duan, X., C. Zhao, Y. Jiang et al., 2020. Parallel evolution of apetalous lineages within the buttercup family (Ranunculaceae): outward expansion of *AGAMOUS1*, rather than disruption of *APETALA3-3*. *The Plant Journal*, **104**, 1169-1181.

[437] Wu, C., L. Jia, and F. Goggin, 2010. The reliability of virus-induced gene silencing experiments using tobacco rattle virus in tomato is influenced by the size of the vector control. *Molecular Plant Pathology*, **12**, 299-305.

[438] Kuhn, A., S. R. Harborough, H. M. McLaughlin, et al. 2020. Direct ETTIN-auxin interaction controls chromatin states in gynoecium development. *eLife*, **9**

Supplementals

1 VIGS

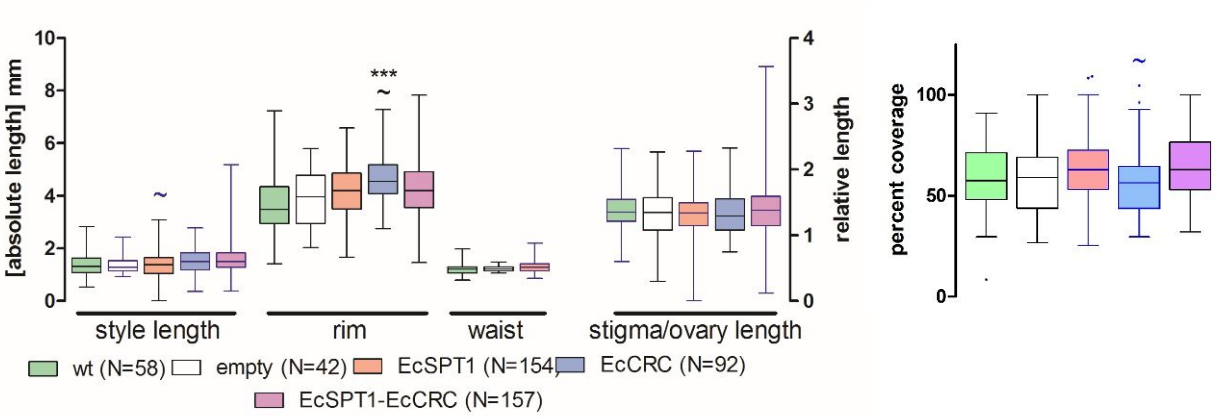

Figure 1: *Dimensions of 523 gynoecia phenotyped for V4 and V6. EcCRC VIGS plants show a significant increase in rim width. Data sets marked in blue vary significantly from normal distribution in Kolmogorov-Smirnov (KS) test (with Dallal-Wilkinson-Lilie (DWL) for P value). Asterisks show statistically significant differences from pTRV2-empty treated plants: (*) 0.01 < p < 0.05, (**) 0.001 < p < 0.01, (***) p < 0.001. ~ show statistically significant differences from EcCRC+EcSPT1 treated plants Significance was tested by Student's t-test for normally distributed samples or Mann-Whitman U test for not-normally distributed samples.*

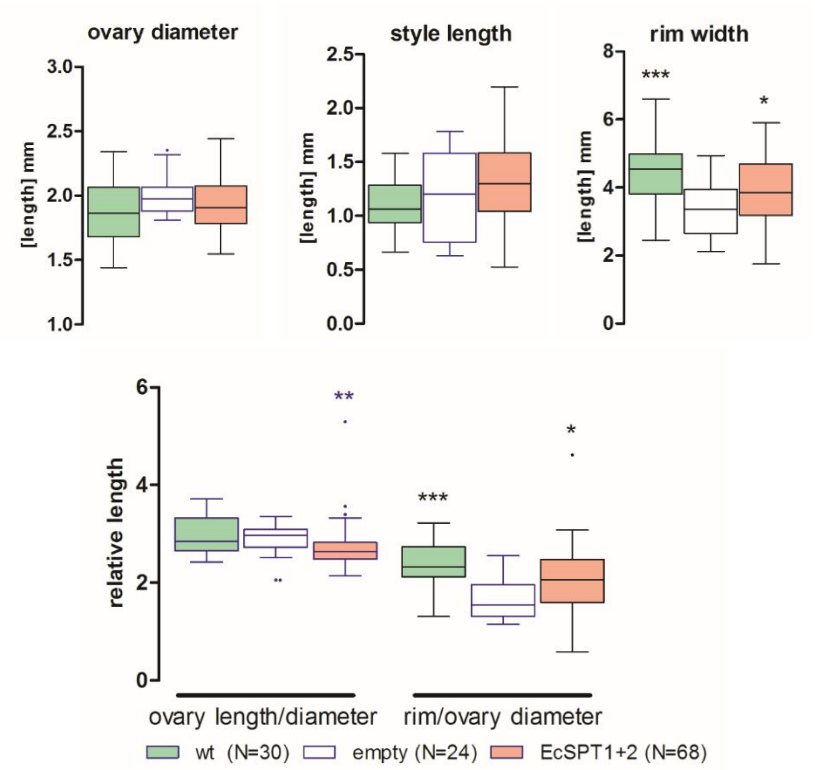

Figure 2: *Gynoecium dimensions measured on 122 gynoecia phenotyped for V8. Border colors and significances as described for fig. 1.*

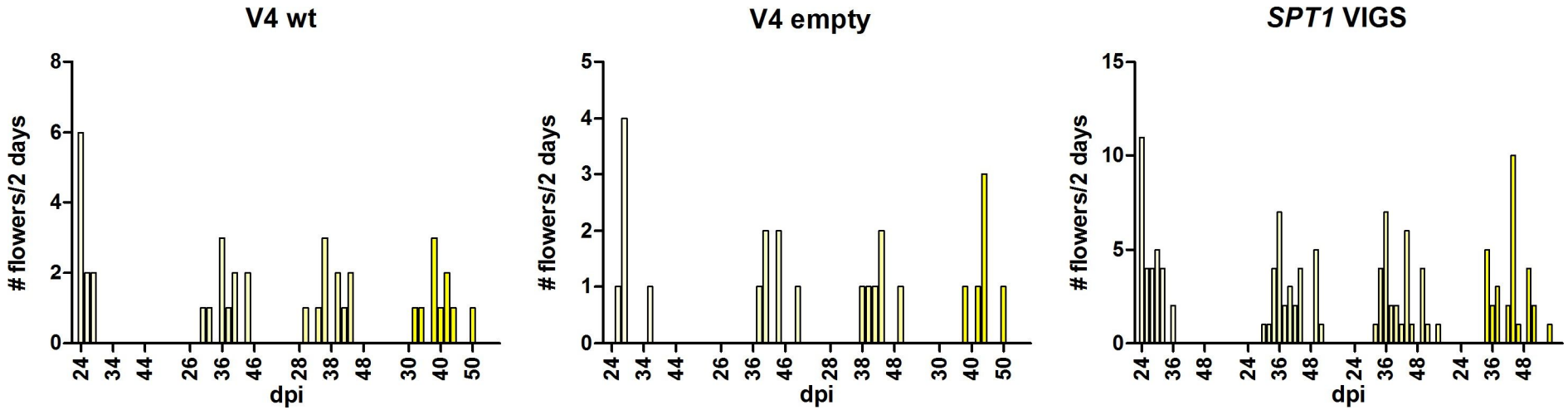

Figure 3: *Detailed frequency analysis of flower formation in experiment V4. VIGS treated plants for knock down of EcSPT1 show a non-Gaussian distribution of flower formation days. Instead a second shoulder or peak in the distribution is seen, indicating a split of the data set in two distinct populations regarding this parameter.*

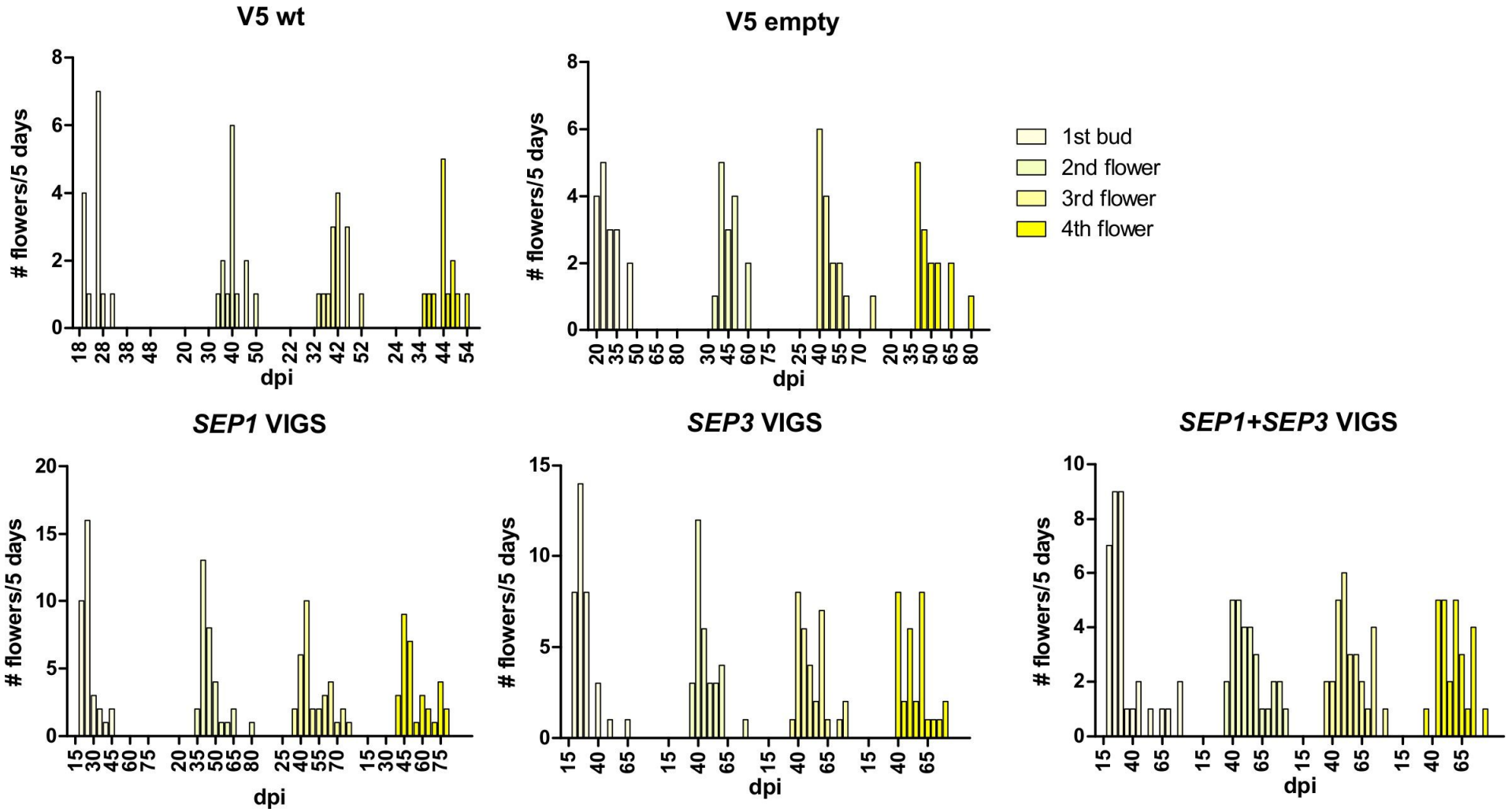

Figure 4: *Detailed frequency analysis of flower formation in experiment V5. VIGS treated plants for knock down of EcSEPs show a non-Gaussian distribution of flower formation days. Instead a second shoulder or peak in the distribution is seen, indicating a split of the data set in two distinct populations regarding this parameter.*

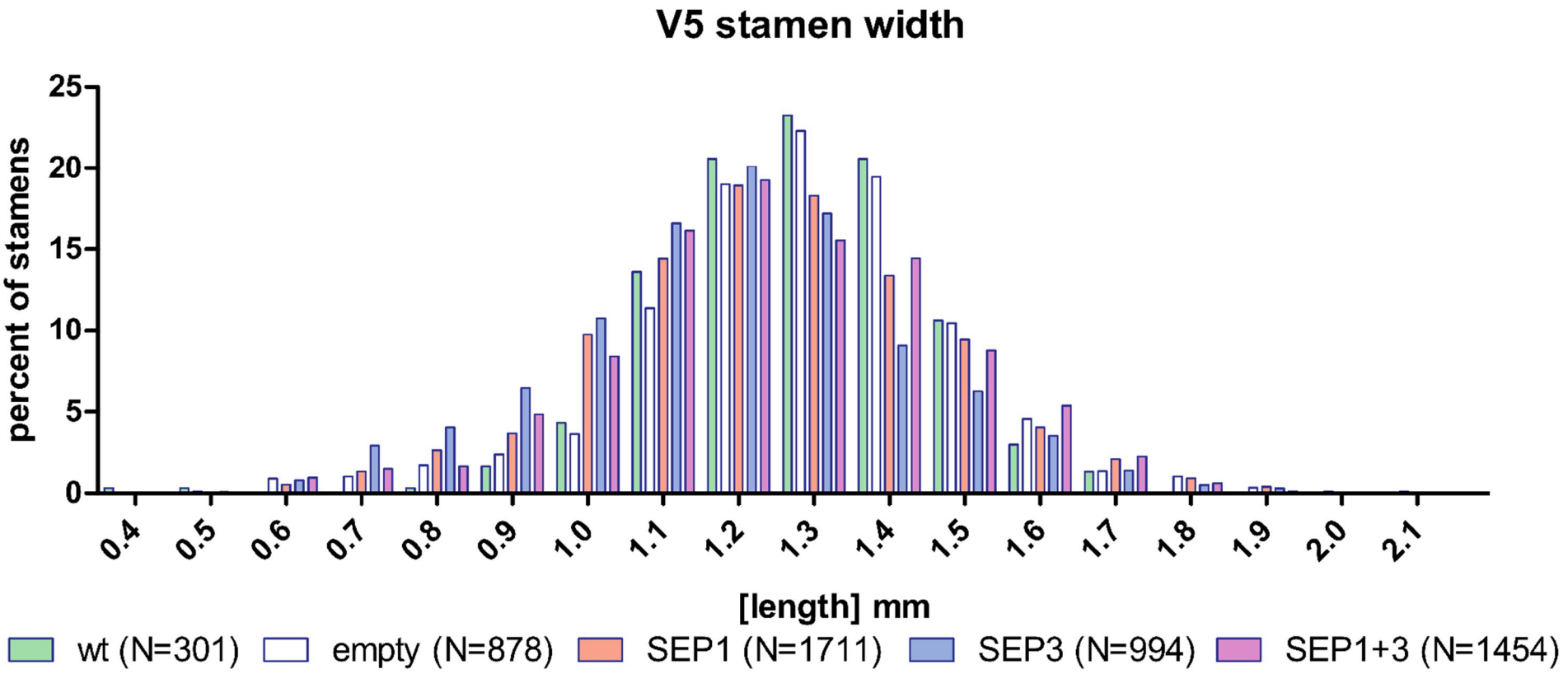

Figure 5: *Detailed frequency analysis of stamen width in experiment V5. All treatments show a non-Gaussian distribution of stamen widths. While wild type and empty vector control show a peak at1.3 mm, the VIGS treated plants show a peak at 1.2 mm and second peaks as shoulders at 1.4 mm and 1.5 mm for EcSEP1-EcSEP2 and EcSEP1 VIGS, respectively*

.

Table 1: *Observation of mosaic organs in buds of the different conducted VIGS experiments. The last column gives the expression strength of the target gene(s) in the first bud of affected plants determined by qPCR, where applicable.*

experiment	treatment	# buds affected	# plants affected	# total buds analysed	expression strength
			leaf-sepal		
V4	*EcSPT1*	1	1	120	not determined
	EcSPT1+EcCRC	3	2	129	not determined
V5	*EcSEP1*	5	4	132	not determined
	EcSEP3	1	1	129	not determined
	EcSEP1+EcSEP3	6	5	122	4 % *EcSEP1*, 20 % *EcSEP3* 160 % *EcSEP1*, 94 % *EcSEP3*
V6a	*EcSPT1*	1	1	86	not determined
V6b	*EcAGO1.1*	1	1	15	not determined
	EcETT	1	1	19	not determined
			sepal-petal		
V4	TRV2-empty	1	1	40	not determined
	EcSPT1	4	4	120	24 % *EcSPT1* 109 % *EcSPT1*
	EcCRC	2	2	124	72 % *EcCRC*
	EcSPT1+EcCRC	3	3	129	not determined
V6a	TRV2-empty	1	1	16	not determined
	EcSPT1	1	1	86	not determined
V6b	untreated	1	1	15	not determined
	EcLUG+EcLUH2	3	3	19	not determined
			petal-stamen		
V4	*EcSPT1*	1	1	93	31 % *EcSPT1*
	EcSPT1+EcCRC	6	5	96	not determined
V5	*EcSEP1*	1	1	97	not determined
	EcSEP1+EcSEP3	4	4	87	14 % *EcSEP1*, 24 % *EcSEP3* 160 % *EcSEP1*, 94 % *EcSEP3*
V6b	untreated	1	1	11	not determined
V8	untreated	1	1	36	not determined
	EcNGA1+EcNGA2	1	1	68	not determined
			stamen-capel		
V5	*EcSEP1+EcSEP3*	1	1	87	160 % *EcSEP1*, 94 % *EcSEP3*

Table 2: *Observation of unfused sepals in buds of the different conducted VIGS experiments. The last column gives the expression strength of the target gene(s) in the first bud of affected plants determined by qPCR, where applicable.*

experiment	treatment	# buds affected	# plants affected	# total buds analysed	expression strength
V4	*EcCRC*	1	1	123	6 % *EcCRC*
	EcSPT1	3	3	120	24 % *EcSPT1*
					59 % *EcSPT1*
					96 % *EcSPT1*
	EcSPT1+EcCRC	4	4	129	not determined
V5	*EcSEP1*	2	2	132	not determined
	EcSEP3	2	1	129	not determined
	EcSEP1+EcSEP3	8	4	122	4 % *EcSEP1*, 20 % *EcSEP3*
					160 % *EcSEP1*, 94 % *EcSEP3*
V6a	*EcSPT1*	1	1	86	not determined
V8a	untreated	1	1	20	not determined
	GFP	1	1	80	not determined
	EcNGA2	1	1	60	216 % *EcNGA2*
	EcNGA1+EcNGA2	1	1	88	not determined
V8b	*EcSPT1+EcSPT2*	4	4	93	not determined
	EcNGA+EcNGA1 +EcNGA2	1	1	69	not determined

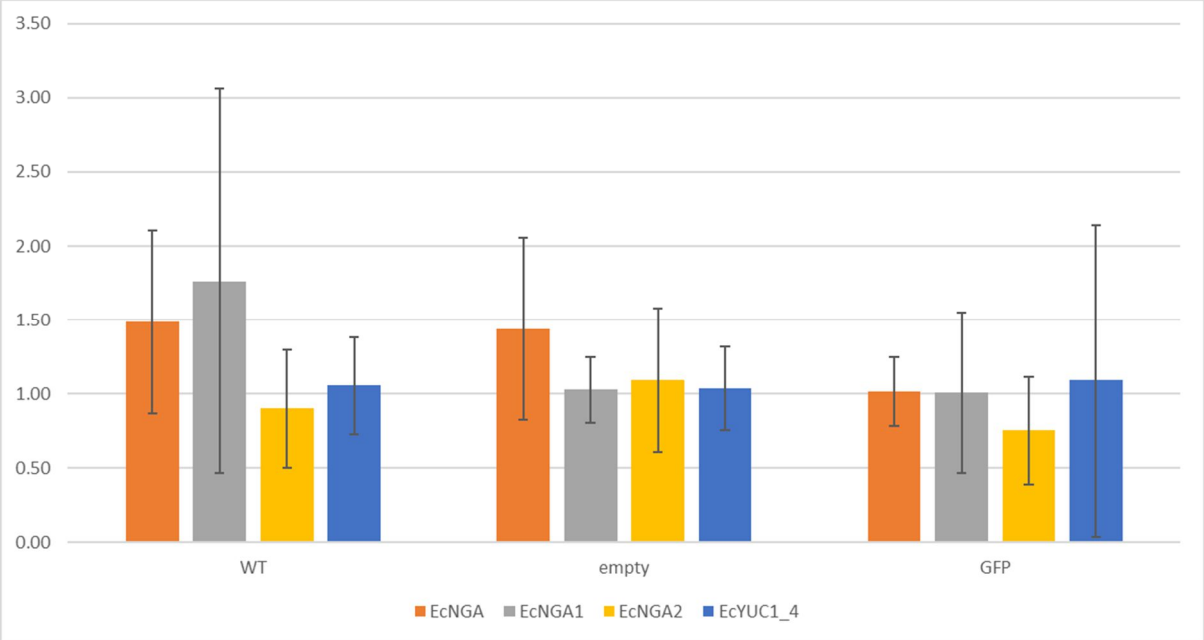

Figure 6: *Expression of selected genes in pTRV2-GFP treated plants compared to other control treatments. Based on 6 biological replicates, expression is normalized to EcGAPDH and shown relative to average expression in empty vector treated plants.*

Table 3: *Expression ration of possible regulator/regulated gene pairs*

	STY-L/SPT	YUC1/4/CRC
WT1	0.97	1.21
WT2	1.92	0.61
WT4	1.45	1.45
Mean	**1.44**	**1.09**
St.Dev.	0.39	0.35
CV	0.27	0.32
empty2	1.31	1.43
empty5	1.28	1.22
empty7	0.60	0.57
Mean	**1.06**	**1.07**
St.Dev.	0.33	0.36
CV	0.31	0.34
SPT1_8	3.80	
SPT1_30	2.00	
SPT1_32	1.95	
Mean	**2.58**	
St.Dev.	0.86	
CV	0.33	
CRC19		22.26
CRC28		25.18
CRC29		23.94
Mean		**23.79**
St.Dev.		1.19
CV		0.05
SPT1CRC4	1.76	
SPT1CRC26	1.47	
SPT1CRC31	1.51	
Mean	**1.58**	
St.Dev.	0.13	
CV	0.08	

VIGS phenotype frequencies

Table 4: F*requencies of phenotypic changes in plants of experiments V4, V6, and V8 (relevant treatments).*

	Treatment / number of treated plants (number of plants flowering, flowers formed)				
phenotype	pTRV-empty / 27 (23, 69)	SPT1 / 68 (53, 123)	CRC / 32 (32, 95)	SPT1+CRC / 69 (52, 154)	SPT1+SPT2 / 30 (23, 68) (experiment V8)
reduced ovary diameter*	-	-	62 flowers on 26 plants	83 flowers on 35 plants	-
reduced / no ovule initiation*	-	-	40 flowers on 19 plants	77 flowers on 36 plants	-
reduced/no ridges on ovary*	-	-	42 flowers on 22 plants	69 flowers on 33 plants	-
green stripe	-	-	42 flowers on 21 plants	58 flowers on 32 plants	-
lack of FM termination*	-	-	40 flowers on 22 plants	38 flowers on 21 plants	-
doubled / lacking marginal stigmatic protrusions	-	4 flowers on 4 plants (in 2 only part of the ovules developed)	40 flowers on 19 plants	56 flowers on 32 plants	-
candle-like ovules	2 flower on 1 plant	2 flower on 1 plant	5 flowers on 4 plants	13 flowers on 10 plants	-
1 marginal stigmatic protrusion not developed	-	5 flowers on 4 plants	2 flower on 2 plants	10 flowers on 9 plants	3 flower on 3 plants
1-2 marginal stigmatic protrusions short	2 flower2 on 1 plant	2 flower on 2 plant	4 flowers on 3 plants	3 flowers on 3 plants	12 flowers on 10 plants
1-2 additional tiny stigmatig protrusions	-	5 flowers on 3 plants	2 flowers on 1 plant		-
gynoecium aborted	-	6 flowers on 3 plant			-

WT
30 plants, 28 flowering, 83 flowers
1 flower on 1 plant: 1 additional stigmatic protrusion
3 flower on 1 plant: marginal stigmatic protrusions short

Table 5: F*requencies of phenotypic changes in plants of experiment V5.*

	Treatment / number of treated plants (number of plants flowering, flowers formed)			
phenotype	pTRV-empty / 20 (16, 46)	SEP1 / 43 (35, 97)	SEP3 / 43 (33, 96)	SEP1+SEP3 / 44 (30, 82)
1-3 additional small stigmatic protrusion	-	2 flowers on 2 plants	2 flowers on 2 plants (SEP3: 106%)	-
Stamen phenotypes (connectives broad/green; stamens long)	3 flowers on 1 plant (SEP1/3: 102/133%)	1 flower on 1 plant (SEP1: 34%)	37 flowers on 14 plants (SEP3: 36%, 106%)	40 flowers on 22 plants (SEP1/3: 4%/20%,363%/360%)
Stamens short	-	-	-	2 flowers on 1 plant
All buds aborted with mosaic sepals	-	-	-	1 plant
candle-like ovules	-	-	1 flower on 1 plant	1 flower on 1 plant
changed carpel number	-	2 flowers on 2 plants	1 flower on 1 plant	-

Wt

15 plants inoculated, 14 plants flowered, 41 flowers phenotyped

3 flowers on 1 plant: marginal stigmatic protrusions short (SEP1/3: 166/186%)

Table 6: F*requencies of phenotypic changes in plants of experiment V8.*

	Treatment / number of treated plants (number of plants flowering, flowers formed)					
phenotype	pTRV-empty / 10 (9, 27)	NGA / 15 (12, 35)	NGA1/15 (13, 39)	NGA2 /15 (15, 45)	NGA1+NGA2 /25 (21, 63)	NGA+NGA1+NGA2 / 20 (18, 51)
2-4 'normal' stigmatic protrusions with bald tips	-	3 flowers on 1 plant	3 flowers on 1 plant	-	2 flowers on 1 plant	-
skirt of additional stigmatic protrusions	-	1 flower on 1 plant	-	2 flowers on 1 plant	-	-
very short stigmatic protrusions	-	1 flower on 1 plant	-	1 flower on 1 plant	3 flowers on 1 plant	-
1-2 additional small stigmatic protrusion*	-	1 flower on 1 plant	-	2 flowers on 1 plant	2 flowers on 2 plants	1 flower on 2 plants
style and stigma barely/not developed, ovules normal	-	-	1 flower on 1 plant	-	-	2 flowers on 1 plant
stigmatic protrusions barely developed, style+ovules normal	-	-	1 flower on 1 plant	-	1 flower on 1 plant	4 flowers on 4 plants
gynoecium aborted	-	-	2 flowers on 1 plant	2 flowers on 1 plant	5 flowers on 2 plants	-
laminar stylar flaps*	-	-	-	4 flowers on 3 plants	15 flowers on 9 plants	3 flowers on 3 plants
Plants only affected in lated buds	-	-	-	1 plant	1 plant	1 plant
Candle-like ovules	2 flowers on 1 plant	-	-	-	-	-

Wt
10 plants inoculated, 10 plants flowered, 30 flowers phenotyped, no irregularities

Empty
10 plants inoculated, 9 plants flowered, 27 flowers phenotyped
2 flowers on 1 plant: petals and pollen white
1 flower on 1 plant: stigmatic protrusions and ovules barely developed

GFP
30 plants inoculated, 28 plants flowered, 84 flowers phenotyped
2 flowers on 1 plant: 1 stigmatic protrusion missing
1 flower on 1 plant: stigmatic protrusions and ovules barely developed

2 Orthologues

Table 7: *Overview of genomic loci identified in this work for previously known, re-evaluated genes. References for these genes can be found in table 8 in the supplementals. The "predicted gene" column gives the identifier from the EGD. Often those transcript sequences predicted in the EGD are not completely identical with regard to start, stop and exon-intron structure to RNAseq data of the Becker lab or sequenced transcripts amplified from cDNA. The last column explains in short the adaptations made to the EGD data to fit the sequenced transcripts. For more details, alignments of transcript sequences with the proposed genomic loci are included in the electronic supplemental files.*

gene/ genomic locus	predicted gene	explanation
EcAG1		
Eca_sc006452.1 137712..131468	–	–
EcAG2		
Eca_sc002195.1 174592..178420	–	–
EcAGL6-like1		
Eca_sc003413.1 1471181..1471405 Eca_sc194781.1 31673..35509	g0030.1	first exon is on Eca_sc003413.1 before 808 nt unresolved sequence, the other exons are on Eca_sc194781.1 behind 3023 nt unresolved sequence, the predicted gene covers exons four, seven, and eight
EcAGL11		
Eca_sc068610.1 Eca_sc049015.1 779293..785207 Eca_sc049015.1 783529..785210	 g0010.1 g1100.1	first exon is on Eca_sc068610.1, the other exons on Eca_sc049015.1 after 997 nt unresolved sequence, part of the cds is doubled on this scaffold
EcAGO1.1		
Eca_sc013049.1 350064..342648 Eca_sc000141.1 222559..225585	–	the region of Eca_sc000141.1 is similar with the transcript with several SNPs, and interestingly has no intron regions
EcBP		
Eca_sc194599.1 517454..523611 Eca_sc029196.1 Eca_sc184534.1	g0540.1 g0310.1	transcript starts on Eca_sc194599.1 before 1236 nt of unresolved sequence, two short scaffolds bridge the gap, carrying parts of the coding sequence, partial overlap of the previously published sequence with Eca_sc194599.1_g0730.1
EcCRC		
Eca_sc027509.1 313465..314997	g0520.1	predicted gene has other first exon, exons three, four, and five are missing

Continued on next page

Table 7 – *Continued from previous page*

gene/ genomic locus	predicted gene	explanation
EcDEF1		
Eca_sc009026.1 390507..392834	g0600.1	–
EcDEF2		
Eca_sc001023.1 920389..918147	g1410.1	predicted sequence skips exon-intron border, ends in first intron
EcDEF3		
Eca_sc194662.1 1201083..1203637 Eca_sc194662.1 1230139..1232545	g2240.1 g2280.1	two nearly identical copies on the same scaffold, differences mainly in introns
EcEBS		
Eca_sc001122.1 2493775..2490385 Eca_sc183462.1 117624..114324	g4900.1 g0160.1	two highly similar genes, the first, second and fourth exon are missing from Eca_sc001122.1_g4900.1 compared to the sequenced transcript and Eca_sc183462.1_g0160.1
EcETT		
Eca_sc000630.1 461534..466002	g0730.1	–
EcFUL1		
Eca_sc001396.1 813540..811487	g0520.1	predicted gene ends prematurely compared to sequenced transcripts and other FUL-related genes, skip of exon-intron border
EcFUL2		
Eca_sc004992.1 359588..368307	g0520.1	predicted gene covers only part of the cds, change in intron-exon border
EcFUL3		
Eca_sc194563.1 118849..121252	g0160.1	–
EcKNAT2/6		
Eca_sc042187.1 584033..575319	g1020.1 g1010.1	g1020.1 ends in the third intron of the sequenced transcript, g1010.1 begins in the third intron and continues to STOP
EcLUG1		
Eca_sc194729.1 502546..511654	g0950.1	predicted gene starts upstream of sequenced transcripts and continues downstream, similarity of previously published transcript in terminal protein sequences to AtLUG

Continued on next page

Table 7 – *Continued from previous page*

gene/ genomic locus	predicted gene	explanation
EcLUG2		
–	–	no genomic locus was found, pub-lished transcript aligns partially with EcLUG1, EcLUG3, Eca_sc187119.1, and Eca_sc072756.1
EcLUG3		
Eca_sc000659.1 196496..188082	g0280.1	–
EcNGA		
Eca_sc194593.1 67172..65970	g0130.1	–
EcNGA1		
Eca_sc010606.1_701353..702603	g1130.1	–
EcSEI		
Eca_sc002821.1 258296..256990 Eca_sc004485.1 606..55	g0440.1 –	transcript starts and ends on Eca_sc002821.1, Eca_004485.1 bridges an unresolved sequence of 641 nt
EcSEP1		
Eca_sc000118.1 310380..307146 Eca_sc114620.1 Eca_sc056349.1	g0530.1 – –	transcript starts on Eca_sc000118.1 before 1980 nt of unresolved sequence, it continues on Eca_sc114620.1 and the last one and a half exons are covered by Eca_sc056349.1
EcSEP3		
Eca_sc194486.1 2122679..2126786 Eca_sc100744.1 Eca_sc177703.1	g3920.1 g0010.1 –	start and end are located on Eca_sc194486.1, the predicted gene covers the only last 2.5 exons, at least 1258 nt of unresolved sequence are in part bridged by Eca_sc100744.1 as well as Eca_sc177703.1, carrying exons three and four and parts of both, exons two and five
EcSPT1		
Eca_sc001754.1 288251..285421	g0390.1	predicted gene has other last exon
EcSRS-like		
Eca_sc009026.1 339180..337704	g0520.1	–

Continued on next page

Table 7 – *Continued from previous page*

gene/ genomic locus	predicted gene	explanation
EcSTM1		
Eca_sc007843.1 42303..404526 Eca_sc010691.1 Eca_sc010690.1	g0040.1 g0010.1 g0010.1	transcript starts on Eca_sc007843.1 before 862 nt of unresolved sequence, continues on Eca_sc010691.1 before reverting to Eca_sc007843.1, the last 1.5 exons are covered by Eca_sc010690.1
EcSTM2		
Eca_sc194544.1 408872..413703	g0720.1	predicted gene starts 57 nt upstream of the published sequence
EcSTY-like		
Eca_sc100701.1 537100..535589	g0990.1	–
EcTCP1		
Eca_sc194426.1 9287..7845 Eca_sc194696.1 156747..156047	– –	on Eca_sc194426.1 the complete transcript sequence can be found, on Eca_sc194696.1 a partial transcript is retained after 944 nt of unresolved sequence
EcTCP2		
Eca_sc005291.1 433475..432510	g0490.1	–
EcTCP3		
Eca_sc000493.1 669056..659683 Eca_sc189724.1	g1190.1 g1200.1 –	three transcripts differing in their exon-intron structure are contained in the databases, 2026 nt of unresolved sequence in Eca_sc000493.1 are partly covered by Eca_sc189724.1
EcWIP		sequenced transcript starts on Eca_sc000058.1 before at least 4238 nt of unresolved sequence, 64 nt overlap with Eca_sc052600.1, where transcript continues. predicted gene g1700.1 has other last exon, g1200.1 is the last exon
Eca_sc000058.1 909893..910703 Eca_sc052600.1 1..1817	g1700.1 g1200.1	
EcWOX4		
Eca_sc000587.1 216335..214505	g0290.1	all EcWOX4 fragments from [259] are parts of the same transcript

Continued on next page

Table 7 – *Continued from previous page*

gene/ genomic locus	predicted gene	explanation
EcWOX4		
Eca_sc000587.1 216335..214505	g0290.1	all EcWOX4 fragments from [259] are parts of the same transcript
EcWOX13		
Eca_sc011255.1 562608..559484	g0910.1	ERXG_scaffold_2017962 and NJKC_scaffold_2007920 from [259] are fragments of the same transcript
EcWOX13-like		
Eca_sc013265.1 362..3001	g0010.1	ERXG_scaffold_2064605, TUHA_scaffold_2019319, NJKC_scaffold_2013864, RKGT_scaffold_2003813, and UNPT_scaffold_2035952 from [259] are fragments of the same transcript
EcYAB1		
Eca_sc049015.1 712815..710287	g1040.1	predicted gene misses first one and a half exons
EcYAB2		
Eca_sc003743.1 29355..28699 Eca_sc147686.1	– g0010.1	transcript sequence starts on Eca_sc003743.1 before 1290 nt of unresolved sequence bridged by Eca_sc147686.1, predicted gene has other last exon
EcYAB3		
Eca_sc003758.1 311321..308166	–	–
EcYAB4		
Eca_sc194697.1 686703..682912	–	–
EcYAB5		
Eca_sc001023.1 375902..378389	–	–

2.1 HEC genes

Compared to the *EcHEC1* fragment identified in Ahmed Bayoumi's master thesis, a modification is proposed here to capture the formerly missing N terminus compared to the *A. thaliana HEC* genes 1 and 2: The nucleotide positions 136 to 237, directly preceding a stretch of 56 unresolved nucleotides, can be aligned as perfect match to the genomic locus identified for *EcHEC1* directly in front of the matching part of the transcript starting at position 293. This results in a new start codon and gives rise to a protein sequence showing high sequence homology with *A. thaliana HECs* 1 and 2 and the *EcHEC2* sequence identified before. The sequences referred to as *EcHEC4* and *EcHEC5* are coded in the EGD by the predicted genes *Eca_sc194573.1_g0990.1* and *Eca_sc001433.1_g1200.1*, respectively. Since no transcript sequences could be recovered from the RNASeq databases, these predicted genes were not further analysed.

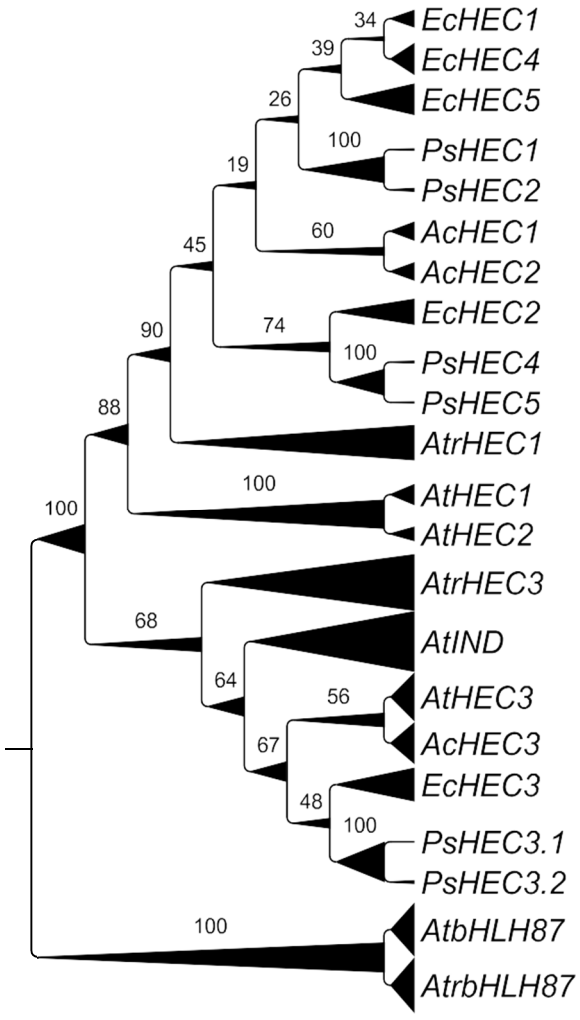

Figure 7: *ML tree of HEC genes rooted with bHLH87 genes. Calculated, using protein sequences from another Papaveraceae species (P. somniferum (Ps)), another ranunculales species (Aquilegia caerulea (Ac)), the basal angiosperm Amborella trichopoda (Atr) in addition to the sequences from A. thaliana (At) and E. californica (Ec); 500 bootstraps. Outgroup chosen according to [23]. Bootstrap values higher than 50 were accepted as reliable. Branch lengths are depicted as width of the triangle at the respective branch. Unnamed paralogous sequences are numbered for better overview. In the EGD two further EcHECs (EcHEC4 and EcHEC5) were predicted but no transcript sequences could be found in the used transcript collections.*

2.2 LUG genes

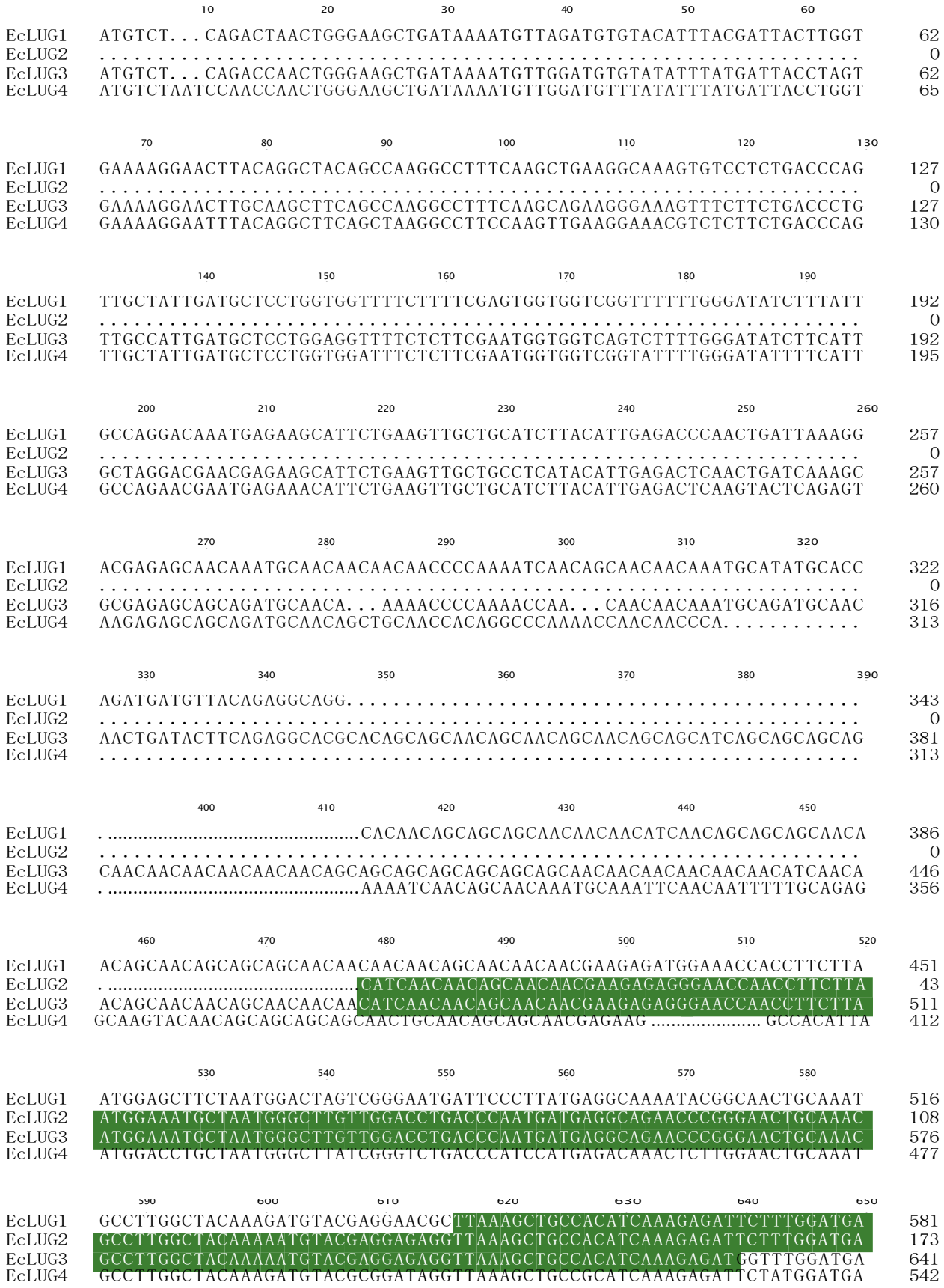
EcLUG1 ATGTCT...CAGACTAACTGGGAAGCTGATAAAATGTTAGATGTGTACATTTACGATTACTTGGT 62
EcLUG2 ... 0
EcLUG3 ATGTCT...CAGACCAACTGGGAAGCTGATAAAATGTTGGATGTGTATATTTATGATTACCTAGT 62
EcLUG4 ATGTCTAATCCAACCAACTGGGAAGCTGATAAAATGTTGGATGTTTATATTTATGATTACCTGGT 65
EcLUG1 GAAAAGGAACTTACAGGCTACAGCCAAGGCCTTTCAAGCTGAAGGCAAAGTGTCCTCTGACCCAG 127
EcLUG2 ... 0
EcLUG3 GAAAAGGAACTTGCAAGCTTCAGCCAAGGCCTTTCAAGCAGAAGGGAAAGTTTCTTCTGACCCTG 127
EcLUG4 GAAAAGGAATTTACAGGCTTCAGCTAAGGCCTTCCAAGTTGAAGGAAACGTCTCTTCTGACCCAG 130
EcLUG1 TTGCTATTGATGCTCCTGGTGGTTTTCTTTTCGAGTGGTGGTCGGTTTTTTGGGATATCTTTATT 192
EcLUG2 ... 0
EcLUG3 TTGCCATTGATGCTCCTGGAGGTTTTCTCTTCGAATGGTGGTCAGTCTTTTGGGATATCTTCATT 192
EcLUG4 TTGCTATTGATGCTCCTGGTGGATTTCTCTTCGAATGGTGGTCGGTATTTTGGGATATTTTCATT 195
EcLUG1 GCCAGGACAAATGAGAAGCATTCTGAAGTTGCTGCATCTTACATTGAGACCCAACTGATTAAAGG 257
EcLUG2 ... 0
EcLUG3 GCTAGGACGAACGAGAAGCATTCTGAAGTTGCTGCCTCATACATTGAGACTCAACTGATCAAAGC 257
EcLUG4 GCCAGAACGAATGAGAAACATTCTGAAGTTGCTGCATCTTACATTGAGACTCAAGTACTCAGAGT 260
EcLUG1 ACGAGAGCAACAAATGCAACAACAACAACCCCAAAATCAACAGCAACAACAAATGCATATGCACC 322
EcLUG2 ... 0
EcLUG3 GCGAGAGCAGCAGATGCAACA...AAAACCCCAAAACCAA...CAACAACAAATGCAGATGCAAC 316
EcLUG4 AAGAGAGCAGCAGATGCAACAGCTGCAACCACAGGCCCAAAACCAACAACCCA..... 313
EcLUG1 AGATGATGTTACAGAGGCAGG... 343
EcLUG2 ... 0
EcLUG3 AACTGATACTTCAGAGGCACGCACAGCAGCAACAGCAACAGCAACAGCAGCATCAGCAGCAGCAG 381
EcLUG4 ... 313
EcLUG1 ...CACAACAGCAGCAGCAACAACAACATCAACAGCAGCAGCAACA 386
EcLUG2 ... 0
EcLUG3 CAACAACAACAACAACAACAGCAGCAGCAGCAGCAGCAGCAACAACAACAACAACAACATCAACA 446
EcLUG4 ...AAAATCAACAGCAACAAATGCAAATTCAACAATTTTTGCAGAG 356
EcLUG1 ACAGCAACAGCAGCAGCAACAACAACAACAGCAACAACAACGAAGAGATGGAAACCACCTTCTTA 451
EcLUG2 ...CATCAACAACAGCAACAACGAAGAGAGGGAACCAACCTTCTTA 43
EcLUG3 ACAGCAACAACAGCAACAACAACATCAACAACAGCAACAACGAAGAGAGGGAACCAACCTTCTTA 511
EcLUG4 GCAAGTACAACAGCAGCAGCAGCAACTGCAACAGCAGCAACGAGAAG.....GCCACATTA 412
EcLUG1 ATGGAGCTTCTAATGGACTAGTCGGGAATGATTCCCTTATGAGGCAAAATACGGCAACTGCAAAT 516
EcLUG2 ATGGAAATGCTAATGGGCTTGTTGGACCTGACCCAATGATGAGGCAGAACCCGGGAACTGCAAAC 108
EcLUG3 ATGGAAATGCTAATGGGCTTGTTGGACCTGACCCAATGATGAGGCAGAACCCGGGAACTGCAAAC 576
EcLUG4 ATGGACCTGCTAATGGGCTTATCGGGTCTGACCCATCCATGAGACAAACTCTTGGAACTGCAAAT 477
EcLUG1 GCCTTGGCTACAAAGATGTACGAGGAACGCTTAAAGCTGCCACATCAAAGAGATTCTTTGGATGA 581
EcLUG2 GCCTTGGCTACAAAAATGTACGAGGAGAGGTTAAAGCTGCCACATCAAAGAGATTCTTTGGATGA 173
EcLUG3 GCCTTGGCTACAAAAATGTACGAGGAGAGGTTAAAGCTGCCACATCAAAGAGATGGTTTGGATGA 641
EcLUG4 GCCTTGGCTACAAAGATGTACGCGGATAGGTTAAAGCTGCCGCATCAAAGAGATTCTATGGATGA 542

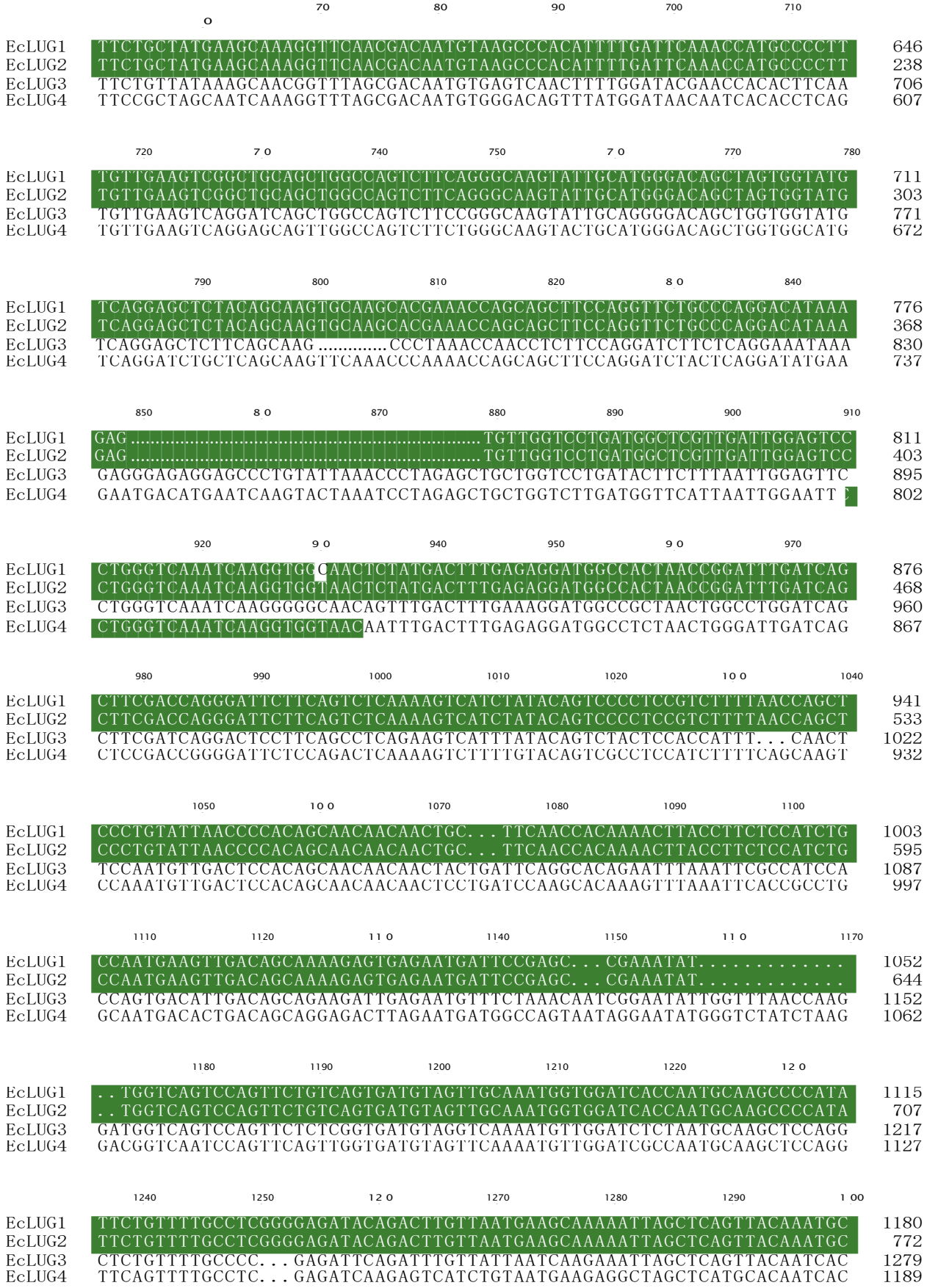
EcLUG1
EcLUG2
EcLUG3
EcLUG4

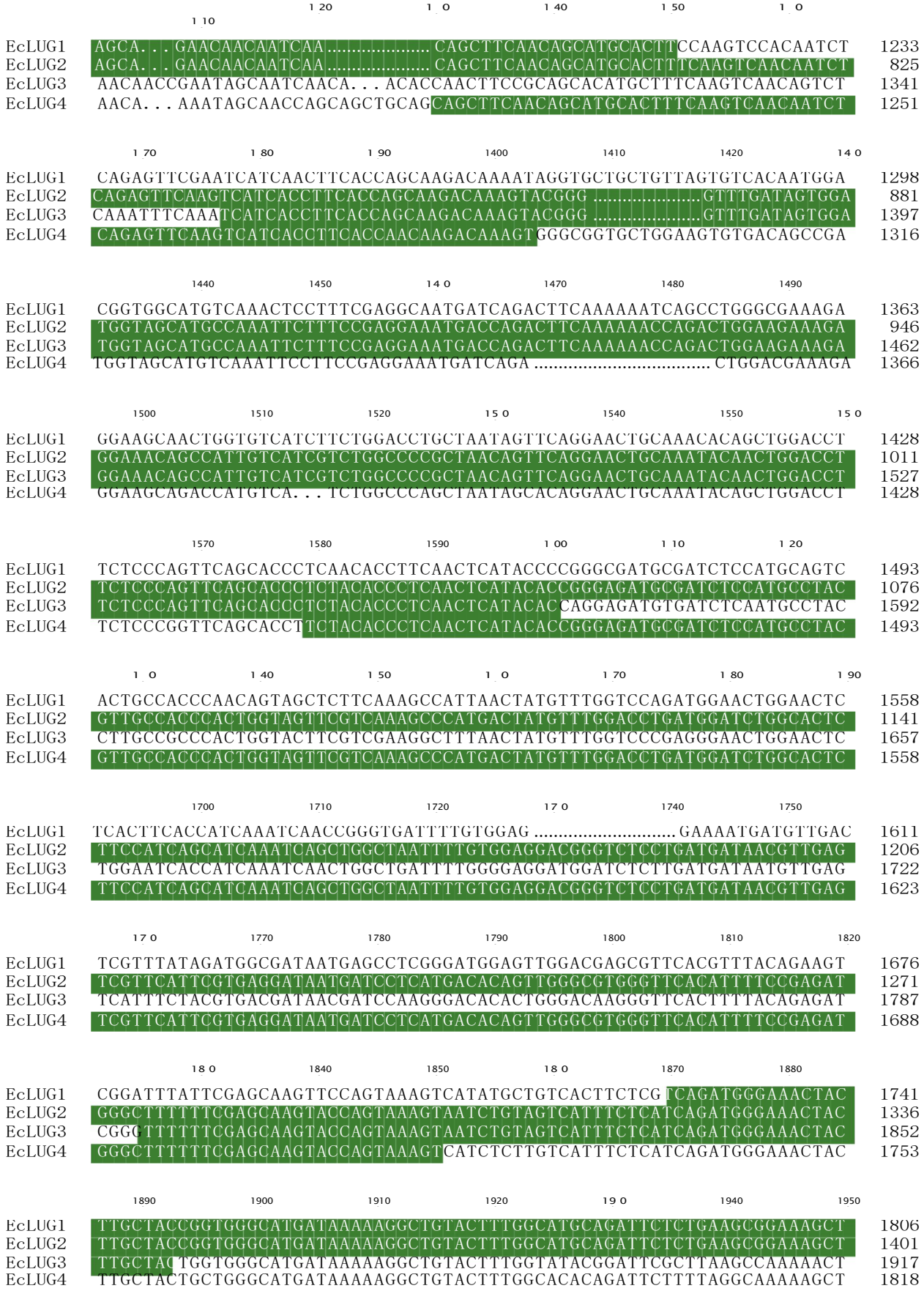
EcLUG1 AGCA...GAACAACAATCAA.....CAGCTTCAACAGCATGCACTTCCAAGTCCACAATCT 1233
EcLUG2 AGCA...GAACAACAATCAA.....CAGCTTCAACAGCATGCACTTTCAAGTCAACAATCT 825
EcLUG3 AACAACCGAATAGCAATCAACA...ACACCAACTTCCGCAGCACATGCTTTCAAGTCAACAGTCT 1341
EcLUG4 AACA...AAATAGCAACCAGCAGCTGCAGCAGCTTCAACAGCATGCACTTTCAAGTCAACAATCT 1251
EcLUG1 CAGAGTTCGAATCATCAACTTCACCAGCAAGACAAAATAGGTGCTGCTGTTAGTGTCACAATGGA 1298
EcLUG2 CAGAGTTCAAGTCATCACCTTCACCAGCAAGACAAAGTACGGG.....GTTTGATAGTGGA 881
EcLUG3 CAAATTTCAAATCATCACCTTCACCAGCAAGACAAAGTACGGG.....GTTTGATAGTGGA 1397
EcLUG4 CAGAGTTCAAGTCATCACCTTCACCAACAAGACAAAGTGGGCGGTGCTGGAAGTGTGACAGCCGA 1316
EcLUG1 CGGTGGCATGTCAAACTCCTTTCGAGGCAATGATCAGACTTCAAAAAATCAGCCTGGGCGAAAGA 1363
EcLUG2 TGGTAGCATGCCAAATTCTTTCCGAGGAAATGACCAGACTTCAAAAAACCAGACTGGAAGAAAGA 946
EcLUG3 TGGTAGCATGCCAAATTCTTTCCGAGGAAATGACCAGACTTCAAAAAACCAGACTGGAAGAAAGA 1462
EcLUG4 TGGTAGCATGTCAAATTCCTTCCGAGGAAATGATCAGA.....CTGGACGAAAGA 1366
EcLUG1 GGAAGCAACTGGTGTCATCTTCTGGACCTGCTAATAGTTCAGGAACTGCAAACACAGCTGGACCT 1428
EcLUG2 GGAAACAGCCATTGTCATCGTCTGGCCCCGCTAACAGTTCAGGAACTGCAAATACAACTGGACCT 1011
EcLUG3 GGAAACAGCCATTGTCATCGTCTGGCCCCGCTAACAGTTCAGGAACTGCAAATACAACTGGACCT 1527
EcLUG4 GGAAGCAGACCATGTCA...TCTGGCCCAGCTAATAGCACAGGAACTGCAAATACAGCTGGACCT 1428
EcLUG1 TCTCCCAGTTCAGCACCCTCAACACCTTCAACTCATACCCCGGGCGATGCGATCTCCATGCAGTC 1493
EcLUG2 TCTCCCAGTTCAGCACCCTCTACACCCTCAACTCATACACCGGGGAGATGCGATCTCCATGCCTAC 1076
EcLUG3 TCTCCCAGTTCAGCACCCTCTACACCCTCAACTCATACACCAGGAGATGTGATCTCAATGCCTAC 1592
EcLUG4 TCTCCCGGTTCAGCACCTTCTACACCCTCAACTCATACACCGGGAGATGCGATCTCCATGCCTAC 1493
EcLUG1 ACTGCCACCCAACAGTAGCTCTTCAAAGCCATTAACTATGTTTGGTCCAGATGGAACTGGAACTC 1558
EcLUG2 GTTGCCACCCACTGGTAGTTCGTCAAAGCCCATGACTATGTTTGGACCTGATGGATCTGGCACTC 1141
EcLUG3 CTTGCCGCCCACTGGTACTTCGTCGAAGGCTTTAACTATGTTTGGTCCCGAGGGAACTGGAACTC 1657
EcLUG4 GTTGCCACCCACTGGTAGTTCGTCAAAGCCCATGACTATGTTTGGACCTGATGGATCTGGCACTC 1558
EcLUG1 TCACTTCACCATCAAATCAACCGGGTGATTTTGTGGAG.....GAAAATGATGTTGAC 1611
EcLUG2 TTCCATCAGCATCAAATCAGCTGGCTAATTTTGTGGAGGACGGGTCTCCTGATGATAACGTTGAG 1206
EcLUG3 TGGAATCACCATCAAATCAACTGGCTGATTTTGGGGAGGATGGATCTCTTGATGATAATGTTGAG 1722
EcLUG4 TTCCATCAGCATCAAATCAGCTGGCTAATTTTGTGGAGGACGGGTCTCCTGATGATAACGTTGAG 1623
EcLUG1 TCGTTTATAGATGGCGATAATGAGCCTCGGGATGGAGTTGGACGAGCGTTCACGTTTACAGAAGT 1676
EcLUG2 TCGTTCATTCGTGAGGATAATGATCCTCATGACACAGTTGGGCGTGGGTTCACATTTTCCGAGAT 1271
EcLUG3 TCATTTCTACGTGACGATAACGATCCAAGGGACACACTGGGACAAGGGTTCACTTTTACAGAGAT 1787
EcLUG4 TCGTTCATTCGTGAGGATAATGATCCTCATGACACAGTTGGGCGTGGGTTCACATTTTCCGAGAT 1688
EcLUG1 CGGATTTATTCGAGCAAGTTCCAGTAAAGTCATATGCTGTCACTTCTCGTCAGATGGGAAACTAC 1741
EcLUG2 GGGCTTTTTTCGAGCAAGTACCAGTAAAGTAATCTGTAGTCATTTCTCATCAGATGGGAAACTAC 1336
EcLUG3 CGGCTTTTTTCGAGCAAGTACCAGTAAAGTAATCTGTAGTCATTTCTCATCAGATGGGAAACTAC 1852
EcLUG4 GGGCTTTTTTCGAGCAAGTACCAGTAAAGTCATCTCTTGTCATTTCTCATCAGATGGGAAACTAC 1753
EcLUG1 TTGCTACCGGTGGGCATGATAAAAAGGCTGTACTTTGGCATGCAGATTCTCTGAAGCGGAAAGCT 1806
EcLUG2 TTGCTACCGGTGGGCATGATAAAAAGGCTGTACTTTGGCATGCAGATTCTCTGAAGCGGAAAGCT 1401
EcLUG3 TTGCTACTGGTGGGCATGATAAAAAGGCTGTACTTTGGTATACGGATTCGCTTAAGCCAAAAACT 1917
EcLUG4 TTGCTACTGCTGGGCATGATAAAAAGGCTGTACTTTGGCACACAGATTCTTTTAGGCAAAAAGCT 1818

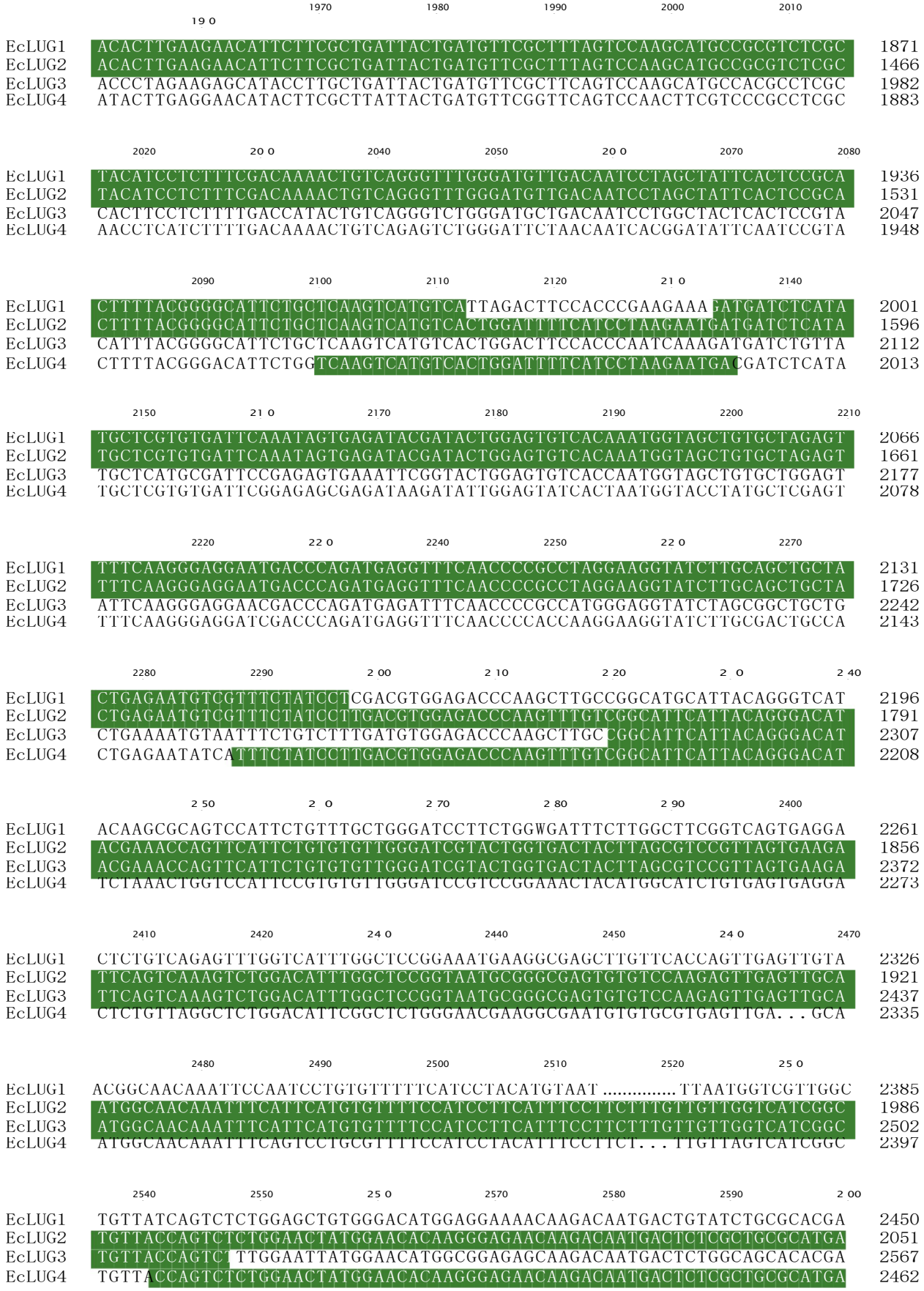
1970 1980 1990 2000 2010
EcLUG1 ACACTTGAAGAACATTCTTCGCTGATTACTGATGTTCGCTTTAGTCCAAGCATGCCGCGTCTCGC 1871
EcLUG2 ACACTTGAAGAACATTCTTCGCTGATTACTGATGTTCGCTTTAGTCCAAGCATGCCGCGTCTCGC 1466
EcLUG3 ACCCTAGAAGAGCATACCTTGCTGATTACTGATGTTCGCTTCAGTCCAAGCATGCCACGCCTCGC 1982
EcLUG4 ATACTTGAGGAACATACTTCGCTTATTACTGATGTTCGGTTCAGTCCAACTTCGTCCCGCCTCGC 1883
2020 2040 2050 2070 2080
EcLUG1 TACATCCTCTTTCGACAAAACTGTCAGGGTTTGGGATGTTGACAATCCTAGCTATTCACTCCGCA 1936
EcLUG2 TACATCCTCTTTCGACAAAACTGTCAGGGTTTGGGATGTTGACAATCCTAGCTATTCACTCCGCA 1531
EcLUG3 CACTTCCTCTTTTGACCATACTGTCAGGGTCTGGGATGCTGACAATCCTGGCTACTCACTCCGTA 2047
EcLUG4 AACCTCATCTTTTGACAAAACTGTCAGAGTCTGGGATTCTAACAATCACGGATATTCAATCCGTA 1948
2090 2100 2110 2120 2140
EcLUG1 CTTTTACGGGGCATTCTGCTCAAGTCATGTCATTAGACTTCCACCCGAAGAAAGATGATCTCATA 2001
EcLUG2 CTTTTACGGGGCATTCTGCTCAAGTCATGTCACTGGATTTTCATCCTAAGAATGATGATCTCATA 1596
EcLUG3 CATTTACGGGGCATTCTGCTCAAGTCATGTCACTGGACTTCCACCCAATCAAAGATGATCTGTTA 2112
EcLUG4 CTTTTACGGGACATTCTGGTCAAGTCATGTCACTGGATTTTCATCCTAAGAATGACGATCTCATA 2013
2150 2170 2180 2190 2200
EcLUG1 TGCTCGTGTGATTCAAATAGTGAGATACGATACTGGAGTGTCACAAATGGTAGCTGTGCTAGAGT 2066
EcLUG2 TGCTCGTGTGATTCAAATAGTGAGATACGATACTGGAGTGTCACAAATGGTAGCTGTGCTAGAGT 1661
EcLUG3 TGCTCATGCGATTCCGAGAGTGAAATTCGGTACTGGAGTGTCACCAATGGTAGCTGTGCTGGAGT 2177
EcLUG4 TGCTCGTGTGATTCGGAGAGCGAGATAAGATATTGGAGTATCACTAATGGTACCTATGCTCGAGT 2078
2220 2240 2250 2270
EcLUG1 TTTCAAGGGAGGAATGACCCAGATGAGGTTTCAACCCCGCCTAGGAAGGTATCTTGCAGCTGCTA 2131
EcLUG2 TTTCAAGGGAGGAATGACCCAGATGAGGTTTCAACCCCGCCTAGGAAGGTATCTTGCAGCTGCTA 1726
EcLUG3 ATTCAAGGGAGGAACGACCCAGATGAGATTTCAACCCCGCCATGGGAGGTATCTAGCGGCTGCTG 2242
EcLUG4 TTTCAAGGGAGGATCGACCCAGATGAGGTTTCAACCCCACCAAGGAAGGTATCTTGCGACTGCCA 2143
2280 2290 2310 2320 2340
EcLUG1 CTGAGAATGTCGTTTCTATCCTCGACGTGGAGACCCAAGCTTGCCGGCATGCATTACAGGGTCAT 2196
EcLUG2 CTGAGAATGTCGTTTCTATCCTTGACGTGGAGACCCAAGTTTGTCGGCATTCATTACAGGGACAT 1791
EcLUG3 CTGAAAATGTAATTTCTGTCTTTGATGTGGAGACCCAAGCTTGCCGGCATTCATTACAGGGACAT 2307
EcLUG4 CTGAGAATATCATTTCTATCCTTGACGTGGAGACCCAAGTTTGTCGGCATTCATTACAGGGACAT 2208
2350 2370 2380 2390 2400
EcLUG1 ACAAGCGCAGTCCATTCTGTTTGCTGGGATCCTTCTGGWGATTTCTTGGCTTCGGTCAGTGAGGA 2261
EcLUG2 ACGAAACCAGTTCATTCTGTGTGTTGGGATCGTACTGGTGACTACTTAGCGTCCGTTAGTGAAGA 1856
EcLUG3 ACGAAACCAGTTCATTCTGTGTGTTGGGATCGTACTGGTGACTACTTAGCGTCCGTTAGTGAAGA 2372
EcLUG4 TCTAAACTGGTCCATTCCGTGTGTTGGGATCCGTCCGGAAACTACATGGCATCTGTGAGTGAGGA 2273
2410 2420 2440 2450 2470
EcLUG1 CTCTGTCAGAGTTTGGTCATTTGGCTCCGGAAATGAAGGCGAGCTTGTTCACCAGTTGAGTTGTA 2326
EcLUG2 TTCAGTCAAAGTCTGGACATTTGGCTCCGGTAATGCGGGCGAGTGTGTCCAAGAGTTGAGTTGCA 1921
EcLUG3 TTCAGTCAAAGTCTGGACATTTGGCTCCGGTAATGCGGGCGAGTGTGTCCAAGAGTTGAGTTGCA 2437
EcLUG4 CTCTGTTAGGCTCTGGACATTCGGCTCTGGGAACGAAGGCGAATGTGTGCGTGAGTTGA...GCA 2335
2480 2490 2500 2510 2520
EcLUG1 ACGGCAACAAATTCCAATCCTGTGTTTTTCATCCTACATGTAAT.....TTAATGGTCGTTGGC 2385
EcLUG2 ATGGCAACAAATTTCATTCATGTGTTTTCCATCCTTCATTTCCTTCTTTGTTGTTGGTCATCGGC 1986
EcLUG3 ATGGCAACAAATTTCATTCATGTGTTTTCCATCCTTCATTTCCTTCTTTGTTGTTGGTCATCGGC 2502
EcLUG4 ATGGCAACAAATTTCAGTCCTGCGTTTTCCATCCTACATTTCCTTCT...TTGTTAGTCATCGGC 2397
2540 2550 2570 2580 2600
EcLUG1 TGTTATCAGTCTCTGGAGCTGTGGGACATGGAGGAAAACAAGACAATGACTGTATCTGCGCACGA 2450
EcLUG2 TGTTACCAGTCTCTGGAACTATGGAACACAAGGGAGAACAAGACAATGACTCTCGCTGCGCATGA 2051
EcLUG3 TGTTACCAGTCTTTGGAATTATGGAACATGGCGGAGAGCAAGACAATGACTCTGGCAGCACACGA 2567
EcLUG4 TGTTACCAGTCTCTGGAACTATGGAACACAAGGGAGAACAAGACAATGACTCTCGCTGCGCATGA 2462

Figure 8: *Alignment of EcLUG genes. Sequences identical to EcLUG2 are marked in green.*

Table 8: *Identified copy numbers of genes considered in this thesis*

Gene	Copy number	Gene	Copy number
EcAG	2	*AtAG*	1
EcAGL6-like	2	*AtAGL6, AtAGL13*	2
EcAGL11	1	*AtAGL11*	1
EcAGO1	2	*AtAGO1*	1
EcARR14	1	*AtARR14*	1
EcATH1.2	1	*AtH1*	1
EcBEL1	1	*AtBEL1*	1
EcBP	1	*AtBP*	1
EcCRC	1	*AtCRC*	1
EcDEF	3(-4)	*AtAP3*	1
EcEBS	1(-2)	*ABS*	1
EcETT	1	*AtETT*	1
EcHEC	3(-5)	*AtHEC*	3
EcLUG	3	*AtLUG*	1
EcNGA	3	*AtNGA*	4
EcPHX	1	*AtPHB, AtPHV*	2
EcPID	3	*AtPID*	2
EcSEI	1	*AtPI*	1
EcSEP	2	*AtSEP*	4
EcSPT	2	*AtSPT, AtALC*	2
EcSTM	2	*AtSTM*	1
EcSTY-like	1	*AtSTY*	2
EcWAG	1	*AtWAG*	2
EcWIP	1	*AtNTT*	1
EcYAB1/2	2	*AtFIL, AtYAB3*	2
EcYUC1/4	1	*AtYUC1, AtYUC4*	2

Table 9: *All sequences used in the identification of orthologues. RNAseq data refers to data generated for AG Becker; AB A. Bayouhmi, personal communication; DT D. Tekleyohans, dissertation; KP K. Pfannebecker, personal communication; TG T. Groß, personal communication; YZ Y. Zhao, personal communication*

name used here	ID/old name	source	publication
AcAGL6-like	Aqcoe7G053700.1	phytozome	
AcAGO1.1	Aqcoe3G009200.1	phytozome	
AcAGO1.2	Aqcoe3G423500.1	phytozome	
AcAGO1.3	Aqcoe3G436100.1	phytozome	
AcARF3	Aqcoe1G248400.1	phytozome	
AcARF4	Aqcoe1G494900.1	phytozome	
AcARF5	Aqcoe4G073400.1	phytozome	
AcARF6	Aqcoe1G185500.1	phytozome	
AcARF8	Aqcoe3G431200.1	phytozome	
AcARR14	Aqcoe3G009700.1	phytozome	
AcATH1	Aqcoe7G132200.1	phytozome	
AcBEE-like	Aqcoe3G034800.1	phytozome	
AcBEL1	Aqcoe5G437300.1	phytozome	
AcHEC1	Aqcoe6G096700.1	phytozome	
AcHEC2	Aqcoe5G150900.1	phytozome	
AcHEC3	Aqcoe5G239900.1	phytozome	
AcKAN2-like	Aqcoe3G169700.1	phytozome	
AcLUG1	Aqcoe7G200300.1	phytozome	
AcLUG2	Aqcoe7G397900.1	phytozome	
AcLUH	Aqcoe5G007900.1	phytozome	
AcNGA	Aqcoe5G472800.1	phytozome	
AcPAN	Aqcoe3G399500.1	phytozome	
AcPHB-like	Aqcoe1G178700.1	phytozome	
AcPID2	Aqcoe7G279900.1	phytozome	
AcSPT	Aqcoe5G147300.1	phytozome	
AcSUP	Aqcoe2G368300.1	phytozome	
AcWAG	Aqcoe6G092400.1	phytozome	
AcWOX1/6	Aqcoe3G000600.1	phytozome	
AcWOX11/12	Aqcoe2G000800.1	phytozome	
AcWOX13	Aqcoe5G119500.1	phytozome	
AcWOX13.1	Aqcoe5G119500.1	phytozome	
AcWOX13.2	Aqcoe6G173100.1	phytozome	
AcWOX2	Aqcoe1G464700.1	phytozome	

Continued on next page

Table 9 – *Continued from previous page*

name used here	ID/old name	source	publi-cation
AcWOX3	Aqcoe2G168200.1	phytozome	
AcWOX4	Aqcoe6G134100.1	phytozome	
AcWOX5/7	Aqcoe2G100800.1	phytozome	
AcWOX8/9	Aqcoe1G245800.1	phytozome	
AcWUS	Aqcoe2G057900.1	phytozome	
AcYUC1/4	Aqcoe7G200400.1	phytozome	
AT2G42300	AT2G42300.1	phytozome	
AT3G57800	AT3G57800.1	phytozome	
AT5G43920	AT5G43920.1	phytozome	
AtABS2	AT2G36080.1	phytozome	
AtAGC1-12	AT3G44610.1	phytozome	
AtAGC1-8	AT5G03640.1	phytozome	
AtAGL6	AT2G45650.1	phytozome	
AtAGL13	AT3G61120.1	phytozome	
AtAGO1	AT1G48410.2	phytozome	
AtAGO10	AT5G43810.1	phytozome	
AtALC	AT5G67110.1	phytozome	
AtARF10	AT2G28350.1	phytozome	
AtARF17	AT1G77850.1	phytozome	
AtARF4	AT5G60450.1	phytozome	
AtARF6	AT1G30330.2	phytozome	
AtARF8	AT5G37020.1	phytozome	
AtARR11	AT1G67710.1	phytozome	
AtARR14	AT2G01760.1	phytozome	
AtBEE1	AT1G18400.1	phytozome	
AtBEE2	AT4G36540.1	phytozome	
AtBEE3	AT1G73830.1	phytozome	
AtBEL1	AT5G41410.1	phytozome	
AtbHLH87	AT3G21330.1	phytozome	
AtBLH1	AT2G35940.1	phytozome	
AtBLH5	AT2G27220.1	phytozome	
AtDPA4	AT5G06250.2	phytozome	
AtETT	AT2G33860.1	phytozome	
AtH1	AT4G32980.1	phytozome	
AtHAF	AT1G25330.1	phytozome	

Continued on next page

Table 9 – *Continued from previous page*

name used here	ID/old name	source	publi-cation
AtHEC1	AT5G67060.1	phytozome	
AtHEC2	AT3G50330.1	phytozome	
AtHEC3	AT5G09750.1	phytozome	
AtIND	AT4G00120.1	phytozome	
AtKAN1	AT5G16560.1	phytozome	
AtKAN2	AT1G32240.1	phytozome	
AtKAN3	AT4G17695.1	phytozome	
AtKAN4	AT5G42630.1	phytozome	
AtLIS	AT2G41500.1	phytozome	
AtLUG	AT4G32551.2	phytozome	
AtLUH	AT2G32700.7	phytozome	
AtNGA1	AT2G46870.1	phytozome	
AtNGA2	AT3G61970.1	phytozome	
AtNGA3	AT1G01030.1	phytozome	
AtNGA4	AT4G01500.1	phytozome	
AtPAN	AT1G68640.1	phytozome	
AtPHB	AT2G34710.1	phytozome	
AtPHV	AT1G30490.1	phytozome	
AtPID	AT2G34650.1	phytozome	
AtPID2	AT2G26700.1	phytozome	
AtPIF3	AT1G09530.2	phytozome	
AtPIF4	AT2G43010.1	phytozome	
AtPIF7	AT5G61270.1	phytozome	
AtRAB	AT5G06070.1	phytozome	
AtREV	AT5G60690.1	phytozome	
AtSAW1	AT4G36870.2	phytozome	
AtSAW2	AT2G23760.1	phytozome	
AtSEP1	AT5G15800.1	phytozome	
AtSEP3	AT1G24260.1	phytozome	
AtSMU1	AT1G73720.1	phytozome	
AtSOD7	AT3G11580.1	phytozome	
AtSPT	AT4G36930.1	phytozome	
AtSUP	AT3G23130.1	phytozome	
AtTGA2	AT5G06950.1	phytozome	
AtTGA5	AT5G06960.1	phytozome	

Continued on next page

Table 9 – *Continued from previous page*

name used here	ID/old name	source	publi-cation
AtTGA6	AT3G12250.4	phytozome	
AtTPL	AT1G15750.1	phytozome	
AtTPR4	AT3G15880.2	phytozome	
AtWAG1	AT1G53700.1	phytozome	
AtWAG2	AT3G14370.1	phytozome	
AtWOX1	AT3G18010.1	phytozome	
AtWOX10	AT1G20710.1	phytozome	
AtWOX11	AT3G03660.1	phytozome	
AtWOX12	AT5G17810.2	phytozome	
AtWOX13	AT4G35550.1	phytozome	
AtWOX14	AT1G20700.1	phytozome	
AtWOX2	AT5G59340.1	phytozome	
AtWOX3	AT2G28610.1	phytozome	
AtWOX4	AT1G46480.1	phytozome	
AtWOX5	AT3G11260.1	phytozome	
AtWOX6	AT2G01500.1	phytozome	
AtWOX7	AT5G05770.1	phytozome	
AtWOX8	AT5G45980.1	phytozome	
AtWOX9	AT2G33880.1	phytozome	
AtWUS	AT2G17950.1	phytozome	
AtYUC1	AT4G32540.1	phytozome	
AtYUC4	AT5G11320.1	phytozome	
AtYUC6	AT5G25620.2	phytozome	
AtYUC7	AT2G33230.1	phytozome	
AtZFP10	AT2G37740.1	phytozome	
AtrAGL6-like	evm_27.model.AmTr_v1.0_scaffold00001.413	phytozome	
AtrAGO10	evm_27.model.AmTr_v1.0_scaffold00044.24	phytozome	
AtrARF3-like	evm_27.model.AmTr_v1.0_scaffold00021.168	phytozome	
AtrARF6	evm_27.model.AmTr_v1.0_scaffold00092.36	phytozome	
AtrARF8	evm_27.model.AmTr_v1.0_scaffold00029.187	phytozome	
AtrARR11-like	evm_27.model.AmTr_v1.0_scaffold00049.51	phytozome	
AtrARR14	evm_27.model.AmTr_v1.0_scaffold00176.20	phytozome	
AtrBEE-like	evm_27.model.AmTr_v1.0_scaffold00079.56	phytozome	
AtrBEL1	evm_27.model.AmTr_v1.0_scaffold00001.384	phytozome	
AtrbHLH87	evm_27.model.AmTr_v1.0_scaffold00036.88	phytozome	

Continued on next page

Table 9 – *Continued from previous page*

name used here	ID/old name	source	publi-cation
AtrHEC1	evm_27.model.AmTr_v1.0_scaffold00008.223	phytozome	
AtrHEC3	evm_27.model.AmTr_v1.0_scaffold00071.86	phytozome	
AtrKAN-like	evm_27.model.AmTr_v1.0_scaffold00059.235	phytozome	
AtrKAN1-like	evm_27.model.AmTr_v1.0_scaffold00048.68	phytozome	
AtrLUG1	evm_27.model.AmTr_v1.0_scaffold00122.38	phytozome	
AtrLUG2	evm_27.model.AmTr_v1.0_scaffold00002.372	phytozome	
AtrLUH	evm_27.model.AmTr_v1.0_scaffold00067.172	phytozome	
AtrNGA	evm_27.model.AmTr_v1.0_scaffold00018.9	phytozome	
AtrPAN	evm_27.model.AmTr_v1.0_scaffold00010.14	phytozome	
AtrPHB-like	evm_27.model.AmTr_v1.0_scaffold00155.45	phytozome	
AtrPID2	evm_27.model.AmTr_v1.0_scaffold00081.20	phytozome	
AtrREV-like	evm_27.model.AmTr_v1.0_scaffold00148.15	phytozome	
AtrSPT	evm_27.model.AmTr_v1.0_scaffold00046.26	phytozome	
AtrSUP	evm_27.model.AmTr_v1.0_scaffold00009.125	phytozome	
AtrWAG	evm_27.model.AmTr_v1.0_scaffold00033.222	phytozome	
AtrWOX1/6	evm_27.model.AmTr_v1.0_scaffold00010.77	phytozome	
AtrWOX11/12	evm_27.model.AmTr_v1.0_scaffold00119.79	phytozome	
AtrWOX13	evm_27.model.AmTr_v1.0_scaffold00044.164	phytozome	
AtrWOX2	evm_27.model.AmTr_v1.0_scaffold00012.85	phytozome	
AtrWOX3	evm_27.model.AmTr_v1.0_scaffold00023.118	phytozome	
AtrWOX4	evm_27.model.AmTr_v1.0_scaffold00051.5	phytozome	
AtrWOX5/7	evm_27.model.AmTr_v1.0_scaffold00029.349	phytozome	
AtrWOX8/9	evm_27.model.AmTr_v1.0_scaffold00021.149	phytozome	
AtrWUS	evm_27.model.AmTr_v1.0_scaffold00405.1	phytozome	
AtrYUC1/4	evm_27.model.AmTr_v1.0_scaffold00122.41	phytozome	
EcAG1	DQ088996.1 *E. californica AG1*	NCBI	[388]
	ok59_2361t3	RNAseq data	
EcAG2	DQ088997.1 *E. californica AG2*	NCBI	[388]
	ok43_6922t7	RNAseq data	
	ta21_R9020089	RNAseq data	
EcAGL6-like1	KC899704.1 *E. californica AGL6-like*	NCBI	[419]
	ok39_11t4	RNAseq data	
	Eca_sc194781.1_g0030.1	EGD	
EcAGL6-like2	ok41_1679t1	RNAseq data	
	c12501tr001	RNAseq data	

Continued on next page

Table 9 – *Continued from previous page*

name used here	ID/old name	source	publi-cation
	Eca_sc194483.1_g1000.1	EGD	
EcAGL11	DQ088998.1 *E. californica AGL11*	NCBI	[388]
	Eca_sc068610.1_g0010.1	EGD	
	Eca_sc049015.1_g1100.1	EGD	
EcAGO1.1	c15008tr001	RNAseq data	KP
	ok49_703t20	RNAseq data	
	Eca_sc013049.1_g0540.1	EGD	
	Eca_sc000141.1_g0310.1	EGD	
EcAGO1.2	sk36_1154729	RNAseq data	
	c20654tr001	RNAseq data	
	Eca_sc001396.1_g0300.1	EGD	
EcARF6	ok55_12273t1	RNAseq data	
	Eca_sc000973.1_g1700.1	EGD	
EcARF8	ok37_11567t102	RNAseq data	
	c1131tr004	RNAseq data	
	c1131tr005	RNAseq data	
	c1131tr007	RNAseq data	
	c1131tr008	RNAseq data	
	Eca_sc193916.1_g0010.1	EGD	
EcARR14	ok37_12075t10	RNAseq data	
	c453tr002	RNAseq data	
	Eca_sc194599.1_g0110.1	EGD	
EcATH1.2	c3161tr001	RNAseq data	KP
	ok23_12173t15	RNAseq data	
	Eca_sc007672.1_g0180.1	EGD	
EcBEE-like	sk33_1302168	RNAseq data	KP
EcBEL1	ok47_28494t1	RNAseq data	
	ta25_R7325110	RNAseq data	
	c8987tr001	RNAseq data	
	c8987tr002	RNAseq data	
EcBP	HQ337627.1 *E. californica KNAT1*	NCBI	[209]
	c2044tr002	RNAseq data	
	ok33_133t5	RNAseq data	
	Eca_sc029196.1_g0010.1	EGD	
	Eca_sc184534.1_g0010.1	EGD	

Continued on next page

Table 9 – *Continued from previous page*

name used here	ID/old name	source	publi-cation
EcCRC	AM946412.1 *E. californica CRC*	NCBI	[288]
	ok61_21050t1	RNAseq data	
	Eca_sc027509.1_g0520.1	EGD	
EcDEF1	EF378697.1 *E. californica DEF1*	NCBI	[344]
	ok29_9841t10	RNAseq data	
	Eca_sc009026.1_g0600.1	EGD	
EcDEF2	EF378698.1 *E. californica DEF2*	NCBI	[344]
	Eca_sc001023.1_g1410.1	EGD	
EcDEF3	HE573239.1 *E. californica DEF3*	NCBI	
	ok25_7449t6	RNAseq data	
	Eca_sc194662.1_g2240.1	EGD	
	Eca_sc194662.1_g2280.1	EGD	
EcEBS	c616tr002	RNAseq data	DT
	ok51_1492t40	RNAseq data	
	ok21_1843t65	RNAseq data	
	Eca_sc183462.1_g0160.1	EGD	
	Eca_sc001122.1_g4900.1	EGD	
EcETT	c793tr002	RNAseq data	KP
	c793tr004	RNAseq data	
	c793tr001	RNAseq data	
	ta24_R7223908	RNAseq data	
EcFUL1	HM592297.1 *E. californica FUL1*	NCBI	
	ok45_17377t4	RNAseq data	
	c13183tr002	RNAseq data	
	c13183tr001	RNAseq data	
	Eca_sc001396.1_g1280.1	EGD	
EcFUL2	HM592298.1 *E. californica FUL2*	NCBI	
	ok51_17321t21	RNAseq data	
	c3873tr001	RNAseq data	
	Eca_sc004992.1_g0520.1	EGD	
EcFUL3	KF500168.1 *E. californica FL3*	NCBI	[420]
	ok49_476t24	RNAseq data	
	c11015tr001	RNAseq data	
	c11015tr002	RNAseq data	
	c11015tr003	RNAseq data	

Continued on next page

Table 9 – *Continued from previous page*

name used here	ID/old name	source	publi-cation
	c11015tr004	RNAseq data	
	Eca_sc194563.1_g0160.1	EGD	
EcHEC1	ok33_33088t4	RNAseq data	AB
	Eca_sc194486.1_g5960.1	EGD	
EcHEC2	ok43_20978t1	RNAseq data	AB
	ok39_20684t1	RNAseq data	
	c13406tr001	RNAseq data	
	Eca_sc001754.1_g0290.1	EGD	
EcHEC3	ok29_33516t5	RNAseq data	AB
	c11220tr001	RNAseq data	
	Eca_sc194732.1_g2620.1	EGD	
EcHEC4	Eca_sc194573.1_g0990.1	EGD	
EcHEC5	Eca_sc001433.1_g1200.1	EGD	
EcKAN1	ok47_16885t3	RNAseq data	
	c19686tr001	RNAseq data	
	c11926tr001	RNAseq data	
	Eca_sc194793.1_g0330.1	EGD	
EcKAN2.1	ok49_12688t8	RNAseq data	TG
	c22447tr001	RNAseq data	
	Eca_sc018558.1_g0690.1	EGD	
EcKAN2.2	ok53_23533t5	RNAseq data	
	Eca_sc007672.1_g0990.1	EGD	
EcKAN2.3	ok45_15151t7	RNAseq data	
	Eca_sc000157.1_g1030.1	EGD	
EcKNAT2/6	HQ337628.1 *E. californica KNAT2/6*	NCBI	[209]
	ok25_11230t7	RNAseq data	
	Eca_sc042187.1_g1020.1	EGD	
	Eca_sc042187.1_g1010.1	EGD	
EcLUG1	c1163tr004	RNAseq data	[391]
	ok49_1064t12	RNAseq data	
	Eca_sc194729.1_g0950.1	EGD	
EcLUG2	c2387tr001	RNAseq data	[391]
EcLUG3	c1487tr001	RNAseq data	[391]
	ok43_3018t90	RNAseq data	
	Eca_sc000659.1_g0280.1	EGD	

Continued on next page

Table 9 – *Continued from previous page*

name used here	ID/old name	source	publi-cation
EcLUG4	ok47_2386t11	RNAseq data	
	c2603tr001	RNAseq data	
	Eca_sc187119.1_g2630.1	EGD	
EcLUH1	c1436tr002	RNAseq data	[391]
	ok57_5277t3	RNAseq data	
	Eca_sc194614.1_g0380.1	EGD	
EcLUH2	c2518tr001	RNAseq data	[391]
	ok55_3276t18	RNAseq data	
	ok41_5003t28	RNAseq data	
	Eca_sc194715.1_g0400.1	EGD	
EcNGA	KF668646.1 *E. californica NGA*	NCBI	[385]
	ok47_18285t3	RNAseq data	
	Eca_sc194593.1_g0130.1	EGD	
EcNGA1	c6319tr001	RNAseq data	[23]
	ok33_64t10	RNAseq data	
	Eca_sc010606.1_g1130.1	EGD	
EcNGA2	ok25_27400t6	RNAseq data	
	Eca_sc003893.1_g1310.1	EGD	
EcPAN	ok39_5605t12	RNAseq data	
	c8664tr001	RNAseq data	
	Eca_sc194588.1_g0860.1	EGD	
EcPHX	c2009tr001	RNAseq data	KP
	ok67_1452t1	RNAseq data	
	Eca_sc007884.1_g0980.1	EGD	
	Eca_sc191652.1_g0010.1	EGD	
	Eca_sc162278.1_g0010.1	EGD	
EcPID1	ok49_3651t1	RNAseq data	
	Eca_sc000493.1_g1340.1	EGD	
EcPID3	ok39_9210t3	RNAseq data	
	c4344tr006	RNAseq data	
	Eca_sc000973.1_g1270.1	EGD	
EcPID2	ok45_14983t4	RNAseq data	
	c8528tr001	RNAseq data	
	Eca_sc003743.1_g3400.1	EGD	
EcSEI	EF378699.1 *E. californica GLO*	NCBI	[344]

Continued on next page

Table 9 – *Continued from previous page*

name used here	ID/old name	source	publi-cation
	ok59_7079t2	RNAseq data	
	Eca_sc002821.1_g0440.1	EGD	
EcSEP1	AY850181.1 *E. californica AGL2*	NCBI	[187]
	ok59_1272t1	RNAseq data	
	Eca_sc000118.1_g0530.1	EGD	
EcSEP3	AY850180.1 *E. californica AGL9*	NCBI	[187]
	ok55_13292t2	RNAseq data	
	Eca_sc194486.1_g3920.1	EGD	
EcSPT1	EVOD-2110824	onekp	[421]
	ta28_R5809015	RNAseq data	
	c21406tr001	RNAseq data	
	c16420tr001	RNAseq data	
	Eca_sc001754.1_g0390.1	EGD	
EcSPT2	ok51_5889t2	RNAseq data	
	c18465tr001	RNAseq data	
	c21579tr001	RNAseq data	
	Eca_sc187119.1_g1320.1	EGD	
	Eca_sc186110.1_g0010.1	EGD	
EcSRS-like	EcSRS-like		[422]
	tr31939c1g4i1	RNAseq data	
	ok25_70226t3	RNAseq data	
	Eca_sc009026.1_g0520.1	EGD	
EcSTM1	HQ337629.1 *E. californica STM1*	NCBI	[209]
	ta40_R3022232	RNAseq data	
	ta28_R5828715	RNAseq data	
	ta32_R4747745	RNAseq data	
	Eca_sc010691.1_g0010.1	EGD	
	Eca_sc007843.1_g0040.1	EGD	
	Eca_sc010690.1_g0010.1	EGD	
EcSTM2	HQ337630.1 *E. californica STM2*	NCBI	[209]
	sk45_725375	RNAseq data	
	ok29_20975t1	RNAseq data	
	Eca_sc194544.1_g0720.1	EGD	
EcSTY-like	c16590tr001	RNAseq data	[391]
	ok33_20301t8	RNAseq data	

Continued on next page

Table 9 – *Continued from previous page*

name used here	ID/old name	source	publi-cation
	Eca_sc100701.1_g0990.1	EGD	
EcSUP	ok23_20347t1	RNAseq data	
	c17714tr001	RNAseq data	
	Eca_sc194641.1_g1000.1	EGD	
EcTCP1	EVOD-2032785	onekp	[423]
	DQ347820.1 *E. californica TCP1*	NCBI	[130]
	Eca_sc194426.1_g0020.1	EGD	
EcTCP2	EVOD-2031455	onekp	[423]
	DQ347824.1 *E. californica TCP2*	NCBI	[424]
	Eca_sc005291.1_g0490.1	EGD	
EcTCP3	c5573tr001	RNAseq data	YZ
	ok27_5762t41	RNAseq data	
	ok31_5780t19	RNAseq data	
	Eca_sc000493.1_g1190.1	EGD	
	Eca_sc000493.1_g1200.1	EGD	
EcWAG	ta44_R2370317	RNAseq data	
	c12880tr001	RNAseq data	
	Eca_sc000066.1_g1570.1	EGD	
EcWIP	c13924tr001	RNAseq data	[23]
	ta27_R6131611	RNAseq data	
	Eca_sc000058.1_g1700.1	EGD	
	Eca_sc052600.1_g0010.1	EGD	
EcWOX1/6	ok45_16071t6	RNAseq data	
	Eca_sc001122.1_g4640.1	EGD	
EcWOX2.1	sk21_1575581	RNAseq data	
	Eca_sc194667.1_g0100.1	EGD	
EcWOX2.2	Eca_sc001061.1_g0100.1	EGD	
EcWOX2.3	Eca_sc002160.1_g0180.1	EGD	
EcWOX3	ok23_14121t7	RNAseq data	
	Eca_sc194507.1_g0670.1	EGD	
EcWOX4	NJKC_scaffold_2057950	onekp	[259]
	UNPT_scaffold_2055913	onekp	[259]
	RKGT_scaffold_2058088	onekp	[259]
	c14637tr001	RNAseq data	
	Eca_sc000587.1_g0290.1	EGD	

Continued on next page

Table 9 – *Continued from previous page*

name used here	ID/old name	source	publi-cation
EcWOX5/7	Eca_sc007206.1_g2890.1	EGD	
EcWOX8/9	c8898tr002	RNAseq data	
	Eca_sc000763.1_g1610.1	EGD	
EcWOX11/12.1	ok25_14388t6	RNAseq data	
	Eca_sc010932.1_g1110.1	EGD	
EcWOX11/12.2	c19392tr001	RNAseq data	
	Eca_sc194509.1_g1500.1	EGD	
EcWOX13.1	ERXG_scaffold_2017962	onekp	[259]
	NJKC_scaffold_2007920	onekp	[259]
	ok57_1522t1	RNAseq data	
	c13428tr001	RNAseq data	
	Eca_sc011255.1_g0910.1	EGD	
EcWOX13.2	ERXG_scaffold_2064605	onekp	[259]
	TUHA_scaffold_2019319	onekp	[259]
	NJKC_scaffold_2013864	onekp	[259]
	RKGT_scaffold_2003813	onekp	[259]
	UNPT_scaffold_2035952	onekp	[259]
	ok21_1644t11	RNAseq data	
	c8474tr001	RNAseq data	
	c8474tr002	RNAseq data	
	Eca_sc013265.1_g0010.1	EGD	
EcWOX13.3	Eca sc004324.1 g2470.1	EGD	
EcWUS	Eca_sc001122.1_g3550.1	EGD	
	TUHA_scaffold_2046381	onekp	
	TUHA_scaffold_2016346	onekp	
EcYAB1	HQ116795.1 *E. californica YAB1*	NCBI	[130]
	ok49_8976t7	RNAseq data	
	Eca_sc049015.1_g1040.1	EGD	
EcYAB2	HQ116796.1 *E. californica YAB2*	NCBI	[130]
	ok45_8287t6	RNAseq data	
	Eca_sc147686.1_g0010.1	EGD	
EcYAB3	HQ116797.1 *E. californica YAB3*	NCBI	[130]
	ok59_11423t4	RNAseq data	
	c12825tr001	RNAseq data	
EcYAB4	HQ116798.1 *E. californica YAB4*	NCBI	[130]

Continued on next page

Table 9 – *Continued from previous page*

name used here	ID/old name	source	publi-cation
	ok53_15441t7	RNAseq data	
	c13080tr001	RNAseq data	
EcYAB5	HQ116799.1 *E. californica YAB5*	NCBI	[130]
	ok59_23166t2	RNAseq data	
	c15693tr001	RNAseq data	
EcYUC1/4	ok25_1392t7	RNAseq data	
	c8481tr001	RNAseq data	
	Eca_sc000659.1_g0290.1	EGD	
PsAGL6-like	XP_026380230.1 *P. somniferum OsMADS6-like*	NCBI	
PsAGO1-like	XP_026387396.1 *P. somniferum AGO1-like*	NCBI	
PsARF17-like	XP_026405523.1 *P. somniferum ARF17-like*	NCBI	
PsARF3-like	XP_026422053.1 *P. somniferum ARF3-like*	NCBI	
PsARF6-like	XP_026394965.1 *P. somniferum ARF6-like*	NCBI	
PsARR14	XP_026387344.1 *P. somniferum ORR21-like*	NCBI	
PsATH1.1	XP_026453303.1 *P. somniferum ATH1-like*	NCBI	
PsATH1.2	XP_026405539.1 *P. somniferum* uncharacter-ized protein	NCBI	
PsATH1.3	XP_026423440.1 *P. somniferum ATH1-like*	NCBI	
PsBEE-like	XP_026397421.1 *P. somniferum BEE1-like*	NCBI	
PsBEL1	XP_026457898.1 *P. somniferum BEL1*-HOMOLOG	NCBI	
PsHEC1	XP_026396880.1 *P. somniferum HEC2-like*	NCBI	
PsHEC2	XP_026449406.1 *P. somniferum HEC2-like*	NCBI	
PsHEC3.1	XP_026390405.1 *P. somniferum HEC3-like*	NCBI	
PsHEC3.2	XP_026403605.1 *P. somniferum IND-like*	NCBI	
PsHEC4	XP_026459122.1 *P. somniferum HEC1-like*	NCBI	
PsHEC5	XP_026450521.1 *P. somniferum HEC1-like*	NCBI	
PsKAN2	XP_026406580.1 *P. somniferum* probable *KAN2*	NCBI	
PsLUG	XP_026389712.1 *P. somniferum LEUNIG -like*	NCBI	
PsLUH	XP_026457644.1 *P. somniferum LEUNIG HOMOLOG-like*	NCBI	

Continued on next page

Table 9 – *Continued from previous page*

name used here	ID/old name	source	publi-cation
PsNGA1	XP_026401707.1 *P. somniferum* Os03g0120900-like	NCBI	
PsNGA2	XP_026406233.1 *P. somniferum* Os03g0120900-like	NCBI	
PsNGA3	XP_026437414.1 *P. somniferum* Os03g0120900-like	NCBI	
PsNGA4	RZC86162.1 *P. somniferum* hypothetical protein C5167_026834	NCBI	
PsPAN	XP_026409251.1 *P. somniferum HBP-1b(c38)-like*	NCBI	
PsPHV-like	XP_026395480.1 *P. somniferum HOX32 -like*, isoform X2	NCBI	
PsPID	XP_026390004.1 *P. somniferum PINOID-like*	NCBI	
PsPID2	XP_026454416.1 *P. somniferum PINOID2-like*	NCBI	
PsREV-like	XP_026413776.1 *P. somniferum REVOLU-TA-like*	NCBI	
PsSPT	XP_026455882.1 *P. somniferum SPATULA-like*	NCBI	
PsSUP1	XP_026453276.1 *P. somniferum SUPER-MAN-like*	NCBI	
PsSUP2	XP_026452900.1 *P. somniferum ZFP11-like*	NCBI	
PsSUP3	XP_026416374.1 *P. somniferum SUPER-MAN-like*	NCBI	
PsSUP4	RZC68675.1 *P. somniferum* hypothetical protein C5167_031836	NCBI	
PsWAG	XP_026394440.1 *P. somniferum WAG1-like*	NCBI	
PsWUS	XP_026432440.1 *P. somniferum WUSCHEL-like*	NCBI	
PsYUC1/4	XP_026460211.1 *P. somniferum* probable *YUCCA4*	NCBI	

3 PPI

Table 10: *Summary of physical interactions between E. californica proteins based on Y2H and BiFC assays conducted in this work.*

protein1	protein2	assay	protein1	protein2	assay
EcAG2	EcAG2	Y2H	EcDEF1	EcNGA	Y2H
EcAG2	EcBP	Y2H	EcDEF1	EcSEI	Y2H
EcAG2	EcDEF1	Y2H, Y2H	EcDEF1	EcSEP1	Y2H, Y2H, Y2H
EcAG2	EcDEF2	Y2H, Y2H	EcDEF1	EcSTM2	Y2H
EcAG2	EcDEF3	Y2H	EcDEF2	EcDEF3	Y2H
EcAG2	EcEBS	Y2H	EcDEF2	EcNGA	Y2H
EcAG2	EcNGA	Y2H	EcDEF2	EcSEI	Y2H
EcAG2	EcPHX	Y2H	EcDEF2	EcSEP1	Y2H, Y2H, Y2H
EcAG2	EcSEP1	Y2H, Y2H, Y2H	EcDEF2	EcSTM2	Y2H
EcAG2	EcSTM2	Y2H, Y2H	EcDEF3	EcSEP1	Y2H, Y2H
EcARR14	EcNGA	BiFC	EcEBS	EcSEP1	Y2H, Y2H
EcARR14	EcSTM2	BiFC	EcNGA	EcNGA	Y2H, BiFC
EcARR14	EcYAB2	BiFC	EcNGA	EcSEP1	Y2H
EcATH1.2	EcBP	Y2H	EcNGA	EcSTM1	Y2H
EcATH1.2	EcSTM2	Y2H	EcNGA	EcSTM2	Y2H, BiFC
EcBEL1	EcNGA	BiFC	EcNGA	EcWIP	BiFC
EcBEL1	EcSTM2	BiFC	EcNGA	EcYAB2	BiFC
EcBEL1	EcYAB2	BiFC	EcPHX	EcPHX	Y2H
EcBP	EcSEP1	Y2H	EcPHX	EcSTM2	Y2H
EcBP	EcSTM2	Y2H	EcSEI	EcSTM1	Y2H
EcBP	EcYAB2	BiFC	EcSEP1	EcSEP1	Y2H, Y2H
EcCRC	EcNGA	Y2H	EcSEP1	EcSTM2	Y2H
EcCRC	EcWIP	BiFC	EcSEP3	EcPHX	Y2H
EcCRC	EcYAB2	BiFC	EcSTM1	EcSTM2	Y2H
EcDEF1	EcDEF1	Y2H	EcSTM2	EcSTM2	Y2H, BiFC
EcDEF1	EcDEF2	Y2H	EcSTM2	EcWIP	BiFC
EcDEF1	EcEBS	Y2H	EcWIP	EcWIP	BiFC

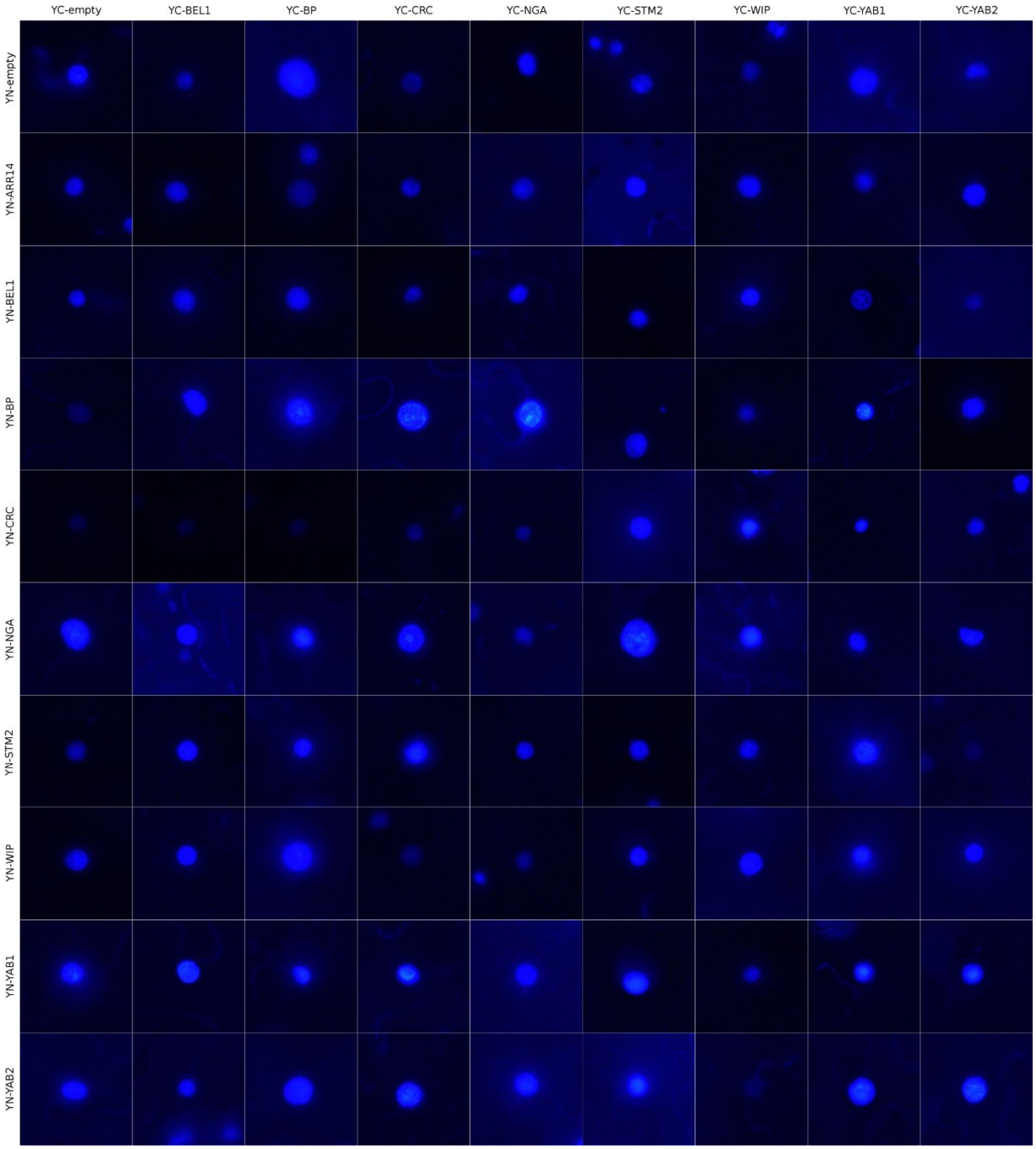

Figure 9: *Summary of all BiFC experiments. DAPI fluorescence at 228 ms exposition time in tobacco leaves. DAPI binds to the minor groove of dsDNA helices at AT-rich sequences, staining the cell nuclei. With RNA DAPI interacts by intercalating in AU-rich sequences. [425]*

Table 11: *Overview of expression strengths in- dicated as transcrips per million (TPM). Partial transcripts are indicated by 'p'.*

		sample IDs																	
gene	**transcript ID**	**SRA bud-r1**	**S1-r1**	**S1-r2**	**S1-r3**	**S2a-r1**	**S2b-r1**	**S2b-r2**	**S3-r1**	**S3-r2**	**S3-r3**	**S4-r1**	**S4-r2**	**S4-r3**	**SRA rootb-r1**	**SRA root-r1**	**SRA leaf-r1**	**SRA stem-r1**	**SRA fruit-r1**	
EcAG1	ok59_2361t3	1.02	212.81	57.54	152.34	195.78	225.94	247.14	248.24	132.12	127.28	138.49	248.51	251.45	0.00	0.42	0.27	371.64	362.70	
EcAG2	ok43_6922t7	0.00	20.98	36.02	18.35	0.00	45.12	23.03	2.59	23.73	14.63	0.00	4.42	0.00	0.00	0.00	0.16	43.54	20.57	
EcARR14	ok37_12075t10	58.65	53.98	63.23	39.29	50.16	46.34	49.85	61.57	58.36	62.71	63.42	50.29	95.01	51.64	58.06	24.46	14.83	49.51	
EcATH1.2	ok23_12173t15	0.00	56.52	38.73	53.69	134.53	28.71	38.24	26.18	56.50	21.51	53.53	4.53	3.44	0.00	0.06	0.47	11.58	0.56	
EcBEL1	ok47_28494t1	38.48	0.43	0.00	2.57	3.10	0.00	20.21	16.66	0.55	0.00	10.87	21.42	4.48	3.20	8.24	37.03	18.86	30.60	
EcBP	ok33_133t5	133.95	24.5	2.62	1.86	0.00	6.76	4.76	0.00	0.00	0.00	0.00	0.16	0.00	71.49	48.44	0.00	12.28	6.67	
EcCRC	ok61_21050t1	0.00	684.28	954.45	568.47	1024.02	2482.12	2656.72	405.11	949.89	2211.21	542.49	75.37	823.26	0.00	0.00	0.00	23.91	3.74	
EcDEF1	ok29_9841t10	7.75	36.23	17.03	86.18	51.73	37.29	24.74	58.98	105.58	82.26	70.56	36.25	53.39	2.45	5.17	9.76	962.42	30.10	
EcDEF3	ok25_7449t6	0.00	80.53	21.42	3.47	0.00	68.08	0.00	0.19	0.00	0.00	0.00	1.18	0.00	0.00	0.00	0.00	424.15	0.41	
EcEBS	ok51_1492t40	0.00	0.00	4.61	0.00	0.00	421.33	928.78	0.00	0.00	0.00	0.00	0.00	4.38	0.05	0.00	0.00	1.09	12.15	
EcNGA	ok47_18285t3	0.00	15.26	0.64	13	68.9	5.54	2.46	42.03	1.46	6.29	24.24	41.83	1.81	1.24	6.57	2.3	9.35	1.2	
EcPHX	ok67_1452t1	39.98	72.84	55.44	52.13	48.11	128.99	104.22	19.00	40.16	27.31	44.12	17.49	20.05	47.27	89.83	5.89	17.69	57.66	p
EcSEI	ok59_7079t2	0.17	173.31	45.57	0.00	0.00	126.62	1.50	0.76	0.00	0.00	0.00	0.00	0.00	0.00	0.00	0.00	754.78	2.20	
EcSEP1	ok59_1272t1	23.36	191.22	176.30	138.16	13.55	2.51	1.78	2.75	95.83	79.27	5.26	10.09	69.70	0.23	0.89	0.00	12.46	19.46	
EcSEP3	ok55_13292t2	42.93	291.26	354.80	356.29	291.79	217.24	128.93	296.17	489.07	252.78	364.34	231.66	198.89	0.30	1.29	0.09	273.59	135.43	
EcSTM1	ta40_R3022232	58.11	92.88	0.53	0.52	0.00	1.50	0.00	0.00	0.00	0.00	0.00	0.00	0.00	23.76	1.30	0.00	7.06	3.28	
EcSTM1	ta28_R5828715	67.06	13.59	2.87	1.41	1.01	18.35	20.28	5.18	5.46	17.93	1.44	10.41	8.17	60.68	88.14	9.37	31.08	34.60	
EcSTM1	ta32_R4747745	13.65	50.12	38.96	43.17	50.41	19.06	26.65	51.49	73.56	30.64	48.80	27.12	34.88	7.59	9.27	1.04	16.19	7.69	
EcSTM2	sk45_725375	3.31	26.51	0.00	30.07	0.00	7.98	0.00	0.00	0.00	0.00	0.00	0.00	0.00	0.00	0.00	0.00	1.85	0.00	p
EcSTM2	tr5989c0g1i1	5.34	4.55	0.00	2.45	0.00	3.73	0.00	0.00	0.00	0.00	0.00	0.00	0.00	0.43	0.00	0.00	0.75	0.00	p
EcSTM2	ok29_20975t1	4.49	0.00	0.00	9.18	0.00	1.41	0.00	0.00	0.00	0.00	0.00	0.00	0.00	0.99	0.00	0.00	1.12	0.00	p
EcYAB2	ok45_8287t6	0.28	97.44	21.66	62.01	0.43	19.97	14.89	28.29	0.00	0.00	12.53	49.69	0.48	0.13	0.10	0.38	17.69	2.07	

Table 12: *Table of predicted TFs binding to genomic sequences 5 kb upstream of E. californica genes, as identified by PlantPan3 [384]. The first two columns show the tested TFs, horizontally the upstream sequences are given. EcDEF3u or d denote the upstream or downstream locus, for EcEBS the scaffold Eca_sc001122.1 is numbered "1" and Eca_sc183462.1 "2". The numbering for EcWIP refers to the different possible TSSs of the same locus. x shows predicted binding motifs for the given TF as well as TFs from other genera, x in italics specifies a predicted site bound only by the given TF from A. thaliana or A. lyrata.*

binding family	TF name	ARR	BELL		bHLH		HD-ZIP III	KNOX I			NGA		
		EcARR14	*EcATH1.2*	*EcBEL1*	*EcSPT1*	*EcSPT2*	*EcPHX*	*EcBP*	*EcSTM1*	*EcSTM2*	*EcNGA*	*EcNGA1*	*EcNGA2*
ARR	AtARR14	x	x	x	x	x	x	x	x	x	x	x	x
ARF	AtETT	x	x	x	x	x	x	x	x	x	-	x	x
	AtMP	x	x	x	x	x	x	x	x	x	-	x	x
	AtARF4/ AtARF6/ AtARF8	x	x	x	x	x	x	x	x	x	-	x	x
AS2	AtAS2	-	-	-	-	-	-	-	-	-	-	-	-
BELL	AtATH1	-	-	-	-	-	-	-	-	-	-	-	-
	AtBEL1	-	-	-	-	-	-	-	-	-	-	-	-
	AtPNY	-	-	-	-	-	-	-	-	-	-	-	-
	AtPNF	-	-	-	-	-	-	-	-	-	-	-	-
bHLH	AtHEC1/ AtHEC2/ AtHEC3	x	x	-	-	-	-	-	-	x	x	-	x
	AtIND	-	-	-	-	-	-	-	-	-	-	-	-
	AtSPT	-	x	-	-	-	-	-	-	x	x	-	x
	AtALC	x	x	x	-	x	-	-	-	x	x	-	x
BTB/ POZ	AtBOP1	-	-	-	-	-	-	-	-	-	-	-	-
	AtBOP2	-	-	-	-	-	-	-	-	-	-	-	-
C2H2	AtSUP	-	-	-	-	-	-	-	-	-	-	-	-
HD-ZIP	AtPHB/ AtREV/ AtHB8	x	x	x	x	x	-	x	x	x	x	x	x
	AtPHV	x	x	x	x	x	x	x	x	x	x	x	x
	AtCNA	x	x	x	x	x	x	x	x	x	x	x	x
FLO/ LFY	AtLFY	-	-	-	-	-	-	-	-	*x*	-	-	-
KNOX I	AtSTM/ AtBP	x	x	x	x	x	x	x	x	x	x	x	x
MADS	AtAG	x	-	-	x	-	-	x	-	x	-	-	-
	OsMADS3/ OsMADS5/ OsMADS13/ OsMADS58/ ZAG2/ ZMM16	x	x	x	x	x	x	x	x	x	x	x	x
	AtPI	-	x	x	-	x	-	-	-	x	-	x	-
	OsMADS2	x	x	x	x	x	x	x	x	x	x	x	x
	OsMADS4	-	-	-	-	-	-	-	-	-	-	-	-
	AtAP3	-	x	x	x	x	x	x	x	-	x	x	x
	OsMADS16	x	-	x	x	x	-	x	x	-	-	x	x
	AtSEP1	-	x	-	-	-	-	x	-	-	-	x	-
	AtSEP2	-	-	-	-	-	-	-	-	-	-	-	-
	ASEP3/ OsMADS7/ OsMADS8	x	x	x	x	x	x	x	x	x	x	x	x
	AtSEP4	-	x	-	x	-	-	x	x	-	-	x	-
	OsMADS1	-	-	-	-	-	-	-	-	-	-	-	-
	AtABS	x	-	x	x	x	-	x	-	-	-	x	x
MYB	AtAS1	-	-	-	-	-	-	-	-	-	-	-	-
NAC	AtCUC1	-	x	x	x	x	x	x	x	x	x	x	x
	AtCUC2	-	x	x	x	x	x	x	x	x	x	x	x
	AtCUC3	-	x	x	x	x	x	x	x	x	x	x	x
NGA	AtNGA1	-	-	-	-	-	-	-	-	-	-	-	-
	AtNGA2	-	-	-	-	-	-	-	-	-	-	-	-
	AtNGA3	x	-	x	-	-	-	-	-	-	-	x	x
	AtNGA4	x	x	-	x	-	x	x	-	x	x	x	x
SHI/ STY	AtSTY1	-	x	x	-	x	x	x	x	x	x	x	x
	AtSTY2	x	x	x	x	x	x	x	x	x	x	x	x
WOX	AtWUS	x	x	-	x	x	x	x	x	x	x	x	x
WIP	AtNTT	-	-	-	-	-	-	-	-	-	-	-	-
YABBY	AtCRC	*x*	*x*	-	*x*	*x*	*x*	*x*	*x*	*x*	*x*	*x*	*x*
	OsDL	-	-	-	-	-	-	-	-	-	-	-	-
	AtFIL	*x*	-	*x*	*x*	-	*x*	*x*	*x*	*x*	*x*	-	*x*
	AtYAB3	*x*	*x*	*x*	-	-	*x*	*x*	*x*	-	*x*	-	*x*
	AtYAB2	-	-	-	-	-	-	-	-	-	-	-	-
	AtINO	-	*x*	*x*	*x*	-	*x*	*x*	*x*	*x*	*x*	*x*	*x*

Continued on next page

Table 12 – *Continued from previous page*

binding family	TF name	MADS *EcAG1*	*EcAG2*	*EcDEF1*	*EcDEF2*	*EcDEF3u*	*EcDEF3d*	*EcSEI*	*EcEBS_1*	*EcEBS_2*	*EcSEP1*	*EcSEP3*
ARR	**AtARR14**	x	x	x	x	x	x	x	x	x	x	x
ARF	**AtETT**	x	-	x	x	x	x	x	-	x	x	x
	AtMP	x	-	x	x	x	x	x	-	x	x	x
	AtARF4/ AtARF6/ AtARF8	x	-	x	x	x	x	x	-	x	x	x
AS2	**AtAS2**	-	-	-	-	-	-	-	-	-	-	-
BELL	**AtATH1**	-	-	-	-	-	-	-	-	-	-	-
	AtBEL1	-	-	-	-	-	-	-	-	-	-	-
	AtPNY	-	-	-	-	-	-	-	-	-	-	-
	AtPNF	-	-	-	-	-	-	-	-	-	-	-
bHLH	**AtHEC1/ AtHEC2/ AtHEC3**	-	-	x	x	-	x	-	-	-	-	x
	AtIND	-	-	-	-	-	-	-	-	-	-	-
	AtSPT	-	-	-	x	-	x	-	-	-	-	x
	AtALC	x	x	x	x	x	x	x	x	x	-	x
BTB/ POZ	**AtBOP1**	-	-	-	-	-	-	-	-	-	-	-
	AtBOP2	-	-	-	-	-	-	-	-	-	-	-
C2H2	**AtSUP**	-	-	-	-	-	-	-	-	-	-	-
HD-ZIP	**AtPHB/ AtREV**	x	-	x	x	x	x	x	x	x	x	x
	AtPHV	x	-	x	x	x	x	x	x	x	x	x
	AtCNA	x	-	x	x	x	x	x	x	x	x	x
FLO/ LFY	**AtLFY**	-	-	-	-	-	-	*x*	-	-	-	-
KNOX I	**AtSTM/ AtBP**	x	x	x	x	x	x	x	x	x	x	x
MADS	**AtAG**	x	x	-	-	x	x	x	x	x	-	x
	OsMADS3/ OsMADS5/ OsMADS13/ OsMADS58/ ZAG2/ ZMM16	x	x	x	x	x	x	x	x	x	x	x
	AtPI	x	-	-	-	x	x	x	-	-	x	x
	OsMADS2	x	x	x	x	x	x	x	x	x	x	x
	OsMADS4	-	-	-	-	-	-	-	-	-	-	-
	AtAP3	x	x	x	x	x	x	-	x	x	x	x
	OsMADS16	x	-	x	x	x	x	-	x	x	-	-
	AtSEP1	-	-	x	x	x	x	-	-	x	-	-
	AtSEP2	-	-	-	-	-	-	-	-	-	-	-
	ASEP3/ OsMADS7/ OsMADS8	x	x	x	x	x	x	x	x	x	x	x
	AtSEP4	x	-	-	x	x	x	-	-	x	-	-
	OsMADS1	-	-	-	-	-	-	-	-	-	-	-
	AtABS	x	-	x	x	x	x	-	x	x	-	-
MYB	**AtAS1**	-	-	-	-	-	-	-	-	-	-	-
NAC	**AtCUC1**	-	-	x	-	x	x	-	-	-	x	-
	AtCUC2	-	-	x	-	x	x	-	x	x	x	x
	AtCUC3	-	-	x	x	x	x	-	-	-	x	-
NGA	**AtNGA1**	-	-	-	-	-	-	-	-	-	-	-
	AtNGA2	-	-	-	-	-	-	-	-	-	-	-
	AtNGA3	-	-	-	-	-	-	-	-	-	-	x
	AtNGA4	x	x	x	-	-	x	x	-	-	-	x
SHI/ STY	**AtSTY1**	x	-	x	x	x	x	x	x	x	x	x
	AtSTY2	x	x	x	x	x	x	x	x	x	x	x
WOX	**AtWUS**	x	x	x	x	x	x	x	x	x	x	x
WIP	**AtNTT**	-	-	-	-	-	-	-	-	-	-	-
YABBY	**AtCRC**	-	*x*	*x*	*x*	*x*	-	*x*	*x*	*x*	*x*	*x*
	OsDL	-	-	-	-	-	-	-	-	-	-	-
	AtFIL	-	-	*x*	*x*	*x*	*x*	*x*	*x*	*x*	*x*	*x*
	AtYAB3	*x*	*x*	-	*x*	*x*	*x*	-	*x*	*x*	-	*x*
	AtYAB2	-	-	-	-	-	-	-	-	-	-	-
	AtINO	*x*	*x*	*x*	*x*	*x*	*x*	*x*	*x*	*x*	*x*	*x*

Continued on next page

Table 12 – *Continued from previous page*

binding family	TF name	Ser/Thr protein kinase				SHI/STY	WIP-domain		WOX	YABBY			YUCCA
		EcPIDa	*EcPIDb*	*EcPID2*	*EcWAG*	*EcSTY-L*	*EcWIP_ATG1*	*EcWIP_ATG2*	*EcWUS*	*EcYAB1*	*EcYAB2*	*EcCRC*	*EcYUC1/4*
ARR	**AtARR14**	x	x	x	x	x	x	x	x	x	x	x	x
ARF	**AtETT**	x	x	x	x	x	x	x	x	x	x	x	x
	AtMP	x	x	x	x	x	x	x	x	x	x	x	x
	AtARF4/ AtARF6/ AtARF8	x	x	x	x	x	x	x	x	x	x	x	x
AS2	**AtAS2**	-	-	-	-	-	-	-	-	-	-	-	-
BELL	**AtATH1**	-	-	-	-	-	-	-	-	-	-	-	-
	AtBEL1	-	-	-	-	-	-	-	-	-	-	-	-
	AtPNY	-	-	-	-	-	-	-	-	-	-	-	-
	AtPNF	-	-	-	-	-	-	-	-	-	-	-	-
bHLH	**AtHEC1/ AtHEC2/ AtHEC3**	x	x	-	x	x	x	x	-	-	-	x	x
	AtIND	-	-	-	-	-	-	-	-	-	-	-	-
	AtSPT	x	x	-	-	x	x	x	-	x	-	x	x
	AtALC	x	x	x	x	x	x	x	-	x	-	x	x
BTB/ POZ	**AtBOP1**	-	-	-	-	-	-	-	-	-	-	-	-
	AtBOP2	-	-	-	-	-	-	-	-	-	-	-	-
C2H2	**AtSUP**	-	-	-	-	-	-	-	-	-	-	-	-
HD-ZIP	**AtPHB/ AtREV**	-	x	x	x	x	x	-	x	x	x	x	x
	AtPHV	x	x	x	x	x	x	x	x	x	x	x	x
	AtCNA	x	x	x	x	x	x	x	x	x	x	x	x
FLO/ LFY	**AtLFY**	-	-	-	-	-	-	-	-	-	-	-	-
KNOX I	**AtSTM/ AtBP**	x	x	x	x	x	x	x	x	x	x	x	x
MADS	**AtAG**	x	x	-	-	-	-	-	x	-	-	-	-
	OsMADS3/ OsMADS5/ OsMADS13/ OsMADS58/ ZAG2/ ZMM16	x	x	x	x	x	x	x	x	x	x	x	x
	AtPI	-	-	x	-	-	-	-	-	x	x	x	-
	OsMADS2	x	x	x	x	x	x	x	x	x	x	x	x
	OsMADS4	-	-	-	-	-	-	-	-	-	-	-	-
	AtAP3	x	x	x	x	x	x	x	x	x	x	-	x
	OsMADS16	x	x	x	x	-	x	x	x	x	-	x	-
	AtSEP1	-	-	-	-	-	-	-	-	-	-	-	-
	AtSEP2	-	-	-	-	-	-	-	-	-	-	-	-
	ASEP3/ OsMADS7/ OsMADS8	x	x	x	x	x	x	x	x	x	x	x	x
	AtSEP4	-	-	-	-	-	-	-	-	-	-	-	-
	OsMADS1	-	-	-	-	-	-	-	-	-	-	-	-
	AtABS	-	-	x	x	-	x	x	x	x	-	x	-
MYB	**AtAS1**	-	-	-	-	-	-	-	-	-	-	-	-
NAC	**AtCUC1**	x	-	x	x	x	x	x	-	x	x	-	x
	AtCUC2	x	-	x	x	x	x	x	x	-	x	-	x
	AtCUC3	x	-	x	x	x	x	x	-	-	x	-	x
NGA	**AtNGA1**	-	-	-	-	-	-	-	-	-	-	-	-
	AtNGA2	-	-	-	-	-	-	-	-	-	-	-	-
	AtNGA3	-	-	-	-	x	-	-	-	-	-	x	-
	AtNGA4	x	-	-	-	x	x	x	-	-	-	-	-
SHI/ STY	**AtSTY1**	x	-	x	-	x	x	x	x	x	-	x	x
	AtSTY2	x	x	x	x	x	x	x	x	x	x	-	x
WOX	**AtWUS**	x	x	x	x	x	x	x	x	x	x	-	x
WIP	**AtNTT**	-	-	-	-	-	-	-	-	-	-	-	-
YABBY	**AtCRC**	*x*	*x*	*x*	*x*	*x*	*x*	*x*	*x*	*x*	*x*	-	*x*
	OsDL	-	-	-	-	-	-	-	-	-	-	-	-
	AtFIL	*x*	-	*x*	*x*	*x*	*x*	*x*	-	-	-	*x*	-
	AtYAB3	*x*	-	-	*x*	*x*	*x*	*x*	*x*	*x*	*x*	*x*	-
	AtYAB2	-	-	-	-	-	-	-	-	-	-	-	-
	AtINO	*x*	-	*x*	*x*	*x*	*x*	*x*	*x*	*x*	-	*x*	*x*

5 Constructs

Table 13: *Vectors used for this thesis. For vectors already present in the group the number of the glycerol stock is given, the other vectors were generated by A. Weisert. Primer sequences are given in the electronic supplemental .fasta files of the respective GOI.*

GOI	Insert	Backbone	Restriction sites	Stock No.
-	-	pGADT7	-	51
-	-	pGBKT7	-	52
-	-	pTRV1	-	253
-	-	pTRV2	-	247
EcAG1 ikc		pGADT7		198
EcAG1 ikc		pGBKT7		201
EcAG2ΔMADS	496 bp	pGADT7	NcoI-BamHI	237
EcAG2ΔMADS	496 bp	pGBKT7	NcoI-BamHI	238
EcAGL11orf		pGADT7		435
EcAGL11orf		pGBKT7		436
EcAGL6		pGADT7		276
EcAGO1.1	cds nt 2416-2617	pTRV2	EcoRI-BamHI	308
EcARR14	YC_complete cds (1971 bp)	pMLBART	EcoRI-BamHI	
EcARR14	YN_complete cds (1971 bp)	pMLBART	EcoRI-BamHI	
EcATH1.2		pGADT7		724
EcBEL1	YC_complete cds (2031 bp)	pMLBART	EcoRI-BamHI	
EcBEL1	YN_complete cds (2031 bp)	pMLBART	EcoRI-BamHI	
EcBP	complete cds (1227 bp)	pGADT7	EcoRI-BamHI	
EcBP	complete cds (1227 bp)	pGBKT7	EcoRI-BamHI	
EcBP	YC_complete cds (1227 bp)	pMLBART	EcoRI-BamHI	
EcBP	YN_complete cds (1227 bp)	pMLBART	EcoRI-BamHI	
EcBP	cds nt 1-430	pTRV2	EcoRI-BamHI	
EcCRC		pGADT7	EcoRI-BamHI	409
EcCRC		pGBKT7	EcoRI-BamHI	296
EcCRC	YC_complete cds (558 bp)	pMLBART	EcoRI-BamHI	
EcCRC	YN_complete cds (558 bp)	pMLBART	EcoRI-BamHI	
EcCRC		pTRV2		30
EcDEF1ΔMADS	528 bp	pGADT7		158
EcDEF1ΔMADS	528 bp	pGBKT7		163
EcDEF2ΔMADS	534 bp	pGADT7	NcoI-BamHI	159

Continued on next page

Table 13 – *Continued from previous page*

GOI	Insert	Backbone	Restriction sites	Stock No
EcDEF2ΔMADS	534 bp	pGBKT7	NcoI-BamHI	164
EcDEF3ΔMADS	531 bp	pGADT7	NcoI-BamHI	281
EcEBS		pGADT7		327
EcEBS		pGBKT7		347
EcETT	complete cds (2340bp)	pGADT7	XmaI-BamHI	
EcETT	complete cds (2340bp)	pGBKT7	XmaI-BamHI	
EcETT		pTRV2		307
EcLUG		pTRV2		615
EcLUG1	complete cds (2547 bp)	pGADT7	NcoI-EcoRI	
EcLUG1	complete cds (2547 bp)	pGBKT7	NcoI-EcoRI	
EcLUH1	cds nt 1706-2034	pTRV2	BsiWI-NheI	616
EcNGA	complete cds (1203 bp)	pGADT7	EcoRI-BamHI	
EcNGA	complete cds (1203 bp)	pGBKT7	EcoRI-BamHI	
EcNGA	YC_complete cds (1203 bp)	pMLBART	EcoRI-BamHI	
EcNGA	YN_complete cds (1203 bp)	pMLBART	EcoRI-BamHI	
EcNGA	cds nt 549-975	pTRV2	EcoRI-BamHI	
EcNGA1	cds nt 577-942	pTRV2	EcoRI-BamHI	
EcNGA2	cds nt 75-470	pTRV2	EcoRI-BamHI	
EcPDS		pTRV2		246
EcPHX	complete cds (2580 bp)	pGADT7	EcoRI-BamHI	
EcPHX	complete cds (2580 bp)	pGBKT7	EcoRI-BamHI	
EcSEIΔMADS	507 bp	pGADT7	NcoI-BamHI	165
EcSEP1	cds nt 330-606	pTRV2	EcoRI-BamHI	
EcSEP1 cds	complete cds	pGADT7		776
EcSEP1 cds	complete cds	pGBKT7		774
EcSEP1 cds+6nt	complete cds+6nt	pGBKT7		775
EcSEP3	726 bp	pGADT7		162
EcSEP3	726 bp	pGBKT7		167
EcSEP3	cds nt 419-504	pTRV2	BamHI-KpnI	
EcSEP3 (ORF)	complete cds	pGADT7		
EcSEP3 (ORF)	complete cds	pGBKT7		
EcSPT		pTRV2		417
EcSPT1	complete cds (1245 bp)	pGBKT7	XmaI-BamHI	
EcSPT2	cds nt 73-448	pTRV2	EcoRI-BamHI	

Continued on next page

Table 13 – *Continued from previous page*

GOI	Insert	Backbone	Restriction sites	Stock No
EcSTM1	complete cds (1095 bp)	pGADT7	NdeI-BamHI	
EcSTM1	complete cds (1095 bp)	pGBKT7	NdeI-BamHI	
EcSTM2	complete cds (1158 bp)	pGADT7	EcoRI-BamHI	
EcSTM2	complete cds (1158 bp)	pGBKT7	EcoRI-BamHI	
EcSTM2	YC_complete cds (1158 bp)	pMLBART	EcoRI-BamHI	
EcSTM2	YN_complete cds (1158 bp)	pMLBART	EcoRI-BamHI	
EcTPC2	complete cds (963 bp)	pGADT7	EcoRI-BamHI	
EcTPC2	complete cds (963 bp)	pGBKT7	EcoRI-BamHI	
EcWIP	cds nt 307-1289	pGADT7	EcoRI-BamHI	
EcWIP	cds nt 307-1289	pGBKT7	EcoRI-BamHI	
EcWIP	YC_cds nt 307-1289	pMLBART	EcoRI-BamHI	
EcWIP	YN_cds nt 307-1289	pMLBART	EcoRI-BamHI	
EcYAB1	complete cds (684 bp)	pGADT7	EcoRI-BamHI	
EcYAB1	complete cds (684 bp)	pGBKT7	EcoRI-BamHI	
EcYAB1	YC_complete cds (684 bp)	pMLBART	EcoRI-BamHI	
EcYAB1	YN_complete cds (684 bp)	pMLBART	EcoRI-BamHI	
EcYAB2	complete cds (657 bp)	pGADT7	EcoRI-BamHI	
EcYAB2	complete cds (657 bp)	pGBKT7	EcoRI-BamHI	
EcYAB2	YC_complete cds (657 bp)	pMLBART	EcoRI-BamHI	
EcYAB2	YN_complete cds (657 bp)	pMLBART	EcoRI-BamHI	
mEGFP		pTRV2		

Erklärung/Declaration of authorship

Ich erkläre: Ich habe die vorgelegte Dissertation selbstständig und ohne unerlaubte fremde Hilfe und nur mit den Hilfen angefertigt, die ich in der Dissertation angegeben habe. Alle Textstellen, die wörtlich oder sinngemäß aus veröffentlichten Schriften entnommen sind, und alle Angaben, die auf mündlichen Auskünften beruhen, sind als solche kenntlich gemacht. Ich stimme einer evtl. Überprüfung meiner Dissertation durch eine Antiplagiat-Software zu. Bei den von mir durchge- führten und in der Dissertation erwähnten Untersuchungen habe ich die Grundsätze guter wis- senschaftlicher Praxis, wie sie in der „Satzung der Justus-Liebig-Universität Gießen zur Sicherung guter wissenschaftlicher Praxis“ niedergelegt sind, eingehalten.

I declare that I have completed this dissertation single-handedly without the unauthorized help of a second party and only with the assistance acknowledged therein. I have appropriately ac- knowledged and cited all text passages that are derived verbatim from or are based on the content of published work of others, and all information relating to verbal communications. I consent to the use of an anti-plagiarism software to check my thesis. I have abided by the principles of good scientific conduct laid down in the charter of the Justus Liebig University Giessen „Satzung der Justus-Liebig-Universität Gießen zur Sicherung guter wissenschaftlicher Praxis“ in carrying out the investigations described in the dissertation.